EEG and TMS-EEG Studies on the Cortical Excitability and Plasticity associated with Human Motor Control and Learning

Myriam Taga

A thesis submitted in partial fulfilment of the requirements of the University of East London for the degree of Doctor of Philosophy

"Learning is making useful changes in the working of our minds", Marvin Minsky

July 2019

Abstract

More than half of the activities of daily living rely on upper limb functions (Ingram et al., 2008). Humans perform upper limb movements with great ease and flexibility but even simple tasks require complex computations in the brain and can be affected following stroke leaving survivors with debilitating movement impairments. Hemispheric asymmetries related to motor dominance, imbalances between contralateral and ipsilateral primary motor cortices (M1) activity and the ability to adapt movements to novel environments play a key role in upper limb motor control and can affect recovery. Motor learning and control are critical in neurorehabilitation, however to effectively integrate these concepts into upper limb recovery treatments, a deeper understanding of the basic mechanisms of unimanual control is needed.

This thesis aimed to investigate hemispheric asymmetries related to motor dominance, to evaluate the relative contribution of the contralateral and ipsilateral M1 during unilateral reaching preparation and finally to identify the neural correlates underlying the formation of a predictive internal model enabling to adapt movements to new environments.

To this end electroencephalography (EEG), transcranial magnetic stimulation (TMS), simultaneous TMS-EEG were employed during a simple motor and a highly standardised robot-mediated task.

The first study used TMS-EEG to examine differences in cortical excitability related to motor dominance by applying TMS over the dominant and non-dominant M1 at rest and during contraction. No hemispheric asymmetries related to hand dominance were found.

The second study assessed the temporal dynamics of bi-hemispheric motor cortical excitability during right arm reaching preparation. TMS was applied either to the ipsilateral or contralateral M1 during different times of movement preparation. Significant bilateral M1 activation during unilateral reaching preparation was observed, with no significant differences between the contralateral and ipsilateral M1. Unimanual reaching preparation was

associated with significant interactions of excitatory and inhibitory processes in both motor cortices.

The third study investigated the neural correlates of motor adaptation. EEG was recorded during a robot-mediated adaptation task involving right arm reaching movements and cortical excitability was assessed by applying TMS over the contralateral M1 and simultaneously recording TMS responses with EEG before and after motor adaptation. It was found that an error-related negativity (ERN) over fronto-central regions correlated with performance improvements during adaptation, suggesting that this neural activity reflects the formation of a predictive internal model. Motor adaptation underlay significant modulations in cortical excitability (i.e. neuroplasticity) in sensorimotor regions. Finally, it was shown that native cortical excitability was linked to motor learning improvements during motor adaptation and explained the variability in motor learning across individuals.

These experiments demonstrated that even unimanual motor control relies on interactions between excitatory and inhibitory mechanisms not only in the contralateral M1 but in a wider range of brain regions, shown by a bi-hemispheric activity during movement preparation, the formation of a predictive model in fronto-central regions during motor adaptation and neuroplastic changes in sensorimotor regions underlying motor adaptation during unimanual reaching.

Declaration

I, Myriam Taga, declare that the work reported in this thesis was carried out in accordance with the regulations of the University of East London. The work is novel except where indicated by special reference in the text and no part of this thesis has been submitted for any other degrees. Any views expressed in the dissertation are those of the author and in no way represent those of the University of East London.

The thesis has not been presented to any other University for examination either in the United Kingdom either overseas.

Myriam Taga

31.07.2019

Table of Contents

List of Figures

List of Tables

List of Equations

Abbreviations

ACC	Anterior Cingulate Cortex
AEP	Auditory-Evoked Potential
AgCL	Silver Chloride
ANOVA	Analysis of Variance
BB	Biceps Brachii
BCI	Brain Computer Interface
BG	Basal Ganglia
CC	Corpus Callosum
CMT	Cortico-Muscular Coherence
CNS	Central Nervous System
CSF	Cerebrospinal Fluid
CSP	Cortical Silent Period
CST	Corticospinal Tract
DC	Direct Current
EEG	Transcranial Magnetic Stimulation
EMA	Early Motor Adaptation
EMG	Electromyography
EOG	Electrooculography
EPSP	Excitatory Postsynaptic Potential
ERD	Event-Related Desynchronisation
ERP	Event-Related Potential
ERPCOH	Event-Related Phase-Coherence
ERS	Event-Related Synchronisation
ERSP	Event-Related Spectral Perturbation
FAM	Familiarisation
FDI	First Dorsal Interosseous
FDR	False Discovery Rate
FF	Force-Field
FFT	Fast Fourier Transform
fMRI	Functional Magnetic Resonance Imaging
FOI	Frequency of Interest
GABA	Gamma-Amino-Butyric Acid

GMFA	Global Mean Field Amplitude
GPT	Grooved Pegboard Task
ICA	Independent Component Analysis
IPSP	Inhibitory Postsynaptic Potential
LFAM	Late Familiarisation
LMA	Late Motor Adaptation
LQ	Laterality Quotient
LTP	Long-term Potentiation
LWO	Late Wash-Out
M1	Primary Motor Cortex
MA	Motor Adaptation
MANOVA	Multivariate Analysis of Variance
MEG	Magnet Encephalography
MEP	Motor Evoked Potential
MLI	Motor Learning Index
MRI	Magnetic Resonance Imaging
MSO	Maximum Stimulator Output
MVC	Maximum Voluntary Contraction
NF	Null-Field
NIBS	Non-invasive Brain Stimulation
OFC	Optimal Feedback Control
PM	Premotor Cortex
rm-ANOVA	repeated-measure Analysis of Variance
RMT	Resting Motor Threshold
ROI	Region of Interest
rTMS	Repetitive Transcranial Magnetic Stimulation
SD	Standard Deviation
SEM	Standard Error Mean
SEP	Somatosensory-Evoked Potential
SMA	Supplementary Motor Area
TEP	TMS-Evoked Potential
tDCS	Transcranial Direct Current Stimulation
TMS	Transcranial Magnetic Stimulation

TMS-EEG	Transcranial Magnetic Stimulation - Electroencephalography
TOI	Time window of Interest
TR-ERPCOH	Task-related Phase Coherence
TRSP	TMS-Related Spectral Perturbation
WO	Wash-Out

Acknowledgements

Three years ago, I embarked this journey to pursue my UEL-funded 3-year PhD in Neurosciences at UEL. During this time, I improved my research skills but also learnt life lessons. This PhD enabled me to learn from and work with remarkable people who influenced my PhD journey.

I would like to thank my supervisor Professor Duncan Turner for giving me the opportunity and providing me with the research setting to investigate the human brain and supporting me throughout this PhD journey. I would also like to thank my second supervisor Professor Cynthia Fu for her valuable support and feedback on the present thesis.

Many thanks go to Doctor Marine Vernet who introduced me to TMS-EEG analysis during a four hour skype conversation. Thanks also go to Doctor Isabella Premoli who kindly agreed to review my first TMS-EEG pilot data and helped me through the first struggles.

I am extremely grateful to have shared a working office with Doctor Sara Pizzamiglio, who showed me that hard work pays off and that science can be more than fun! I gained an amazing friendship and talking science with her never becomes boring. Our shared love of yoga reminds us and will probably always remind us that the right work – pleasure balance is necessary to keep a calm mind even in the most stressful situations.

I am truly thankful to all of the people in the Neurorehabilitation lab who have made these past 3 years stimulating and enjoyable. I am especially grateful to have had the honour to supervise Annacarmen Curci during her internship at UEL; it was a pleasure to work with her. Many thanks go to Annacarmen Curci and Irene Lacal for working with me on EEG data and especially for getting proficient in MATLAB together, it was a lot of fun and hard work!

I would also like to mention Irene Faiman, who also completed an internship in our lab. Sharing our love and passion about science but also our concerns about scientific rigour were always fun. Her support through ups and downs during the PhD and meetings at UCL library helped me to energise and complete writing this thesis.

"The brain is imprisoned inside the skull, a silent, dark, and motionless place; how can it learn what it's like outside? The surface of the brain itself has not the slightest senses of touch, it has no skin with which to feel, it is only connected to skin. Nor can a brain see, for it has no eyes, it only is connected to eyes. The only paths from the world to the brain are bundles of nerves like those that come in from the eyes, ears, and skin. How do the signals that come through those nerves give rise to tour sense of "being in" the outside world? The answer is that this sense is a complicated illusion. We never actually make any direct contact with the outside world. Instead, we work with models of the world that we build inside our brains."

A quote from Marvin Minsky in from his book: The society of Mind (Minsky, 1988).

Chapter 1 - Introduction

1.1. Overview

1.1.1. The human brain and movement control

The human brain is to me the most fascinating organ of our bodies. It is not only the single organ which named itself but is also the organ with which we communicate with the external world. In a famous TED talk Professor Daniel Wolpert even goes as far as to say that the real and only reason we have a brain is "to produce adaptable and complex movements" (Wolpert, 2011). He says: *"Movement is the only way you have of affecting the world around you. Now that's not quite true. There's one other way, and that's through sweating. But apart from that, everything else goes through contractions of muscles. So, think about communication - speech, gestures, writing, sign language - they're all mediated through contractions of your muscles. So, it's really important to remember that sensory, memory and cognitive processes are all important, but they're only important to either drive or suppress future movements. There can be no evolutionary advantage to laying down memories of childhood or perceiving the colour of a rose if it doesn't affect the way you're going to move later in life."* (Wolpert, 2011). Regardless if we agree with this statement or not, without doubt, movement control is a key factor in our daily activities. Even if we take it for granted that we can intentionally move with ease and great flexibility without thinking about it, complex control mechanisms engaging the central nervous system take place.

Voluntary movement is a result of signals transmitted through communication channels linking the internal world in our brains to the physical world around us. In brief, the signals from the brain travel through the nervous system to converge on muscles that eventually generate displacements and forces on the external world (Schwartz, 2016). It is easy to forget the actual complexity of what is going on in our brain when we perform simple tasks in everyday life until something goes wrong, such as after a brain injury. Upper limb problems following brain injury, such as following a stroke are debilitating and can significantly impair the quality of life of survivors (Nichols-Larsen et al., 2005).

Damage to specific parts of the brain can lead to impaired motor control and adaptation, and highlight the complexity with which the CNS has to deal with to enable flexible and adaptable movements. It has been demonstrated that adaptation is important for rehabilitation by making movement flexible and can be used to determine if some patients can generate a more normal motor pattern (for review see Basteris et al., 2014).

1.1.2. Focus and structure of the thesis

Since, the majority (50 %) of the activities of daily living rely on upper limb functions (Ingram et al., 2008) and that upper limb impairments are often observed following stroke (Nichols-Larsen et al., 2005), this thesis focussed on upper limb movements to gain more insights into the neural mechanisms underlying unimanual motor control. Specifically, the thesis will investigate the role motor dominance, bi-hemispheric motor activity and adaptive neural mechanisms in unimanual motor control. This was done in order to understand how these factors could have an impact on upper limb recovery. Gaining more insights into the mechanisms underlying unimanual motor control could provide novel insights on neural mechanisms that could be important for stroke patients to help them to regain a normal motor pattern.

In **Chapter 2** research on these aspects of motor control will be reviewed and gaps in the literature as well as open questions will be highlighted to show how the present thesis tried to expand findings from the literature.

Chapter 3 will provide an overview of the neuroimaging tools and experimental tasks used to investigate unimanual motor control.

In **Chapter 4** hemispheric asymmetries related to motor dominance will be explored, in order to identify the neural substrates underlying differences of motor dominance related to handedness. This was of particular interest since it is still unclear how and why motor dominance impacts upper limb recovery in stroke (for review see Sainburg and Duff, 2006). Specifically, upper limb recovery and lateralised cortical activity depend on whether the dominant or the dominant hemisphere is affected in stroke (Harris and Eng, 2006; Lüdemann-Podubecká et al. , 2015, Liew et al., 2018).

In **Chapter 5-7** robot-mediated reaching tasks were employed, particularly because they represent a highly standardised tool to evaluate reaching movements providing both measurement reliability and movement controllability (for review see Huang and Krakauer, 2009). The robotic device and its mechanism of action will be detailed in **Chapter 3.** Since, this robotic device is increasingly used in clinical settings to assess upper limb function in stroke and has the potential to be used in neurorehabilitation (for review see Basteris et al., 2014, Bastian, 2008, Shishov et al. 2017), **Chapter 5-7** employed a highly standardised robot-mediated reaching task in healthy individuals with the aim to extract normal neuronal and patterns of activations and link them to behavioural performances. This could be used as baseline measurements in healthy individuals and thus relevant for studying the mechanisms of brain plasticity and recovery in stroke patients. Parallel to the applicability in neurorehabilitation, robot-mediated reaching tasks can also be used to study motor adaptation in healthy individuals and give further insights into the neural mechanisms of error-based learning that are thought to be a key mechanism allowing flexible movements in changing environments.

Specifically, **Chapter 5** aimed to explore the hemispheric contribution of the ipsilateral and contralateral motor cortex during unimanual robot-mediated reaching preparation to gain a deeper understanding on the normal balance of activity between both motor cortices. Investigating bi-hemispheric activity during movement preparation was deemed important, since in stroke plasticity leading to interhemispheric imbalances can have an impact on unimanual movement control and recovery (for review: Dodd et al., 2017).

Chapter 6 aimed to identify the neural correlates and neuroplastic changes involved in motor adaptation using a robot-mediated reaching task. This was done to gain a deeper understanding of the neural substrates driving motor learning. Specifically, it has been shown that even in healthy individuals motor learning capacities vary largely across participants (Faiman et al., 2018, Ozdenizci et al., 2017). Identifying the neurophysiological mechanism driving this response variability, could help to harness these differences to best utilise the brain's capacity to learn.

Chapter 7 aimed to further exploit the neural mechanisms of the robot-mediated adaptation task used in **Chapter 6**. Specifically, this chapter focussed on extracting normal patterns of cortical activity on a regional and network level during unimanual reaching. This could provide novel insights on how to extract these normal patterns of activity and be exploited by brain computer interfaces (for review see Daly and Wolpraw, 2008).

Chapter 8 summarises and discusses the main results and achievements of the thesis and introduces potential directions for future investigations.

1.1.3. Tools to study the human brain

Neuroimaging and brain stimulation techniques allow the investigation of the human brain and can thus help us to gain insights into the neural mechanism underlying motor control. This thesis will focus on two techniques, namely electroencephalography (EEG) and transcranial magnetic stimulation (TMS) to investigate the neural correlates of motor control.

EEG provides a measure of cortical activations and interactions between brain regions with millisecond precision, and TMS-EEG co-registration can examine motor system excitability and plasticity. Applying TMS to the motor cortex and recording motor evoked potentials (MEPs) with electromyography (EMG) in the targeted muscle as well as cortical evoked potentials with EEG can quantify not only corticospinal but also direct cortical excitability. In **Chapter 3** these neuroimaging tools and their mechanism will be reviewed in detail.

Crucially, by combining TMS-EEG this work aimed to identify cortical biomarkers of movement control, which can be measured independently from the integrity of the corticospinal tract (CST). This is especially relevant when translating the results into clinical populations, such as stroke patients who commonly present with damages in the CST, limiting the use of TMS-EMG outcome measures because typically no MEPs can be evoked in the targeted muscle as this relies on an intact corticospinal system (for review see Sato et al., 2015).

1.2.   Research questions and aim of the research project

The specific research questions of the thesis are:

- Can the characteristic TMS-evoked cortical EEG responses reported in the TMS-EEG literature be reliably reproduced in all participants?

- What is the neural substrate of motor dominance? Is motor dominance reflected in interhemispheric cortical excitability asymmetries?

- Are both hemispheres engaged in unimanual reaching movements? Is the excitability of the ipsilateral M1 similarly modulated to the contralateral M1 during movement preparation?

- What is the neural correlate of motor adaptation? What is the neural substrate of the formation of a predictive internal model?

- What neuroplastic changes does motor adaptation underlie?

- What neural mechanism drives the inter-subject variability in motor learning?

- Is regional and interregional activity enhanced during perturbed compared to unperturbed reaching? What dynamical fluctuations in regional and network activity does robot-mediated reaching underly?

Chapter 2 - Literature Review

2.1. Human motor system

2.1.1. The human brain

The cortex, the largest part of the human brain, plays a central role in higher brain functions including, thought and action. The cerebral cortex consists of a convoluted sheet of neural cells on the outer surface of the brain under the skull and the cerebrospinal fluid (CSF). Deep, distinct fissures divide the cerebral cortex into four lobes, namely: the frontal, parietal, occipital and temporal lobe. These lobes are separated by different sulci: the frontal from the parietal lobe by the central sulcus and the temporal lobe from the frontal and temporal lobes by the lateral sulcus (also called the Sylvian fissure). A deep fissure splits the cerebral cortex into two halves, the left and right hemispheres, which are connected by a thick bundle of axons, known as the corpus callosum (CC). Functionally the cerebral cortex is divided into three groups: the sensory, motor and association cortices.

The cerebral cortex is also organised into different cell layers, with the number and functional organisation varying throughout the cortex (Heimer, 1995). However, the most common form of neocortex is divided into six layers, numbered from the outer pial surface of the cortex to the white matter and containing a mixture of cell bodies and local fibres (Figure 2-1).
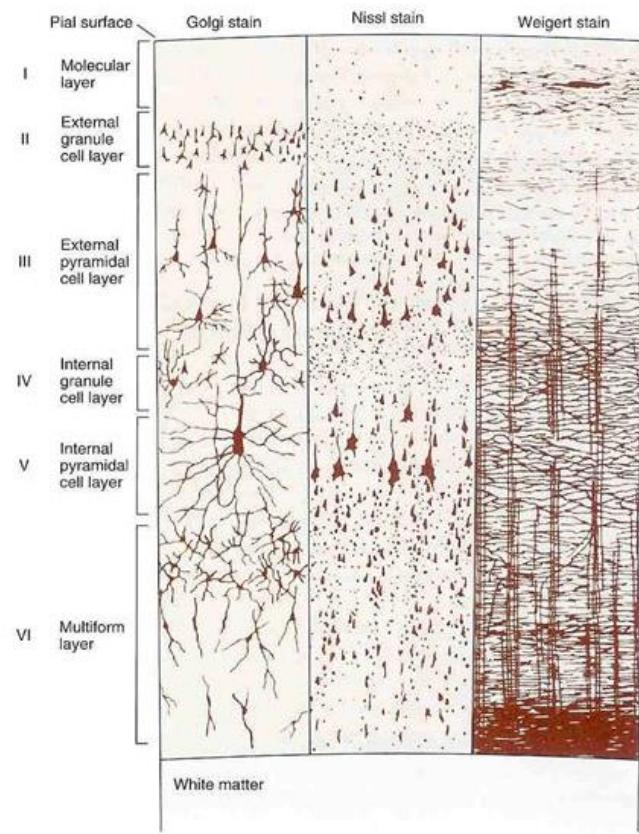
Figure 2-1: The six layers of the cerebral cortex. Figure taken from Heimer (1995).

The cerebral cortex contains over 21-26 billion neurons (Herculano-Houzel, 2009; Pelvig et al., 2008) divided into two major neuronal cell type are interneurons and projection neurons (pyramidal cells). While interneurons project only locally using the inhibitory neurotransmitter Gamma-amino-butyric acid (GABA) and are located in all layers, pyramidal cells project more globally into remote cortical structures using primarily the excitatory amino acid glutamate and are mainly located in layers III, V and VI (Zilles et al., 2004). These neurons are hugely interconnected with a single pyramidal cell receiving around 60 000 synaptic inputs and being able to directly project to an estimated 5000 other neurons (Cragg, 1967).

Although the global anatomical and functional organisation of the cerebral layers vary, in general, the first four layers receive input projections from other cortical structures, the brainstem as well as subcortical structures whereas layer V-VI comprise the output projection layers. Layer V mainly contains large pyramidal cells and is prominent in the motor cortex. This layer contains giant pyramidal cells called Betz cells, which are exclusive in the motor cortex and give rise to a portion of the descending pyramidal tract (Meyer, 1987).

Neurons in the neocortex are not only organised in layers but also in columns across layers in sections perpendicular to the long axis of the pre-central gyrus running parallel to the long axis of the gyrus. Neurons within a column share common characteristics and build microcircuits, forming basic functional units (Mountcastle, 1997). In particular, the dendrites and cell body of pyramidal cells in layers III and V have a preferential orientation in the same direction, parallel to the main axis of the gyrus (Meyer, 1987).

2.1.2. Control of skeletal muscles

The primary motor cortex (M1) is one of the major brain areas involved in motor function and is associated with the generation of motor control and limb movements. The M1 is located in the frontal lobe in the pre-central gyrus and has a somatotopic map of different regions of the body, referred to as motor homunculus (Penfield and Boldrey, 1937) (Figure 2-2). This somatotopic map is arranged in an ordered manner along the central sulcus, representing the

toes at the top and the mouth at the bottom of the cerebral hemisphere, close to the lateral sulcus. The motor homunculus is split in half, with the motor representation for each body side on the contralateral side of the brain. The size of brain matter representing each body part depends on the amount of control that the M1 has over that particular body part. This gives rise to a disproportionate map of the body, with, for example, a large cortical space devoted to the hand and fingers, which require very complex and fine motor control (Figure 2-2). Furthermore, it has been demonstrated that rather than being homogenous, the primary sensory cortex (area 3b) and M1, (area 4), are subdivided into individual cortical fields, each representing a main body part (Villringer et al., 2017). Recent research underlines the importance of studying the anatomical connections between M1 (located in the pre-central gyrus) and the primary sensory gyrus (located in the post-central gyrus), to re-evaluate the homunculus within an extended network of cortico-cortical and cortico-subcortical connections enabling precise and complex movement control (Catani, 2017).

The corticospinal tract (CST) is the major neural tract in motor function and is mainly involved in the functional use of distal extremities, such as fine motor coordination (Baek et al., 2013; Chang et al., 2015; Kondo et al., 2015; Kwon et al., 2016; for review see Martin, 2005). The main cortical origin of the CST is the M1, but other cortical origins include the supplementary motor area (SMA) and premotor cortex (PM) (for review see Lemon and Griffiths, 2005; Martin, 2005; Yang et al., 2017) (Figure 2-3). The CST, consisting of approximately one million fibres, is the only direct pathway from the cortex to the spine and is considered as the most functionally important pathway for controlling distal limb muscles. Neurons located in layer V of the M1 directly project to motor neurons, or interneurons, in the ventral horn of the spinal cord via the CST. The axons of the CST descend through the subcortical white matter, the internal capsule, and the cerebral peduncle (Figure 2-2). The fibres descending fibres of the CST form the medullary pyramids on the ventral surface of the medulla, and the entire projection is referred to as the pyramidal tract. At the level of the lower medulla, 85 % of the fibres of the CST cross at the midline to the opposite side of the spinal cord before travelling down the

spinal cord and are referred to as the lateral CST (for review see Lemon, 2008) (Figure 2-2). The remaining fibres (~ 10-15 % of CST fibres) that do not cross the midline, travel down on the ipsilateral side and are called the anterior CST. The axons of the CST travel down their respective tract until they reach their appropriate spinal level where they will directly or indirectly (via interneurons) synapse with motor neurons in the anterior horn of the spinal cord. These motor neurons will end at the neuromuscular junction of the targeted muscle. Most corticospinal axons projected from M1 to the spinal motor neurons form monosynaptic connections, establishing direct cortico-motoneuronal (CM) synapses, important for individuated finger movements. The axons of the CST also project to interneurons in the spinal cord and form indirect connections, which play a key role for the coordination of larger muscle groups in behaviours including walking and reaching.

Even though the CST is the dominant, direct and fastest descending motor pathway (for review see Lemon, 2008), multiple indirect pathways including cortico-bulbospinal pathways and CST tracts from the SMA and the PM) run in parallel (Figure 2-3). In the healthy population, the contributions from indirect pathways are relatively small compared to the CST tract. However, when the CST is damaged, e.g. after a stroke (Schwerin et al., 2008, 2011), indirect pathways may become more dominant.

KEY

→ Axon of upper-motor neuron

⇨ Lower-motor neuron

Motor homunculus on primary motor cortex of left cerebral hemisphere

To skeletal muscles

Corticobulbar tract

Motor nuclei of cranial nerves

Cerebral peduncle

MESENCEPHALON

To skeletal muscles

Motor nuclei of cranial nerves

MEDULLA OBLONGATA

Decussation of pyramids

Pyramids

Lateral corticospinal tract

Anterior corticospinal tract

To skeletal muscles

SPINAL CORD

Figure 2-2: The primary motor cortex and its descending projections. Figure adapted from the book Human anatomy © Pearson 2012 (Martini et al., 2012). The cerebral cortex with the primary motor cortex marked in green (on the right) and the descending pyramidal tract (on the left).

2.1.3. Evolutionary importance of direct cortico-motoneuronal (CM) system

The CM system has developed differently across species (for review see Lemon, 2008; Lemon and Griffiths, 2005) and is a unique trait of primates (Kuypers, 1981). Converging research has shown that the CM system has developed to a variable extent in different primates (for review see Isa, 2017) and that less dexterous animals, including cats (Illert and Tanaka, 1978), rodents (Alstermark et al., 2004) and even some primates like marmosets (Kondo et al., 2015) have no direct connection between CST axons and spinal motoneurons. The evolution of the CST and specifically the formation of the CM system parallels the development of dexterous hand movements, both phylogenetically (Bernhard and Bohm, 1954; Heffner and Masterton, 1983) and ontogenetically (Armand et al., 1997; Olivier et al., 1997). Studies in macaque monkeys provide evidence that the continuous post-natal expansion of CM projections to hand motor neurons parallels the development of dexterous hand movements (Armand et al., 1997) and that fine finger movements are not seen before the robust establishment of functional CM connections.

2.1.4. Contralateral and ipsilateral CST

The predominant role of the contralateral over the ipsilateral CST projecting from M1 in controlling upper limb movements has been established and explains why patients with unilateral motor cortical lesions, such as after a stroke present with contralateral motor deficits (Gerloff et al., 2006). However, it has been suggested that the ipsilateral M1 is also actively engaged during unilateral movements, since some patients with unilateral motor stroke present with deficits in control of the ipsilateral arm in addition to the more severely affected contralateral arm (Noskin et al., 2008). The extent to which the ipsilateral M1 contributes to unilateral upper limb movement is still poorly understood but the ipsilateral CST has been suggested to form a parallel control system to the contralateral CST, which becomes more important following unilateral motor lesions (for review see Alawieh et al., 2017).

At the anatomical level up to 10 -15 % of CST fibres descend ipsilaterally to the spinal cord enabling M1 to access ipsilateral muscles. However, the extent

to which ipsilateral projections are related to axial and proximal muscles relative to distal forearm and hand muscles is not clear and the functional role of these connections in relation to voluntary movements is still poorly understood. Ipsilateral corticospinal projections to upper limb muscles have been evidenced with TMS in proximal (Wassermann et al., 1992) as well as distal (Ziemann et al., 1999) muscles in healthy adults. It has been shown that these ipsilateral corticospinal connections become scarcer after the age of 10, most probably due to an increased transcallosal inhibitory influence during development (Muller et al., 1997). Following stroke these ipsilateral connections can become unmasked due to a cortical reorganisation in motor output of the unaffected M1 (Netz et al., 1997).

Recovery of motor function following stroke heavily depends on the extent of the lesion in the ipsilesional CST and activity of M1 (Gerloff et al., 2006). In their review, Alawieh et al. (2017) report that studies have collectively shown that activity of ipsilesional M1 and its contralateral CST projections mainly determine motor recovery following stroke, but that the contribution of the ipsilateral CST remains debatable. In a multimodal imaging study, Gerloff et al. (2006) showed that effective motor recovery relies on both ipsilesional and contralesional resources. Their findings provide evidence that the contralesional activity does not facilitate recovery through ipsilateral CST projections but rather promotes recovery of motor function at a higher-order processing level, such as movement selection and preparation.

2.1.5. Sensorimotor system

Voluntary movement control is initiated in the brain but also relies on somatosensory feedback (for review see Baker, 2007). A handful of studies show that the oscillatory cortico-muscular interactions originate not only from descending motor commands but are also affected by ascending somatosensory feedback (Baker and Baker, 2003; Campfens et al., 2013, 2014; Witham et al., 2010). Thus, the sensorimotor system can be viewed as a closed-loop system, consisting of descending motor pathways and ascending somatosensory feedback (Figure 2-3).

Functional connections between cortical regions and muscles can be indexed with cortico-muscular coherence - a measure that quantifies coherence between EEG from the scalp and EMG from the muscle (for review see Yang et al., 2017). Specifically, cortico-muscular coherence measures the synchrony between oscillations from the cortex and the muscles (for review see Liu et al., 2019). The communication between the cortex and the periphery is bidirectional; therefore EEG and EMG signals are both influenced by the descending output and ascending somatosensory feedback (for review see Yang et al., 2017). Since voluntary motor action is typically reflected in modulations of oscillatory power in the beta frequency band (13 – 30 Hz) in the motor cortex (Pfurtscheller and Andrew, 1999), a large number of research has focused on studying cortico-muscular coherence in this specific frequency band (for review see Yang et al., 2017). It has been shown that the strength of beta-band cortico-motor coherence depends on the type of motor task: whereas cortico-motor coherence is increased in isometric contraction, it is decreased/ suppressed in dynamic motor tasks (Kilner et al., 2000). It is assumed that cortico-muscular coherence partly reflects the information propagation from the motor cortex to the periphery via descending pathways (Baker et al., 2003). However, since subcortical regions such as basal ganglia cerebellum and brainstem can also affect the cortico-muscular interactions via the cortico-subcortical loops and subcortical-spinal tracts (Airaksinen et al., 2015; Akkal et al., 2007; Park et al., 2009), cortico-muscular coherence is also influenced by these subcortical regions.

Even though cortico-muscular coherence is a useful measure to quantify cortico-peripheral interactions, a major limitation of it is that it does not specify the directionality (for review see Yang et al., 2017). However, by experimentally manipulating descending or ascending pathways, the individual contributions of each pathway on cortico-muscular coherence can be revealed. For example, Baker et al. (2003), showed that enhancing beta-band oscillations in the motor cortex through the administration of benzodiazepine diazepam, did not result in an increased cortico-muscular coherence, suggesting that this measure does not solely depend on motor cortex signal propagation. The contribution of somatosensory pathways has

been evidenced by manipulating afferent pathways, revealing that cooling the arm to prevent somatosensory feedback affected cortico-muscular coherence (Riddle and Baker, 2005).
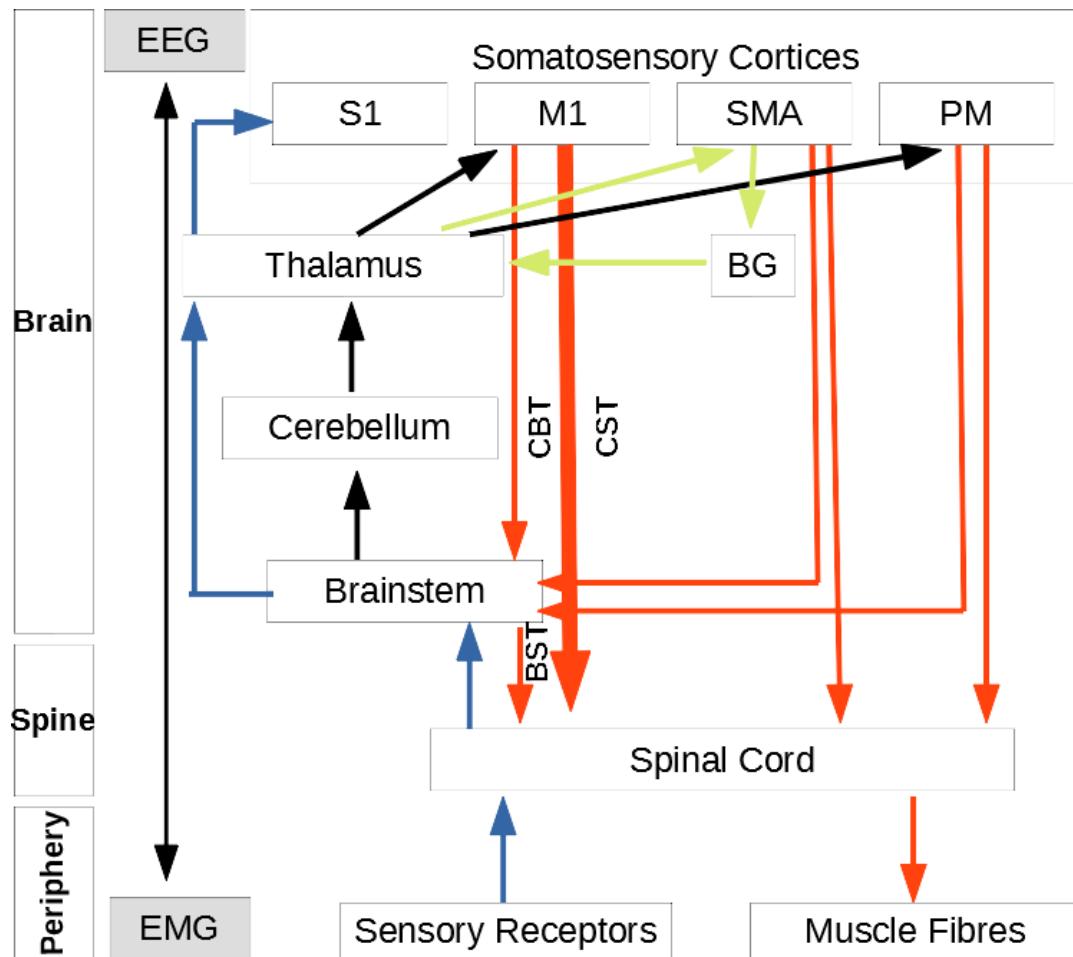
Figure 2-3: General overview of the sensorimotor system. Figure adapted from Yang et al. (2017). The sensorimotor system forms a closed-loop, consisting of descending motor output, illustrated with red lines and ascending somatosensory feedback pathways, illustrated with blue lines. The CST is highlighted with a red thick line. The cortico-basal ganglia loop is illustrated with green lines. Abbreviations: BG: basal ganglia; BST: bulbo-spinal tract; CBT: cortico-bulbar tract; M1: primary motor cortex; PM: premotor cortex; S1: primary sensory area; SMA: supplementary motor area.

2.1.6. Brain lateralisation and specialisation

2.1.6.1. The evolutionary advantage of brain lateralisation and asymmetry

Asymmetric functional specialisation (i.e. distinctive roles) of the two hemispheres of the brain is a basic organisational feature of the vertebrate nervous system which arose 500 million years ago evolution even before the emergence of vertebrates (for review see MacNeilage et al., 2009). It has been hypothesised that separating neural circuits across the hemispheres increases efficient behaviour by reducing interference between potentially competing processes (for review see Corballis, 2017; Lemon, 2008).

Rogers et al. (2004) propose that the main advantage of brain lateralisation lies in increasing neural processing capacity, specifically the ability to perform multiple tasks simultaneously. In other words, engaging only one hemisphere in a task leaves the other hemisphere to engage in other functions. Their findings suggest that the left hemisphere specialises in well-established patterns of behaviour under familiar conditions, whereas the right hemisphere is specialised in responding to unforeseen environmental events (for review see MacNeilage et al., 2009).

Sainburg et al. (2014) expanded these findings to motor control and proposed a dynamic dominance model of motor lateralisation, which is based on fundamental principles of optimal movement control theories. Two important mechanisms are involved in accurate and efficient movement control: predictive mechanisms that specify efficient and accurate movements to minimise costs and, impedance control mechanisms that assure stability and accuracy of steady-state postures, relevant for postural stability under unpredictable conditions (for review see Scott, 2012). The dynamic model of motor lateralisation as reviewed by Sainburg et al. (2014) states that these two control mechanisms are specialised in different hemispheres: The left hemisphere (in right-handers) controls mainly predictive mechanisms, whereas the right hemisphere is proficient in impedance control mechanisms.

Growing evidence suggests that the pressure of lateralisation and asymmetries of the two hemispheres is driven by the evolution of new and more specialised circuits and are the result of a trade-off for space (as the

17

brain cannot expand infinitely) and of maximising neural capacity (Corballis, 2017). However, it should be noted that while brain lateralisation might be important for efficiency, it is also plastic and can dynamically change shifting from one hemisphere to the other (for review see Corballis, 2017). For example, lateralisation shifts have been reported in patients, with brain tumours in language areas in their dominant hemisphere (commonly the left side), who showed a functional shift to their non-dominant language area in the right hemisphere (Krieg et al., 2013).

2.1.6.2. Hemispheric asymmetries – handedness

Humans use their hands asymmetrically in daily activities with a lateralised preference towards one hand, referred to as handedness. The term handedness is commonly defined as the hand that performs faster or more precisely on manual tasks and/ or the hand that one prefers to use, regardless of performance. It is thought that the asymmetrical functions of the hands reflect an asymmetrical neural control. Handedness is a uniquely human trait (Annett, 2002; McManus, 2002) and is one of the characteristics that separate us from most other primates.

The proportion of right and left-handers in humans were described more than 5000 years ago (Coren and Porac, 1977). Nowadays, 90 % of humans are right-handed (Perelle and Ehrman, 2005). The advantages of being right-handed compared to left-handed have been explored and it has been suggested that left-handedness is associated with a decreased survival fitness (Coren and Halpern, 1991). In a recent study, it has been shown that heart asymmetry (i.e. thoracic anatomic asymmetry) might have played a role in the evolution of handedness, giving right-handed individuals a survival advantage (Larsson, 2017).

2.1.6.3. Manifestation of handedness

Both, cross-sectional (Fagard, 1998; Gesell and Ames, 1947; Michel et al., 1985; Morange and Bloch, 1996) as well as longitudinal (Coryell and Michel, 1978; Lynch et al., 2008; Michel, 2018; Michel et al., 1985; Provins, 1992; Ramsay, 1985) studies suggest that handedness becomes evident with the emergence of voluntary reaching (for review see Scharoun and Bryden, 2014).

A recent study (Parma et al., 2017) investigated lateralised reaching biases in foetuses by analysing kinematics of arm movements (such as reaching towards the eyes,) during ultrasonography. Strikingly, they have shown that by using the kinematic data (movement times or deceleration estimates), handedness could be inferred with a high accuracy ranging from 89-100% from gestational week 18.

The development of hand preference is driven by both genetic and environmental factors (for review see Cochet and Byrne, 2013). The origins of this cerebral specialisation are still debated and it is unclear whether there is a common substrate for language and handedness. In their review, Cochet and Byrne (2013) suggested that developmental processes link the development of handedness with the development of left-hemispheric specialisation for speech processing. Some research even suggests that language lateralisation evolved from manual gesture (for review see Corballis, 2002). For instance, Rizzolatti and Arbib (1998) proposed that the mirror-neuron system represents the neurophysiological system from which language evolved. This was derived from the fact that mirror neurons were activated when observing actions done by others in brain regions in monkeys that are thought to be homologous to language regions in humans including Broca's area.

Cerebral specialisation and hemispheric asymmetries have extensively been studied with EEG, establishing correlations in EEG asymmetry patterns, as markers of functional asymmetries and behavioural traits (for review see Kline, 2004). Frontal EEG alpha asymmetry is commonly used in studies investigating the lateralisation of emotional processing (for review see Allen et al., 2018), and can also be applied to a wider range of research, such as the study of handedness (Ocklenburg et al., 2018).

A greater dominance of the left hemisphere over the right hemisphere according to motor and language function is commonly seen in resting state activity during wakefulness. Two studies examining the relationship between EEG asymmetry and the degree or consistency of hand preference in right-handers found a negative correlation between frontal asymmetries and the

degree of handedness (Papousek and Schulte, 1999, Propper et al., 2012). Both reported a greater relative right hemisphere activity (i.e. greater left hemisphere alpha power). Ocklenburg et al. (2018) expanded these findings to a wider range of brain regions and frequency bands (delta, theta alpha and beta) showing that EEG asymmetries beyond frontal alpha power are modulated by handedness: stronger right-handedness predicted greater left (compared to right activity).

Together these findings suggest that EEG asymmetries represent markers of asymmetric brain function, possibly reflecting hemispheric specialisation. Interestingly, it has been shown that this hemispheric asymmetry is reversed during sleep showing a right hemispheric dominance in right-handers (Park and Shin, 2017). The authors suggest that the reversal of left hemispheric dominance can be due to the fact that the dominant hemisphere is more active during the day and as a result needs more "rest" compared to the non-dominant hemisphere and uses sleep to restore its function.

2.2.   Motor dominance and hemispheric asymmetries

A wide range of research has focussed on investigating anatomical and functional asymmetries related to handedness within the M1 and its corticospinal projections due to their key role in upper limb movements as reviewed by Hammond et al. (2002). Specifically, anatomical differences include a larger hand motor cortex in the dominant compared to the non-dominant hemisphere (Volkmann et al., 1998), a deeper central sulcus in the dominant compared to the non-dominant hemisphere and more horizontal connections in the dominant M1 reflecting a wider distribution of basic movement representations (Amunts et al., 1996).

Several motor cortical output map studies have been employed to characterise anatomical and functional asymmetries by studying cortical excitability differences between the dominant and non-dominant M1 but reported contradictory results. While some studies found no significant interhemispheric differences (Bashir et al., 2014, Cicinelli et al., 1997, Civardi et al., 2000, Rossini and Rossi, 1998), others found significant differences between the

dominant and non-dominant hemisphere (Koski et al. 2005, Macdonell et al., 1991, Triggs et al., 1994).

In the same vein, corticospinal excitability differences within the CST are contradictory, with findings of no interhemispheric differences (Kazumoto et al., 2017; Saisanen et al., 2008) as well as reports of higher levels of corticospinal excitability in the dominant (De Gennaro et al., 2004) or in the non-dominant (Daligadu et al., 2013) hemisphere.

So far, no clear link between CST asymmetries and handedness has been established. Similarly no link between anatomical CST asymmetries were detected, with studies reporting leftward volume asymmetries in corticospinal fibres in both right- and left-handers (Rademacher et al., 2001; Thiebaut de Schotten et al., 2011, Westerhausen et al., 2007). More recently it has been shown that frontoparietal tracts, as opposed to the CST, correlate with handedness and manual specialisation from diffusion tractography (Howells et al., 2018). Together these findings suggest that handedness seems to be related to motor cortical asymmetries which are not reflected in the CST but most probably at a more cortical level.

Therefore, directly measuring cortical as opposed to corticospinal excitability differences by using simultaneous TMS-EEG could enable to identify neural differences related to motor dominance. To gain further insights into hemispheric asymmetries related to motor dominance, **Study I** (**Chapter 4**) of this thesis employed simultaneous TMS-EEG allowing to capture both cortical and corticospinal activity. Specifically, the study investigated if cortical excitability as measured with TMS-evoked cortical responses (measured with EEG) as well as peripheral responses (measured with EMG) would reveal hemispheric asymmetries in excitability related to motor dominance.

2.3. Upper limb reaching

Most research on the development of handedness and asymmetric movement control comes from reaching studies as reviewed by Scharoun and Bryden (2014). In fact, handedness investigated through the observation of hand selection in reaching have yielded deep insights into the development of hand preference and unimanual skill. This is not surprising considering that a

handful of daily life activities such as drinking, pointing and eating require reaching movements. The control over these movements relies on the cohesive framework of three systems of the motor system, namely motor behaviour, limb mechanics and neural control. These different levels of control need to build a cohesive network to accurately control movement (for review see Scott, 2004). The ability to reach is very often impaired after a stroke and dramatically reduces the quality of life of survivors. Understanding the basic physiological and neurological mechanisms controlling reaching is therefore key to develop better upper limb neurorehabilitation therapies.

2.3.1. Reaching definition

Different forms of reaching are required in everyday activities and can be studied in laboratory settings, including reach-to-target, reach-to-release, reach-to-manipulate and reach-to-pull movements. All these forms of reaching require the ability to use visuospatial cues and transform them into motor signals (visuomotor transformations). In research settings, reach-to-target has been investigated in several experiments and has been mostly studied in the horizontal plane. It has been shown that forward reaching leads to the emergence of interaction torque between segments, namely action of the forearm on the upper-arm and also within segments, among the three main degrees of freedom of the shoulder joint for the upper arm in 3D. To accurately control this complex interaction of muscles and joints, the CNS relies on an effective computational and neural system (for review see Scott, 2012; Shadmehr and Krakauer, 2008). Specifically, a series of sensorimotor transformations have to take place between distinct representations or coordinate frames (Figure 2-4). A crucial computation that is needed is the conversion from a kinematic (i.e. spatial location of the target, hand position, trajectory, angular motion) to a kinetic (i.e. joint torques, muscular activity) representation (Scott, 2000).

Simple reach-to-target movements can be described in terms of kinematics, including the planned trajectory, velocity and magnitude: The path refers to the hand position sequence in the surrounding space (2D or 3D). The trajectory defines the time sequence of the different hand positions in space (2D or 3D).

In general, unconstrained movement is characterised by a curvilinear shaped trajectory (Hollerbach and Flash, 1982). The velocity refers to the speed in time of the hand in a particular direction and is usually bell-shaped and single peaked during reach. With practice, the shape can become asymmetric, with an ascending steeper than descending trace. The accuracy depends on target, velocity and visual guidance. In general, slow movements are more accurate and errors detected halfway of the movement and eventually corrected by additional movements. The visual guidance is needed to locate the target in space, monitor the hand/ arm movement and adjust the hand/arm to reach. Experiments in which reaching was performed in the dark or with prevented vision demonstrated the importance of visual guidance not only to locate the target in space, to monitor the arm but also to perform online adjustments to reach the target (Reichenbach et al., 2009).

Reaching movements, such as reach-to-target movements, require the activation of several muscles at different times and intensities depending on their role during movement execution (Georgopoulos et al., 1986). For example, it has been shown that the Anterior Deltoid muscle is activated first, to protract the shoulder, followed by the recruitment of the Triceps and Biceps Brachii to guide the extension of the elbow to the end position. The co-contraction of several muscles is another mechanism that is important to perform accurate movements for different types of reaching and it has been shown that their level of activation depends on the type (Pizzamiglio et al., 2017b) and difficulty (Thoroughman and Shadmehr, 1999) of reaching.

Figure 2-4: A goal-directed motor action: reach-to-target. A series of sensorimotor transformations have to take place between distinct representations of coordinate frames. A crucial computation that is needed is the conversion from a kinematic (i.e. spatial location of the target, hand position, trajectory, angular motion) to a kinetic (i.e. joint torques, muscular activity) representation (Scott, 2000).

2.3.2. Neural correlates of reaching preparation and execution

Reaching movements can be decomposed into two main stages (Takiyama and Sakai, 2016); a motor planning and motor execution phase. The former process is necessary to prepare the appropriate motor commands (such as direction and muscle selection) to achieve that goal. The latter process refers to the execution level that causes muscle activity via the activation of motor cortical neurons that project to the spinal cord where they synapse on motor neurons, which then activate muscles and enable movement. In general, the motor planning phase is defined as the phase before the onset of reaching movement, whereas movement execution is defined as the phase around the onset of movement. Both of these phases are crucial for accurate movement control. Recently, it has been suggested that the complete specification of the motor command is already accomplished in the planning phase occurring before movement onset (for review see Wong et al., 2014).

The motor cortex has an established role in movement preparation and execution (for review see Georgopoulos and Carpenter, 2015). Neurons in many cortical and subcortical regions change their firing rate progressively during movement preparation and execution (Kilavik et al., 2014). Reaching programming can be decomposed in high-level (abstract) processing and low-level processing (motor commands) stages. While parietal regions are crucial for the programming of reaching at the highest level of abstractness, before the real motor command is specified in terms of muscle activations, torques and joint angles; the primary motor cortex is the key region involved in the lowest level of abstractness, sending out the final motor commands (Scott, 2000).

In humans, non-invasive brain imaging techniques such as EEG have been employed to delineate the neural correlates of reaching movements. It has been shown that several brain regions work together to enable voluntary externally cues reaching movements (Dipietro et al., 2014; Naranjo et al., 2007), such as the premotor, prefrontal, paracentral and parietal areas which are activated during reaching preparation and execution.

Initially, time-locked spontaneous changes in the activity of neuronal populations induced by specific sensory events, referred to as event-related potentials (ERPs) were employed to investigate the timing of activation of different brain regions. By recording ERPs evoked by a visual cue to start reaching movements with the right hand, it has been shown that several brain regions are activated both sequentially and in parallel in time. Specifically, it has been demonstrated that the premotor, prefrontal, paracentral and parietal areas are activated between 140 and 170 ms after visual cue. Shortly after, the occipital cortex is activated around 210 ms, joined by the bilateral superior parietal lobules until 300 ms, after which ERPs decreased until movement onset (Naranjo et al., 2007).

Later studies have also focused on studying event-related power modulations related to movement preparation and execution. These studies revealed that visually-triggered voluntary reaching movements are characterised by increases and decreases of oscillatory power in specific frequency bands. It has been reported that low and high frequencies (<8Hz and > 35Hz) show an increase of oscillatory power, whereas a decrease of oscillatory power is observed at frequencies between 10 Hz and 30 Hz with respect to a rest condition (Storti et al., 2016; Waldert et al., 2008). The increase and decrease of oscillatory activity follow a particular spatiotemporal evaluation during movement preparation and execution. Specifically, high-frequency oscillatory activity (> 30 Hz) increases, showing an event-related synchronisation (ERS) around movement onset and offset over the contralateral M1 (Ball et al., 2008) and frontal areas (Babiloni et al., 2016). These oscillations have been linked to the fast information processing during movement execution.

In contrast to this increased activity, oscillatory power of middle frequencies (alpha and beta frequency band) usually decreases, showing an event-related desynchronisation (ERD) during voluntary movement which thought to reflect ongoing sensorimotor integration processes (for review see Engel and Fries, 2010; Pfurtscheller and Andrew, 1999). After movement execution, beta-band oscillatory power usually increases and is commonly referred to as post-movement beta synchronisation or beta rebound. This phenomenon is thought

to reflect neural processes related to movement accuracy such as trial-by-trial error detection and to update neural mechanisms of motor control (Tan et al., 2016; Torrecillos et al., 2014).

2.3.3. The role of M1 during reaching preparation and execution

Using non-invasive imaging techniques in humans, such as EEG, magnetic resonance imaging (MRI) and TMS have been successfully used to assess the modulation in cortical excitability of the motor cortex during movement preparation and execution. Specifically, it has been shown that the generation of a voluntary movement involves an interaction between intracortical facilitatory and inhibitory processes within the M1 which are essential for motor control. These cortical excitability changes are already occurring at early stages of movement preparation even before movement onset (Chen, 2004; Kennefick et al., 2014; Reynolds and Ashby, 1999; Zaaroor et al., 2003). The time course of corticospinal excitability during movement preparation and execution has previously been studied with TMS and revealed that corticospinal excitability is increased above resting around 100 ms before and after the response, except for a short period between 75 and 150 ms before movement onset, suggesting an interaction between facilitatory and inhibitory mechanisms in the motor cortex during movement preparation (Zaaroor et al., 2003).

Motor related activations during movement preparation and execution have previously been studied in humans using different imaging techniques such as TMS (Kennefick et al., 2014, Zaaroor et al., 2003) or EEG (Naranjo et al., 2007). Recently, the combination of both techniques (i.e. TMS-EEG) has been used to study modulations of motor cortex excitability during movement preparation. Specifically, Nikulin et al. (2003), revealed that cortical TMS-evoked inhibitory potentials measured with EEG over the contralateral M1 to the task limb were attenuated in M1 and the MEP in the targeted muscle were larger in the preparation period compared to a resting condition in a simple reaction time task involving unimanual thumb abductions. Kičić et al. (2008) expanded these findings by applying TMS over both motor cortices and reported that unilateral reaching preparation requiring thumb abductions is

associated with bilateral changes in cortical excitability and only in the contralateral hemisphere these modulations were associated with changes in MEPs.

The enhanced corticomotor excitability during movement preparation found in these studies was not reported in more complex movements such as robot-mediated reaching in an unperturbed environment (Hunter et al., 2011). Specifically, Hunter et al. (2011) applied TMS to the contralateral M1 during unimanual reaching preparation and reported no significant changes in corticomotor excitability as measured with MEPs in an unperturbed environment. To expand Hunter et al.'s (2011) findings and assess if cortical excitability changes could be detected at the cortical level, as measured with TEPs as opposed to the corticospinal level as measured with MEPs, **Study II** (**Chapter 5**) used simultaneous TMS-EEG recordings during robot-mediated reaching movement preparation. Moreover, to assess the involvement of both motor cortices during unimanual unperturbed reaching, TMS was not only applied to the contralateral but also ipsilateral M1 to the reaching arm.

2.4. Models of motor control

2.4.1. Internal models

When humans perform movements, they have to take into account the outer world and combine them with their internal models (motor programs; memory). As such, the motor system is controlled by the constant interaction of the body part being controlled and the controller (internal model) (Figure 2-5). The concept of internal models in a key theoretical mechanism in motor control (Kawato and Wolpert, 1998). Internal models comprise feedforward and inverse models: A forward model refers to the ability to produce a predicted sensation based on the state and the action. In other words, a forward model predicts the consequences of a given action in the context of a given state. Internal models represent/ mimic the normal behaviour of the motor system in response to an outgoing motor command and can predict their sensory feedback. For instance, when a motor command is issued by a controller, an estimated output of the new state is generated. In addition, internal models also model the external physical environment and predict the behaviour of the

external world. On the other hand, inverse models are used to produce an action as a function of the current state and the desired sensation. Here the controller inverts the transformation from actions to sensations (Wolpert and Miall, 1996).

2.4.2. Forward models: Motor efference copy

Goal-directed behaviour relies heavily on feedback and feedforward sensory systems that input into the controller (for review see Scott, 2004; Scott et al., 2015). Visual and proprioceptive feedback are both important for optimal movement control (van Beers et al., 1999). These feedback signals arrive with a delay to the controller and hence can only influence the accuracy of the generated movements with time delays of approximately 190-260 ms for visual feedback (Miall et al., 1985, 1986) and longer than 100 ms for proprioceptive feedback (Dietz, 2002). The relative contribution of each feedback is currently debated, but pointing towards the dominance of vision over proprioception (Pistohl et al., 2013; Touzalin-Chretien et al., 2009). In the context of neurorehabilitation, the importance of proprioceptive feedback has been highlighted for both restoring functional recovery of the impaired limb and for controlling a prosthetic limb (Blank et al., 2008; Kuchenbecker et al., 2007). In their systematic review, Aman at al. (2015) show that proprioceptive training is an effective method to improve sensorimotor control. Neuroprosthetic designs increasingly seek to incorporate proprioceptive feedback in upper-and lower limb prosthetic devices, since it has been shown that artificial proprioceptive feedback can improve movement accuracy of these non-self-entities (Blank et al., 2008; Pistohl et al., 2013).

In contrast to feedback control, which is inherently associated with time delays, feedforward mechanisms make predictions of the actual sensory feedback to modulate internal models. Internal models integrate both signals and feedforward control is adjusted to the actual sensory feedback (for review see Scott et al., 2015).

Forward models are used by the CNS to internally simulate the behaviour of the motor system in planning, control and learning (Wolpert and Miall, 1996). When a motor signal from the CNS is sent to the periphery (i.e. motor

efference), a copy of this motor outflow (i.e. efference copy) is generated. This efference copy inputs to the internal model which can estimate the sensory consequences of the motor command, thus generating the predicted sensory feedback. This forward mechanism is used to anticipate and cancel the sensory effects of movement. Sensory signals in the periphery result from environmental influences on the body (i.e. afference) or by self-generated movements (i.e. reafference) (Wolpert and Miall, 1996). In general, the sensory consequences of self-generated movements can be accurately predicted and thus attenuate the sensory effects of the movement. It has been suggested that the efference copy mechanism and the ability to inhibit sensation as a result, is the underlying reason why we cannot tickle ourselves. (Blakemore et al., 2000).

2.4.3. Optimisation of motor control

When producing a voluntary movement, the motor system encounters two problems, namely sensory feedback is noisy and delayed and the relationship between the motor command and the movement it produces is variable, because of muscle fatigue or changes in the environment for example (Figure 2-5).

Two main theories have been proposed to explain how the motor system deals with these problems and how motor control is optimised (for review see Latash et al., 2010, Shadmehr, 2010): the equilibrium-point (i.e. Lambda) model (Feldman 1986) and the optimal feedback control model (OFC) (Todorov and Jordan, 2002).

2.4.3.1. Equilibrium-point (Lambda) model

Voluntary movements are elicited by a modification of muscle force and activity. The equilibrium-point theory is based on the stretch reflex, a monosynaptic reflex in response to stretching within a muscle which provides an automatic regulation of the muscle length. According to equilibrium point-model the control of a single muscle can be described with changes in the threshold of motor unit recruitment during slow muscle stretches (i.e. tonic stretch reflex threshold) (Feldman, 1986). In the presence of proprioceptive feedback, the brain sends signals to motoneurons which are transformed into

changes in the threshold muscle lengths or joint angles at which these motoneurons are recruited, setting the spatial activation range. It is thought that the CNS specifies where, in terms of spatial coordinates, muscles are activated without relying on exact details on when and how they are activated. The main idea behind the equilibrium-point theory is that the CNS does not control muscles independently of the muscle-stretch reflex system. In other words, it assumes that the brain can only modify muscle (i.e. EMG) patterns and thus limb movements indirectly through the control over parameters specifying the equilibrium state of the motor system. Thus, the model supposes that the CNS is inherently dependent on the state of the sensory system that measures muscle length. •

2.4.3.2. Optimal Feedback Control (OFC)

The notion of OFC has recently been introduced to explain the interaction between actual and predicted sensory feedback to update internal models (for review see Scott, 2004; Scott et al., 2015; Shadmehr and Krakauer, 2008). According to the OFC theory the internal model has to incorporate three aspects to control movements: i) predict the sensory consequences of the planned movement, ii) update the current state estimation by comparing the predicted against the actual sensory feedback, iii) update the state of the limb based on the cost and reward of the task (for review see Scott et al., 2015).

The optimal strategy for combining sensory inputs and the predictions of the internal model is thought to rely on a forward model (i.e. Kalman filter) (Todorov and Jordan, 2002). According to this model, delayed sensory feedback is overcome by using an optimal state estimation: a Kalman filter that integrates efference copy signals with delayed sensory feedback. The filter aims to minimise the variance in the estimated states and thereby optimises motor control. Properties of the musculoskeletal system are used to achieve a balance between behavioural performance and associated motor costs by providing an optimal control policy (i.e. feedback gains).

In OFC, the concept of feedback gain depends on the motor task and a cost function describing the rewarding states and nature motor costs. In contrast to the equilibrium point model, where the feedback controller is at the spinal level

31

and acts on proprioceptive feedback, the OFC model relies on a hierarchical feedback control involving all levels of the CNS (Figure 2-6).
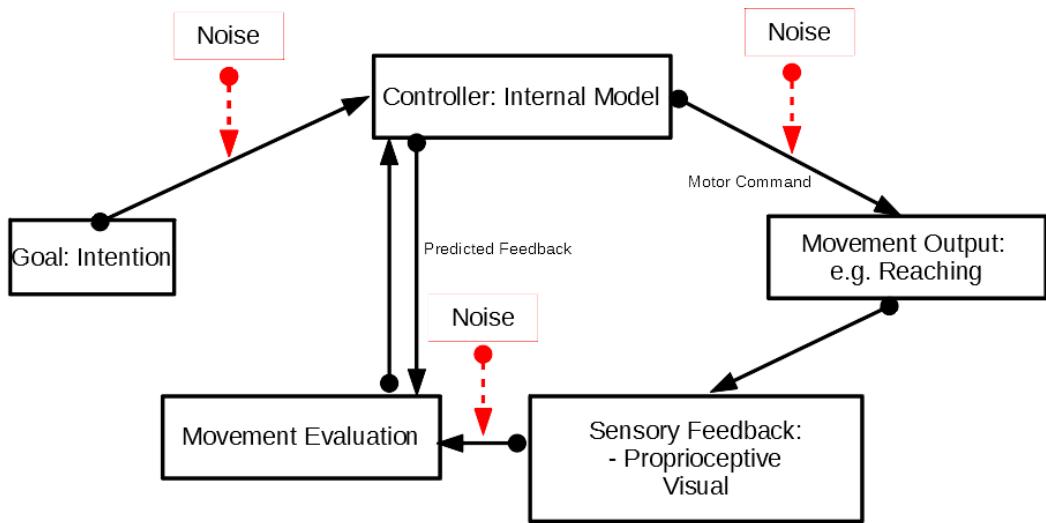
Figure 2-5: General motor control and motor learning computational model. The internal model theory states that the motor system is controlled by the constant interaction of the body part being controlled and the controller (internal model, i.e. the CNS). Internal models are controlled by feedback mechanisms and feedforward control. Specifically, the controller compares the predicted feedback against the sensory feedback to evaluate the movement. Noise that is present in the system and in the external environment produced by perturbations, leads to mismatches between the predicted and the actual sensory feedback. Information from the outer world and the internal models have to be combined to control accurate movements.

2.5. Neural correlates of motor control

A growing number of studies are concerned with investigating the neural bases of the computational models of motor control. Specifically, neuroimaging and lesion studies have been used to identify the anatomical and functional correlates of these internal models to build neuroanatomical and physiological models of motor control. Crucially, these models have to consider and integrate three systems: neural control, musculoskeletal mechanics and motor behaviour (for review see Scott, 2012; Shadmehr and Krakauer, 2008; Shadmehr and Wise, 2005).

In the last decades, several brain regions involved in motor control have been revealed including cortical regions, such as, M1, the premotor cortex, the parietal cortex, the supplementary motor area as well as subcortical regions, such as the basal ganglia and the cerebellum (for review see Shadmehr and Krakauer, 2008, Nowak et al., 2007) (Figure 2-6). The cerebellum is thought to play a key role in building internal models that predict sensory consequences of motor commands and correct motor commands through internal feedback (Smith and Shadmehr, 2005; Wolpert et al., 1998). The parietal cortex, on the other hand, is thought to integrate the predicted sensory consequence and compare it to both the actual proprioceptive and visual feedback (Day and Brown, 2001; Grea et al., 2002). It is thought that the parietal cortex uses the comparison of the predicted and actual feedback to update the estimated state of the system (such as arm location in space) and sends this information to M1 via the SMA to generate new motor commands (Desmurget et al., 1999; Grea et al., 2002; Wolpert et al., 1998). The M1 and premotor cortex then implement the control strategy into motor commands (for review see Shadmehr and Krakauer, 2008).

.
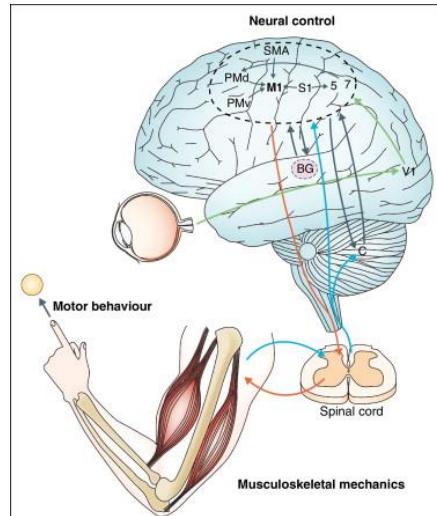
Figure 2-6: Anatomical and neurophysiological model of movement control.
Figure taken from Scott et. al. (Scott et al., 2015). The cortical regions involved in
movement control include the primary motor (M1) and somatosensory (S1) region,
the supplementary motor area (SMA), the area 5, (A5), the dorsolateral premotor
region (dPM).

2.6. Motor learning

2.6.1. Model-based and model-free learning

Motor control and motor learning are both important to perform accurate movements, such as reaching and pointing movements. Motor learning takes many aspects and includes: i) learning over the generations of reflexes and innate motor programs that become genetically encoded, ii) learning new tasks (i.e. skills) to improve the inherited motor repertoire and adapting to maintain a performance at a given level, iii) learning when and what movements to make (for review see Wise & Shadmehr, 2002).

An important distinction in motor learning is made between de novo learning (i.e. skill learning) and motor adaptation. Specifically, motor skill learning relies on the generation of a completely new movement (e.g. learning to play tennis), while motor adaptation relies on the modification of a known movement (e.g. adjusting the force with which you hit the tennis ball under windy conditions). In their review on motor learning Haith and Krakauer (2012) argue that these two forms of learning underly two different mechanisms namely a model-free (for skill learning) and model-based (for motor adaptation) mechanism. Model-free systems assume that learning is driven by the reinforcement of successful actions and directly guided by the controller, while the model-based systems rely on an internal forward model of the environment that is updated based on prediction errors. Since this thesis investigates motor adaptation, it will focus on the model-based rather than the model-free mechanism.

In research settings, motor learning is most commonly studied with motor adaptation paradigms, in which individuals have to learn to compensate for a systematic perturbation. In the case of arm movements two types of adaptation paradigms are used, namely a visuomotor adaptation and force-field adaptation task. While visuomotor adaptation (Krakauer et al., 2000) uses a perturbation that distorts the visual consequences of the motor command without altering the proprioceptive consequences, force-field adaptation (Shadmehr and Mussa-Ivaldi, 1994) alters both the visual and proprioceptive consequences of the motor command through the introduction of a physical

perturbation. Both of these types of adaptation depend on sensory prediction errors and most probably on the formation of a predictive internal model (for review see Shadmehr et al., 2010).

During these tasks, an initial rapid improvement and then slower improvement closer to initial baseline levels, resulting in an approximately exponential learning curve, is observed. This nearly exponential fit implies that the amount of improvement on each trial is proportional to the error (Thoroughman and Shadmehr 2000; Donchin et al. 2003). This fast trial-by-trial reduction in systematic errors is typically referred to as adaptation. Specifically, adaptation is a form of error-based learning (for review see Seidler et al., 2013), which uses information about the difference between an actual behaviour and the desired/intended behaviour (i.e. error), to update and modify the next behaviour to reduce errors (minimise the difference between actual and desired behaviour) (Diedrichsen et al., 2010; Rumelhart et al., 1986).

Force-field adaptation tasks (relevant for this thesis) involve making reaching movements in transient novel force environments. To make accurate reaching movements the motor system makes estimations of the forces that will act on the arm based on previous experiences. When no external perturbations are applied (e.g. no force-field) the estimations of the forces are usually correct and the actual movement resemble the intended movement. However, when perturbing forces are applied, movements are first deviated from the ideal intended trajectory, causing a discrepancy between the predicted and the observed force. To minimise this difference and cancel the perturbation during the next movement, the motor system produces a force that counteracts the predicted force of the perturbation. This process is referred to as motor adaptation. Behavioural performance during motor adaptation paradigms is characterised by a reduction in movement trajectory errors (Hunter et al., 2009; Ozdenizci et al., 2017; Pizzamiglio et al., 2017b) and by a reduction in muscle co-contraction (Pizzamiglio et al., 2017a, Thoroughman and Shadmehr, 1999).

It is assumed that the improvement in performance correlates with the improvement of internal models that estimate/ predict external forces. The

successful formation of internal models can be tested by studying after-effects. Specifically, by removing external perturbations, movements are usually overcompensated to the previously applied perturbation causing deviations from the desired trajectory (errors). It is thought that these after-effects are indicative of the successful formation of an internal model to counteract the force-field (Hunter et al., 2009).

2.6.2. Neural correlates of motor adaptation (i.e. error-based learning)

The computational mechanisms of error-based learning suggest that the CNS learns a model from experience that predicts the motor commands that should be produced to compensate for the novel environment (external perturbations) (Thoroughman and Shadmehr, 1999).

Seidler et al. (2013) reviewed the neurocognitive mechanisms of error-based learning and highlighted three neural regions that have been demonstrated to play a key role in this process namely, the cerebellum, the basal ganglia and the anterior cingulate cortex (ACC)

Specifically, it is thought that error-processing and learning underly common neural mechanisms showing extensive neural overlaps in the cerebellum (Diedrichsen et al. 2005). Krebs et al., (1998) used a force-field motor adaptation task and suggested that while the cortico-striatal loop plays a significant role during early learning, the cortico-cerebellar loop becomes more important during later stages of learning

Spatiotemporal neural dynamics of error-processing have first been investigated through the recording of event-related potentials (ERPs) using EEG (Falkenstein et al., 1995; Gehring et al., 1993). These studies have found an association between error commission and a negative ERP component, commonly referred to as error-related negativity (ERN) (for review see Gehring et al., 2018). The ERN is a negative deflection seen in the ERP locked to the time in which incorrect responses are made. The ACC is thought to be the neural generator of the ERN (for review see Holroyd and Coles, 2002). The ERN was initially studied in paradigms in which errors a characterised in a binary way (i.e. present or absent). During motor learning and adaptation, however, errors persist over time and continuously change in size.

Specifically during motor adaptation paradigms, trajectories (i.e. deviations from intended trajectories - errors) can be continuously monitored and related to dynamic brain responses with ERP components (Anguera et al., 2009 Contreras-Vidal and Kerick, 2004, Torrecillos et al., 2014).

Visually-triggered movements rely on visuomotor transformations and it is important to disentangle visual, motor and error-related potentials recorded with EEG in these paradigms as they might overlap in time and location (Dipietro et al., 2014; Naranjo et al., 2007). In a recent review, Krigolson et al. (2015) pointed out that the dominating contribution of motor related potentials over visual and error-related potentials can make it hard to identify small peaks.

Voluntary movements elicit ERP components, including a negative deflection around movement onset (Wiese et al., 2005) and a frontal peak related to sensory feedback (Tarkka and Hallett, 1991). The spatiotemporal dynamics of movement preparation have been identified in the fronto-parietal network characterised by two peak activations between 170 and 240 ms in the prefrontal cortex and between 170 and 260 ms in the parietal cortex (Naranjo et al., 2007).

Visual processes play a key role during movement control and learning.The time course, as well as the function of individual ERP components following visual cues to move have been extensively studied. In their review Krigolson et al. (2015) summarised the main ERP components that have been identified and linked to specific cognitive mechanisms: i) the N100, a negative deflection around 100 ms post-visual cue linked to corrective responses in the presence of a perturbation, ii) the N200, a negative deflection occurring around 200 ms post-visual cue associated with movement planning, iii) the P300 a positive deflection around 300 ms post-visual cue related to feedforward mechanisms and iv) the N300, a negative deflection around 300 ms post-visual cue reflecting feedback mechanisms.

The functional role of the P/N300 component has been the focus of attention in recent years and their distinct contribution to motor adaptation mechanisms

were investigated. More recently, the P300 has been linked to learning processes, whereas the N300 (also termed ERN) with error-processing (MacLean et al., 2015).

It has been shown that fronto-central ERP components peaking around 300 ms post-visual cue play a key role in processing online motor correction (Dipietro et al., 2014). Specifically, it has been reported that the negative fronto-central ERP component (i.e. ERN) correlates with error size in catch trials in a force-field adaptation task (Torrecillos et al., 2014), and with the size of errors in visuomotor task (Anguera et al., 2009). Together these findings suggest that the fronto-central ERN is a marker of error-processing.

During a force-field mediated adaptation task (Pizzamiglio, 2017), ERN-like activity was reported and it was suggested that this activity reflects the formation of a predictive internal model. However, no link between this activity and motor performance improvement was established. **Study III** (**Chapter 6**) aims to expand these findings by using the same motor adaptation paradigm and investigating the association between ERN activity and kinematic performance improvements to determine if this neural activity scales with the necessary motor-command adjustment resulting in performance improvements.

2.6.3. Motor adaptation underlies cortical plasticity

Neuroplasticity refers to the ability of the brain to continuously change structurally and functionally throughout an individual's life (for review see Hummel and Cohen, 2005, Voss et al., 2017). At a cortical level, plasticity can refer to modifications including neuronal responsiveness, synaptic and functional connectivity and grey matter volume and white matter structure.

It is well established that de novo skill learning and re-learning of a skill such as after stroke depend on the plasticity of neurons and circuits in the motor system (for review see Hosp et al., 2011, Hummel and Cohen, 2005). Specifically, it has been shown that cortical plasticity is a crucial mechanism to continuously adapt movements to a changing environment and is involved

in error-based learning (for review see Ostry and Gribble, 2016 and Tyc and Boyadjian, 2006).

For instance, it has been shown that force-field learning underlies structural neuroplastic changes involving changes in resting-state sensory and motor networks (Vahdat et al., 2011, Vahdat et al., 2014). Functional changes have also been observed as assessed by cortical excitability modulations following visuomotor adaptation (Schintu et al., 2016). Similar changes in corticospinal excitability occur when participants observe motor learning paradigms without moving (McGregor et al., 2017). Namely, participants who observed a force-field reaching task with a learnable force showed increased cortical excitability post-observation, whereas participants watching an unlearnable force-field did not, demonstrating that the effects are specific for observation of motor learning (McGregor et al., 2017).

The neuronal mechanism underlying plasticity is explained by the theory of Hebbian learning, which states that the synaptic strength between two neurons increases when they are activated simultaneously (Wiesel and Hubel, 1965). The driving forces of synaptic plasticity-related to motor learning rely on long-term potentiation (LTP) and long-term depression (LTD) mechanisms (Ilic and Ziemann, 2005; Stefan et al., 2006; Ziemann et al., 2004). Specifically, the strengthening of synaptic connections in M1 driven by LTP-like mechanisms can produce changes in cortical excitability. (Ilic and Ziemann, 2005).

TMS is a useful tool to explore the ability of M1 to adapt/change during motor skill acquisition as reviewed by Tyc and Boyadjian, 2006. Methods include TMS mapping protocols to study cortical reorganisation, as measured with changes in cortical output maps or cortical excitability modulations as measured with changes in MEPs or TMS-evoked potentials (TEPs). In this thesis, we will refer to neuroplasticity, measured as changes in cortical excitability. As such, this thesis only measures short-term plasticity changes by capturing cortical excitability modulations, i.e. functional changes and not structural changes, such as enlargements/ expansions of cortical representations. Specifically, **Study III (Chapter 6)** measures neuroplastic

changes (i.e. modulations in cortical excitability) underlying motor adaptation to test whether increased plasticity is associated with better motor performance improvements.

2.7. Research contributions and novelty

This thesis aims to investigate neural mechanisms underlying unimanual upper limb motor control in different tasks, including unilateral isometric contractions and unilateral arm-reaching tasks (with and without an external perturbation). Upper limb function is necessary in everyday life but often impaired after brain injury, leaving stroke survivors with poor quality of lives. Understanding the mechanisms of upper limb control can aid in the design of better neurorehabilitation therapies. This thesis employs neuroimaging tools including EEG and TMS-EEG in combination with a highly standardised robot-mediated reaching task. The benefits and the impact of using these techniques will be outlined here. This will provide an overview on how the present research can contribute to advance our understanding on neural factors underlying unimanual motor control and delineate how the identified mechanisms of motor control and learning can be exploited for neurorehabilitation.

2.7.1. Novelty and contribution of using TMS-EEG

Since the development of TMS-compatible EEG systems, simultaneous TMS-EEG has emerged as a powerful tool to assess cortical activity non-invasively in humans (for review see Farzan et al., 2016). This thesis used this recently developed neuroimaging technique to directly assess cortical and corticospinal excitability related to upper limb motor control. The simultaneous recording of EEG in combination with TMS stimulation enables to capture cortical excitability and connectivity in a time-resolved manner.

So far, a large body of research has used TMS (without EEG recordings) to assess cortical excitability and plasticity in M1 by using MEPs as a readout (for review see Ziemann, 2017). However, MEPs are known to reflect both the state of neurons in M1 as well as in the spinal cord and muscle properties, thus the term corticospinal activity is commonly used to highlight the indiscriminability of MEPs between cortical and spinal influences. Directly recording TMS responses using EEG can be used to address this issue and TMS evoked responses captured at a cortical level with EEG (i.e. TMS-evoked potentials (TEPs) and induced oscillations) can provide a more direct readout

of cortical excitability. Moreover, direct cortical readouts such as TEPs can be used to assess cortical excitability without relying on an intact CST in contrast to MEPs. This is relevant when assessing cortical excitability in the clinical population who present with damages to the CST. For instance, in stroke patients MEPs can often not be elicited and recorded from the targeted muscle due to damage to the CST (for review see Sato et al., 2015). TMS-EEG can be used to overcome this issue by directly measuring cortical readouts such as TEPs or TMS-induced oscillations and provide a direct index of cortical excitability even in patients with damages to the neuromuscular system affecting the CST.

These direct EEG readouts cannot only partially substitute MEPs but also give a more complete picture of cortical activity, since different TEP components are thought to reflect activity in distinct subsets of cortical neurons (for review see Farzan et al., 2016). It has been shown that EEG readouts and MEPs can be sensitive to different changes in cortical excitability, thereby providing complementary information on neurophysiological mechanisms. For instance, studies reported that TEPs can be significantly modulated with no significant change in MEPs (Harrington et al., 2018, Kičić et al., 2008). Thus, EEG readouts can represent a more sensitive approach to capture and unravel predominantly cortical processes.

Finally, as highlighted in their methodological paper on concurrent TMS-EEG, Ilmoniemi et al. (2010) showed that TMS-evoked EEG can provide an index of cortical excitability in a wider range of brain regions than TMS-MEP which is limited to motor areas. In particular, when stimulating a specific brain region with TMS, whole scalp EEG recordings can capture the spreading of activity and thereby be used as an index of cortico-cortical connectivity.

This thesis employed TMS-EEG, by focusing on TEPs as a main readout of excitability, to gain deeper insights into cortical hemispheric excitability asymmetries related to motor dominance, track bi-hemispheric motor cortical activity related to unimanual reaching and finally to measure cortical excitability and plasticity related to motor learning.

2.7.2. Implication of using a highly standardised robotic task

This thesis employed a highly standardised robot-mediated reaching task to assess neural processes involved in movement preparation as well as to investigate neural mechanisms underlying motor adaptation (e.g. error-based learning).

Using a robotic device offers many benefits and besides its applicability in neurorehabilitation, it also enables the investigation of basic mechanisms of motor control in healthy individuals. As highlighted by Huang and Krakauer (2009) robotic devices such as the MIT-Manus robotic manipulandum, used in this thesis provide high measurement reliability and controllability in upper limb reaching tasks representing a highly standardised way to assess the motor system.

This thesis employed the robotic device in two-ways: The first was to study neural mechanisms associated with robot-mediated reaching preparation and the second was to investigate neural correlates of motor adaptation during robot-mediated reaching in an unperturbed and perturbed environment.

The thesis focussed on upper limb reaching since more than half of the activities in daily living require upper limb movements (Ingram et al., 2008) and upper limb impairments are often observed in stroke. Studying robot-mediated reaching can be exploited in two-ways: it can give more insights into the mechanisms underlying motor control and adaptation (i.e. error-based learning), and it can also help to understand how robot-mediated tasks can be employed in rehabilitation to generalise to 'real world' movements and thus be used in neurorehabilitation settings to improve upper limb recovery (Kluzik et al.,2008).

The thesis employed a robot-mediated force-field adaptation task. This task was chosen since it is commonly used in research settings in healthy individuals as well as in stroke patients. For instance, Scheidt and Stoeckmann (2007) compared force-field adaptation in stroke and healthy individuals and demonstrated that stroke patients can adapt movements to the novel environment but need more practice to do so compared to healthy individuals. Another study, showed that error-enhancing tasks using robot-meditated

45

force-field adaptation may represent a promising strategy for upper limb recovery (Patton et al., 2006). Specifically, they showed that adaptive training can lead to a more normal motor pattern in stroke patients and might help to restore impaired motor function.

In the context of motor rehabilitation aiming to recover upper limb function, robot-mediated training is now increasingly used in clinical trials and practice (for review Basteris et al., 2014). However, the basic neurophysiological mechanisms underlying motor adaptation are still not fully understood. Motor learning is highly variable even in healthy individuals and it is important to identify which neural factors contribute to these differences in order to best harness individual brain activity to boost motor learning. This thesis employed EEG to record neural activity during robot-mediated adaptation to expand previous findings of cortical activity related to motor adaptation reported by Pizzamiglio (2017) by directly investigating neural correlates of motor performance derived from motor learning indices. Moreover, this research is the first one to employ TMS-EEG in the context of robot-mediated motor adaptation training to identify potential neural biomarkers of motor adaptation in a healthy population. This could potentially pave the way for the development of cost-effective biomarkers of motor adaptation and be exploited in neurorehabilitation.

2.8. Goals and hypotheses of the thesis

Hemispheric asymmetries related to motor dominance, imbalances between contralateral and ipsilateral M1 excitability and the ability to adapt to novel environments play a key role in upper limb motor control and can affect upper limb recovery. This thesis aimed to investigate neural correlates of unimanual upper limb movement to gain further insights into how these factors contribute to motor control in healthy individuals.

Specifically, the goal of this research was to identify hemispheric asymmetries related to motor dominance, to evaluate the relative contribution of the contralateral and ipsilateral M1 during unimanual reaching preparation and finally to investigate the neural correlates underlying the formation of a

predictive internal model enabling the adaptation of movements to new environments.

The specific research questions with their aims and hypothesis will be outlined here and results of these studies will be presented in the different chapters of the thesis.

Chapter 4 (**Study I**) introduces the technique of TMS-EEG co-registration and tests whether motor cortical excitability can be reliably assessed with TMS-evoked cortical responses (i.e. TEPs and TMS-induced oscillations) in both hemispheres. Specifically, the study aims to replicate the characteristic TMS evoked responses at the cortical level reported in the literature to test the reproducibility of this relatively new neuroimaging technique across participants in our research lab. The second goal of the study is to investigate if motor dominance is related to hemispheric cortical excitability asymmetries between the dominant and non-dominant M1 and whether this difference is enhanced in an active motor contraction state compared to rest. To this end, TMS was applied to M1 of the dominant and non-dominant M1 in right-handed healthy individuals during a resting and an active isometric contraction condition using a within-subject design.

Hypothesis 1: TMS over M1 will produce evoked cortical responses measured with EEG that follow well-characterised negative and positive deflections (i.e. TEP components) as well as increases and decreases of oscillatory power following the TMS pulse.

Hypothesis 2: Motor dominance and motor state will have a significant effect on cortical excitability. It is expected that cortical excitability will be higher in the dominant M1 and that motor state, i.e. changing from a resting to an active contraction would enhance this difference.

Chapter 5 (**Study II**) explores neurophysiological correlates of unimanual reaching in M1 of both hemispheres, with a special emphasis on the role of the ipsilateral hemisphere. Specifically, cortical excitability

modulations during unilateral right-arm reaching preparation at different times during reaching preparation will be investigated. To this end this study uses a between-subject design in which right-handed individuals are divided into two groups, each receiving either TMS stimulation over the contralateral (left) or ipsilateral (right) M1 to the task arm (right) at different time delays from visual cue during movement preparation.

Hypothesis 1: Motor cortical excitability will be significantly modulated during reaching preparation, reflected with increases and decreases of TMS-evoked responses.

Hypothesis 2: The modulation of excitability will be less enhanced in the ipsilateral compared to the contralateral M1 to the reaching arm.

Chapter 6 (**Study III**) aims to identify neural correlates and biomarkers of error-based learning using a robot-mediated force-field adaptation task. This study employs a within-subject design in which right-handed individuals performed a reaching task with their right arm in an unperturbed (non-adapting condition) and in a force-field perturbed (adapting condition) environment while EEG was recorded. TMS over the contralateral (left) M1 is applied before and after the motor adaptation condition to measure cortical excitability with TEPs.

Hypothesis 1: Neural activity related to error-processing will be significantly higher during motor adaptation compared to unperturbed reaching.

Hypothesis 2: Cortical excitability will be significantly increased after motor adaptation. Native cortical excitability measured prior to motor adaptation will be associated with performance improvements during motor adaptation.

Lastly, **Chapter 7** aims to expand the analysis of the data acquired in **Study III (Chapter 6)** during the motor adaptation task to the time-frequency domain in order to explore regional and interregional cortical activations during the preparation and execution of the reaching task. This **Chapter** uses an

exploratory approach to identify potential differences between unperturbed and perturbed reaching as measured with changes in regional cortical activity and interregional connectivity and to investigate the spatiotemporal dynamics in brain activity and brain network configuration during the highly standardised reaching task.

Hypothesis 1: Regional brain activity and interregional connectivity will be significantly higher during perturbed compared to unperturbed reaching.

Hypothesis 2: Functional dynamics in regional activity and network configuration will be significantly modulated during different phases of robot-mediated reaching.

Chapter 3 - General Methods

This Chapter will describe general methods used for participant recruitment and introduce the neuroimaging tools and methodological techniques implemented in the thesis. A detailed description of protocols, data and statistical analysis can be found in the method sections of the individual chapters of the thesis.

3.1. Ethics

All experimental procedures were conducted in accordance with the Declaration of Helsinki for Human Experimentation (48th World Medical Association General Assembly, Somerset West, Republic of South Africa, October 1996) and were approved by the University of East London ethics committee (UREC_1617_23 and UREC_1718_03, see **Appendix A.1** and **A.2**). Each participant was first orally informed about the experiment upon recruitment and was given written detailed information on the day of the experiment. Before testing, participants were required to fill out a medical questionnaire to ensure that there were no contraindications to participate to the studies (e.g. contraindications to TMS such as history of neurological, psychiatric or muscular disorders, see **Appendix C**), and lastly gave their written informed consent (see **Appendix E.1** and **E.2).** Participants could withdraw from the studies at any time without specifying the reason from the experiment. After completion of the experiment, participants received a monetary remuneration for their participation.

3.2. Participant recruitment

All the studies took place at the Neurorehabilitation Unit, School of Health, Sports and Bioscience, College of Applied Health and Communities, University of East London, at the Stratford campus. Participants were recruited from both the university and general public through flyer distributions, emails and face-to-face recruitment (**Appendix B.1** and **B.2**).

The recruitment started with a general requirement for right-handed, healthy young (18-45 years old) participants without any neurological or psychiatric disorders and having normal or corrected to normal vision. Once a person expressed interest in the study, their age, handedness and health status of the potential participant was enquired. To objectively quantify handedness, the Edinburgh Handedness Inventory questionnaire was used (**Appendix D**) (Oldfield, 1971). For eligibility to participate in TMS studies, potential participants had to complete a medical questionnaire (**Appendix C**) according to international guidelines for TMS safety inclusion and exclusion criteria (Rossi et al., 2009).

The duration of every experiment was between 2 and 3 hours (including setup preparation and testing). Throughout every experiment, participants were given breaks in between testing to prevent fatigue and assure that participants could maintain attention throughout the task.

3.3. Neuroimaging tools

3.3.1. Transcranial Magnetic Stimulation (TMS)

TMS is a non-invasive and painless neuroimaging tool widely used in clinical and research settings to stimulate excitable tissues with an electric current by an external time-varying magnetic field (Ridding and Rothwell, 2007). In their pioneering work in 1985, Barker et al. introduced TMS to study the integrity of the corticospinal pathways in humans. TMS has since been established as a safe neurophysiological tool that can be used to trigger and modulate neural activity (Rossini et al., 2015). Most commonly, TMS has been used to study corticospinal pathways by applying TMS measuring MEPs from the targeted muscle activated by TMS over the motor cortex. TMS can be used to investigate cortical excitability and connectivity. In this thesis, single-pulse TMS over M1 was used to investigate cortical excitability and plasticity.

The currents that pass through a TMS coil induce the production of a magnetic field which can affect large populations of individual neurons to study cellular characteristics, including neuronal firing (Hallett, 2007; Ridding and Rothwell, 2007). Specifically, in TMS, time-varying currents are generated in an

induction coil positioned over the area of interest on the scalp. This leads to the generation of a magnetic field (Faraday's law of electrical current induction), which in turn induces a secondary electric current in brain structures parallel to the orientation of the coil. These induced currents can either lead to direct depolarisation of neural structures resulting in the production of action potentials or modify the state of tissue excitability (for review see: Farzan et al., 2016).

3.3.1.1. Physics of TMS

TMS uses electromagnetic induction to induce and interfere with neural activity (Figure 3-1). A TMS device consists of a TMS coil (the inductor L) connected to the main TMS stimulator unit. This main unit comprises the voltage source that generates the magnetic field in the coil with a capacitor charged to very high voltage and when discharged producing a current of thousands of amperes into the coil over a short period (around 100 µs). This high speed of discharge enables the magnetic field to rapidly rise and then to decay more slowly around 1 ms.

The magnetic field pulse is generated by inducing a current pulse I (t) the coil, which in turn can induce a secondary electrical current flow in an underlying conducting medium such as the brain. According to Lenz's law, this induced current flow is parallel but opposite in direction to the current in the coil. The basic system required for TMS stimulation consists of a stimulator and a stimulating coil. Specifically, the magnetic stimulator comprises a capacitor (capacitance C), a thyristor (switch S) and the stimulating coil (inductance L), with a series resistance (R) in the coil, forming an RLC oscillator. A capacitor C is charged to up to 3kV, then the circuit is closed via an electronic switch allowing the current flow to start and gating the thyristor into the conducting state. This induced a current forming a sine wave of several kilo Amperes (≤ 10 kA). In rapid-rate stimulators, during the second half cycle of the oscillation, the current flows in the opposite direction, returning the charge to the capacitor. In case the thyristor gating is ended during the second half, the oscillation terminates when the cycle is completed. The induced electric field and the current density induced in the underlying conducting tissue such as

the brain is proportional to the induced electrical field in the coil. The electrostatic energy discharged by the capacitor and transformed into the coil's magnetic energy. This peak energy depends on the coil's inductance and the peak current in the coil. The two most commonly-used coil shapes are the circular and figure-of-eight coils.

The figure-of-eight coil allows a greater precision than the original circular coil and enables a relatively focal cortical activation. The figure-of-eight coil consists of two loops in which the current flows in opposite directions (clockwise and anticlockwise), creating the strongest induced electric field at the intersection of the coil winding. The induced electric field (E) strength for brain stimulation should be around 100V/m (max strength 140V/ m) and is the temporal derivative of the magnetic field.
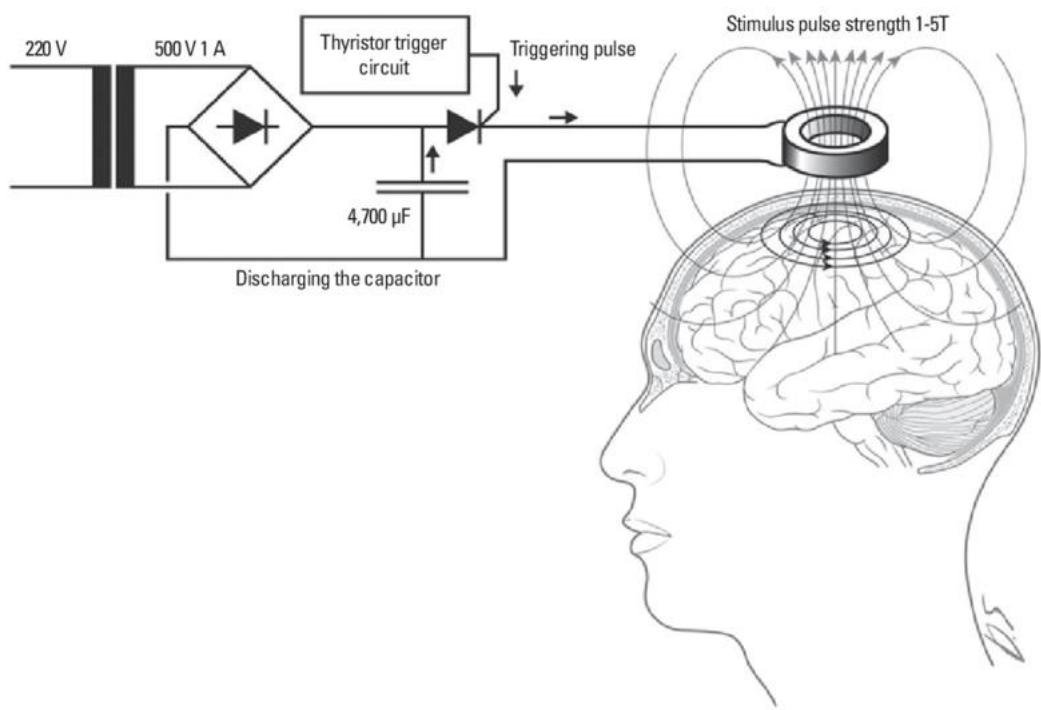
Figure 3-1: Underlying principle of transcranial magnetic stimulation (TMS). Figure taken from Kleinjung et al. (2007).

3.3.1.2. TMS excitation of neural structures

TMS can activate neural regions under the coil by inducing an electric current in the CNS (Tofts, 1990). The fast-changing magnetic field in the coil creates circular electrical currents which flow in a plane orthogonal to the magnetic field. The strength and the direction of the induced electric field are both dependent in the underlying neural structures and can be reduced by extracerebral tissues, such as the scalp, bone and meninges. If the electric field is high enough, networks in the cortex can be activated by depolarising superficial axons. It has been shown that TMS preferentially activates neurons oriented horizontally in a plane that is parallel to the coil and the brain surface.

3.3.1.3. TMS over the motor cortex

When single TMS pulses are applied over the motor cortex muscle, action potentials can be generated in the target muscle in the periphery, called MEPs. These MEPs are most commonly characterised but their amplitude and latency and enable the assessment of the integrity of the CST. TMS applied over the motor cortex is thought to activate mostly corticospinal axons close to the initial segment of the axon, called the axon hillock (Barker et al., 1985). After depolarising neurons in the motor cortex, descending volleys in the pyramidal tract are generated and project onto spinal motor neurons along the CST.

Motor neuron activation induced by TMS induces an MEP in the targeted muscle and can be recorded via EMG by using surface electrodes over the muscle belly. TMS activates a variety of neuron types in the cortex and the stereotyped output in corticospinal neurons is most probably a result of a complex interplay between neurons. The response to TMS to the motor cortex consists of the production of two main waves. The first waves originate from direct activation of the axons of fast-conducting pyramidal neurons in layer V and are referred to as D-waves whereas the later waves originate from indirect, transsynaptic activation of the pyramidal neurons and are referred to as I-waves.

TMS preferentially stimulates superficial parts of the brain. Due to the anatomical layered structure of the cerebral cortex it is thought that pyramidal neurons which are in deeper cortical layers, are mostly activated trans-synaptically, via interneurons located in more superficial layers closer to the surface of the brain thereby to the coil (Day et al., 1989; Di Lazzaro and Ziemann, 2013). The magnitude and orientation of the induced current in the motor cortex determine whether TMS induces predominantly I- or D- waves (Di Lazzaro et al., 1998). It has been shown that the hand muscle recruitment with TMS over the motor cortex is similar to the one with voluntary contraction. In fact, voluntary contraction and TMS over the motor cortex recruit motor units in the same ordered manner from the smallest to the largest (Hess et al., 1987).

The response to TMS in the motor cortex can be quantified by measuring MEPs at the targeted muscle at rest and serve as an indicator of motor cortical excitability (Figure 3-2). Most commonly, the peak-to-peak amplitude and latency of MEPs, as well as the resting motor threshold (RMT) defined as the minimum TMS intensity to evoke MEPs of at least 50 µV in 50% of 5 to 10 consecutive trials are used to quantify the excitability of corticospinal pathways. MEPs recorded during a voluntary contraction of the target muscle is followed by an interruption of the background EMG activity, a phenomenon referred to as cortical silent period (CSP) and is a measure of inhibitory activity. Whereas, the initial part of the inhibitory process is mediated by spinal mechanisms, the later part (50-100 ms) by cortical mechanisms. At the cortical level, the CSP is thought to be mediated through $GABA_B$ receptors (Farzan et al., 2013; Werhahn et al., 1999). Commonly, the duration of the silent period is used to quantify inhibitory activity. Thus, single-pulse TMS over the motor cortex can be used as a tool to quantify excitatory, as well as inhibitory activity using MEPs and CSP duration as biomarkers of the integrity of cortical and corticospinal pathways.
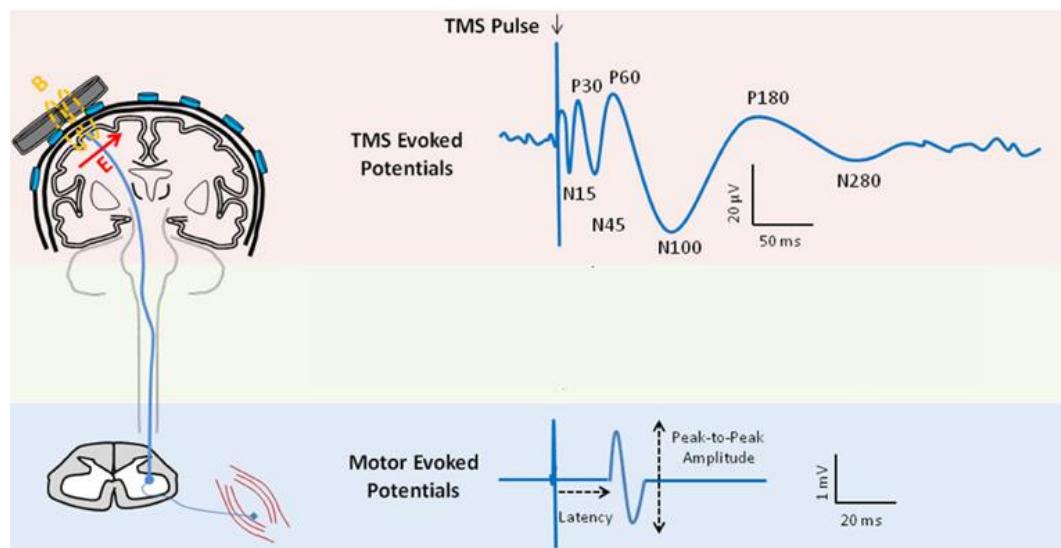
Figure 3-2: The basic principle of transcranial magnetic stimulation. Figure taken from Farzan et al. (2016).

The absence of low amplitude MEP responses to single-pulse TMS are linked to a loss of neurons of axons in the CST and has been used as an early-stage prognostic indicator of motor and functional recovery in stroke patients (Escudero et al., 1998; Kim et al., 2016; Wu et al., 2015). The integrity and structure of the CST is commonly represented using diffusion tract tractography (DTT), an imaging method which produces a three-dimensional representation of CST structure, which is derived from diffusion tensor imaging.

A recent study combined TMS and DTT imaging in patients who suffered a middle cerebral artery stroke to evaluate if these measurements can predict motor recovery (Kim et al., 2016). Specifically, Kim et al. (2016) applied TMS to the vertex to elicit MEPs from the affected and non-affected tibialis anterior muscles in a relaxed state. Patients were classified into four groups according to the presence of MEPs in the affected muscle and observed CST integrity, measured with DTT. Groups were defined according to the following classifications: preserved CST and a presence of MEP, absence of CST and a presence of MEP, preserved CST and an absence of MEP and absence of CST and an absence of MEP (Figure 3-3). Kim et al. (2016) have found that patients with the presence of both MEPs and a preserved CST showed better functional recovery than other groups at the 4-week follow-up. Furthermore, among the group of patients with a present MEP, those with a preserved CST showed better recovery of paretic lower extremities.
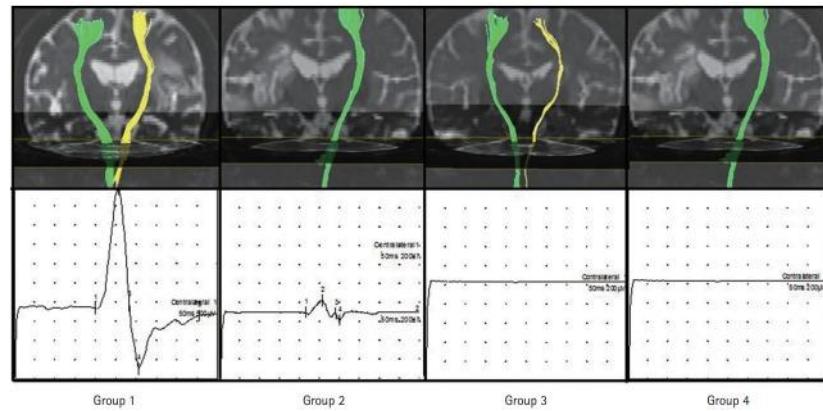
Figure 3-3: The relationship between the integrity of CST and the presence of MEP.
Figure taken from Kim et al. (Kim et al., 2016). Patients were classified into groups according to DTT and TMS results. Upper panels show the coronal DTT images and lower panels the TMS results. Group 1 has a preserved CST and a presence of MEP, group 2 has an absence of CST and a presence of MEP, group 4 has a preserved CST, and an absence of MEP and group 4 has an absence of CST and an absence of MEP.

3.3.2. Electroencephalography (EEG)

EEG is a non-invasive functional neuroimaging technique measuring the electrical activity of the human brain by capturing changes in voltage over time (Berger, 1929). Similarly, to TMS, EEG enables to determine the timing of brain activity in response to external stimuli. While TMS induces electric current creating neuronal activity, EEG records changes in cortical neuronal activity from wide regions of the brain by capturing subtle changes of voltages across the scalp and is completely non-invasive (Figure 3-4).

EEG uses non-invasive electrodes positioned over the scalp recording the electrical potentials generated within the brain and as such reflect the sum and cancellation of potentials from neighbour neurons rather than the activity of single neurons (i.e. both action potentials and post-synaptic potentials) (Schomer et al., 2017). Specifically, electrodes can detect voltage fluctuations resulting from ionic current within the neurons of the brain. At rest, the interior of a neuron is negatively charged compared to the extracellular fluid. When an action potential is triggered, an influx of sodium ions causes the neuron's polarity to change, making the interior positively charged. An increase of potassium efflux combined with a decrease in sodium influx stops the action potential and the neuron's membrane returns to its resting state potential.

Action potentials can be transmitted between neurons and traverse long axonal distances without loss of amplitude. When an action potential is generated, a passive current downstream from the action potential is elicited and depolarises the membrane potential in adjacent regions of the axon, opening sodium channels. This local depolarisation results in another action potential and propagates until the end of the axon is reached. Post-synaptic potentials can be elicited through neurotransmitter release at chemical synapses. The probability that an action potential will be produced in the postsynaptic cell depends on the postsynaptic potential. If the membrane is depolarised, the potential is called an excitatory postsynaptic potentials (EPSP), whereas, if it is hyperpolarised, the potential is termed an inhibitory postsynaptic potential (IPSP). While EPSPs facilitate the generation of an action potential by bringing the membrane's potential closer to threshold

potential, IPSPs maintain the membrane potential more negative than the threshold potential thus making it harder to generate an action potential. In chemical synapses, the type of neurotransmitter released and the type of postsynaptic receptor activated determine the event of an EPSP or IPSP. In the cerebral cortex, the principal CNS excitatory neurotransmitter synthesised and released by neurons is glutamate. The remaining neuronal population (i.e. interneurons) release GABA, the main inhibitory neurotransmitter of the cortex. EPSPs and IPSPs sum up in time through synchronisation and in space and can be captured with EEG via surface electrodes by measuring voltage differences (Schomer et al., 2017). Importantly, the EEG signal arises from thousands of synchronised pyramidal cell post-synaptic potentials and does not reflect the activity of a single neuron. Several factors influence and modify the original signal and depend on the anatomy of the thickness and shape of the scalp, skull, dura and the conductive properties of the CSF.

Despite having a limited spatial resolution, the time resolution of EEG is the highest of current neuroimaging techniques with a millisecond precision (Kappenman and Luck, 2012).
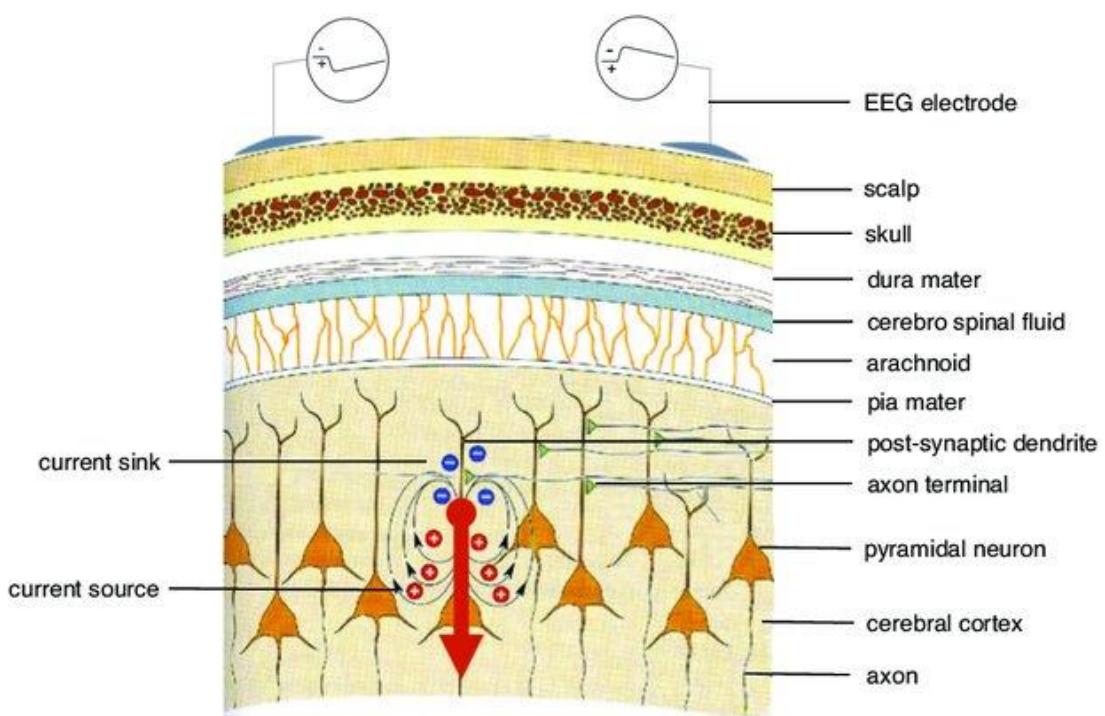
Figure 3-4: Biophysical basis of EEG. Figure taken from Strobbe et al. (2015).

3.3.2.1. EEG components

Neural oscillations can be captured by EEG and appear as sinusoidal waves with a peak-to-peak amplitude ranging from 0.5 to 100 μV in amplitude (Aurlien et al., 2004). The first described brain waves were characterised by Hans Berger in 1929, where he recorded the first human alpha wave at around 10Hz. Since then other identifiable brain waveforms have been characterised and classified by their frequency into five basic groups: delta (1-4 Hz), theta (4-7 Hz), alpha (8-13 Hz), beta (13-30 Hz) and gamma (30-80 Hz) (Herrmann et al., 2016).

EEG can be used to record spontaneous cortical activity and cortical responses to external stimuli. Cortical responses to external stimuli can be characterised in the time domain to study event-related potentials/ fields or in the time-frequency domain to study oscillatory activity.

3.3.2.2. Event-related potentials (ERPs)

Due to the small signal to noise ratio of brain oscillations, a method for extracting meaningful brain potentials with larger amplitudes is to average recorded EEG activity over time. This averaging technique enables to visualise even small potentials that were not discernible in the raw EEG recording. This now commonly used EEG technique enables the measurement of brain responses to specific events. Specifically, it means that EEG responses are recorded with respect to an eliciting stimulus and these time-locked responses are then averaged over a number of repetitions (trials) of that stimulus.

The averaged response is typically referred to as event-related potential (ERP) (Kappenman and Luck, 2012). ERPs are thought to reflect with high temporal resolution the neuronal activity over time evoked by a specific stimulus. The two main assumptions in the ERP technique are that that the stimulus (internal or external) is invariant over trials and that the background EEG (i.e. noise) is random in each trial. The analysis of ERPs is a commonly used methodology to study cognitive and sensorimotor processes. ERP research focuses on the relationship between ERP components and cognitive or sensorimotor processes in the brain. Specifically, ERP waveforms are characterised by a

set of positive and negative deflections, which are related to underlying brain processes. The term ERP component is used to denote a particular feature of an ERP waveform and is characterised by its polarity, amplitude and latency. Usually, the ERP components are referred to with acronyms containing a letter P for positive and N for a negative deflection followed by a number, typically indicating the latency in milliseconds, e.g. N100 (Kappenman and Luck, 2012). In the last two decades, other tools to study more complex brain dynamics have been developed such as decomposing brain signals in the time and frequency domain (Grandchamp and Delorme, 2011). In this thesis, we used two types of measures: event-related spectral perturbation (ERSP) and channel event-related phase coherence (ERPCOH).

These signal processing techniques transform a one - dimensional signal (representing a signal in either the time domain or the frequency domain) into a two-dimensional signal (combining time and frequency domain). To do this, a signal in the real domain is transformed into the time-frequency domain via a Fourier transform or wavelet transform.

3.3.2.3. Event related spectral perturbation (ERSPs)

ERSP measures changes in spectral power induced by a specific stimulus (event). Calculating the time-frequency evolution of the ERSP requires computing the power spectrum over a sliding latency window and then averaging across trials (similarly to ERPs). For a given number of trials (n), being F_k (f,t) the spectral estimate of trial k at frequency f and time t using a fast Fourier transform (FFT) or wavelet transform:

$$\text{ERSP}(f, t) = \frac{1}{n} \sum_{k=1}^{n} |F_k (f, t)|^2$$

Equation 3-1: Time-Frequency transformation: ERSP.

The time-frequency sliding window dimensions can be fixed or mutable. Commonly, a mutable sliding window is used, with sliding window getting shorter along the time axis and longer along the frequency axis with increasing frequencies. This allows to emphasise the content of higher frequencies, whose amplitudes are typically low, by smoothing over a bigger frequency range.

3.3.2.4. Event-related phase coherence

Event-related phase-coherence (ERPCOH) was introduced by Rappelsberger et al. (1994) to measure the coherence between EEG channels related to specific events across a temporal dimension. It provides information about the dynamic interaction of brain regions (Andrew and Pfurtscheller, 1996) and can be used as a measure of functional connectivity. In this thesis, ERPCOH (Grandchamp and Delorme, 2011), which estimates the complex linear relationship between two signals, has been applied.

For a and b, two given time series (e.g. from two EEG channels), being F_k $(f,)$ the spectral estimate of trial k at frequency f and time t:

$$\text{ERPCOH}^{a,b}(f,t) = \frac{1}{n}\sum_{k=1}^{n}\frac{\sum_{k=1}^{n} F_k^a(f,t)\, F_k^b(f,t)^*}{|F_k^a(f,t)\, F_k^b(f,t)|} \quad ,$$

Equation 3-2: Time-Frequency transformation: ERPCOH.

N is the number of trials and $F_k^a(f,t)\, F_k^b(f,t)^*$ is the cross-spectrum between two given time series from *a* and *b*. ERPCOH values are real numbers between 0 and 1, where 1 symbolises perfect synchronisation and 0 an absence of synchronisation between two signals. With n nodes (electrodes) the number of electrode combinations (connections) is n(n-1)/2.

In order to reduce the effect of the averaged reference, volume conduction issues, inter-subject and inter-electrode variability, task-related coherence was employed. Specifically, ongoing coherence measurements were corrected for a baseline value. Task-related coherence was calculated by subtracting the baseline coherence (in a resting condition, e.g. before a visually cued movement) from an active condition (e.g. during visually guided movements) similar to the literature (Formaggio et al., 2015; Fuggetta et al., 2005) according to following subtraction:

$$\text{TR ERPCOH} = \text{ERPCOH(active)} - \text{ERPCOH(baseline)}$$

Equation 3-3: Task-related coherence: TR-ERPCOH.

in which positive values represent increases in coherence magnitude and negative values represent decreases in coherence.

3.3.3. TMS - EEG

Using TMS over the motor cortex while recording whole scalp EEG enables the identification of both local and distant effects of TMS, by not only measuring local excitability of the stimulated patch of the motor cortex but also the spreading of TMS-evoked responses (activity) in a wider cortical network. The overall TMS-evoked responses are highest under the stimulated area and decrease with increasing distance from the stimulation point. Locally, within one hemisphere, increased EEG activity can be seen in neighbouring electrodes, reflecting the spread of TEPs to anatomically interconnected cortical areas (Ilmoniemi et al., 1997; Paus et al., 2001).

An important characteristic of TMS-evoked response topography is that by stimulating TMS unilaterally in one cortical hemisphere, bilateral EEG responses are evoked with different features. It is thought that TMS-evoked activity spreads from the stimulation site ipsilaterally via association fibres and contralaterally stimulated hemisphere via transcallosal fibres and to subcortical structures via projection fibres (Ferreri et al., 2011; Ilmoniemi et al., 1997; Komssi et al., 2002). Combining TMS-EEG is, therefore, a non-invasive brain imaging technique enabling the study of cortico-cortical interactions by applying TMS to one brain region and measuring responses in remote but interconnected areas.

3.3.3.1. TMS-evoked responses

TMS can induce electric currents, which in turn induces cell membranes to depolarise leading to the opening of voltage-sensitive ion channels and triggering action potentials. The resulting synaptic activations are directly reflected in EEG by recording a linear projection of postsynaptic current distribution (for review see Ilmoniemi and Kičić, 2009). These EEG signals can be analysed to quantify and locate the recorded synaptic current distributions and can be used to make inferences on local and global excitability and functional connectivity in the brain.

When TMS is targeted to a specific brain region in a repeatable, stable and well-controlled way from pulse to pulse (hence, trial-by-trial), TMS - evoked responses are usually highly reproducible and less variable than MEPs

(Lioumis et al., 2009). Single-pulse TMS can be used to characterise TMS-evoked responses in the time and frequency domain.

TMS - evoked responses are time-locked to the TMS pulse (external stimulus), and when averaged across trials, in the same way than ERPs, these responses are referred to as TMS-evoked potentials (TEPs). TEPs allow the direct response of cortical neurons to an external perturbation (TMS pulse) and are used as an index of cortical excitability.

In the last decade, it has been shown that TEP responses are characterised by positive and negative components with a specific shape and latency (Komssi et al., 2002; Paus et al., 2001). Single-pulse TMS evokes EEG activity lasting up to 300 ms and consists of a sequence of positive and negative deflections. In particular, specific TEP components, such as the N15, P30, N45, P60, N100, P190 and N280 (Figure 3-2), have been identified and their functional significance studied (for review see Farzan et al., 2016). The functional role and origin of the N100 component has been primarily studied and has been established as a biomarker of inhibitory processes, representing the activity of $GABA_B$ receptors and is believed to reflect local GABA and Glutamate balance (Du et al., 2018).

TMS - evoked responses can also be characterised in the frequency domain (Pellicciari et al., 2017). TMS can trigger oscillatory activity as well as perturb ongoing oscillatory activity, eliciting event-related synchronisation (ERS) (Rosanova et al., 2009) or desynchronisation (ERD) (Fecchio et al., 2017). Single-pulse TMS over M1 induces a brief period of synchronised activity in the stimulated brain area (Fecchio et al., 2017; Fuggetta et al., 2005; Paus et al., 2001). It has been hypothesised that TMS pulses synchronise spontaneous activity of a population of neurons, termed the resetting hypothesis. Single-pulse TMS-induced oscillations are also thought to uncover natural rhythms and endogenous brain activity of different brain regions.

3.3.3.2. TMS-EEG as a research tool

TMS enables to study cortical excitability, connectivity and brain plasticity in at least two very different scenarios. First, it can be used to investigate brain activity independent of behaviour, with the recorded variations in neural

activity reflecting the brain reactivity to the stimulus directly without being confounded with the participant's capability to perform a task or by other strategies employed. Secondly, TMS can directly perturb local brain networks while participants are engaged in a specific task.

In the series of experiment, this thesis applied TMS over M1 to measure cortical excitability at rest (**Study I**) and during motor tasks (**Study I and II**) using TEPs and MEPs amplitudes as readouts. In **Study III**, cortical excitability was measured with TEP amplitudes before and after a motor task (i.e. motor adaptation) and cortical plasticity indexed with TEP modulations (i.e. from pre and post-motor adaptation).

3.4. Experimental recording systems

3.4.1. TMS acquisition

A monophasic stimulator and figure-of-eight coil have been used for all studies (Figure 3-5).

Figure 3-5: Monophasic stimulator and figure-of-eight coil.

Hardware and software used for the application of TMS were provided by Magstim (Magstim Co, Whitland, Dyfeld, UK) and CED signal (Cambridge Electronic Design, Cambridge, UK), consisting of:

- 70mm Figure-of-eight coil (Magstim Co, Whitland, Dyfeld, UK)
- Magstim stimulator: Magstim 200^2 stimulator (monophasic pulse) (Magstim Co, Whitland, Dyfeld, UK)
- CED Signal 1902 amplifier
- CED 1902-11/4 electrode adaptor box
- CED 1401: data acquisition unit

Single-pulse TMS in all experiments was performed with the Magstim 200^2 stimulator (monophasic pulse) connected to a figure-of-eight coil with an average diameter for each wing of 70 mm.

3.4.1.1. EMG acquisition

EMG is a neurophysiological technique used to evaluate and record electrical activity produced by skeletal muscles (myoelectric signals). EMG recordings can be acquired invasively, using needle electrodes to capture single-fibre activities, or non-invasively. This thesis employed surface EMG electrodes allowing to record the sum of multiple single-fibre/motor-units activities (Basmajian and Luca, 1985).

The shape of the motor unit potentials in the EMG depends on many factors, including the composition of the motor unit, number of muscle fibres per motor unit and metabolic type of muscle fibres. EMG is thought to be the indirect measure of the activity of motor neurons of the spinal cord due to their one-to-one correspondence with muscle fibres (Li et al., 2012).

Surface EMG was used to record responses from the first interosseous (FDI) muscle of the right and left hand (**Study I**) and from the Biceps Brachii (BB) of the left and right arm (**Study II-III**). Two disposable Ag/AgCl electrodes were attached to the skin over each muscle in a belly to tendon montage and along the muscle fibres direction following the SENIAM guidelines (Hermens et al., 2000), and the ground electrode was placed over the right forearm.

Raw EMG signals were sampled at 5kHz with a Micro CED 1401 analogue-to-digital laboratory interface (Cambridge Electronics Design, UK), amplified and filtered (bandpass filter 45 Hz high pass, 1kHz low pass) with a CED 1902 amplifier (Cambridge Electronics Design, UK). Data were stored for offline analysis on a laboratory computer for online visual display and additional offline analysis through the software Signal (Cambridge Electronics Design, UK).

3.4.1.2. TMS – EMG acquisition

In all the studies, TMS was applied over the primary motor cortex (left and right M1 in **Study I and II** and left M1 in **Study III**).

Each TMS testing session started with determining the "motor hotspot" for the targeted muscle (FDI in **Study I** and BB muscle in **Study II and III**) and followed with determining the resting motor threshold (RMT).

Neuronavigation systems are increasingly used to improve TMS stimulation location site and make measurements more reliable (for review see Farzan et al., 2016). However, such a system was not available in the lab and individual MRI images were not acquired for the studies. For these reasons the optimal scalp position to target the motor representation of the FDI (**Study I**) and BB (**Study II and III**) was identified as the position that elicited maximal MEP activity in the targeted muscle as recommended by Rossini et al. (2015) for clinical and research application.

To target the M1, coil position was adjusted to produce an MEP of maximal peak-to-peak amplitude in the target muscle. Specifically, the approximate location of the hand motor area on the stimulated hemisphere was explored in 1-cm steps until reliable MEPs could be evoked. This site was marked with a washable pen on the EEG cap to ensure consistent coil positioning throughout the experiment and the handle of the coil pointed backwards, perpendicular to the presumed direction of the central sulcus, approximately 45 degrees to the midsagittal line.

The direction of the TMS-induced current in the brain tissue was posterior-anterior. The RMT, defined as the minimum stimulus intensity that elicited MEP of more than 50 microvolts in at least five out of ten trials (Rossi et al., 2009), was determined by applying single-pulses of TMS to the identified motor hotspot.

3.4.2. EEG acquisition

EEG activity was recorded non-invasively using equipment from ANT Neuro (www.ant-neuro.com) consisting of the following hardware and software:

- 64-channel (i.e. electrodes) Waveguard cap (ANT Neuro, Entschede, Netherlands)
- EEGoPro amplifier (ANT Neuro, Entschede, Netherlands)
- USB adaptor to connect the amplifier to the recording computer (tablet)
- Analogue-to-digital converter to digitise the amplified voltage potential differences

In each experiment, neural oscillations were recorded non-invasively through a 64-channel (i.e. electrodes) Waveguard cap (ANT Neuro, Entschede, Netherlands) with electrodes placed according to the 10-20 international system (Jasper, 1958).

Electrode positions are usually given identifiable names and to describe their location on the scalp with respect to the underlying areas of the cerebral cortex. Usually four reference points are taken to divide the scalp into four arcs: the nasion (point between forehead and nose), the inion (lowest point of the skull from the back of the head), and the left/ right pre-auricular points anterior to the ears. The vertex is the point of intersection between the longitudinal and the lateral arc. All electrodes are located at 10 % or 20 % of the total longitudinal or lateral distance from the vertex (Klem et al., 1999). The names and locations of the electrodes are shown in Figure 3-6.

To acquire the best EEG recording and to assure the best electrode to scalp contact and minimise electrode movement, several steps were taken. First, the participant's head circumference was measured the appropriate cap size

was chosen (i.e. small, medium and large). Then, the electrodes in the cap were placed at their appropriate site (10/20 system).

The distance between nasion-inion (between the most indented point on the bridge of the nose and the bony protrusion at the back), as well as the distance between the left and right pre-auricular points of the ear, were carefully measured. The cap was then shifted until Cz was at 50% of the nasion-inion distance and 50% of the left and right ear distance. To maintain the cap fixed, the chin strap was attached and strapped.

Wet electrodes were used to improve the quality and amplify the EEG signal. After the positioning of the EEG cap on the participant's head, a gel solution was injected between the scalp and the electrodes to lower the impedances and to improve the quality of electrode-skin connection.

To optimise the quality of the EEG data, impedances were always kept below 5 kΩ. EEG signals were recorded continuously during each experiment in all studies with the ground electrode located in AFz position and the reference electrode (used as reference for measurements by the other electrodes) in CPz. EEG data without TMS was recorded at a sampling frequency of 1000 Hz, whereas simultaneous TMS-EEG data was recorded at a sampling frequency of 2048 Hz. EEG and simultaneous TMS-EEG data were amplified by an EEGoPro amplifier (ANT Neuro, Entschede, Netherlands).

Electrooculography (EOG) was not recorded as it has been shown that ICA decomposition can be used to reliably detect and remove eye movement artefacts, such as lateral eye movements and blinks without the need for extra EOG recordings during offline pre-processing (Rogasch et al., 2014; Zhou and Gotman, 2009).
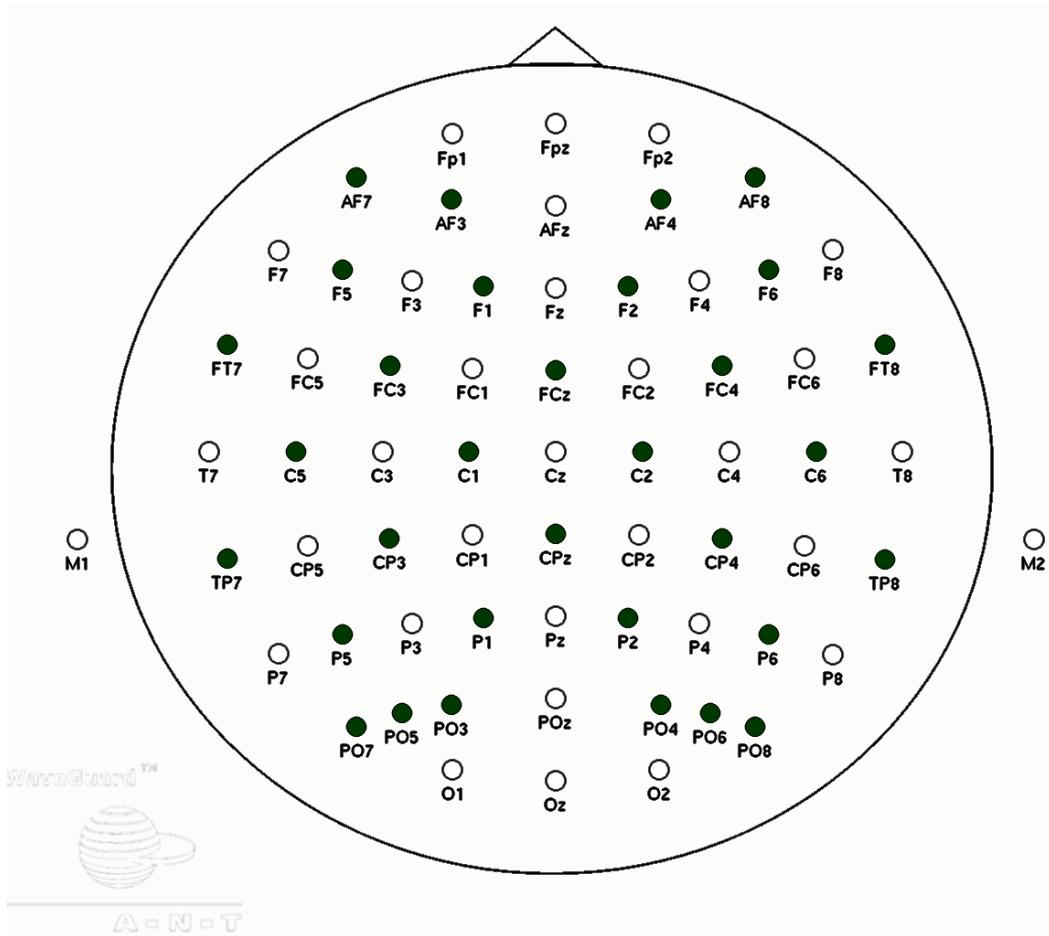
Figure 3-6: 64-channel Waveguard cap (ANT Neuro, Entschede, Netherlands). This electrode scheme allows the positioning of 64 electrodes in total. Ground electrode: AFz. Reference Electrode: CPz (Figure adapted from www.ant-neuro.com official website).

3.4.3. Simultaneous TMS – EEG acquisition

The synchronisation of EEG and TMS

In all studies, we used simultaneous TMS-EEG recordings over M1 to probe cortical excitability and plasticity. A crucial aspect of our experimental protocols is the integration of peripheral and central responses within TMS paradigms. All TMS data presented here combine both types of activity by using EEG and EMG recordings obtained concurrently with TMS applied over M1. For these measurements, it is indispensable that event-triggers in all recording devices are registered for later off-line data analysis. The triggering scheme between all the devices is shown in Figure 3-7. Most importantly, the output triggers from the magnetic stimulator (Magstim 200^2) were collected as an indication that the TMS pulse was fired in both the EEG and EMG recording devices.

Special equipment

Simultaneous TMS-EEG is technically challenging and requires special TMS-compatible EEG equipment as well as a careful experimental set-up in order to acquire clean EEG data without confounds.

EEG amplifier

TMS induces a strong electrical field and can lead to the saturation of the EEG amplifier. In the last decade, several TMS-EEG amplifier systems have been developed, including gain-control and sample-and-hold circuits that lock the EEG signal for several milliseconds immediately after the TMS pulse. More recently, DC amplifiers with a wide dynamic range allow continuous data recording without EEG signal saturation and no data loss. In this thesis, the TMS-compatible DC Waveguard amplifier from ANT was used.

EEG electrodes

It is necessary to use TMS-compatible electrodes to reduce electronic artefacts such as the polarisation of the electrolyte-electrode interface.

Usually, Ag/AgCl electrodes with a small contact or ring electrodes with a slit to reduce the magneto-electric induction in the electrodes.

TMS clicking noise

Each TMS pulse produces a loud clicking sound ranging from 100-120 dB with a rise of time lower than 0.5 ms. This time-locked sound produces auditory evoked potentials (AEPs) confounding the brain signals recorded with EEG. The TMS-induced AEP produces the well- characterised N100-P190 complex. To attenuate the AEPs, hearing protection such as earplugs or playing loud white noise at approximately 90 dB trough earphones are commonly used (Farzan et al., 2016). In all of the experiments of this thesis, we applied white noise through earphones into the participant's ears.
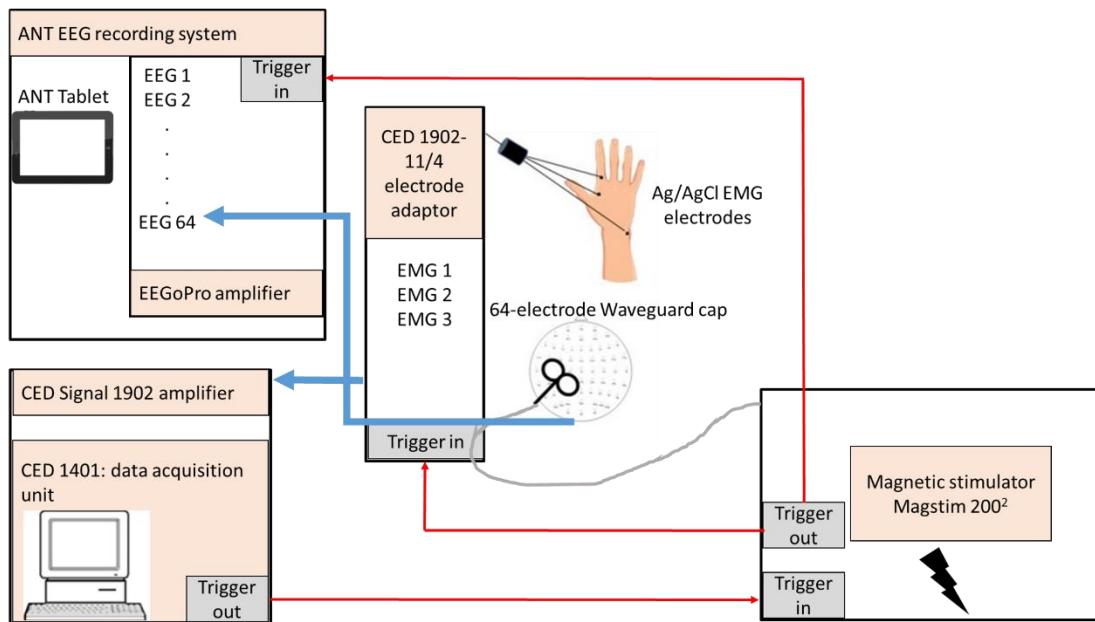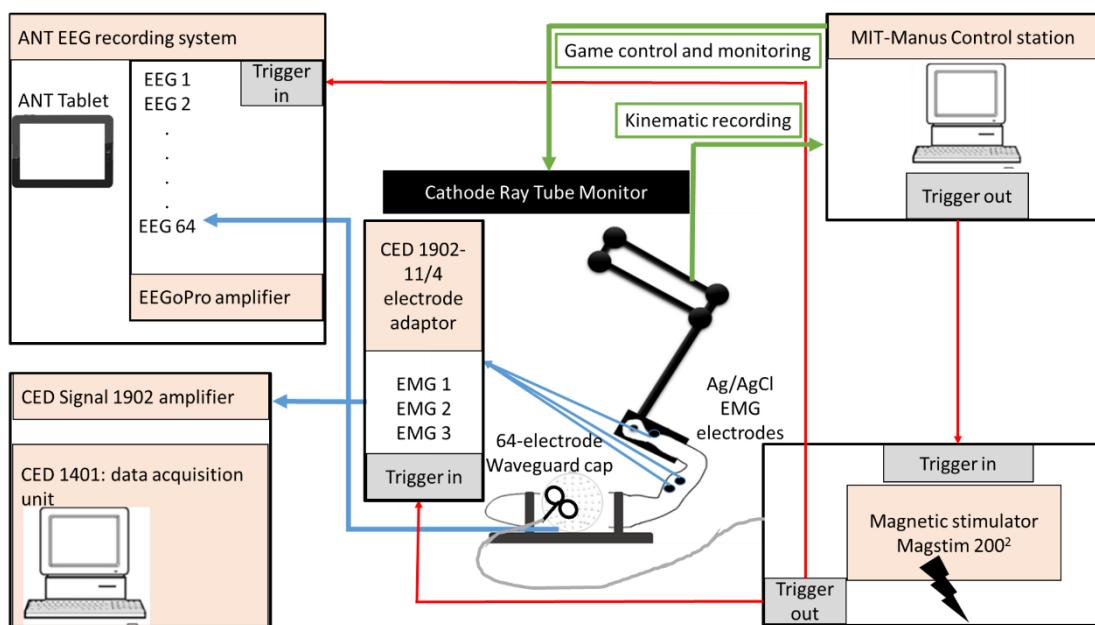
Figure 3-7: A schematic overview of the experimental setup used to record simultaneous TMS-EEG activity. It illustrated the equipment needed for the recording of EEG and EMG responses to TMS for **Study I (A)**, and for **Study II** and **III (B).**

3.5. Experimental equipment and set-up

In all experiments, we used TMS and EEG.

- **Study I:** rest and isometric contraction: TMS-EEG and pinch meter
- **Study II-III:** robot-mediated reaching protocol, TMS-EEG

3.5.1. Study I: TMS-EEG

3.5.1.1. Experimental set-up

Prior to the TMS-EEG recording, participant's manual dexterity was evaluated with the grooved pegboard task (GPT, Lafayette Instrument Co) (Klove, 1963) (Figure 3-8A) to obtain a quantitative measure of hand skill. The GPT consists of inserting 25 small pegs into small grooves using a fine precision grip as fast as possible. The time needed to insert the 25 pegs was measured for each hand.

During the TMS-EEG experiment, participants sat in a comfortable chair with their hands resting on a pillow placed on their laps. Participants were asked to maintain relaxation as EMG was monitored on a computer screen unless instructed to contract their muscle (Figure 3-8B).

A)
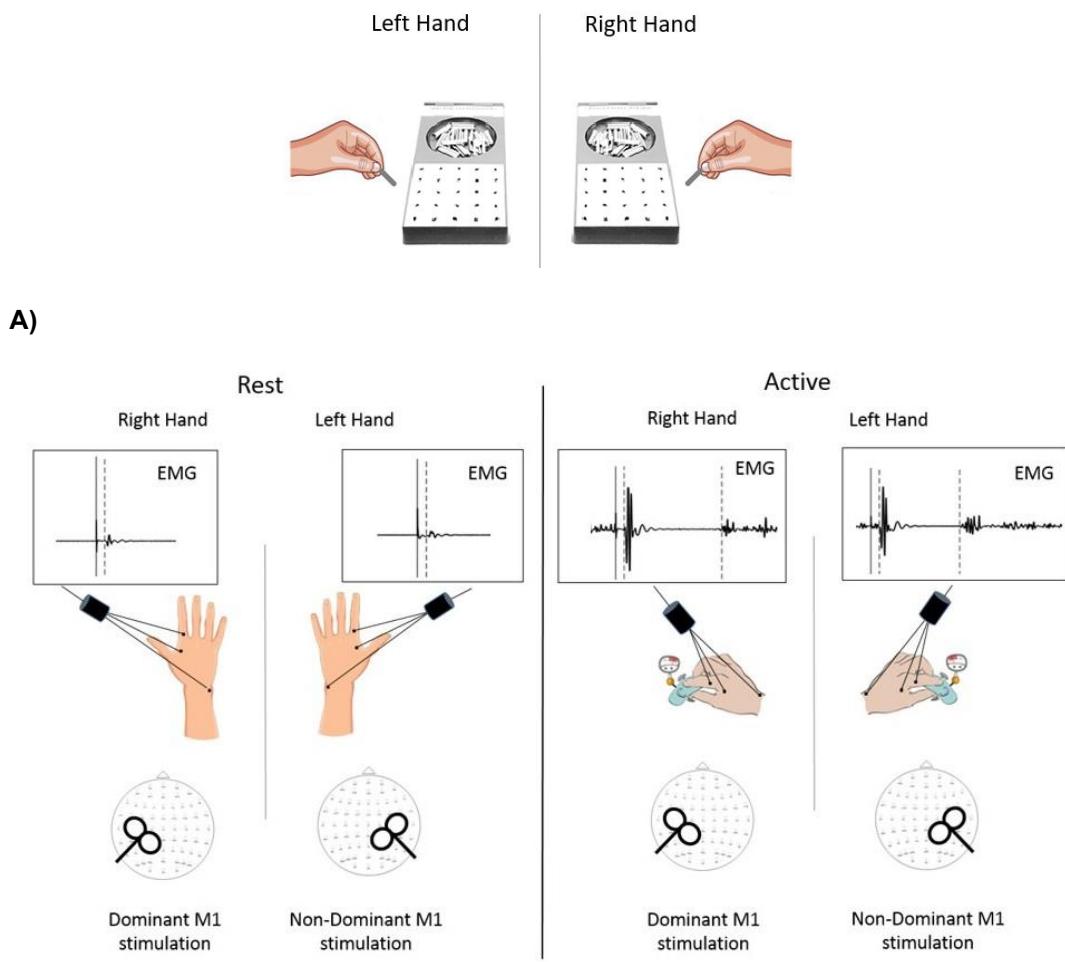
B)

Figure 3-8: Experimental equipment used in Study I. Throughout the experiment participants were comfortably seated on a chair. **A)** Grooved Pegboard Task. **B)** A total of 80 TMS single-pulses were delivered over the dominant and non-dominant M1 at 130% RMT at rest and during contraction. In the rest condition, participants were required to relax both of their hand an in the contraction condition, participants were required to hold an isometric contraction with the hand muscle contralateral to the stimulated hemisphere by pressing on the pinch meter at 40 % of their maximal voluntary contraction (MVC) for a total duration of 7 min, with breaks of 1 min every 50 s. Visual feedback was provided via a computer screen using Biometrics System (Biometrics Ltd., UK) throughout the experiment to ensure that participants maintained an isometric contraction.

3.5.2. Study II-III: Robotic device

3.5.2.1. Robot Equipment

In studies II and III a MIT-Manus robotic manipulandum (IMT2, InMotion Technologies, Cambridge, MA, USA) was used to examine different aspects of upper limb reaching movements. The robotic equipment consists of a MIT-Manus control station connected to a robot and to a vertical stimulus presentation screen. The control station is operated by a Linux software using a 16-bit analogue-to-digital and digital-to-analogue card with 32 digital lines and controls the robotic game, gives visual feedback and records the kinematic data from the robot.

The robot has 2 degrees of freedom, allowing free movements of the upper limb restricted to the horizontal plane (i.e. no vertical movements). The angular positions of the two joints of the robotic arm (later converted into Cartesian coordinates) is recorded with a sampling rate of 200 Hz by 16-bit position encoders inside the robot motors.

The robotic games are displayed on a vertical screen in front of the participant at a distance of 0.75 m. The end-effector is represented by a cursor of 0.5 cm of diameter whose position on the screen reflects the position of the joystick in the horizontal plane, serving as online feedback for participants. The manipulandum can operate in several different modalities (Figure 3-9) including:

- Non-assistive mode (no external perturbation): In this modality, the motors of the robot are switched off and participants are required to perform voluntary movements with their upper limb.
- Resistive mode (external perturbation): In this modality, the robot can apply different types of resisting forces (i.e. against the movement) while participants are required to perform voluntary movements with their upper limb and have to counteract these forces.

In both modes, kinematics is monitored by the position and force encoders throughout the reaching movements. In this thesis, we used the non-assistive

mode for **Study II** and the non-assistive and resistive modes in **Study III**. The main force-field used in this thesis is a velocity-dependent force-field as previously employed (Milner and Franklin, 2005; Thoroughman and Shadmehr, 1999) according to the formula:

$$\begin{bmatrix} F_x \\ F_y \end{bmatrix} = B \cdot \begin{bmatrix} \cos\theta & -\sin\theta \\ \sin\theta & \cos\theta \end{bmatrix} \cdot \begin{bmatrix} V_x \\ V_y \end{bmatrix}$$

Equation 3-4: Robot-mediated velocity-dependent force-field.

in which Fx and Fy are the resisting force produced in the respective directions, Vx and Vy are the end-effector velocities in the x- and y-direction respectively, B is the intensity of the force-field generated by the robot motors, and the angle θ is equal to -90° or 90° respectively for clockwise or counter-clockwise practice (Bays et al., 2005; Brashers-Krug et al., 1996).

This robot equipment, where force-fields were modified to specific protocol designs, has been extensively used in studies investigating motor adaptation and motor learning (Finley et al., 2009; Krebs et al., 1998; Krebs et al., 2001). In this thesis, a velocity-dependent force-field in the clockwise direction as has been used in previous motor adaptation studies was employed (Figure 3-9) (Hunter et al., 2009; Pizzamiglio et al., 2017b).

3.5.2.2. Reaching task

During the reaching task, participants sat in a standardised position with their right arm holding the robotic joystick (the end effector of the robot) (Figure 3-9). The right shoulder was in 70° flexion and the elbow in 90° flexion with the forearm semi-pronated. The forearm of the participant was placed in a thermoplastic trough fixed to the joystick, supporting the arm against gravity. Then the height of the chair was adjusted to ensure that the participant's shoulder was at the same level as the end effector. To minimise trunk movements, shoulder straps were used.

Participants faced a vertical screen situated at eye -level at a distance of approximately 0.7 m. The screen was used to display the robotic game and gave online feedback on the position of the displaced robot handle. The

screen displayed 8 peripheral circular targets (1 cm diameter) were positioned at a constant radial distance of 14 cm and at 45° intervals relative to a central start position (1 cm diameter) (Figure 3-10). Participants were required to displace the cursor from the central to the peripheral targets with the real-time hand position represented on the screen. The actual distance to move was 15 cm. Participants were instructed to reach the peripheral target located in the north-west direction (135°) within 1.0–1.2 s from the appearance of a visual cue (peripheral target turning red) and to stay on the target until the robot relocated the joystick at the central start position.

Reaching time feedback was visually displayed after each trial. If the participants reached the target within the required time, the text: "good" appeared. If they moved too slowly, the text: "early" appeared and when moving too fast, the text "late" turned up. Visual feedback was given throughout the duration of the experiment to ensure consistent movement speed.

Before each reaching experiment, participants received the following oral instructions:

- Make reaching movements from the centre circle the target at the circumference of the dartboard toward the north-west direction.
- Make smooth and straight movements towards the target.
- Aim to get the feedback: good as often as possible and adapt your speed if you get the feedback "slow" or "fast".
- Once you reached the target, remain in this position and wait until the robot will help you to move your arm back to the central position.
- In some trials, the robot might interfere with your movement and push or pull you off your reaching trajectory. In this case, try to keep reaching with the same speed and straightness towards the target as possible.
- Try to relax as much as you can and retract from moving your head, clenching your teeth or make jaw movements during the experiment.

3.5.2.3. Trajectory recording

During the reaching experiments, kinematic data were recorded with 16-bit position encoders embedded within the two robotic joystick joints. Specifically, the angular position of these two robotic joints was recorded and used to extract the position and velocity of the joystick in Cartesian coordinates. The position (m) and velocity (m/ s) of the end-effector in the horizontal plane (along the x and y axes), as well as the forces exerted by the participant in the 3D space (along the x, y and z axes; N) were recorded with a sampling rate of 200 Hz and stored for offline analyses on the computer.

3.5.2.4. Experimental protocol

There were two main experimental set-ups using a robotic-manipulandum to assess upper arm reaching movements. In **Study II**, visually triggered upper limb movements were assessed, and in **Study III**, motor adaptation to an external perturbation (all trials with FF) during visually-triggered movements were investigated. The experimental protocols of these studies are all based on the use of a robotic manipulandum (IMT2, Interactive Motion Technologies, Cambridge, MA, USA).

3.5.2.4.1. Study II

In **Study II**, the non-assistive mode was used to study visually-triggered upper limb movements during natural reaching (Figure 3-9).

Before the experiment, participants performed a training block consisting of 25 trials of reaching movements to familiarise with the task. The experimental protocol consisted of 360 movement trials. Each trial consisted in performing a voluntary movement with the right arm to a north-west target starting after the presentation of the visual cue from a central position, followed by a passive return to the starting position. The intertrial interval (interval between visual cues) was 3 s. Participants were asked to respond quickly to the visual cue, so that the latencies of motor responses would be between 300 and 500 ms. This latency range allowed to investigate the modulatory effects of movement preparation on evoked responses in the time range 10-220 ms

post-visual cue prior to onset of voluntary EMG. Previous experiments using a similar experimental paradigm in the same laboratory have shown that the onset of EMG activity in the BB muscle starts around 260 ms post-visual cue (Hunter et al., 2011).

The experiment consisted of 6 experimental conditions: no-TMS, TMS10, TMS130, TMS160, TMS190 and TMS220, based on a previous study investigating cortical excitability changes during movement preparation (Hunter et al., 2011). The no-TMS condition consisted of 45 trials, whereas a higher number of trials was used for TMS conditions (each consisting of 63 trials), as it has been shown that TMS-EEG data contain more artefacts and it was expected that in the TMS conditions more trials will be rejected compared to the no-TMS condition (for review see Farzan et al., 2016; Rogasch et al., 2014). Each session began with the no-TMS condition in which participants performed movements without any perturbation. This was followed by the TMS condition trials, in which TMS was applied to the contralateral or ipsilateral primary motor cortex at one of five possible timings from visual cue during movement preparation. In each of these trials, single-pulse TMS was applied at 10, 130, 160, 190 or 220 ms (i.e. referred to condition TMS10, TMS130, TMS160, TMS190 and TMS220 respectively) after visual cue similar to previous studies (Hunter et al. 2011, Turner et al., 2013). Trials of the TMS condition were counterbalanced and randomised.

3.5.2.4.2. Study III

The non-assistive and resistive mode of the robot manipulandum were used to examine visually-triggered upper limb movements during natural reaching and perturbed reaching (Figure 3-9).

The experiment was composed of 288 trials. Each trial consisted in performing a voluntary movement with the right arm to a north-west target starting after the presentation of the visual cue from a central position, followed by a passive return to the starting position. The intertrial interval (interval between visual cues) used in **Study III** of 6 s was higher compared to **Study II**. This choice was based on findings from a previous study, which demonstrated that

intertrial intervals shorter than 5 s can worsen motor adaptation performance (Francis, 2005). Since **Study III** primarily aimed to study motor adaptation processes, it was deemed reasonable to increase the intertrial interval to 6 s in line with previous studies (Faiman et al., 2018; Pizzamiglio, 2017).

The experiment comprised 3 experimental conditions: 1) familiarisation, 2) motor adaptation, and 3) wash-out conditions. During the familiarisation and wash-out conditions reaching movements were performed under a null-field and participants movement were unperturbed by the robot. In the motor adaptation condition, the robot applied a velocity-dependent force-field in the clockwise direction of 25Ns/m absolute intensity, perpendicular to the trajectory of the joystick and as such perturbed participants movements in a constant manner.

Each condition consisted of 96 trials, grouped in blocks of 4. After each block of 24 trials, a break of one minute was given. Each experiment started with 4 blocks of familiarisation, followed by 4 blocks of motor adaptation and ending with 4 blocks of wash-out. The protocol used in **Study III** is consistent with standard paradigms reported in the literature (for review see Della-Maggiore et al., 2015).
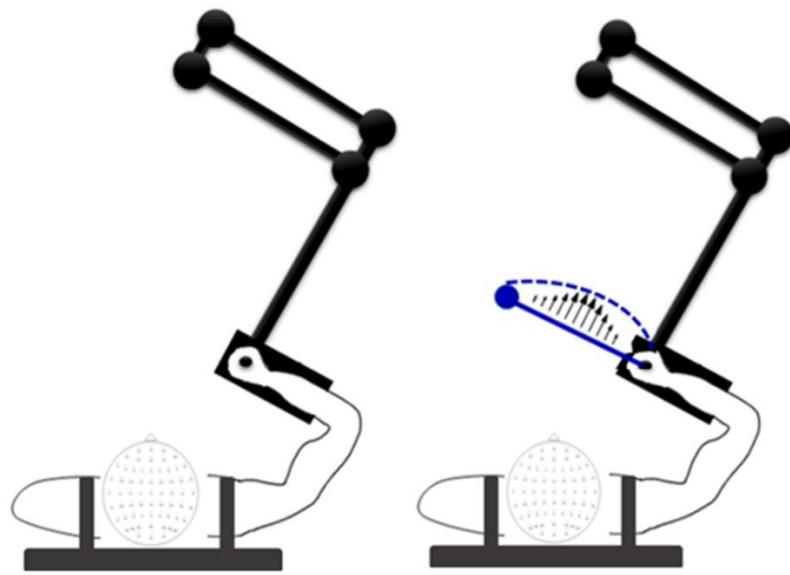
Figure 3-9: Robotic device: non-assistive (Null-Field) and resistive-mode (Force-Field).
In the non-assistive mode, the robotic device does not exert any forces (Null-Field, left panel)
on the participant's arm. In the resistive mode, the robot applies velocity dependent-forces in
the clockwise direction indicated by the arrows (right panel). The blue line represents the ideal
reaching trajectory, and the blue dashed line the trajectory deviation due to the force-field.
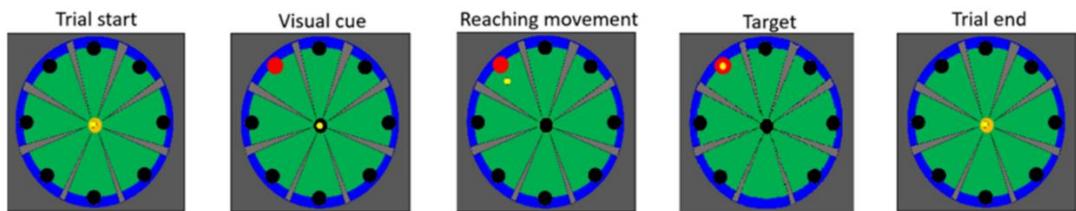
Figure 3-10: The visual display during Study II and III from a cathode-ray tube monitor. Throughout each experiment, the screen displayed a dartboard including a central circle (diameter of 1 cm) and eight peripheral target circles (each of 1 cm in diameter) positioned at a constant radial distance of 14 cm and a 45 ° intervals relative to the central circle. A cursor (yellow dot) tracked the real-time hand position of participants and was projected on the screen. Each trial started with the yellow cursor at the central position (orange dot). After the appearance of the visual cue at the target circle (north-west direction), indicated by the target turning red, the participant was required to move the yellow cursor towards the target circle and hold this position until the cursor (i.e. the hand) is passively returned by the robot to the central start position.

3.6. Signal processing

All data analyses were performed with MATLAB 2016 (The MathWorks Inc.).

3.6.1. Kinematics

Kinematics is concerned with the study of the motion of object and bodies without reference to mass or force, hence without taking care of the causes of the movement itself. Acceleration, velocity and position are all measures used in this work to describe the evolution of upper limb movements.

Reaching movements were described by a starting time point (i.e. movement onset, the time point at which the speed profile exceeds the threshold of 0.03 m/ s) and by an end time point (i.e. movement offset, the time point at which the speed profile is lower than the threshold of 0.03 m/ s post-movement onset). Modulations in movement onset and offset were monitored throughout the whole duration of the experiments in **Study II-III** to capture eventual changes in reaction times and movement durations. Reaching movements could evolve following a straight trajectory connecting the starting point and the end target, but even practised movements show small deviations from this ideal straight path.

Applying an external perturbation during movement preparation, such as by stimulating M1 with single-pulse TMS (**Study II**) or by applying a robot-mediated motor adaptation protocol (**Study III**), induces even bigger offsets from the ideal straight line.

Several methods exist to quantify movement accuracy during reaching movements including maximum and summed deflections from the ideal straight trajectory path (Hunter et al., 2009; Ozdenizci et al., 2017). This thesis used summed errors (Hunter et al., 2009), consisting in calculating the sum of the perpendicular distance (path offset) between the actual and the ideal trajectory at each time point from movement onset to offset (Figure 3-11).

Improvement of movement accuracy, reflected by a reduction in trajectory errors is characteristic of motor adaptation processes, during which

participants learn to compensate for external perturbations, such as external force-fields (Hunter et al., 2009). Since changes in movement speed and exerted forces to counteract the applied perturbation and to support the adaptation process were expected (Hunter et al., 2009; Pizzamiglio et al., 2017b), maximum velocity (m/s) and maximum force (N) were also evaluated and monitored during movement execution.
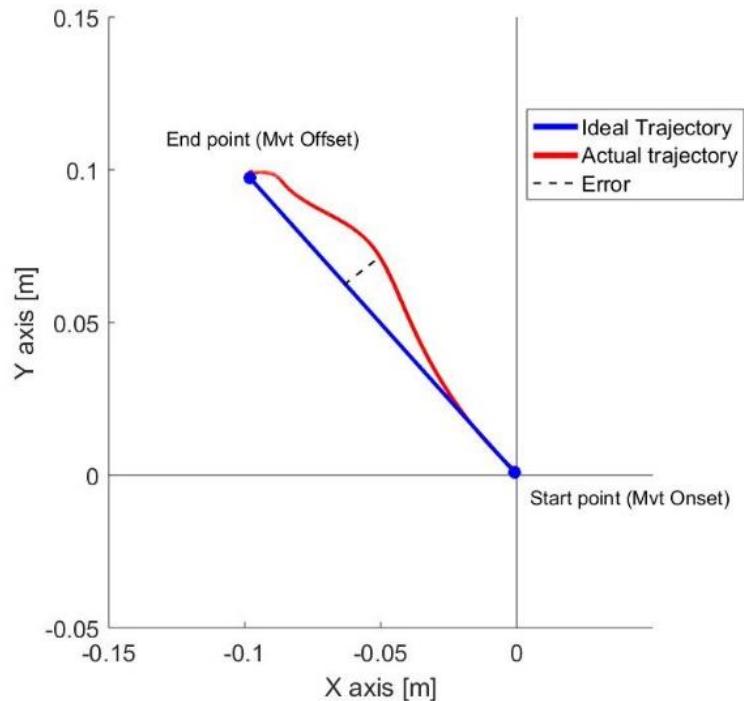
Figure 3-11: Summed error calculation. To quantify movement accuracy, summed errors were calculated as the sum of the perpendicular distance (path offset; represented with the dotted line) between the actual and the ideal trajectory at each time point from movement onset to offset.

3.6.2. EMG

EMG trials were visually inspected, and trials contaminated with physiological, and TMS artefacts were deleted using the software Signal (Cambridge Electronics Design, UK). Specifically, all TMS epochs were visually inspected: All trials with TMS pulse artefacts (Study I and II) were deleted and all trials with pre-TMS EMG activity were deleted in Study I in the rest condition and Study II in all conditions.

3.6.3. EEG

EEG

All EEG pre-processing analysis was performed on the MATLAB platform (MathWorks 2016) using the EEGLAB toolbox (Delorme et al., 2011) and its open-source extension called TMS-EEG Signal Analyser (TESA) (Rogasch et al., 2017). All EEG data were imported from the ANT software into MATLAB (MathWorks 2016).

TMS-EEG

Combining TMS with EEG introduces additional artefacts to regular EEG data recordings. These artefacts are prone to distort the underlying TMS-evoked neural activity. In this thesis, artefacts refer to any part of the EEG signal that is not primarily of interest, in opposition to TMS-evoked neural activity or ongoing neural activity. These artefacts can be diminished, and some avoided with a carefully designed experimental set-up such as using auditory masking noise to minimise auditory-evoked potentials (AEPs), careful EEG preparation (impedances below 5 kOhm), holding the TMS coil still during the recording to avoid electrode movements. However, some artefacts introduced by the interaction between the EEG recording system and the large, time-varying magnetic field generated by TMS, hence the TMS pulse artefacts, decay artefacts and electrode noise remain and have to be dealt with in the offline pre-processing analysis.

To achieve this, a semi-automated TMS-EEG pre-processing pipeline, called TESA, has been developed (Rogasch et al., 2017) and has been established

as a good cleaning pipeline that minimises the artefacts while maintaining the integrity of the neural system. This TMS-EEG pre-processing pipeline was used in this thesis, and all the steps will be detailed here. In this pre-processing pipeline, we used a method of independent component analysis (ICA) to remove artefactual data offline to reduce non-biological (TMS) and biological (eye and muscular) artefacts.

3.6.3.1. Independent Component Analysis method

ICA is a statistical and computational method that uncovers hidden factors underlying sets of random variables, measurements or signals. It consists in generating a model for observed multivariate data (Hyvärinen and Oja, 1997). The primary assumptions of the model are that the data variables are linear mixtures of some unknown latent variables, and the mixing of the system is unknown. These latent variables are thought to be non-Gaussian and mutually independent and are referred to as independent components of the observed data. These independent components can be revealed by using an ICA decomposition.

ICA can be used to decompose multivariate data such as EEG data recorded from several channels. The method of ICA consists in performing a blind source separation to find underlying or hidden independent components by separating the measured data matrix into two new matrices. The columns of the first new matrix represent the topographies of the hidden sources and the rows of the second new matrix represent the time-dependent amplitudes of the sources (Onton et al., 2006).

Each resulting component is an estimate of the unmixed signal from a single source. This method is based on three main assumptions: i) the EEG signal comprises a linear combination of activity from several cortical and non-cortical sources, ii) these sources are stationary in space, iii) these sources activity in time is independent (Onton et al., 2006). To identify and remove artefactual contributions the power spectral, the spatial and the temporal features of each independent component were inspected and those representing stereotypical artefacts were eventually discarded.

In this thesis, ICA decomposition was used to reject artefactual components of the EEG signal and performed with the 'symmetric approach' and the 'tanh' function using the FastICA algorithm (Korhonen et al., 2011). This approach was used twice: A first round of ICA decomposition was used to only identify and reject TMS-related muscle artefacts before filtering the data. A second round of ICA was used to then identify additional artefacts related to eye movements and persistent muscle activity. The identification and rejection of these artefacts were done using a semi-automated algorithm using TESA plugins. The detailed threshold selection is specified here:

Semi-automated ICA 1 and 2 component selection

1) **The threshold for semi-automated component selection for ICA1:**
    i)   **Decay artefact: TMS evoked muscle activity (Figure 3-12 and 3-13):** This artefact is detected by comparing the mean absolute amplitude of the component time course within 11 to 30 ms post-TMS pulse and the mean absolute amplitude across the entire component time course. The threshold used to detect such artefacts was set to 8, meaning the mean absolute amplitude within +11 to +30 ms post-TMS pulse is eight times bigger than the mean absolute amplitude across the entire time course.

2) **The threshold for semi-automated component selection for ICA2 (Figure 3-14 and 3-15):**
    ii)   **Eye movements:**
        a. **Blinks:** This artefact is detected by comparing the mean absolute z-score (calculated on the component topography weights) of two electrodes in the vicinity of the eyes (here FP1 and FP2). The threshold set for detecting this type of artefact was set to 2.5, meaning that the mean absolute z-score of the two electrodes should not exceed 2.5.
        b. **Lateral eye movements:** This artefact is detected by comparing the mean absolute z-score (calculated on the component topography weights) on either side of the

93

forehead (here F7 and F8). The z-score must be positive for one and negative for the other electrode and the threshold set for detecting this type of artefact was set to 2, meaning that z-score of one electrode should be greater than 2 and less than two for the other electrode.

    iii) **Persistent muscle activity:** This artefact is detected by comparing the mean power of the component time course frequency distribution between 30 and 100 ms and the mean across all frequencies (calculated using an FFT across all trials). The threshold set for detecting this type of artefact was set to 0.6, meaning that the high-frequency power is greater than 60% of the total power.

    iv) **Electrode noise:** This artefact is detected by comparing the z-scores in individual electrodes (calculated on the component topography weights). The threshold for detecting this type of artefact was set to 4, meaning that one or more electrodes have an absolute z-score greater than 4.

3.6.3.1. Step by step pre-processing of simultaneous TMS-EEG recordings

1. **Epoch Data:** EEG data were epoched from -1000 to +1000 ms around the TMS pulse.

2. **Demean Data:** EEG epochs were demeaned by performing a baseline correction from -1000 to +1000 ms around the TMS pulse to remove the DC offset.

3. **TMS pulse artefact:** The TMS pulse artefact is an early, short-lived electromagnetic artefact of the TMS pulse with a large bandwidth and no distinct spatiotemporal characteristics. This artefact is not easily detected by ICA, and its large amplitude can limit the application of some artefact rejection algorithms to the data. Therefore, the time segment contaminated with this artefact is removed prior to ICA. The most common method for eliminating the TMS pulse artefact is to remove the affected data and replace it with cubic interpolation (Casula et al., 2012; Thut et al.,

94

2011). Interpolation is important for minimising sharp transition edges which can interact with filters that will be applied later in the workflow. Specifically, the data from -2 to +10 ms around the TMS pulse were removed and a cubic interpolation using MATLAB's polyfit function was used to interpolate the missing data. A cubic function was fitted on the data either side of the removed data. Removed data was then replaced with artefact free data using data from -7 to -2 and +10 to +15 ms using cubic interpolation.

4. **Down-sample:** EEG epochs were down-sampled from 2048 Hz to 1000 Hz.

5. **Bad electrode and trial deletion:** EEG epochs were visually inspected and excessively noisy (containing mechanical artefacts) electrodes and trials were deleted. Specifically, electrodes with flat or noisy activity resulting from poor contact or mechanical artefacts, such as electrode movement were deleted. Similarly, trials with excessive noise were deleted. In particular, trials contaminated with non-stereotyped artefacts (i.e. those which cannot be eliminated with ICA), such as those due to subject motion (i.e. head movement, jaw clenching, talking, swallowing and throat clearing) were deleted.

6. **ICA1 decomposition:** Prior to ICA1, the interpolated data from step 2 was replaced with constant amplitude (zeros) which is a crucial step to improve the performance of ICA. In fact, it has been shown that adding information to the data by interpolating time points or missing electrodes can change the performance of ICA and should, therefore, be avoided (Korhonen et al., 2011; Rogasch et al., 2017, 2014). A first ICA decomposition was performed using FASTICA (Rogasch et al., 2014).

7. **ICA1 component rejection (Figure 3-12 and 3-13):** Following the ICA1 decomposition, one component representing the decay artefact caused by the TMS evoked muscle activity from the stimulation of scalp muscles, was selected based on amplitude and removed.

8. **Extend data removal:** To remove any residual muscle activity not removed with the ICA1 component rejection, data removal was extended to +15 ms post-TMS. Specifically, data between -2 and +15 ms around the TMS pulse were removed and missing data is replaced by cubic interpolation. A cubic function was fitted on the data either side of the removed data. Removed data was then replaced with artefact free data using data from -7 to -2 and +15 to +20 ms using cubic interpolation. This step is necessary prior to filtering the data, as it has been shown that it prevents sharp edges and steps in the data that can interfere with filtering. cubic interpolation prior to filtering the data is necessary, as it avoids sharp edges and steps in the data.

9. **Filter Data:** Filtering is used to exclude signals outside the bandwidth of interest. Importantly, the filtering step is performed after extracting the large-amplitude TMS artefact from the data to prevent ringing artefacts and it precedes the second round of ICA to prevent the loss of ICA components to sources outside the bandwidth of interest. Specifically, EEG epochs were first band-pass filtered using a fourth-order, Butterworth, zero-pass band-pass filter from 1-80 Hz. Then, the data was band-stop filtered fourth-order, Butterworth, zero-pass band-stop filter from 48-52 Hz to filter out and reduce power line noise.

10. **ICA2 decomposition:** Prior to ICA2 the interpolated data from step 9 was replaced with constant amplitude (zeros) which is a crucial step to improve the performance of ICA. A second ICA decomposition was performed using FASTICA to identify additional artefacts (Atluri et al., 2016; Rogasch et al., 2014).

11. **ICA2 component rejection (Figure 3-14 and 3-15):** Artefactual ICA components were identified and rejected based on five different categories: i) TMS-evoked muscle artefact ii) blink artefacts and lateral eye movements, iii) persistent muscle activity, iv) electrode movement, v) other sensory artefacts.

12. **Bad electrode and trial deletion:** EEG epochs were visually inspected and residual noisy electrodes and trials were removed. Here, the same rejection criteria described in step 5 was applied.

13. **Data interpolation:** Missing electrodes were interpolated using spherical interpolation. For visual (aesthetic) purposes, removed data were replaced with artefact free data using data from -7 to -2 and +15 to +20 ms using cubic interpolation.

14. **Reference Data:** EEG data were re-referenced to common average.

Decay artefact caused by TMS-evoked muscle activity
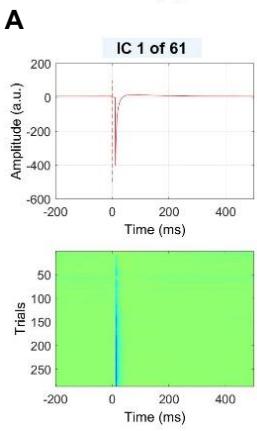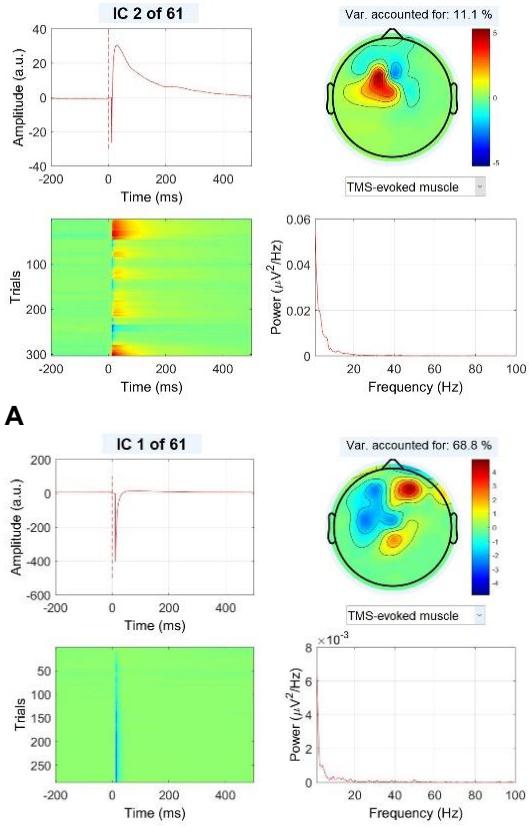
Neural Activity
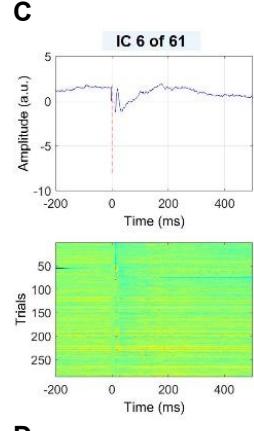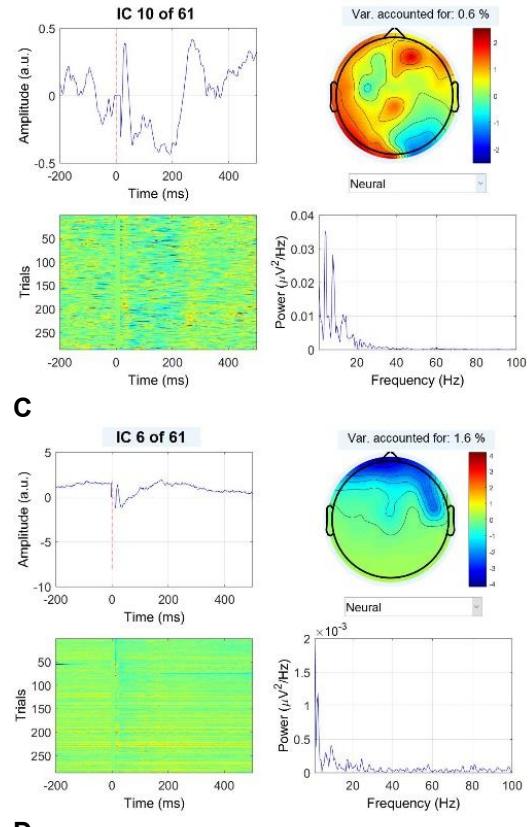
Figure 3-12: Stereotypical TMS artefacts in one representative participant: ICA1: Decay artefact caused by TMS-evoked muscle activity versus a neural component. ICA components are shown for one representative participant from **Study I**. In each subplot (**A, B, C and D**) the time course of the ICA component is displayed in the left top panel, the topographical weights of the ICA components are shown in the right top panel, the time course by trial of the ICA component is shown in the left bottom panel, and the frequency analysis of the time course of the ICA component is plotted in the right bottom panel. Classification of components is made using three main properties of the ICA component: the time course, the frequency distribution of the time course and the topography weights.
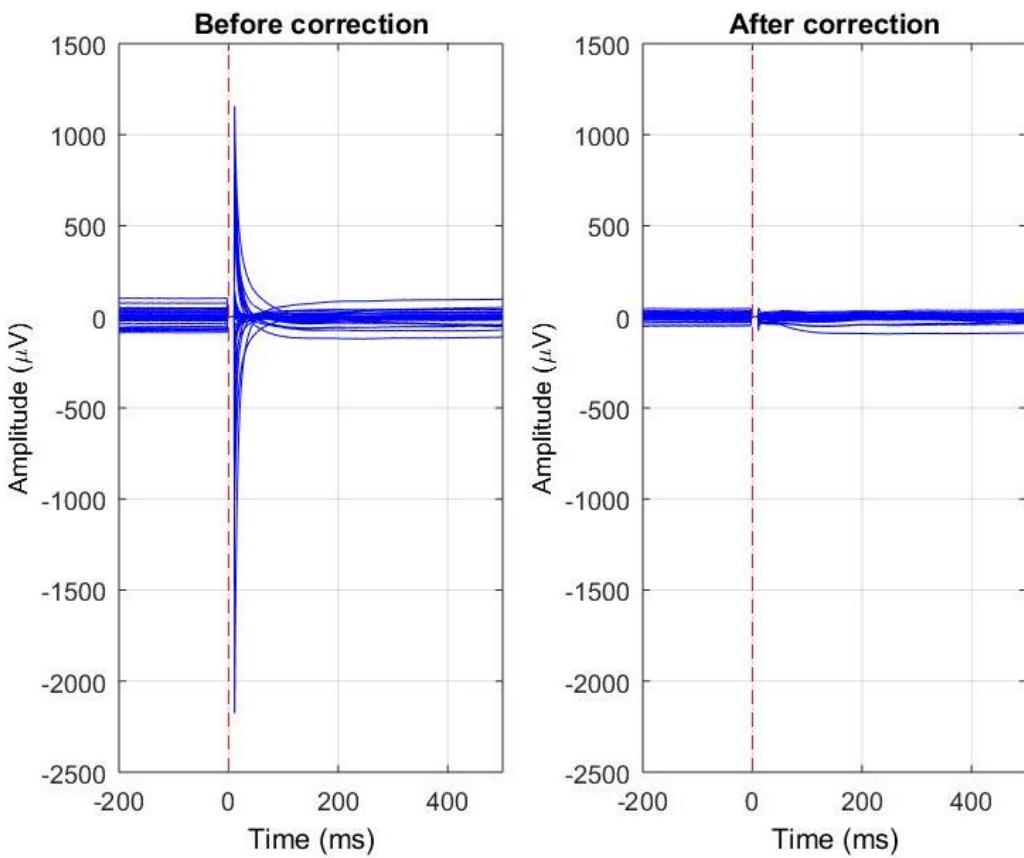
Figure 3-13 Butterfly plots of averaged epochs pre-and post-ICA1. TMS-evoked EEG activity from all electrodes (N=63) averaged across trials pre-ICA1 (left panel) and post-ICA1 (right panel). The data is represented for one representative participant from **Study I**. After removing ICA components related to the TMS decay artefact (shown in Figure 3-12) eliminates the non-physiological data from the EEG signal resulting in a drastic change of amplitude from very high amplitudes (left panel) to amplitudes in the microvolt range (right panel), corresponding to the normal physical amplitude range of neural data.
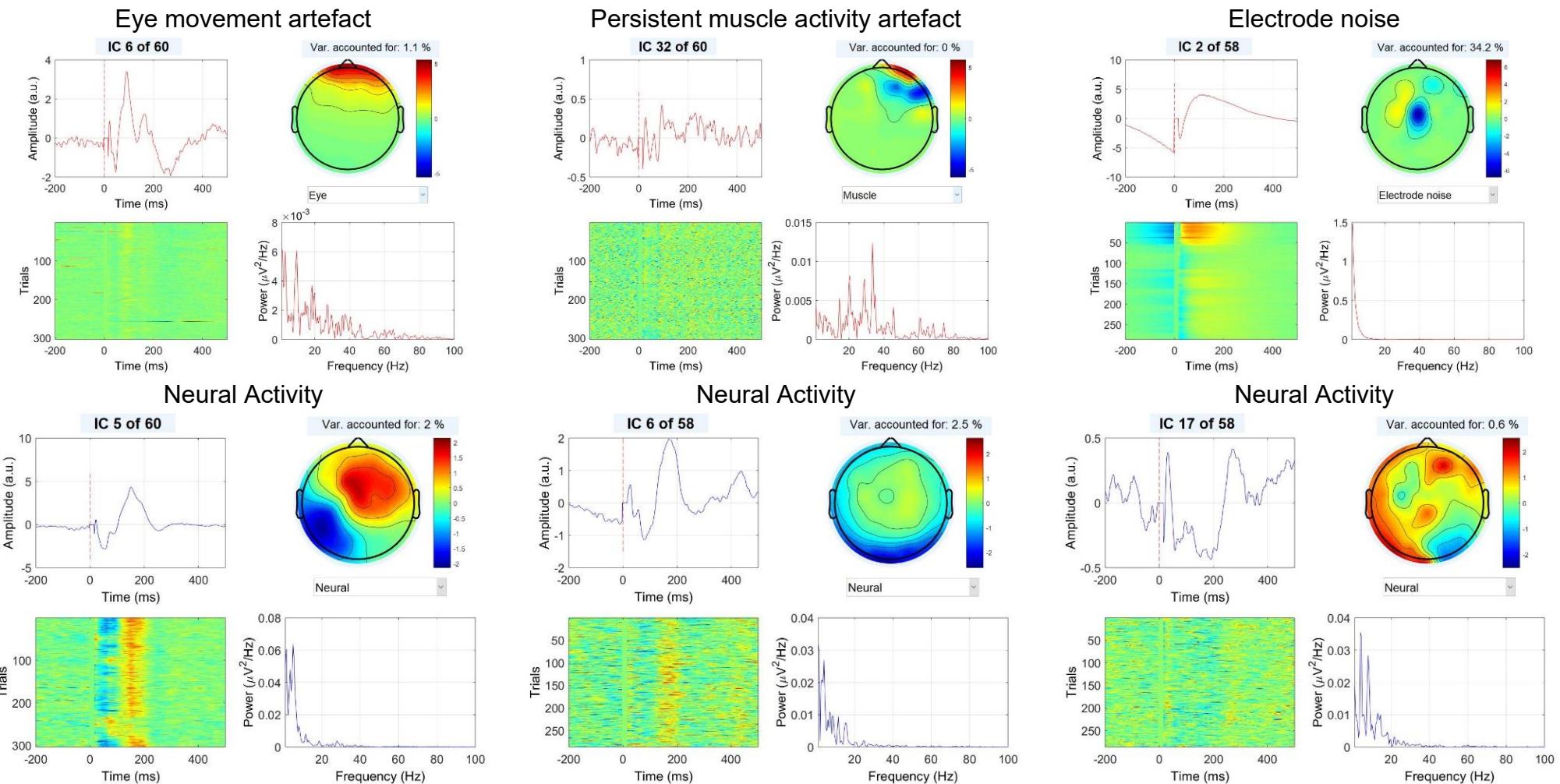
Figure 3-14: Stereotypical TMS artefacts in one representative participant: ICA2: Artefacts related to eye movements, persistent muscle activity or electrode noise versus neural activity. ICA components are shown for one representative participant from **Study I**. In each subplot the time course of the ICA component is displayed in the left top panel, the topographical weights of the ICA components are shown in the right top panel, the time course by trial of the ICA component is shown in the left bottom panel, and the frequency analysis of the time course of the ICA component is plotted in the right bottom panel. Classification of components is made using three main properties of the ICA component: the time course, the frequency distribution of the time course and the topography weights
.
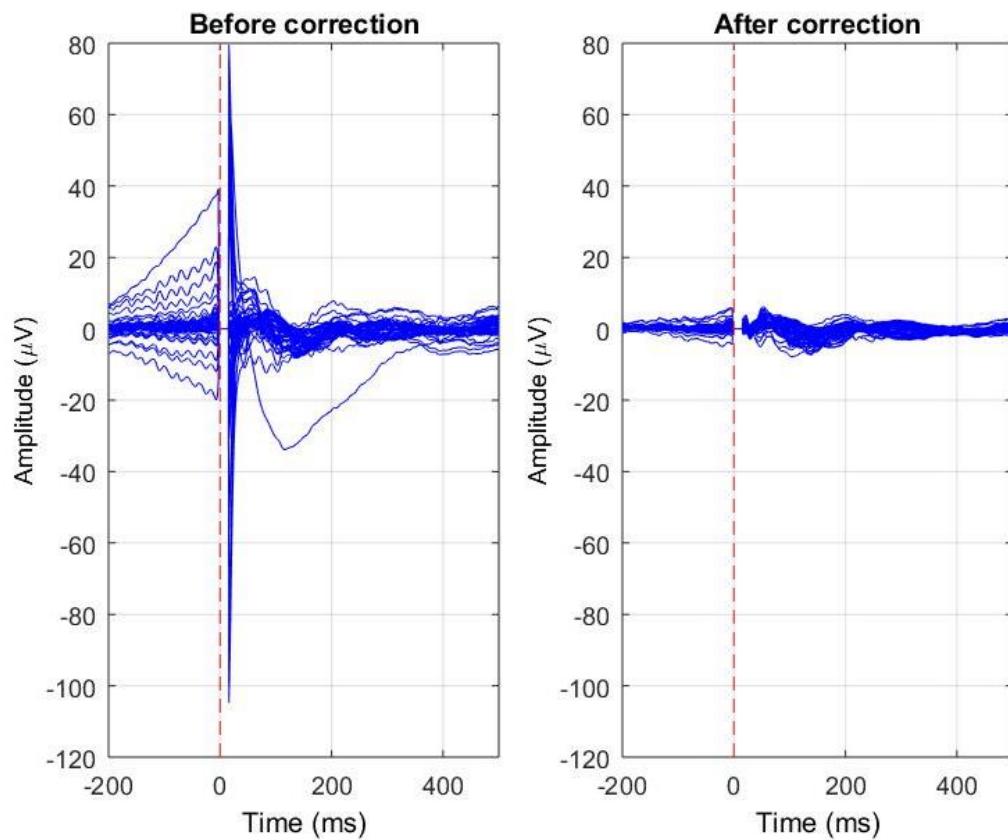
Figure 3-15: Butterfly plots of averaged epochs pre-and post-ICA2. TMS-evoked EEG activity from all electrodes (N=63) averaged across trials pre-ICA2 (left panel) and post-ICA2 (right panel). The data is represented for one representative participant from **Study I.** The right panel shows the resulting cleaned TMS-evoked EEG activity after removing ICA components related to eye movements, persistent muscle activity and electrode noise (shown in Figure 3-14).

3.6.3.2. Step by step pre-processing of EEG recordings without TMS

1. **Down-sample Data:** EEG data was down-sampled from 2048 to 1000 Hz

2. **Filter Data:** EEG data was first band-pass filtered using a fourth-order, Butterworth, zero-pass band-pass filter from 1-80 Hz. Then, the data was band-stop filtered fourth-order, Butterworth, zero-pass band-stop filter from 48-52 Hz to filter out and reduce power line noise.

3. **Epoch Data:** EEG data was epoched -1000 to +1000 ms around the visual cue.

4. **Electrode and Trials deletion:** EEG epochs were visually inspected and excessively noisy (containing mechanical artefacts) electrodes and trials were deleted. Specifically, electrodes with flat or noisy activity resulting from poor contact or mechanical artefacts, such as electrode movement were deleted. Similarly, trials with excessive noise were deleted. In particular, trials contaminated with non-stereotyped artefacts (i.e. those which cannot be eliminated with ICA), such as those due to subject motion (i.e. head movement, jaw clenching, talking, swallowing and throat clearing) were deleted.

5. **ICA decomposition:** ICA decomposition was performed using FASTICA.

6. **ICA component rejection:** Artefactual ICA components were identified and rejected based on five different categories: i) blink artefacts and lateral eye movements, ii) persistent muscle activity, iv) electrode movement, v) other sensory artefacts.

7. **Electrode and Trials deletion**: EEG epochs were visually inspected and residual noisy electrodes and trials were removed. Here the same rejection criteria described in step 4 was applied.

8. **Data interpolation:** Missing electrodes were interpolated using spherical interpolation.

9. **Re-reference Data:** Epochs were re-referenced to common average.

3.7. Statistical analyses

Prior to all other statistical tests, normal distribution of the data was always checked using the Shapiro-Wilk test. This test was chosen above that of Kolmogorov-Smirnov because it was more appropriate for the small sample size.

Sample sizes used in the three studies were similar to those reported in the literature but no a prior power calculations were performed to determine how many participants were needed to reach significant results.

In order to discuss whether negative findings reported in the studies could be linked to underpowered studies, a series of power analyses based on the used sample sizes were conducted for selected comparisons using Cohen's d (Cohen, 2013) as the measure of effect size.

Power analyses were performed in G Power version 3.1 (Faul et al., 2007), using standard assumptions of alpha = 0.05, power (1-β) = 0.80, and two-tails for t-tests. Effect size index f were estimated from the partial eta squared (η2) for multivariate analysis of variance (MANOVA) and ANOVA and from group parameters (mean and standard deviation (SD)) for paired comparisons (t-tests or Wilcoxon signed rank tests).

3.7.1. Kinematics and EMG

When comparing two conditions paired t-tests were applied if data was normally distributed. If the assumption of normal distribution was not met, non-parametric Wilcoxon rank tests were employed. In these comparisons, a statistically significant difference was set at an alpha = 0.05.

In studies, which compared more than two groups, in case of normally distributed data, repeated-measure MANOVA and/or ANOVA were first performed and if significant they were followed by post-hoc ANOVAs or paired t-tests, respectively, with Bonferroni correction applied. If the data were non-normally distributed a Friedman test, followed by post-hoc Wilcoxon sign rank tests were performed.

3.7.2. EEG: non-parametric permutation-based statistics

The multidimensionality (spatiotemporal or spatiotemporal-spectral) of the EEG data creates an enormous number of multiple comparisons in statistical analysis and needs to be taken into account. Differences across experimental conditions are indeed evaluated at a high number of (electrode, time)-pairs or (electrode, time, frequency)-triplets. Non-parametric permutation-based t-tests or repeated-measure ANOVAs implemented in EEGLAB can be used to minimise the number of false discoveries.

This method offers great flexibility to test a global hypothesis in EEG analysis. The main advantage of this method is that the tests are distribution free, no assumptions of an underlying correlation structure are needed and it provides exact p-values for any number of time points and recording sites (Fields and Kuperberg, 2018). The function statcond as implemented in EEGLAB (statcond.m, 2000 permutations, $p < 0.05$ (False Discovery Rate (FDR); (Benjamini and Yekutieli, 2001)), was used to determine the electrodes in which EEG outcome measures were statistically different. Specifically, each EEG outcome measure from each electrode from each participant is permuted (2000 permutations) across conditions. In this way, the t-test or ANOVA was performed with surrogate data (i.e., shuffle participants across conditions, which represents the null hypothesis that the conditions come from the same distribution, hence no mean difference) for 2000 times. These 2000 F statistics form the null distribution and any electrode with a t- or F-value in the unpermuted data that was greater than 95 % (i.e. $p < 0.05$) of values in this null distribution was considered significant. FDR correction was applied to adjust for multiple comparisons.

When EEG data were analysed in a single electrode or a single region of interest the same statistical tests explained in the previous section (applied to EMG and kinematic data) were performed.

3.7.3. Correlations and linear regressions

The relationship between behavioural data and neural data was tested using Pearson's correlation when data were normally distributed, and Spearman correlations if this assumption was not met.

To investigate neural predictors of behavioural data, linear regressions were performed. If the residuals were not normally distributed, a bootstrapping (Efron and Tibshirani, 1986) method was used, which helps to estimate the properties of the sample distribution from the sample data.

All statistical tests were performed using MATLAB statistical toolbox (MathWorks Inc., Natick, MA, United States), EEGLAB (Delorme et al., 2011) statistical tools and SPSS (IBM SPSS Statistics for Windows, Version 24.0). For all statistical analyses, the level of significance was a priori set to $\alpha = 0.05$.

Chapter 4 - Cortical Excitability: Dominant versus Non-Dominant M1

4.1. Introduction

Humans use their hands asymmetrically in daily activities with a lateralised preference towards one hand, with 90 % of individuals showing a rightward preference (Perelle and Ehrman, 2005). The term handedness is commonly defined as the hand that performs faster or more precisely on manual tasks and/ or the hand that one prefers to use, regardless of performance. It is thought that the asymmetrical functions of the hands reflect an asymmetrical neural control, sensorimotor organisation and cortical excitability.

Due to the key role of the M1 and its projections in controlling fine upper limb movements, much research has focussed on investigating neural asymmetries at this level of motor control. In humans, the M1 located in the pre-central gyrus is the area associated with limb movements (Penfield and Boldrey, 1937) and is the start of the final motor command pathway: Neural signals from M1 project down to the spinal cord and control the execution of movement (Scott et al., 2000).

The pyramidal tracts consisting of the corticobulbar tract and CST constitute the main descending pathway for controlling movement. The CST is the principal motor pathway for controlling upper limb voluntary movement (Lemon et al. 2008). A person's ability to perform skilled finger activities is dependent on the lateral corticospinal pathway from M1 to the spinal motor neurons controlling the fingers and hand muscles (Porter and Lemon, 1993). These lateral corticospinal fibres project inferiorly to the contralateral side, providing a robust contralateral control of hand and finger muscles (for review see Lemon, 2008).

4.1. The impact of motor dominance

Motor (hand) dominance plays a key role in motor recovery (for review see Sainburg and Duff 2006). Specifically, motor recovery and lateralised cortical

activity depend on whether the dominant or the dominant hemisphere is affected in stroke (Harris and Eng, 2006; Lüdemann-Podubecká et al. , 2015, Liew et al., 2018,). Motor recovery of the affected upper limb is determined by dominance of the affected hemisphere (Lüdemann-Podubecká et al., 2015), with a stroke of the dominant hemisphere being associated with poorer improvements of the affected upper limb. Furthermore, while an inhibitory rTMS stimulation over the contralesional M1 significantly improves dexterity of the affected hand in patients with a lesion in the dominant hemisphere, it does not in those with lesion in the non-dominant hemisphere. Furthermore, shifts in lateralised cortical activity post-stroke are influenced by hand dominance. In an fMRI study, Liew et al. (2018) demonstrated that stroke patients with right hemisphere lesions have a greater activity in the dominant (left hemisphere) rather than the ipsilesional (right) hemisphere during action observation. This left-lateralisation was similar to the patients with left dominant hemisphere stroke. These findings highlight the importance of carefully considering dominance and laterality when assessing post-stroke neural activity and recovery.

4.1.2. Anatomical asymmetries

Anatomical asymmetries between motor cortices related to handedness have been investigated with functional imaging studies, reporting a leftward asymmetry in the size of M1 in consistent right-handers in healthy male individuals (Hervé et al., 2006, 2009, 2005, Angstmann et al., 2016). It has also been shown that consistent right-handers have a deeper central sulcus and more horizontal connections in the left (dominant) M1 (Amunts et al., 1996). Attempts have been made to link corticospinal asymmetries to handedness. A leftward asymmetry of the volume of the corticospinal fibres has consistently been reported (Nathan et al., 1990; Rademacher et al., 2001; Thiebaut de Schotten et al., 2011), but this asymmetry was not related to handedness, since the leftward shift was found in both right and left-handers (Kertesz and Geschwind, 1971; Westerhausen et al., 2007). Recently, however, it has been shown that asymmetries in frontoparietal tracts, as opposed to those in CSTs, are more robustly correlated with handedness and manual specialisation (Howells et al., 2018).

The asymmetrical anatomical findings do not translate into clear corresponding functional neurophysiological asymmetries as measured with corticomotor excitability using TMS. For instance, motor cortical output map studies investigating differences between the dominant and non-dominant M1 have reported contradictory results. Some studies found no significant interhemispheric differences (Cicinelli et al., 1997, Civardi et al., 2000, Rossini and Rossi, 1998), while others reported significant differences between the dominant and non-dominant hemisphere (Koski et al. 2005, Macdonell et al., 1991, Triggs et al., 1994). These inconsistent findings can be attributed to individual anatomical cortical differences. Using neuronavigation in combination with individual MRIs can improve precision of TMS measurements and is increasingly used in TMS studies. Using this more precise method by applying a navigated TMS mapping, Bashir et al. (2013) reported no significant interhemispheric differences.

TMS studies of hemispheric differences in cortical excitability have also produced conflicting results with regard to handedness as reviewed by Hammond et al. (2002). For example, while some studies found asymmetries in resting motor threshold (RMT) with lower values for the dominant M1 (Cicinelli et al., 1997), others reported an opposite result in showing that the non-dominant M1 is more excitable than the dominant M1 in both right- and left-handers (Daligadu et al., 2013). These conflicting results could be related to differences in TMS protocols but also to the fact that most commonly handedness was measured as a dichotomous and not continuous variable (i.e. degree of lateralisation), which could have contributed to the diverse findings as pointed out by Bernard et al. (2011). However, even when using a three-way classification (right-, left- and mixed handedness), Davidson et al. (2013) reported no significant influence of the degree of handedness and no hemispheric asymmetries in corticospinal excitability (as measured with RMT, MEP amplitude and motor output mapping).

4.1.3. TMS-EEG to assess asymmetries in M1 and CST

Several TMS protocols that can be used to probe cortical excitability (for review see Ziemann, 2017). By applying single-pulse TMS over M1 active

excitatory and inhibitory processes acting on the output cells in M1 can be revealed. TMS over M1 can produce MEPs or cortical silent periods (CSPs). While MEPs reflect the ability to induce action potentials in the CST (Rossini et al., 2015), CSPs correspond to the inhibitory activity of M1. Single TMS pulses over M1 during voluntary contraction of a contralateral muscle evoke an MEP followed by a silent period in the EMG activity. The duration of the CSP is a measure of intracortical inhibition due to activation of $GABA_B$ interneurons that synapse on pyramidal neurons and can be used as a biomarker of inhibition (Siebner et al., 1998, Werhahn et al., 1999).

Recently, the simultaneous recording of TMS-EEG has been established as a useful tool to study both cortico-cortical and corticospinal axons. Cortical responses to TMS can be captured with EEG as a series of evoked potentials (TEPs) (Bonato et al., 2006, Ilmoniemi et al., 1997, Paus et al., 2001), as well as in a modulation of spontaneous oscillatory activity (TRSP) (Fecchio et al., 2017, Rosanova et al., 2009). Cortical responses to TMS measured with EEG could expand the previously mentioned findings from TMS studies by capturing asymmetries directly at the cortical level and corticospinal level. Given that hemispheric asymmetries might rely on motor cortical asymmetries outside the CST (Howells et al, 2018, Westerhausen et al., 2006), this method could provide further insights into the neural correlates underlying motor dominance.

Since so far, the neural correlates leading to motor dominance are still not fully understood in healthy individuals but seem to have an impact on stroke recovery, this study aimed to investigate neural asymmetries underlying motor dominance.

Specifically, this TMS-EEG study examined hemispheric asymmetries between motor cortices in right-handers in two different motor states (at rest and during contraction) by applying single-pulse TMS to the dominant and non-dominant M1. The study used several excitability readouts including cortical responses to TMS measured with EEG (i.e. evoked potentials and induced oscillations) and peripheral responses measured with EMG (MEP and CSPs) to evaluate hemispheric asymmetries related to motor dominance.

As a first aim, this study was to replicate characteristic TMS evoked cortical responses reported in the literature to test whether TMS-evoked components were reliably elicited in all participants. It was expected that single-pulse TMS would elicit the characteristic TMS-evoked responses in the time domain (positive and negative deflections post-TMS pulse, which are reported in the literature (i.e. P30, N45, P60, N100, P190 and N280) and in the time-frequency domain (i.e. ERS followed by ERD post-TMS pulse).

The second aim, was to identify potential motor cortical excitability differences linked to motor dominance. It was hypothesised that cortical excitability will be higher in the dominant compared to the non-dominant M1 and that this difference would be further increased when holding an active contraction compared to rest.

4.2. Methods

4.2.1. Research Design

This study used a within-subject design to test the effect of hemispheric motor dominance and motor state by applying single-pulse TMS to the dominant and non-dominant M1 at rest and during contraction. The independent variables were Hemisphere (dominant versus non-dominant) and State (rest versus contraction). The main outcome measures were cortical excitability measures including six TEP components (P30, N45, P60, N100, P190 and N280) and TMS induced time-frequency responses (ERS and ERD). Secondary outcome measures included peripheral corticospinal excitability measures (MEP amplitudes and CSP durations) as well as behavioural outcome measures (MVC and GPT speed). Before the TMS protocol, several behavioural tests were carried out including measures of handedness, dexterity and MVC. The whole experimental session with EEG preparation and TMS hotspot definition lasted around 3 hours.

4.2.2. Participants

Sixteen right-handed healthy young participants (14 females, mean age ± SD = 26 ± 5 years, age range: 20 - 43 years) were recruited. Since the primary goal of the study was to determine if TEP and TRSP reported in TMS-EEG studies could reliably be reproduced with the current setting, the sample size

was determined by matching the one from previous TMS-EEG studies. Furthermore, no a priori sample size calculation was performed using a power calculation, since no previous data on the effect of motor dominance and motor state on TEPs and TRSPs was available. The sample size was similar to other TMS-EEG studies (N = 9, 4 females (Bonnard et al., 2009), N = 6, 3 females (Bonato et al., 2006), N = 17, 12 females (Petrichella et al., 2017)) reported in the literature. However, in order to discuss whether the study was underpowered to detect effects of motor dominance, post-hoc power calculations were performed and will be reported in the discussion in order to determine if lack of significance could be due to an underpowered study.

4.2.3. Behavioural tests prior to the experimental protocol

4.2.3.1. Handedness

Participants hand preference was assessed with the Edinburgh Handedness Inventory (Oldfield, 1971), a 10-item questionnaire which yields a lateralisation quotient ranging from -100 (consistent left-handedness) to +100 (consistent right-handedness). The laterality quotient (LQ) was derived as following: [(Right-Left)/ (Right + Left)] *100, where positive scores between +30 to +100 indicate right-handedness, negative scores between -100 to -30 left-handedness and scores between -30 and +30 ambidexterity (Fagard et al., 2015). The LQ served as a more objective measure of handedness and allowed to evaluate the accuracy of self-reported right-handedness. Specifically, we wanted to make sure that participants were right-handed according to the LQ with scores above +30 (Fagard et al., 2015).

Hand dexterity was further tested with the grooved pegboard task (GPT, Lafayette Instrument Co) (Klove, 1963) to obtain a quantitative measure of hand skill. The GPT consists of inserting 25 small pegs into small grooves using a fine precision grip as fast as possible. The time needed to insert the 25 pegs was measured for each hand and the dexterity laterality score was derived as following [(Right$_{GPT}$ –Left$_{GPT}$)/ (Right$_{GPT}$ + Left$_{GPT}$)]*100.

4.2.3.2. Maximal voluntary contraction (MVC)

Since participants were required to hold a contraction at 40% of their maximal voluntary contraction (MVC) during the experimental TMS protocol, the MVC was first assessed in both hands prior to the experiment. Specifically, thumb index finger pinch strength was assessed using a small pinch gauge meter (Hand Pinch Pinchmeter P200, Biometrics Ltd., UK). This test provided an index of the pinch strength (by measuring the force load in N) elicited by the first dorsal interosseous muscles (FDI) during maximal muscle contraction. Participants performed 3-second contractions for three trials with either hand with 20 s breaks, and the average of the trials of each hand provided a measure of MVC (Newtons, pinch strength).

4.2.4. EEG and EMG acquisition

Following the behavioural tasks, participants sat in a comfortable chair in the experiment room: the EEG cap was placed to record cortical signals; EMG electrodes were placed on the right and left FDI muscles to record EMG activity. A detailed description of EMG and EEG recording and the set-up refer to **Chapter 3** (section 3.4.1.1 and 3.4.2 respectively). EEG and EMG were continuously recorded during the experimental protocol.

4.2.5. TMS targeting: RMT

Single-pulse TMS were applied over the dominant (left) and non-dominant (right) M1 at 130% RMT targeting the dominant (right) hand muscle (FDI) and non-dominant (left) hand muscle (FDI) respectively. A detailed description of the motor hotspot and RMT selection is presented in **Chapter 3** (General Methods; section 3.4.1.2). In brief, RMT for each M1 was determined after the positioning of the EEG cap. This intensity corresponded to an average of 52 ± 6 % of maximum stimulator output (MSO) for the left M1 and of 53 ± 7 % of MSO for the right M1.

This study employed a stimulation intensity of 130% RMT, which is the most commonly reported in the literature when measuring CSP (Orth and Rothwell, 2004, Poston et al., 2012, Werhahn et al., 1999). The relatively high

stimulation intensity ensured that the elicited CSP duration is long enough to be accurately quantified compared to shorter CSP durations elicited by lower TMS intensities. Moreover, since long CSP durations (> 75 ms) reflect exclusively cortical mechanisms (Chen et al., 1999; Fuhr et al., 1991; Inghilleri et al., 1993) as opposed to short CSP durations (< 75 ms) which reflect spinal mechanisms (Chen et al., 1999; Fuhr et al., 1991), the high stimulation intensity used in this study ensured that intracortical mechanisms were investigated (Poston et al., 2012). MVC was set to 40 % similar to Farzan et al. (2013) and not higher to avoid muscle fatigue. To minimise the influence of muscle fatigue on TMS responses, periodic rest breaks (every 10 trials) were provided during the TMS protocol. The level of MVC when assessing the CSP duration vary across studies, but it has been shown that the level of contraction does not influence the CSP duration (Saisanen et al., 2008).

4.2.6. Experimental Protocol

Participants were seated in a comfortable chair with their hands resting on a pillow placed on their laps. Participants were asked to maintain relaxation unless instructed to contract their muscle and EMG was monitored on a computer screen (Figure 4-1).

Two TMS paradigms were applied to investigate hemispheric asymmetries in different states (rest versus contraction). In the rest condition, participants were required to relax both of their hands. In the contraction condition, participants were required to hold an isometric contraction with their hand muscle (FDI) contralateral to the stimulated hemisphere. Participants were asked to press on the pinch meter at 40% of their MVC.

Visual feedback was provided via a computer screen using the Biometrics System (Biometrics Ltd., UK) throughout the experiment to ensure that participants maintained an isometric contraction. Specifically, the force level output was displayed on the monitor in front of the participant and visible to the investigator. If the contraction dropped below 40% MVC prior to the TMS pulse, the TMS protocol was paused and a break was given. This was done, in order to ensure that varying forces would not influence the CSP durations

or MEP amplitudes. This measure of precaution was taken, even if previously it has been shown that muscle force does not have to be accurately controlled to get reliable CSP measurements (Saisanen et al., 2008).

A total of 80 single-pulse TMS were delivered over the dominant and non-dominant M1 in four blocks for each condition (dominant M1 stimulation rest, dominant M1 stimulation contraction, non-dominant M1 stimulation rest and non-dominant contraction). The interstimulus interval between TMS pulses was, on average, 5 s (random intertrial interval variation of 20 % to reduce anticipation of the next trial). Breaks every 10 trials were given to minimise muscle fatigue and to control for participant's attention and engagement in the task. The order of stimulation targets and conditions were counterbalanced across participants.
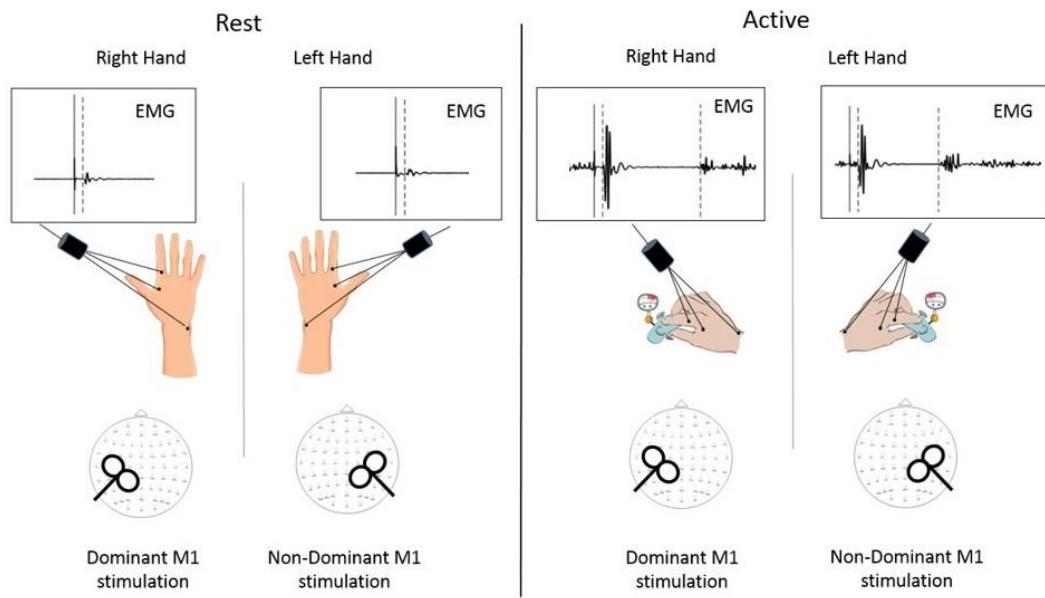
Figure 4-1: Experimental set-up. Throughout the experiment, participants were comfortably seated on a chair. A total of 80 TMS single-pulses were delivered with an interstimulus interval of 5 seconds and a variance of 20 % over the dominant and non-dominant M1 at 130 % RMT in four blocks for each condition (dominant M1 stimulation at rest and during contraction, non-dominant M1 stimulation at rest and during contraction,) The order of stimulation targets and conditions were counterbalanced across participants. In the rest condition, participants were required to relax both of their hands. The schematic EMG trace illustrates the MEP. In the contraction condition, participants were required to hold an isometric contraction with their hand muscle (FDI) contralateral to the stimulated hemisphere by pressing on a pinch meter at 40 % of their maximal voluntary contraction (MVC) for a total duration of 7 min, with breaks of 1 min every 50 s. Visual feedback was provided via a computer screen throughout the experiment to ensure that participants maintained an isometric contraction. The schematic EMG trace illustrates the MEP followed by a CSP.

4.2.7. EMG Pre-processing and analysis

In the rest and contraction conditions, EMG was continuously recorded and MEP peak-to-peak amplitudes of the FDI muscle contralateral to the stimulation site was recorded and analysed offline. In the contraction condition, the silent period was recorded during the 40 % voluntary isometric contraction of the FDI muscle contralateral to the stimulation site. EMG trial data were visually inspected, and trials contaminated with physiological (e.g. EMG activity pre-TMS in the rest condition), and TMS pulse artefacts were deleted using the software Signal (Cambridge Electronics Design, UK). After trial rejection, each condition contained at least 77 artefact free trials. Specifically, the dominant rest condition contained 79 ± 4 trials, the dominant contraction condition 78 ± 6 trials, the non-dominant rest condition 78 ± 5 trials and the non-dominant contraction condition 77 ± 8 trials.

For each participant, the mean peak-to-peak amplitude of MEPs was measured trial-by-trial as the difference between the maximum, and minimum peak detected 10-40 ms post-TMS. The CSP duration was measured trial-by-trial as the time between the first MEP peak and the first reoccurrence of EMG signal (CSP offset) according to commonly used methods (Farzan et al., 2013; Saisanen et al., 2008).

4.2.8. EEG Pre-processing and analysis

4.2.8.1. TMS-EEG pre-processing

EEG data of rest and contraction condition were merged for dominant M1 stimulation and non-dominant M1 stimulation in two separate files and pre-processed together. Data were epoched (- 1 to + 2 s) around the TMS pulse. Epochs were demeaned by subtracting the average between - 1 to + 2 s from each epoch to remove the DC offset. This was done instead of using a baseline correction (e.g. from -1 to 0), since it has been demonstrated that it improves the subsequent ICA reliability compared to baseline removal (Groppe et al. 2009, Rogasch et al., 2017).

The TMS pulse artefact was removed from - 2 to + 10 ms around the TMS pulse and removed data was replaced with artefact free data using data from - 7 to - 2 and + 10 to + 15 ms using cubic interpolation. EEG data were then down-sampled from 2048 Hz to 1000 Hz. Electrodes and epochs with mechanical artefacts were identified by means of visual inspection and rejected. After this step, each condition contained at least 75 artefact free trials, specifically, the dominant M1 rest condition contained 77 ± 7 trials, the dominant M1 contraction condition contained 76 ± 4 trials, the non-dominant M1 rest condition contained 79 ± 3 trials and the non-dominant M1 contraction condition contained 77 ± 8 trials on average across participants. On average across participants 3 ± 1 electrodes (i.e. 5 ± 1.6 % of total electrodes) were deleted.

Data were then submitted to an ICA decomposition using the FASTICA algorithm (Korhonen et al., 2011) and components representing TMS evoked muscle artefacts were identified and rejected. In the dominant M1 condition 3 ± 1 components (i.e. 6 ± 2 % of total ICA components) and in the non-dominant M1 condition 3 ± 1 components (i.e. 6 ± 2 % of total ICA components) were rejected on average across participants. Data between -2 and +15 ms around the TMS pulse were removed and replaced with artefact free data using data from -7 to - 2 and +15 to + 20 ms using cubic interpolation. A bandpass filter (1-80 Hz, zero-phase Butterworth filter, order = 4) and bandstop filter (48-52 Hz, zero-phase Butterworth filter, order = 4) to remove line noise (50 Hz) were applied. Then, a second round of ICA decomposition was performed and all the remaining artefacts (eye-blinks, lateral eye movements, electrode movement and electrical artefacts) were identified and removed.

In the dominant M1 condition 31 ± 4 components (i.e. 54 ± 8 % of total ICA components) and in the non-dominant M1 condition 33 ± 5 components (i.e. 56 ± 9 % of total ICA components) were rejected on average across participants. Deleted electrodes were interpolated using a spherical interpolation and the data were re-referenced to common average. A more detailed description of the pre-processing steps can be found in **Chapter 3**

(General Methods section 3.6.3). To examine TMS-evoked responses in the time domain, all clean trials were baseline corrected (- 800 to - 100 ms pre-TMS) and then averaged for each electrode. The average of cleaned epochs for each electrode is referred to as TEP.

4.2.8.2. TMS-evoked potential (TEP) and Global Mean Field Amplitude (GMFA)

The Global Mean Field Amplitude (GMFA) was calculated in each condition for each participant with the following equation. adapted from Lehmann and Skandries (1980):

$$
GMFA(t) = \sqrt{\left(\frac{\left[\left(\sum_{i}^{k}(Vi(t) - Vmean(t))2\right)\right]}{K}\right)}
$$

Equation 4-1: GMFA.

where t is time, K the number of electrodes, Vi the voltage in electrode I and V_{mean} is the mean of the voltages in all electrodes. GMFA represents the root of the mean of the squared TEP differences at all electrodes (i.e., $V_i(t)$) from the mean of instantaneous TEP across electrodes (i.e., $V_{mean}(t)$). GMFA identifies the maximum amplitude of the evoked field and has been used in previous TMS-EEG studies (Farzan et al., 2013; Komssi et al., 2004) to measure the global brain response to TMS.

The TEP and GMFA were calculated for each participant as a function of time. Using butterfly TEP plots (Figure 4-2 and 4-3) and the GMFA (Figure 4-4) curve of the cleaned data, commonly observed TMS–EEG deflections were identified: namely the P30, N45, P60, N100, P190 and P280. For the TEP peak amplitude extraction of each TEP component, the following time windows of interest (P30 TOI (25-40 ms post-TMS), N45 TOI (35-60 ms post-TMS), P60 TOI (50-70 ms post-TMS), N100 TOI (75-150 ms post-TMS), P190 TOI (160-220 ms post-TMS) and N280 TOI (240-360 ms post-TMS) were used, based on our data and in line with previous TMS-EEG literature (Farzan et al., 2013; Komssi et al., 2004; Mutanen et al., 2016; Paus et al., 2001; Premoli et al., 2014).

Peak Extraction

The peak amplitude of the TEPs component were extracted in the previously specified time windows of interest. Specifically, TEP peak analysis was performed in every electrode using the tep_extract function of the TESA toolbox. Peaks were defined as a data point that is greater than (positive) or less than (negative) 5 data points on either side of the peak. If multiple peaks were detected within a time window, the largest peak was used.

Region of interest

For TEPs one region of interest (ROI) covering the ipsilateral motor region of the stimulated hemisphere were selected. The ROI was composed of the two electrodes closest from the stimulated M1, namely FC1 and C1 for the dominant (left) M1 stimulation and FC2 and C2 for the non-dominant (right) M1 stimulation.

4.2.8.3. Time Frequency Representation and TMS-related-spectrum perturbation (TRSP)

The time-frequency representation of cortical activity for each participant and electrode was calculated between 1 and 45 Hz by means of a Hanning Fast Fourier Transform (FFT) tapering using the 'newtimef' function in EEGLAB (Farzan et al., 2013; Grandchamp and Delorme, 2011). To calculate the TMS-related-spectrum perturbation (TRSP) a spectral normalisation first at the single-trial level performing a full-epoch length single-trial correction and then by a pre-stimulus baseline correction (- 700 to - 100 ms pre-TMS) on the resulting TRSP averaged across all artefact free trials was applied (Delorme and Makeig, 2004). A sliding window size of 200 ms in width was applied to the single-trial clean data over a 3-second time interval (-1000 ms to +2000 ms post-TMS) to optimally separate out both, the low and high-frequency components.

The average TRSP of the two electrodes in the ipsilateral ROI was then calculated for each participant and used for analysis.

4.2.9. Statistics

Unless stated otherwise, all data were assessed using parametric statistical tests following confirmation of normal distribution of data using the Shapiro-Wilk test. All statistical procedures were performed using SPSS (IBM SPSS Statistics for Windows, Version 24.0).

For behavioural outcome measures and the CSP duration, paired t-tests (for normally distributed data) or Wilcoxon-signed rank tests (if data was non-normally distributed, as was the case for MVC, pre-TMS EMG activity and MEP facilitation) were used to test for significant differences between dominant and non-dominant M1 stimulation.

Since MEP peak-to-peak amplitudes were not normally distributed, a Friedman test was used to assess differences across the four conditions (dominant M1 at rest, non-dominant M1 at rest, dominant M1 during contraction, non-dominant M1 during contraction) If a significant main effect was detected, post-hoc Wilcoxon signed rank tests were performed to test for differences in MEP peak-to-peak amplitude between dominant and non-dominant M1 at rest and between dominant and non-dominant M1 during contraction (Bonferroni corrected p-value < 0.025).

TEP peak amplitude differences were tested using a two-way MANOVA with factor State (rest versus contraction) and Hemisphere (dominant versus non-dominant hemisphere) on the six dependent TEP components of interest (P30, N45, P60, N100, P190 and N280). If significant effects were detected, follow-up two-way ANOVAs were performed for each TEP component separately.

To test for potential differences in TRSP across conditions a permutation-based two-way ANOVA (2000 permutations) was used to control for multiple comparisons in the frequency (1-45 Hz) and time (- 700 to + 1700 ms). To control for multiple comparisons, the Benjamini and Hochberg (Groppe et al., 2011) procedure FDR correction was applied.

4.3. Results

Unless stated otherwise, all results presented in text, Figures and Tables are presented in mean ± SD.

4.3.1. TMS-evoked responses: cortical and peripheral

Single-pulse TMS over both dominant and non-dominant M1 evoked EEG activity lasting up to 300 ms composed of a sequence of deflections of negative and positive polarity peaks, as reported previously in the literature (Farzan et al., 2013; Komssi et al., 2004; Mutanen et al., 2016; Paus et al., 2001; Premoli et al., 2014). TEPs resulting from dominant M1 and non-dominant M1 stimulation are shown in Figures 4-2 and Figure 4-3 along with their scalp topographies to illustrate the spatiotemporal evolution of TMS-evoked activity.

At the peripheral level, single-pulse TMS over the dominant and non-dominant M1 produced an MEP in the rest condition and an MEP followed by a CSP in the contraction condition in the targeted hand muscle (FDI). The EMG traces for one representative participant are shown in Figure 4-5.
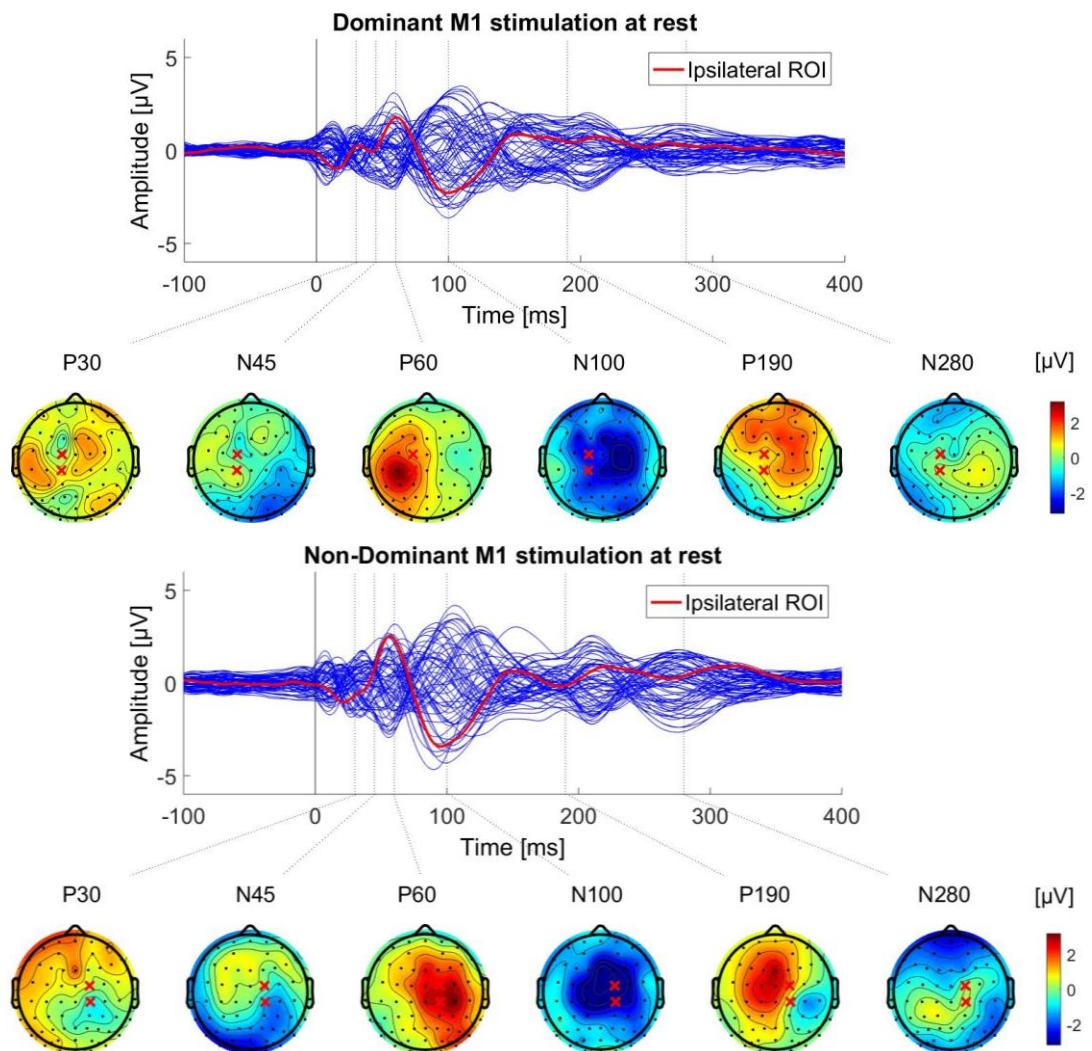
Figure 4-2: Cortical components following single-pulse TMS stimulation over the dominant and non-dominant M1 in the rest condition. Butterfly plot of the average TEPs from all electrodes (N = 63) averaged across all 16 participants in the dominant M1 (upper panel) and non- dominant M1 (lower panel). The red line corresponds to the averaged TEP of the electrodes in the ipsilateral ROI (FC1 and C1 for dominant M1, and FC2 and C2 for the non-dominant M1; denoted with 'x' on the head plots). Single-pulse TMS produced TEP peaks at 30, 45, 60, 100, 190 and 280 ms post-TMS pulse as indicated with the vertical dashed lines, reproducing the TEP components reported in the literature (Farzan et al., 2016) referred to as P30, N45, P60, N100, P190 and N280 respectively. The X-axes represent time in ms, and Y-axes the amplitude in μV. The topographic representation of the identified TEP components illustrates the spatiotemporal evolution of TEPs, showing a spreading of activity from the stimulated (ipsilateral) motor region to central motor and parietal regions, along with frontal regions.

Figure 4-3: Cortical components following single-pulse TMS stimulation over the dominant and non-dominant M1 in the contraction condition. Butterfly plot of the average TEPs from all electrodes (N = 63) averaged across all 16 participants in the dominant M1 (upper panel) and non- dominant M1 (lower panel). The red line corresponds to the averaged TEP of the electrodes in the ipsilateral ROI (FC1 and C1 for dominant M1, and FC2 and C2 for the non-dominant M1; denoted with 'x' on the head plots). Single-pulse TMS produced TEP peaks at 30, 45, 60, 100, 190 and 280 ms post-TMS pulse as indicated with the vertical dashed lines, reproducing the TEP components reported in the literature (Farzan et al., 2016) referred to as P30, N45, P60, N100, P190 and N280 respectively. The X-axes represent time in ms, and Y-axes the amplitude in µV. The topographic representation of the identified TEP components illustrates the spatiotemporal evolution of TEPs, showing a spreading of activity from the stimulated (ipsilateral) motor region to central motor and parietal regions, along with frontal regions.

Figure 4-4: GMFA following dominant and non-dominant M1 stimulation at rest and during contraction. Grand-average across participants (N = 16) and SEM (shaded area) are plotted.
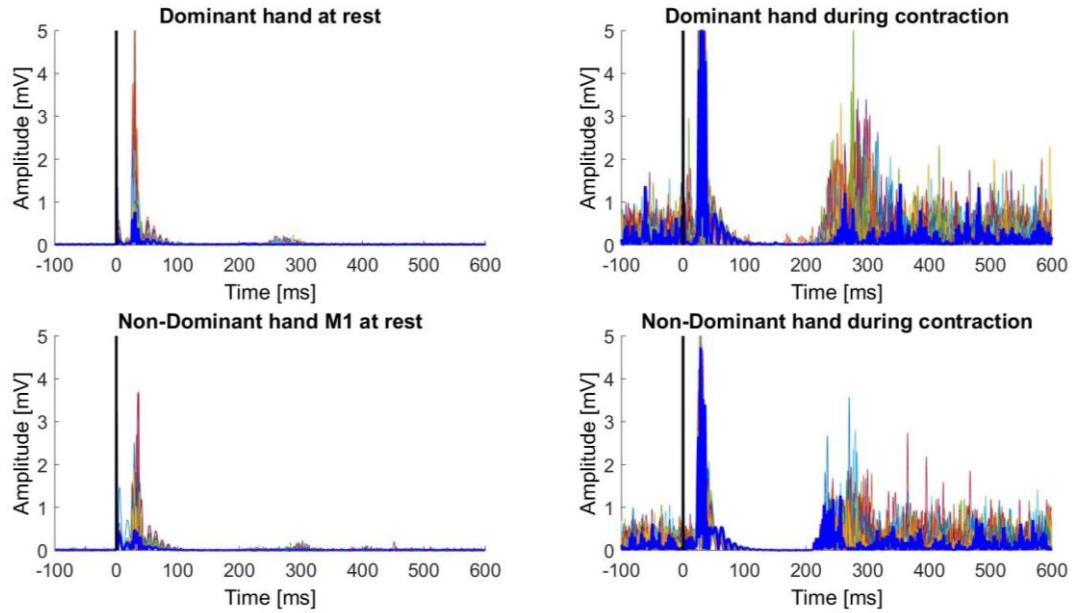
Figure 4-5: Peripheral responses following single-pulse TMS stimulation over the dominant and non-dominant M1 in one representative participant. Waveforms represent the rectified EMG recording form the FDI muscle for all trials (coloured waveforms) and averaged across trials in one representative participant (the blue waveform) for each condition. MEPs in the rest condition in the dominant and non-dominant hand are shown in the left upper and lower panel, respectively. MEPs followed by the CSP in the active contraction condition in the dominant and non-dominant hand are shown in the right upper and lower panel respectively. The Y-axis represents EMG amplitude in mV and the X-axis represents time in ms. The solid vertical black line represents the TMS pulse.

4.3.2. Behavioural and EMG results

The Shapiro-Wilk test revealed that the MEP peak-to-peak amplitude, the MEP facilitation, the pre-TMS EMG activity and the MVC were not normally distributed. For this data non-parametric tests such as the Friedman test and the Wilcoxon signed rank test were employed instead of repeated-measure ANOVAs and paired t-tests.

4.3.2.1. Behaviour

The LQ assessed with the Edinburgh Handedness Inventory confirmed that all participants were right-handed (84 ± 16.7). The MVC was higher in the dominant (15.0 ± 6 N) compared to the non-dominant hand (13.1 ± 6.1 N, z = 2.6, p = 0.01), indicating that participants were significantly stronger with their dominant hand. Participants were significantly faster with their dominant hand (65.3 ± 7.6 s) compared to the non-dominant hand (75.7 ± 9.5 s) in the GPT (t (15) = - 5.70, p < 0.0001). There was no significant difference between the RMT in the dominant (52 ± 6 %) and non-dominant hand (53 ± 7 %, t (15) = - 1.25, p > 0.05).

4.3.2.2. EMG

Group-level (Mean ± SD) and single subject results are shown in Figure 4-6A for peak-to-peak MEP amplitudes and in Figure 4-6B for CSP durations.

The Friedman test showed that there was a significant difference in MEP peak-to-peak amplitudes across conditions (χ^2 (3) = 39, p< 0.0001). Post-hoc Wilcoxon signed-rank tests between dominant and non-dominant M1 with Bonferroni adjusted p-values showed that the peak-to-peak MEP amplitude was not significantly different in the dominant compared to the non-dominant hand at rest (z = 1.1, p = 0.51) and in the contraction condition (z = 2.17, p = 0.06).

The CSP duration was not significantly different between the dominant and non-dominant hands (t (15) = - 0.83, p = 0.42).

126

Pre-TMS EMG activity was significantly higher in the dominant compared to the non-dominant hand (z = 2.07, p = 0.04).

All other EMG measures showed no significant differences between the dominant and non-dominant hand (p > 0.05) and are reported in Table 4-1.
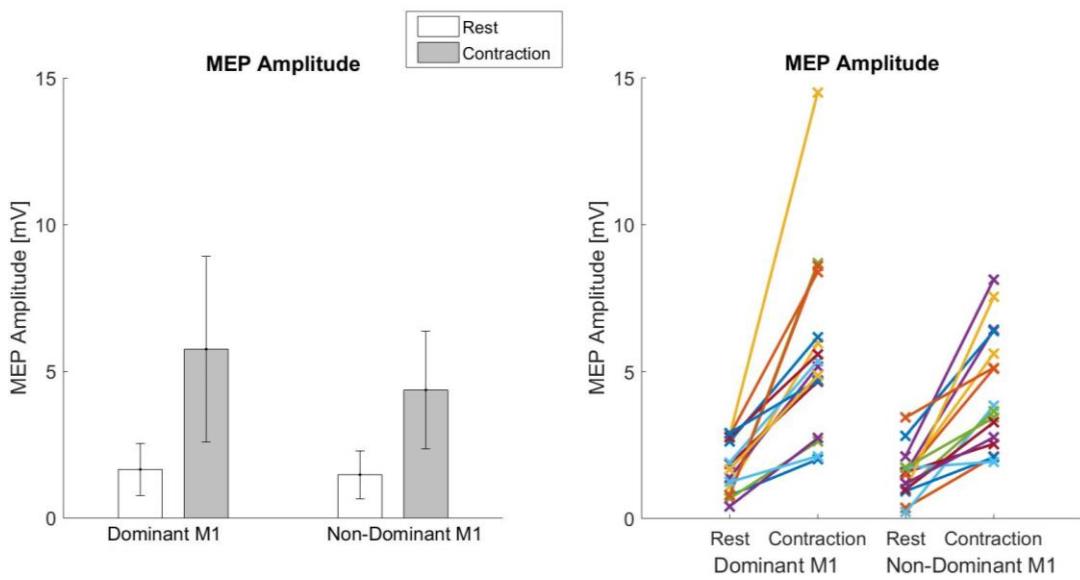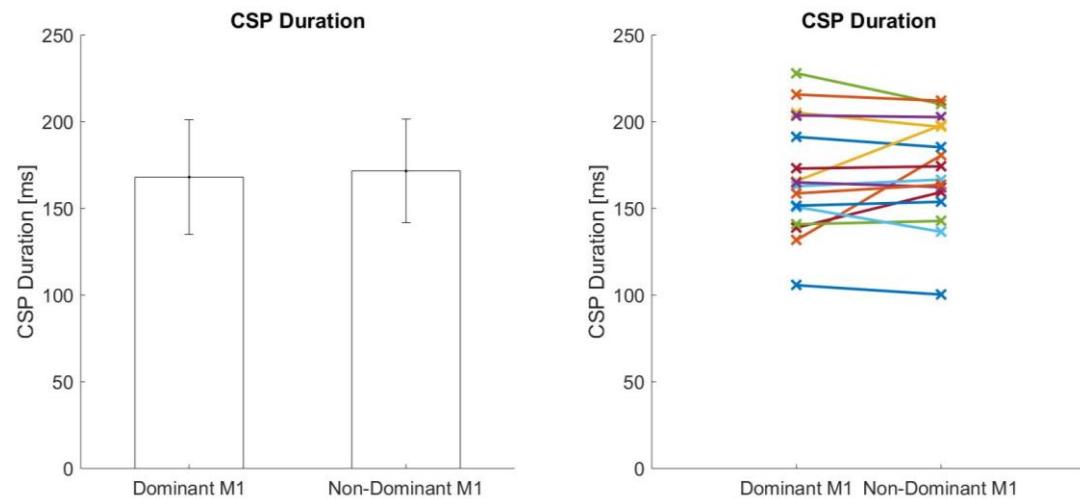
Figure 4-6: EMG response to TMS. A) MEP peak-to-peak amplitude (Mean ± SD) are shown in the dominant and non-dominant hand in the rest and contraction condition in mV in the left panel. White bars represent MEPs elicited at rest and grey bars MEPs elicited during contraction. Single-subject MEP peak-to-peak amplitudes are shown in the right panel. **B) CSP duration (Mean ± SD)** in ms in the contraction condition in the dominant and non-dominant hand are shown in the left panel. Single-subject CSP durations are shown in the right panel.

128

Table 4-1: Mean, SD and test statistic (paired t-test or Wilcoxon-signed rank test) results between the dominant and non-dominant hand.

	Dominant Hand	Non-Dominant Hand	Test-statistic	p
Behavioural				
GPT speed [s]	65.25 [7.50]	75.67 [9.49]	t = 5.7	<0.0001
MVC [N]	15 [5.7]	13.1 [6.0]	z = 2.6	0.01
RMT [%]	52 [6]	53 [7]	t = - 3.049	0.212
Rest Condition				
MEP peak-to-peak amplitude [mV]	1.66 [0.89]	1.48 [0.82]	z = 1.1	0.51
MEP onset [ms]	21.54 [2.75]	21.78 [0.96]	t = - 0.35	0.73
Contraction Condition				
MEP peak-to-peak amplitude [mV]	5.76 [3.16]	4.37 [2.01]	z = 2.2	0.06
MEP onset [ms]	19.42 [3.18]	18.71 [3.11]	t = 0.77	0.45
Pre-TMS EMG activity [mV]	0.07 [0.04]	0.05 [0.03]	z = 2.07	0.04
CSP duration [ms]	168 [33]	172 [30]	t = - 0.83	0.42
MEP facilitation ($\frac{MEP\ contraction}{MEP\ rest}$)	4.27 [2.96]	4.18 [4.14]	z = 0.621	0.54

4.3.3. TEP

The TMS-evoked activity resulting from dominant and non-dominant M1 stimulation in the ipsilateral ROI is shown in Figure 4.7 showing a consistent pattern of positive and negative peaks in the evoked response. Figure 4-7. shows the group average TEP activity in the ipsilateral ROI for the dominant and non-dominant M1 stimulation at rest (upper panel) and during contraction (lower panel). The peak amplitude of the six peaks of interest (P30, N45, P60, N100, P190 and N280) was extracted from the time-domain response of the EEG activity.

The two-way MANOVA on the six TEP dependent component of interests (P30, N45, P60, N100, P190 and N280) with factor State (rest versus contraction) and Hemisphere (dominant versus non-dominant M1) revealed no significant effects of State (Pillai's trace = 0.459, $F(6,10) = 1.412$, $p = 0.300$, $\eta_p^2 = 0.459$), Hemisphere (Pillai's trace = 0.251, $F(6,10) = 0.559$, $p = 0.754$, $\eta_p^2 = 0.251$) and no interaction between State and Hemisphere (Pillai's trace = 0.420, $F(6,10) = 1.207$, $p = 0.377$, $\eta_p^2 = 0.420$). Mean and SD of each TEP component are shown in barplots in each condition in Figure 4-8.
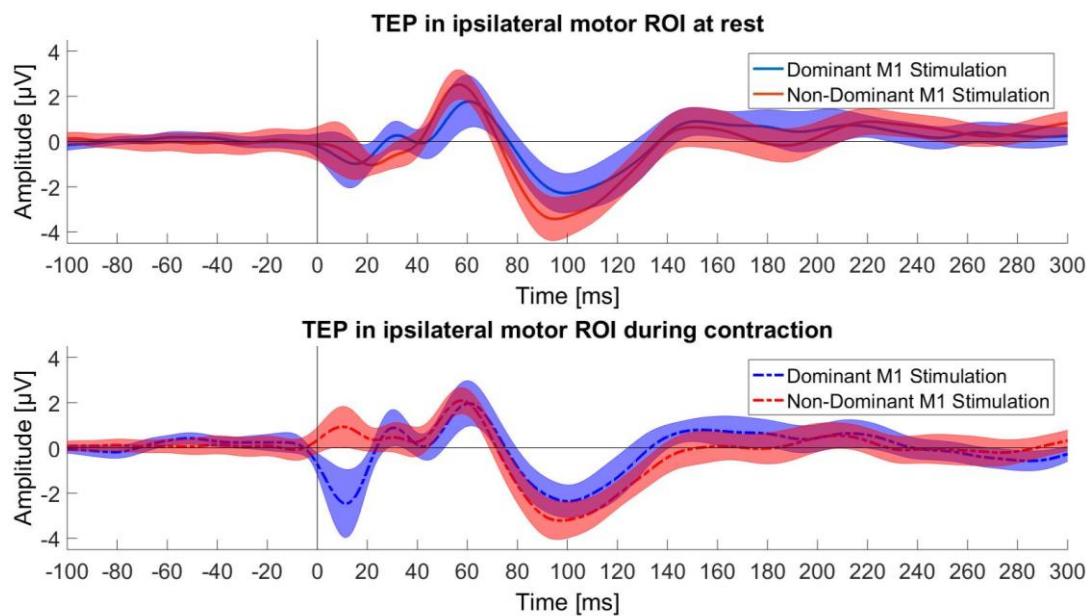
Figure 4-7: TMS-evoked potentials at rest and during contraction following single-pulse TMS over the dominant and non-dominant M1. Grand-average TEP plots (N = 16) in the ipsilateral ROI (FC1, C1 for dominant M1 and FC2, C2 for non-dominant M1). Shades represent ± SEM. The solid vertical bar represents the TMS pulse. Six characteristic TEP components were identified, namely the P30, N45, P60, N100, N190 and P280, and peak amplitudes were extracted for statistical analysis
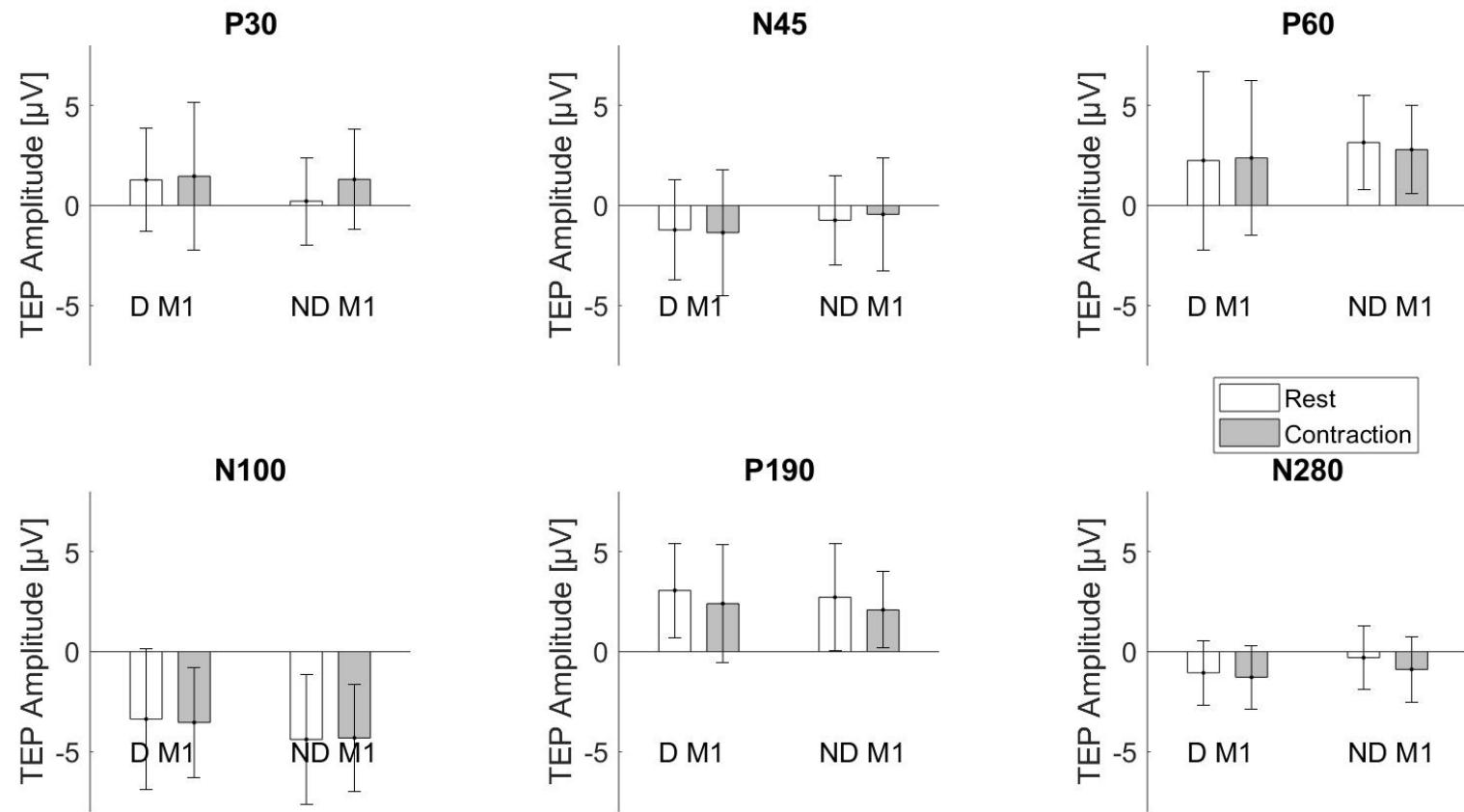
Figure 4-8: TEP peak amplitudes. Bar plots represent TEP amplitudes (Mean ± SD) following single-pulse TMS over the dominant (D M1) and non-dominant (ND M1) during rest and contraction for each component. Group-level (N = 16) TEPs in the ipsilateral ROI (FC1, C1 for dominant M1 and FC2, C2 for non-dominant M1) are represented with white bars for the rest condition and with grey bars for the contraction condition.

4.3.4. TRSP

With respect to the EEG responses in the time-frequency domain (TRSP), the present results showed that dominant and non-dominant M1 stimulation responded to TMS with a broadband increase of spectral power lasting up to approximately 250 ms (Figure 4-9A) at rest and during contraction. After this first activation, spectral power showed a statistically significant desynchronisation (ERD; blue colour in Figure 4-9A) from 250 - 400 ms post-TMS in the dominant and non-dominant M1 stimulation at rest and from 250 - 1600 ms post-TMS during contraction in the alpha and beta frequency band. While a statistically significant synchronisation (ERS, red colour) was seen between 500 - 1000 ms post-TMS in both the dominant and non-dominant M1 at rest, during contraction, there was no ERS but the ERD persisted until the end of the epoch.

The two-way ANOVA with factor Hemisphere (dominant versus non-dominant M1) and State (rest versus contraction) reported a significant effect of State, suggesting a significant higher ERD during contraction compared to rest 400-1200 ms post-TMS for both the dominant and non-dominant M1 stimulation (Figure 4-9B).
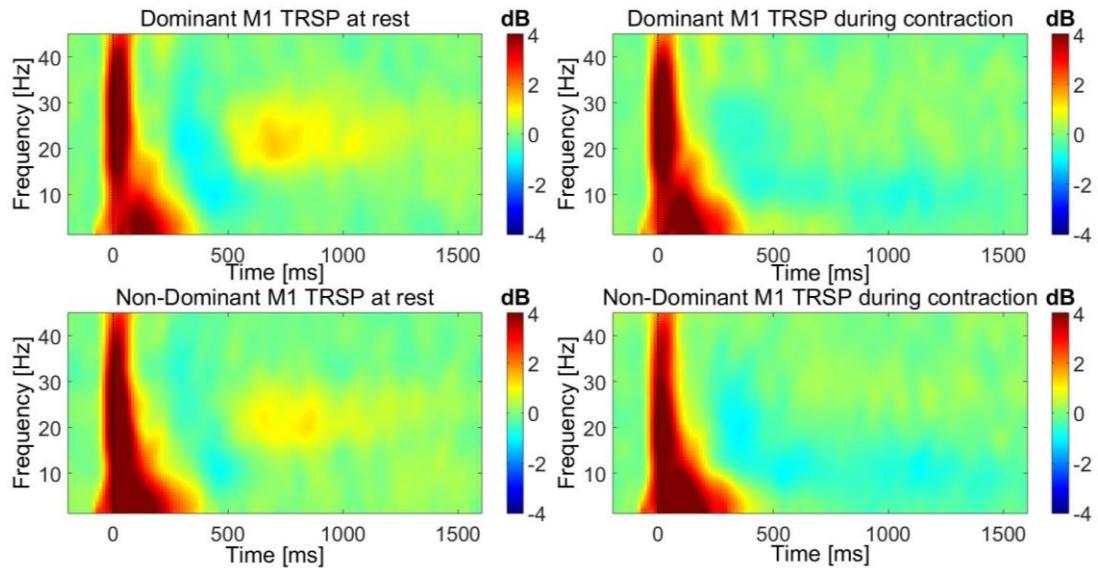
A)
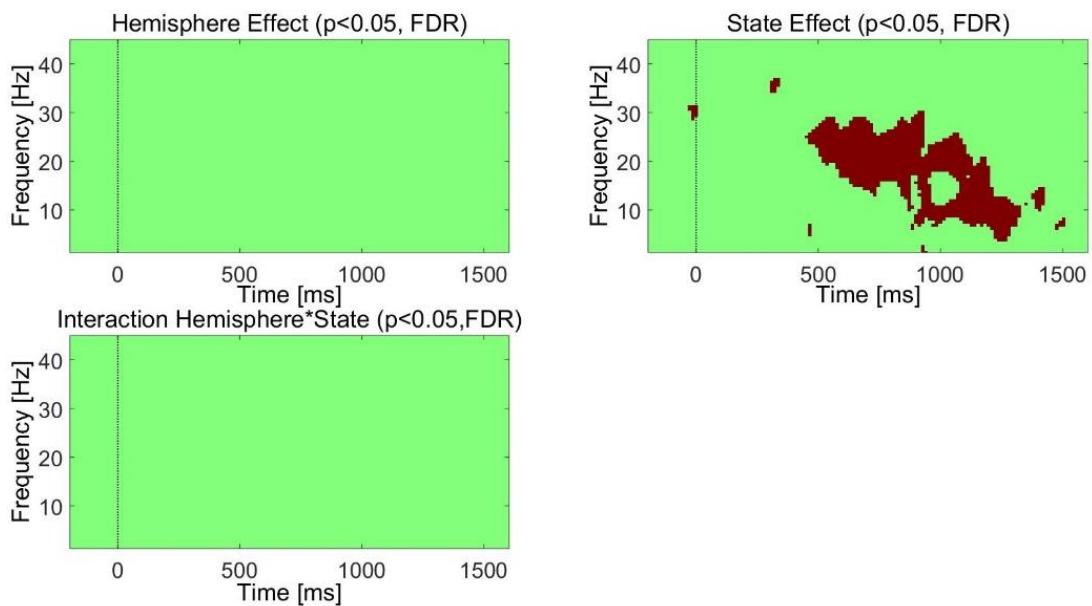
B)

Figure 4-9: Illustration of dominant M1 and non-dominant stimulation TMS-induced power in the rest and in the contraction condition. A) Grand-average TRSP plots (N = 16) in the ipsilateral ROI (FC1, C1 for dominant M1 and FC2, C2 for non-dominant M1). is presented in the dominant M1 stimulation rest, non-dominant M1 stimulation rest, dominant M1 stimulation contraction and non-dominant M1 stimulation contraction condition in log dB scale. An FFT transform has been applied at the single-trial level. The significance threshold for bootstrap statistics is set at α < 0.01. Non-significant activity is set to zero (green), red colours indicate a significant increase (ERS) with respect to the baseline, while blue colours indicate a significant decrease (ERD) compared to the baseline. The dashed vertical line indicates the time of the TMS pulse. Colour intensity is proportional to the value of TRSPs in dB. **B) Permutation-based ANOVA results:** Significant main effects of State (rest versus contraction), Hemisphere (dominant versus non-dominant M1) and the interaction of State and Hemisphere are shown. The significance level is 0.05, and permutation-based tests are corrected for multiple comparisons using FDR. Significant effects are coloured in dark red and non-significant effects in green.

4.4. Discussion

First, the present study presents findings that were consistent with previous literature reporting similar activation patterns in the time (TEP) (Paus et al., 2001; Petrichella et al., 2017; Premoli et al., 2014) and time-frequency (TRSP) (Fecchio et al., 2017) domain, indicating that the TMS-EEG set-up in the lab is appropriate for testing cortical excitability in the next studies in this thesis. In line with previous studies (for review see Farzan et al., 2016), this study therefore confirms that TEPs and TRSPs measured with EEG activity in response to TMS are reliable readouts of cortical excitability.

The study showed that M1 produces specific responses to TMS possibly reflecting specific neurophysiological and functional properties. Single-pulse TMS of both dominant and non-dominant M1 evoked EEG activity lasting up to 300 ms post-TMS pulse of a sequence negative and positive deflections and increases and decreases of oscillatory power.

Second, as expected, the study revealed significant effects of motor state on cortical reactivity revealed with TRSP but not with TEPs. Namely, ERD in beta band was significantly enhanced during contraction between 400 and 1200 ms post-TMS compared to rest possibly reflecting motor task-related ERD.

Third, the study reported no significant difference in cortical and corticospinal excitability related to motor dominance. However, this lack of significance is not a prove of no hemispheric difference and it is possible that the sample size was too small to detect differences in cortical excitability as measured with MEPs, CSPs and TEPs. A power analysis calculation using the G power software revealed that a sample size of 24 individuals was needed to detect a significant effect of hemisphere (i.e. motor dominance) in the main outcome measure, namely TEP amplitudes (6 components) with a power of 80%. This was based on an estimated effect size derived from the present data of $f = 0.25$, and α significance level of $p = 0.05$ in a within-subjects design experiment with a total of 6 measures and 4 conditions. Similarly, a power analysis for differences in cortical excitability as measured by MEP amplitude and CSP duration related to motor dominance (dominant versus non-

dominant hand), revealed that a sample size of 21 (with an estimated effect size of f = 0.66) for MEPs and 34 (with an estimated effect size of f = 0.18) for CSPs was needed. Since this study had a sample size of 16 participants, it is likely that the lack of significance is due to a too small sample size and according to the power calculations, future studies should seek to have sample sizes of at least 34 participants to reliably detect differences related to motor dominance measured with TEPs, MEPs and CSPs.

4.4.1. Peripheral asymmetries

Humans use their hands asymmetrically in everyday life and in this study, the findings demonstrated that this asymmetrical use is reflected in the strength (pinch strength) and dexterity (GPT speed). The maximum pinch strength was higher in the dominant hand, which is in line with previous research showing that the maximum voluntary contraction force is higher in the dominant hand (Saisanen et al., 2008).

No significant differences in RMT and CSP duration between dominant and non-dominant M1 stimulation were observed, suggesting that motor cortex excitability is similar in both hemispheres at rest, corroborating previous findings (Saisanen et al., 2008). Similarly, non-significant differences in functional mechanisms between both hemispheres have also been reported with threshold tracking paired-pulse TMS (Kazumoto et al., 2017). Kazumoto et al. (2017) found no differences between dominant and non-dominant M1 as measured by MEP amplitude, latency, central motor conduction time, CSP, short-interval intracortical inhibition and facilitation, compound muscle action potential amplitude and latency, F-wave latency. Together, these findings suggest that there is no difference in cortical function measured with corticospinal excitability measures at rest between the motor cortices.

Even though pre-TMS EMG activity was significantly higher in the dominant compared to the non-dominant hand, it did result in significant differences in corticospinal excitability, as MEP amplitudes were not significantly different between the dominant and non-dominant hand. This finding contradicts previous reports of a greater facilitation in the dominant hemisphere compared

to the non-dominant hemisphere during contraction. Specifically, Brouwer et al. (2001), found a larger MEP facilitation in the dominant hand compared to the non-dominant hand in a subgroup of right-handers with LQ scores between 0 and 85 % (similar to our participants: LQ= 84 ± 16.7 %), and a larger facilitation in the non-dominant hand in a subgroup of right-handers with LQ scores higher than 85%.

It needs to be acknowledged that the lack of significant differences between EMG measures in the present study could be due to the high variability specifically in MEP amplitudes between the right and left hand. In fact, even though care was taken to place the electrodes in the same way on the right and left FDI, this could have made the MEP measurements between hands more variable. One way to reduce this variability would have been to normalise MEPs to maximal motor responses and would have helped to more reliably compare MEP amplitudes between different muscles (left and right FDI) (Rossini et al. 2015, Hallett et al. 2007). Therefore, measuring the maximal motor response by stimulating the ulnar nerve prior to the TMS protocol, would be advised, when planning a future study to detect differences in MEPs related to hemispheric asymmetries.

4.4.2. Cortical asymmetries

4.4.2.1. TEP

Previous TMS-EEG studies have reported a well-characterised pattern of activation following TMS to the left M1 in which TMS produced large deflections in scalp voltage primarily near the site of stimulation but also on the contralateral side (Fecchio et al., 2017; Paus et al., 2001; Petrichella et al., 2017; Premoli et al., 2014). The present study demonstrated similar positive and negative TEP deflections reported in the literature following both, dominant (left) and non-dominant (right) M1 TMS stimulation (Petrichella et al., 2017). TMS over the dominant and non-dominant M1 resulted in local neuronal activation, with TEPs spreading from the stimulated (ipsilateral) motor region to central motor and parietal regions, along with frontal regions as shown in the spatiotemporal representation of TEPs in Figures 4-2 and 4-

3. Similar TEP distributions have been reported following left M1 stimulation at rest (Ilmoniemi et al., 1997) and during contraction (Farzan et al., 2013). Together these findings suggest that TEPs originate from stimulated (ipsilateral) M1 and engage excitatory and inhibitory mechanisms of more distant brain regions at longer latencies.

Overall, the timing of evoked activity is generally consistent with previous studies including motor areas (Bonato et al., 2006; Farzan et al., 2013; Komssi et al., 2004; Premoli et al., 2014). The lack of significant differences between both hemispheres is consistent with previous findings during which TMS was applied to the dominant and non-dominant M1 at rest (Petrichella et al., 2017). Furthermore, the present study extends previous findings by demonstrating that there are also no significant differences between dominant and non-dominant M1 stimulation during contraction.

4.4.2.2. TMS-induced oscillations: spectral responses to single-pulse TMS

TMS- induced ERS

Corroborating previous findings (Farzan et al., 2013; Fecchio et al., 2017), the global mean-field amplitude (GMFA) (Figure 4-4) showed characteristic peaks in response to TMS at different time delays post-TMS, with a return to baseline amplitudes 500 ms post-TMS. In the time-frequency domain, TMS-induced oscillations are shown in Figure 4-9. Oscillatory responses to TMS over M1 have been characterised in previous studies (Pellicciari et al., 2017). Single-pulse TMS over M1 induced a brief period of synchronised activity in the stimulated brain area (Paus et al., 2001).

It has been hypothesised that TMS pulses synchronise spontaneous activity of a population of neurons, called the resetting hypothesis (Fuggetta et al., 2005; Paus et al., 2001; Vernet et al., 2013). It has been shown that TMS-induced oscillations are of physiological nature and reveal 'natural rhythms' of different regions (Rosanova et al., 2009). The present study showed that dominant and non-dominant M1 stimulation responded to TMS with a broadband increase of spectral power lasting up to approximately 250 ms (Figure 4-9A) at rest and during contraction. Using different TMS intensities

138

of stimulation over the left M1, Fuggetta et al. (2005) demonstrated that the intensity level modulates the ERS, with higher intensities eliciting an enhanced ERS post-TMS (Fuggetta et al., 2005). Moreover, even subthreshold TMS intensities (which do not elicit MEPs) synchronise the activity of neurons in the vicinity of the stimulation site. TMS induces the strongest electrical fields in the superficial cortical layers (Rothwell et al., 1991). Subthreshold TMS intensities produce direct and indirect excitation of pyramidal neurons in the grey matter through transsynaptic volleys, whereas suprathreshold TMS results in a direct activation of axonal pathways (Day et al., 1989). Fuggetta et al. (2005) suggested that EEG activity at subthreshold intensities reflect the activation of superficial layers, whereas suprathreshold TMS reflects the activation of cortical as well as subcortical regions. As such, the synchronous activation of cortical and subcortical neuronal structures by depolarisation produced by TMS may be responsible for the short-lasting synchronisation of the oscillatory activity. In this study, the finding of an increased ERS post-TMS might, therefore, reflect the activation of neurons in the vicinity of the stimulation site leading to the depolarisation of neurons and thus activating the targeted muscle, by eliciting MEPs.

TMS- induced ERD

After the first synchronisation of neuronal activation, spectral power showed a statistically significant desynchronisation compared to baseline (ERD; blue colour in Figure 4-9A) from 250-400 ms post-TMS in the dominant and non-dominant M1 stimulation at rest and from 250-1600 ms post-TMS during contraction (Figure 4-9B). The present study replicated the M1-related ERD observations at rest over the dominant (left) M1 (Fecchio et al., 2017). It has been suggested that ERD is reflective of the somatosensory feedback of the targeted muscle activation (Fecchio et al., 2017). By stimulating brain regions that do not elicit MEPs (the parietal, prefrontal, premotor cortex) and the M1 which elicits an MEP response at suprathreshold TMS, Fecchio et al. (2017) showed that only the M1 response was associated with late ERD (around 300 ms post-TMS). Moreover, splitting trials in low-MEP and high-MEP amplitudes

after M1 stimulation revealed that the late ERD was modulated by the amplitude of MEPs (Fecchio et al., 2017).

The ERD observed in the present study and the one reported in the literature (Fecchio et al., 2017) resemble the localized desynchronisation of the ongoing EEG oscillations in the μ-bands (8-13 Hz) induced by the execution of a voluntary movement (Kuhlman, 1978) and by somatosensory stimulation (Stancák, 2006). Similarly, ERD in the beta-band (15 – 30 Hz) recorded from sensory-motor cortices has been associated mechanical finger stimulation (Gaetz and Cheyne, 2006), with electrical nerve stimulation (Muller et al., 2003) and as well as with movement (Pfurtscheller and Aranibar, 1979) and motor imagery (Pfurtscheller et al., 1999). The similarity of the frequency-specific spectral profiles brought about by peripheral activations and the broadband ERD post-TMS (Figure 4-9) found in the present study suggest that the oscillatory response to TMS reflects direct and indirect cortical activation. Specifically, it is possible that the activation of specific cortico-spinal circuits (Shitara et al., 2013), as well as the sensory feedback from the activated muscle (Gaetz and Cheyne, 2006; Stancák, 2006), contributed to the characteristic ERD in response to single-pulse TMS at rest and during contraction. Specifically, the ERD response can correspond to the re-entry of proprioceptive feedback associated with the target muscle in which TMS produced an MEP reflecting specific anatomo-functional properties of the sensorimotor system (Yang et al., 2017). It has also been suggested that ERD in the alpha and beta band reflects the level of cortical excitability, with increases in excitability being associated with increases in ERD magnitude (Cremoux et al., 2013; Kasuga et al., 2015; Matsumoto et al., 2010).

4.4.2.3. Task-related oscillations: effect of motor state on spectral properties

TMS at rest and during contraction resulted in the activation of the targeted muscle, eliciting MEPs recorded from the contralateral FDI muscle for both dominant and non-dominant M1 (Figure 4-5). This first activation of the targeted muscle was followed by a brief interruption of EMG activity during voluntary FDI contraction, referred to as the CSP. The CSP duration lasts approximately 170 ms and EMG activity reoccurs 200 ms post-TMS. At the

cortical level, the spectral features of muscle contraction are reflected with a sustained ERD post-EMG re-emergence (500-1200 ms post-TMS). This enhanced ERD seems to be related to the motor task, namely the isometric contraction (for review see Pfurtscheller and Andrew, 1999). In fact, ERD during contraction is significantly enhanced compared to rest.

ERD is sustained during isometric contraction upper limb (elbow flexor) (Cremoux et al., 2013) and lower limb (Gwin and Ferris, 2012). Specifically, it has been demonstrated that ERD in the alpha and beta band is related to sustained muscle activation (for review see Pfurtscheller and Andrew, 1999). The sustained ERD during the contraction condition, in the present study, may, therefore, be linked to the muscle contraction, specifically to the EMG activity re-occurrence after the silent period induced by TMS.

ERD in the alpha and the beta band is proposed to reflect the level of cortical excitability, with increases in excitability being associated with increases in ERD magnitude (Cremoux et al., 2013; Kasuga et al., 2015; Matsumoto et al., 2010). In the present study, an enhanced ERD during contraction (after re-occurrence of EMG activity following the CSP) duration compared to rest was observed between 400-1200 ms post-TMS. It can be hypothesised that sustained ERD between 400-1200 ms during contraction compared to rest reflects the activity related to voluntary muscle contraction. This is supported by Pfurtscheller and Andrew's review (1999), reporting that sustained muscle contraction is reflected in oscillatory activity in M1 in the alpha and beta band.

4.4.3. Novel findings

No study to our knowledge has evaluated the potential difference between the dominant and non-dominant M1 stimulation during two motor states (rest and contraction) by evaluating MEPs, CSPs and TEPs simultaneously. Previous studies investigated the relationship between the CSP and cortical oscillations only in the dominant hemisphere (left M1) (Farzan et al., 2013) and, the influence of the presence or absence of CST activity, measured through

MEPs and TEPs in the dominant and non-dominant hemisphere (right and left M1) (Petrichella et al., 2017).

The present study detected significant differences in cortical excitability related to motor state in the dominant and non-dominant hemisphere as measured with EEG revealing an increased ERD during contraction compared to rest. However, the study failed to detect significant differences between the dominant and non-dominant hemisphere, which is most likely due to a too small sample size and as such the study was underpowered to test for hemispheric asymmetries.

4.4.4. Limitations and future work

The most important limitation of the current study related to motor dominance is that it investigated cortical asymmetries only in right-handers, reporting no differences in cortical or peripheral neurophysiological mechanisms between hemispheres as measured with TMS. The study did not include left-handed individuals for two reasons: First, it is known that left-handed individuals are less consistent in using their hands asymmetrically compared to right-handers and neurophysiological differences are usually higher in consistent right-handers (Bernard et al., 2011, Hervé et al., 2006, Oldfield et al., 1971). Second, the response to TMS has a high degree of intra-subject and inter-subject variability (Koski et al., 2005, Orth and Rothwell, 2004). Since this study applied TMS to both hemispheres and in order to enhance the power of finding group differences related to hemispheric asymmetries, left-handed and ambidextrous individuals were not included in this study. However, it needs to be acknowledged that the present study gives an incomplete picture of cortical asymmetries related to motor dominance and handedness, and future work should incorporate left-handers, as well as ambidextrous individuals to gain further insights into the neurophysiological mechanisms contributing to handedness (Davidson and Tremblay, 2013).

Future work could also investigate how peripheral activity can influence cortical activity, by including not only a rest and contraction condition as

outlined in the present study but also include conditions with varying contraction levels.

It should be noted that although white noise was used to mask the auditory artefact in the EEG data, it cannot be ruled out that the present data are not contaminated with the artefact overlying the N100 amplitude. However, this artefact would have affected and contaminated all the experimental conditions is the same way so that any potential differences in the N100 amplitude would reflect true neural differences and not caused by this artefact.

In terms of analysis, the analysis of the present data can be extended in more depth in future work (outside of the scope of this thesis), by looking at measures of connectivity between different ROIs such as in the work of Fuggetta et al. (2005).

Chapter 5 - Bi-hemispheric Modulation during Movement Preparation

5.1. Introduction

5.1.1. Movement control

M1 is one of the major brain areas involved in motor function and is associated with the generation of motor control and limb movements (for review see Lemon, 2008). In particular, in humans, pyramidal cells that form a monosynaptic connection with alpha-motor neurons in the spinal cord via the CST are predominantly located in the M1. These alpha-motor neurons innervate extrafusal muscle fibres of skeletal muscle leading to their contraction. In humans, the CST has direct control over the activation of alpha motor neurons and muscle contraction(for review see Lemon, 2008). Corticospinal axons descend ipsilaterally through the internal capsule to the brainstem where a large majority of fibres (approximately 80 %) cross the midline to the contralateral side in the spinal cord (Kertesz and Geschwind, 1971; Nathan et al., 1990). This results in a predominantly contralateral control of movement, namely one cerebral hemisphere predominately controls movement on the other side (contralateral) of the body. During voluntary unilateral movements of the upper limb, the M1 contralateral to the active limb plays, therefore, a major role (for review see Lemon, 2008), but, there is substantial evidence that the ipsilateral M1 to the active limb is also engaged during unilateral movement (Buetefisch et al., 2014; Chiou et al., 2014; Chye et al., 2018; Duque et al., 2010; Howatson et al., 2011; McMillan et al., 2006; Perez et al., 2013; Perez and Cohen, 2008). The functional role of the ipsilateral activity in M1, however, remains unclear. Previous studies have attempted to link cortical activity in both motor cortices with upper limb movements studied reaching movements.

Reaching with the upper limb can be divided into several temporal stages thought to represent certain stages of neuronal activity. Specifically, visually-triggered movements can be divided into four phases early visual information

processing (Thut et al., 2000), movement preparation (Simon et al., 2002), movement execution (Sainburg and Kalakanis, 2000) and movement termination (Andrew and Pfurtscheller, 1996). These distinct movement stages are associated with active processing and involve both excitatory and inhibitory neuronal information exchange (Zaaroor et al., 2003).

The initiation of voluntary arm reaching is often associated with large-scale modulations of neurons in M1 (Churchland and Abbott, 2012; Maynard et al., 1999). It is well established that M1 plays a central role in controlling upper limb reaching movements. Studies in monkeys have revealed that many neuronal characteristics of cortical processing involved in reaching movements can be recorded by single-cell and field potential recordings in M1 (Georgopoulos et al., 1986; Georgopoulos and Carpenter, 2015; Schwartz, 2007; Schwartz and Moran, 1999). However, ever since M1 was identified, there is a continuous debate over whether there is a muscle-based representation, a kinematic representation of direction and velocity detectable in M1, or both (for review: (Cisek and Kalaska, 2010). The activity of many M1 neurons co-varies with movement parameters including dynamic and static force (Kalaska et al., 1989; Schwartz and Moran, 1999; Murphy et al., 1985). Furthermore, it has been shown that the discharge of neuronal populations in M1 are linked with the direction, velocity and trajectory hand movement (Truccolo et al., 2008).

To identify the functional role of ipsilateral M1 activation during unimanual movement, Chye et al. (2018) applied TMS over the ipsilateral M1 and demonstrated that forces produced with the active arm were reflected in increased excitability in the ipsilateral M1. Their finding suggests that ipsilateral motor cortical activity during unilateral movement preparation reflects the state of the active arm rather than representing a subliminal motor plan to support coordination between the arms in case a bimanual movement would be required.

The M1 contralateral to a moving hand undergoes excitatory and inhibitory modulations during movement preparation and execution, but much less is known about the role of the ipsilateral M1 (Chye et al., 2018). Activity in

145

neurons within the ipsilateral M1 depends on the type of upper limb movement, as demonstrated in single-cell recordings in monkeys (Cisek et al., 2003; Tanji et al., 1988) and functional MRI (Dai et al., 2001; van Duinen et al., 2008) studies. TMS studies in humans have reported that parametric increases in unimanual force modulate the activity of the ipsilateral M1(Hess et al., 1986; Hortobágyi et al., 2003; Muellbacher et al., 2000; Tinazzi and Zanette, 1998). Perez and Cohen (2008) revealed that interactions between M1s contribute to control activity-dependent changes in corticospinal output to a resting hand during force generation by the opposite hand. Even though the involvement of ipsilateral M1 during unilateral motor task performance has been demonstrated, the cortical mechanisms controlling the corticospinal output originated in the ipsilateral M1, and the non-task hand remain unclear.

Coding movement in M1 is acquiring more and more interest due to its fundamental importance in neuro-prosthetic implications involving brain-computer interfaces (BCIs). Decoding movement information from the discharges of motor cortical cells using their directional tuning and population coding has driven successful neuro-prosthetic applications. Specifically, BCIs that used signals recorded in M1 have provided promising results for the control of robotic arms and in patients' own paralysed limbs through functional electrical stimulation (Bouton et al., 2016; Ganguly and Carmena, 2009; Hochberg et al., 2012; Velliste et al., 2008).

5.1.2. Movement preparation and cortical excitability

Modulations of the contralateral M1 activity occur as early as during movement preparation, even before movement onset. In humans, motor-related activations during movement preparation and execution have previously been studied using non-invasive brain stimulation (NIBS) such as TMS (Kennefick et al., 2014) or neuroimaging techniques such as EEG (Krigolson et al., 2015; Naranjo et al., 2007). Recently the combination of both techniques allows to directly probe cortical excitability with TEPs as well as corticospinal excitability with MEPs. By applying single-pulse TMS over M1 active excitatory and inhibitory processes acting on the output cells in M1 can be revealed. TMS over M1 can produce MEPs reflecting the ability to induce

action potentials in the CST (Bonato et al., 2006). Simultaneous TMS over M1 and EEG has been proven to be a useful tool to study both cortico-cortical and corticospinal axons resulting in TEPs and MEPs, respectively. Time-locked EEG responses are characterised by positive and negative components labelled P30, N45, P60, N100, P190 and N280 (Farzan et al., 2016; Paus et al., 2001). The most thoroughly studied TEP is the N100 and has been established as a measure of cortical inhibition representing the activity of $GABA_B$ receptors (Premoli et al., 2014).

By applying TMS to M1 to record MEPs during movement preparation, it has been demonstrated that the generation of a voluntary movement involves an interaction between intracortical facilitatory and inhibitory processes within M1 which are essential for motor control (Chen, 2004; Kennefick et al., 2014; Reynolds and Ashby, 1999; Zaaroor et al., 2003). Zaroor et al. (2003) have investigated the time course of corticospinal excitability during movement preparation applying TMS at different time points before movement onset and revealed that corticospinal excitability is increased above resting from 100 ms before to 200 ms after movement onset, except for a short period around 150 ms before movement onset without increased excitability, suggesting an interaction between facilitatory and inhibitory mechanisms in the motor cortex during movement preparation. These TMS studies have indirectly probed cortical excitability by using MEPs which reflect corticospinal activity as outcome measures. Only two studies to date have used simultaneous TMS-EEG (Kičić et al., 2008, Nikulin et al., 2003) to directly investigate cortical excitability modulations during movement preparation in a simple reaction task requiring unilateral thumb movements. Nikulin et al. (2003) reported a decrease in the N100 amplitude in the contralateral M1 during movement preparation compared to rest, possibly reflecting increased excitability. Kičić et al., (2008) expanded these findings by applying TMS to the contralateral as well as the ipsilateral M1 to measure bilateral activations. They found significant changes in the N100 amplitude in both the ipsilateral and contralateral M1 but only found a significant modulation in MEPs in the contralateral thumb, suggesting a dissociation between cortical and corticospinal mechanisms in unilateral movement.

All these TMS studies have investigated corticospinal excitability modulations in M1 during unilateral movement preparation in reaction time tasks, which required simple finger, thumb or wrist movements and not in more complex movements such as arm reaching. One previous study used TMS over the contralateral M1 during unilateral arm reaching preparation using a robot-mediated reaching task (Hunter et al., 2011). Hunter et al. (2011) reported no modulation of excitability measured with MEPs during reaching preparation in an unperturbed environment, but a significant increase in MEPs during movement preparation closer to movement onset in a perturbed environment during which an external force-field was applied. So far, bi-hemispheric modulations during movement preparation have been investigated in simpler tasks, such as choice-hand reaction tasks involving simple wrist flexions and extensions (McMillan et al., 2006), unilateral contraction tasks (Howatson et al., 2012) or unilateral thumb abductions (Kičić et al., 2008), reporting increased excitability in the task and non-task arm as measured with MEPs.

The present study aimed to expand the findings to directly investigate bi-hemispheric cortical modulations of the motor cortices using a more complex task, namely unilateral arm reaching preparation. The goal of the study was to investigate the temporal evolution of bi-hemispheric motor cortical excitability during movement preparation by applying TMS over M1 at different time delays from visual cue during movement preparation. This was accomplished by using combined TMS-EEG to record cortical and peripheral responses to single-pulse TMS over M1 (contralateral or ipsilateral) at different delays from visual cue during movement preparation of the right arm.

The novelty of this study is two-fold: i) Using TEPs as outcome measure allowing to directly probe cortical excitability and not only corticospinal activity (MEPs), ii) Applying TMS to both the contralateral and ipsilateral M1.

It was hypothesised that:

i)   Cortical excitability will be more modulated in the contralateral compared to the ipsilateral M1 during movement preparation due to its greater involvement in unimanual motor control.

ii)   The temporal dynamics of cortical excitability will be significantly modulated in both hemispheres, as measured by modulations in TEPs and MEPs during movement preparation.

5.2.   Methods

5.2.1. Research Design

This study used a between-subject design to test differences of cortical excitability during movement preparation related the hemispheric stimulation site and timing of TMS. Participants were divided into two groups and each group either received TMS to the contralateral M1 or ipsilateral M1 to the task arm. The between subject-factor was Hemisphere (contralateral TMS M1 stimulation versus ipsilateral TMS M1 stimulation) and the within-subject factor TMS delay (TM10, TM130, TM160, TMS190 and TMS220). All TMS conditions were counterbalanced within the TMS session. The main outcome measures were measures of cortical excitability (5 TEP component amplitudes: P30, N45, P60, N100 and P190), corticospinal excitability (MEP amplitude). Secondary outcome measures included kinematics measures (movement onset, offset, movement time and summed errors).

5.2.2. Participants

Twenty-eight right-handed healthy young participants (15 females, mean age ± SD = 24 ± 3 years, age range: 19-33 years) were recruited and randomly assigned to one of two experimental conditions: contralateral (left) M1 stimulation and ipsilateral (right) M1 stimulation. Prior to the study, participants were assessed for any contraindications to TMS (Rossi et al., 2009). The sample size was similar to previous TMS-EEG studies investigating movement-related excitability changes (N = 7, all male (Nikulin et al., 2003), N = 8, 4 females (Bonnard et al., 2009), N = 6, 3 females (Bonato et al., 2006). However, in order to discuss whether the study was underpowered to detect effects of TMS stimulation site and TMS time delay, post-hoc power calculations were performed and will be reported in the discussion in order to determine if lack of significance could be due to an underpowered study.

5.2.3. Experimental task

The experimental task is shown in Figure 5-1. Participants performed visually-triggered reaching movement with their dominant (right) hand rested in a robotic manipulandum (IMT2, Interactive Motion Technologies, Cambridge, MA, USA). The experiment was carried out in one continuous session and lasted approximately 2.5 hours and was composed of 360 reaching trials. To reduce muscle fatigue five-minute breaks were given after each block of 63 trials.

Each trial consisted in performing a voluntary movement with the right arm to a north-west target starting after the presentation of the visual cue from a central position, followed by a passive robot-assisted return to the starting position. Before each trial the participants were to hold the joystick within the starting central circle and wait for a visual cue; movement initiation was then indicated by the peripheral target turning from red to yellow. The intertrial interval (interval between visual cues) was 3 s.

Participants were asked to respond quickly to the visual cue so that the latencies of motor responses would be between 300 and 500 ms. This latency range allowed us to study the modulatory effects of movement preparation on evoked responses in the time range 10-220 ms post-visual cue prior to the onset of voluntary EMG. Previous experiments using a similar experimental paradigm in the same laboratory have shown that the onset of EMG activity in the BB muscle in the reaching task is around 260 ms post-visual cue (Hunter et al., 2011). For a detailed description of the reaching task and the kinematic recordings refer to **Chapter 3** (General Methods section 3.6.1). EEG was continuously recorded throughout the experiment.

Trial Start   **Visual Cue**   **Reaching towards the target**   **Trial End**

Movement Preparation   Movement Execution

A)

Trial Start   **Visual Cue**   **Reaching towards the target**   **Trial End**

Movement Preparation   Movement Execution
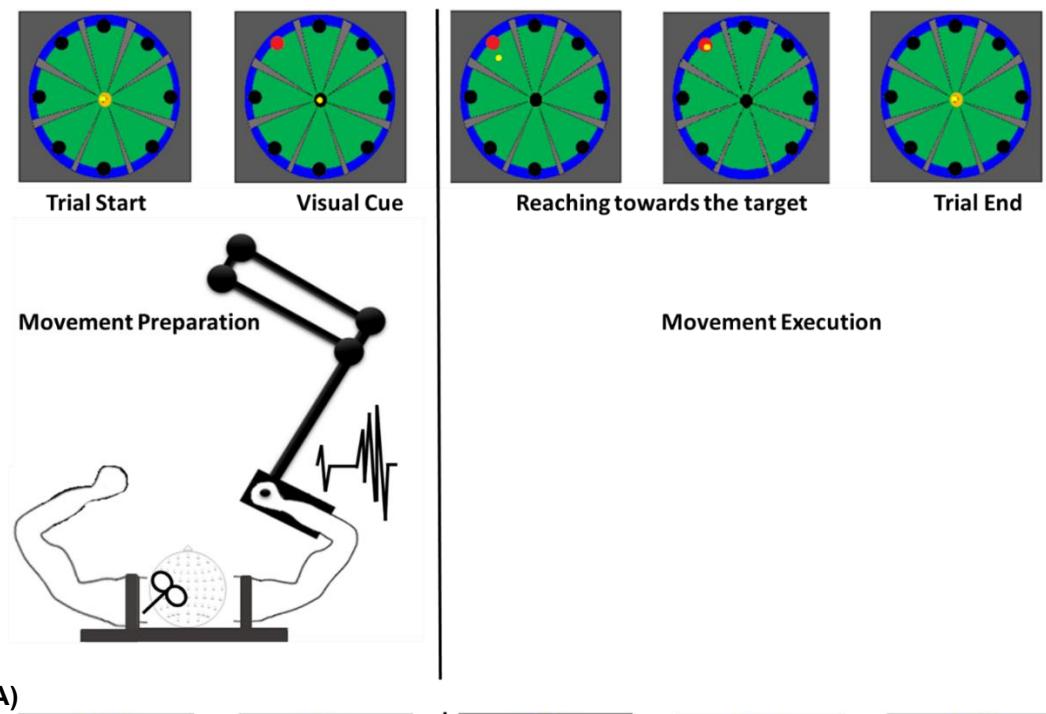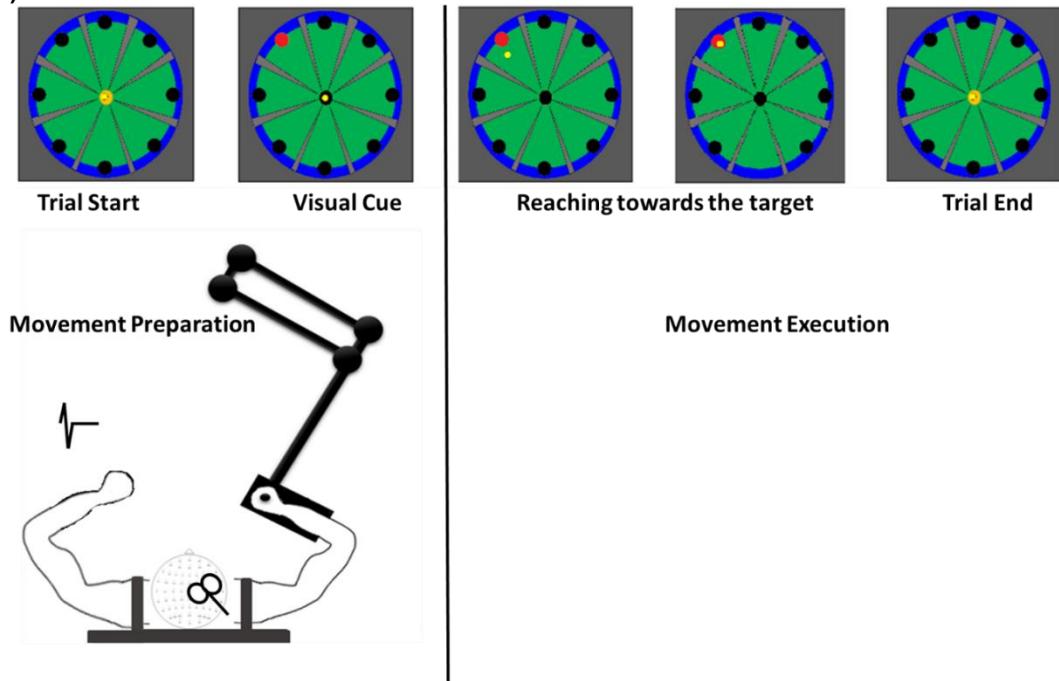
B)

Figure 5-1: Experimental Task. A) TMS applied to the left (contralateral) M1 eliciting MEPs in the task-arm (right BB) and **B)** TMS applied to the right (ipsilateral) M1 eliciting MEPs in the non-task arm during unilateral right arm reaching preparation.

5.2.4. TMS Protocol

For a detailed description of TMS hotspot definition and EMG recording please refer to **Chapter 3** (General Methods, section 3.4.1). TMS was applied at 110% RMT, which is high enough to consistently elicit MEPs and low enough to minimise the number of artefacts induced by TMS on EEG data compared to higher intensities (Farzan et al., 2016). In **Study I**, however, to reliably elicit long enough CSPs a higher intensity seemed more appropriate. For the experimental group contralateral M1 TMS stimulation, the RMT of the left M1 targeting the right BB was determined after the positioning of the EEG cap on the head. The RMT intensity corresponded to an average of 42 ± 4 % of maximum stimulator output (MSO). For the experimental group ipsilateral M1 TMS stimulation, the RMT of the right M1 targeting the left BB was determined after the positioning of the EEG cap on the head. The RMT intensity corresponded to an average of 45 ± 4 % of MSO. During the experiment single-pulse TMS was applied at 110% RMT.

5.2.5. Experimental procedure -timeline

To assess the modulation of cortical excitability during movement preparation, single-pulse TMS was applied over the left M1 (experimental group: contralateral M1 TMS stimulation) or right M1 (experimental group: ipsilateral M1 TMS stimulation) while participants prepared a reaching movement with their right arm.

Five single-pulse TMS conditions were performed with increasing delay from visual cue during movement preparation, namely 10 ms (TMS10), 130 ms (TMS130), 160 ms (TMS160), 190ms (TMS190) and 220 ms (TMS220) after visual cue similar to a previous study (Turner et al., 2013). These TMS timings range between 10-220 ms post-visual cue ensured that elicited MEPs will not be confounded with ongoing EMG activity, as it has been shown that the onset of EMG activity in the BB muscle in the same reaching task starts around 260 ms post-visual cue (Hunter et al., 2011).

TMS10 was chosen as a baseline measurement to establish a baseline of motor cortical excitability and was delivered as close as possible to the visual

cue (10 ms after visual cue). This baseline choice is similar to previous TMS reaction time paradigms (Quoilin et al., 2016; Wilhelm et al., 2016), where TMS was applied at the onset of a fixation cross. This baseline condition was chosen because it helped to control for the visual attentional focus and serves as an active/ internal control, as participants were already in a state of attention and expectation. This baseline choice was expected to be a better active control rather over a baseline at rest, which would not control for the visual cue or expectation to move.

Before the experiment, participants performed a training block consisting of 25 trials of reaching movements to familiarise with the task. The experimental protocol consisted of 360 movement trials divided in 6 experimental conditions: no-TMS, TMS10, TMS130, TMS160, TMS190 and TMS220. The no-TMS condition consisted of 45 trials, whereas a higher number of trials was used for TMS conditions (each consisting of 63 trials), as it has been shown that TMS-EEG data contain more artefacts and it was expected that in the TMS conditions more trials would be rejected compared to the no-TMS condition (for review see Farzan et al., 2016).

Each session began with the no-TMS condition in which participants performed movements without any perturbation. This was followed by the TMS condition trials, in which TMS was applied to the contralateral or ipsilateral primary motor cortex at one of five possible timings from visual cue during movement preparation. Trials of the TMS condition were counterbalanced and randomised.

EEG was continuously recorded throughout the experiment. Participants were instructed to relax completely before each trial began and this was confirmed by visual inspection of the EMG signal. To minimise the auditory evoked potentials resulting from the TMS discharge, participants listened to white noise played through earplugs (<70dB in each ear) for the duration of the TMS session.
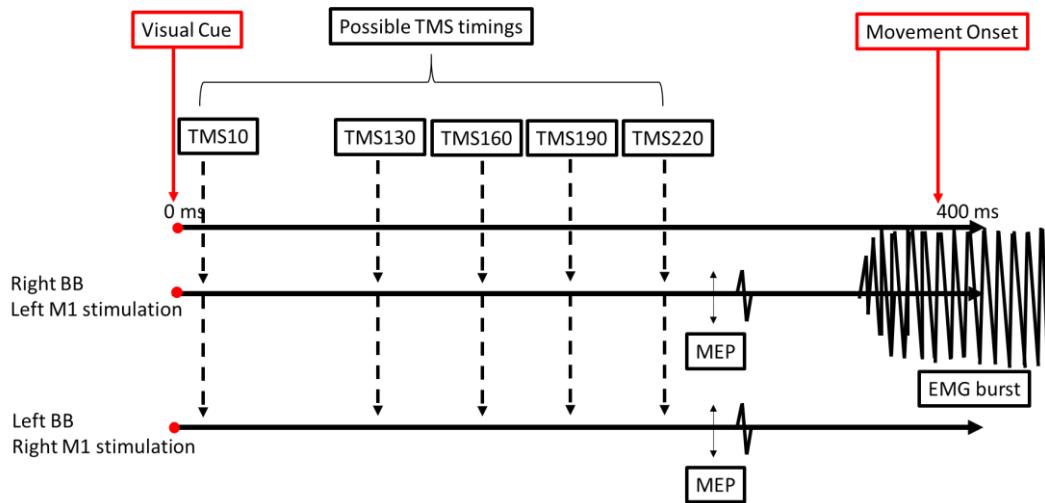
Figure 5-2: Experimental timeline: TMS timings. Previous experiments in the laboratory have shown that in this simple reaching task the mean movement onset is around 400 ms. TMS was applied in this time interval at five different delays from visual cue (TMS10, TMS130, TMS160, TMS190 and TMS220). TMS10 to TMS220 were given 10 ms post-visual cue (98 % pre-movement onset), 130 ms post-visual cue (68 % pre-movement onset), 160 ms post visual cue (60 % pre-movement onset), 190 ms post visual cue (53 % pre-movement onset), 220 ms post visual cue (45 % pre-movement onset) respectively. One single TMS pulse was delivered in each trial at one of five possible timings. For the experimental group contralateral M1 TMS, TMS was applied to the left M1 and EMG were recorded from the right BB (task arm), for the experimental group ipsilateral M1 TMS, TMS was applied to the right M1, and EMG recorded from the left BB (non-task arm).

154

5.2.6. Trajectory Recording

During each trial, trial-by-trial kinematic measures were recorded with 16-bit position encoders embedded within the two robotic joystick joints. Specifically, the angular position of these two robotic joints was recorded and used to extract the position and velocity of the joystick in Cartesian coordinates. The position (m) and velocity (m/ s) of the end-effector in the horizontal plane (along the x and y axes), as well as the forces exerted by the participant in the 3D space (along the x, y and z axes; N) were recorded with a sampling rate of 200 Hz and stored for offline analyses on the computer.

5.2.7. EEG and EMG recording

At the start of the experiment, participants sat in a comfortable chair in the experiment room and the EEG cap was placed on their head to record cortical signals and EMG electrodes were placed on the right BB muscle for the experimental group contralateral M1 stimulation and on the left BB muscle for the experimental group ipsilateral M1 stimulation to record EMG activity. For a detailed description of the EMG and EEG recording and the set-up refer to **Chapter 3** (General Methods, section 3.4.1.1 and 3.4.2 respectively). EEG and EMG were continuously recorded during the experimental protocol.

5.3.   Pre-processing

5.3.1. Kinematics

Reaching movements were described by a starting time point (i.e. movement onset, the time point at which the speed profile exceeds the threshold of 0.03 m/s) and by an end time point (i.e. movement offset, the time point at which the speed profile is lower than the threshold of 0.03 m/ s post-movement onset). Modulations of movement onset and offset were monitored throughout the whole duration of the experiment to capture eventual changes in reaction times and movement durations. Movement time was calculated as the difference between movement onset and offset. Reaching movements could ideally evolve following a straight trajectory connecting the start point and the end target.

To quantify movement accuracy, summed errors (Hunter et al., 2009) were calculated as the sum of the perpendicular distance (path offset) between the actual and the ideal trajectory at each time point from movement onset to offset.

5.3.2. MEP

EMG trial data were visually inspected, and trials contaminated with physiological (i.e. EMG activity pre-TMS pulse), and TMS pulse artefacts were deleted using the software Signal (Cambridge Electronics Design, UK). After trial rejection, each condition contained at least 55 artefact free trials. Specifically, on average across participants TMS10 contained 58 ± 4, TMS130 57 ± 4, TMS160 55 ± 4, TMS190 55 ± 4 and TM220 56 ± 4 trials in the experimental group contralateral M1 stimulation and TMS10 contained 55 ± 7, TMS130 56 ± 4, TMS160 56 ± 4, TMS190 56 ± 4 and TMS220 56 ± 4 trials in the experimental group ipsilateral M1 stimulation group.

The peak-to-peak MEP amplitude in the BB was determined semi-automatically using the Signal software in CED in a time window of 10 to 40 ms after TMS pulse for every single trial. To ensure that the measurements were taken accurately, data were also visually inspected trial-by-trial. MEP peak-to-peak amplitude averages for each TMS condition were then calculated. In order to reduce the inter-subject variability in MEP amplitudes, MEP amplitude of conditions I = TMS130, TMS160, 1TMS90 and TMS220 were expressed as percentage change from TMS10 and used for statistical analysis ([TMSi/ TMS10] * 100).

To compute pre-TMS baseline EMG activity and EMG activity associated with movement, the EMG signals were full-wave rectified and pre-TMS EMG activity was calculated as the mean EMG activity 100 ms pre-TMS.

5.3.3. EEG: ERP and TEP

5.3.3.1. ERP

First, EEG data were down-sampled from 2048 Hz to 1000 Hz. A bandpass filter (1-80 Hz, zero-phase Butterworth filter, order = 4) and bandstop filter (48-

52 Hz, zero-phase Butterworth filter, order = 4) to remove line noise (50 Hz) were applied. Data were epoched from - 1 to 1 s around the visual cue. Electrodes and trials with mechanical artefacts were identified by means of visual inspection and rejected. On average across participants, 42 ± 5 artefact free trials remained in the experimental group contralateral M1 stimulation and 43 ± 2 artefact free trials remained in the experimental group ipsilateral M1 stimulation. On average across participants 3 ± 1 electrodes (i.e. 5 ± 2 % of total electrodes) were deleted in the experimental group contralateral M2 stimulation and 2 ± 0 electrodes (i.e. 3 ± 0 % of total electrodes) in the experimental group ipsilateral M1 stimulation.

To remove artefacts such as eye-blinks, lateral eye movements and electrode movements, an ICA decomposition was performed using the FASTICA algorithm (Korhonen et al., 2011). Deleted electrodes were then interpolated using spherical interpolation and the data were re-referenced to common average. To examine evoked responses in the time domain, all clean trials were baseline corrected (-800 to 0 ms pre-visual cue) and then averaged for each electrode. The average of cleaned trials for each electrode is referred to as ERP.

5.3.3.2.   TEP

EEG data from each TMS condition (TMS10, TMS130, TMS160, TMS190 and TMS220) were merged into one file and pre-processed together. Data were epoched (- 1 to + 1 s) around the TMS pulse. Epochs were demeaned by subtracting the average between - 1 to + 1 s from each epoch to remove the DC offset. The TMS pulse artefact was removed from - 2 to + 10 ms around the TMS pulse and removed data were replaced with artefact free data using data from - 7 to - 2 and +10 to + 15 ms using cubic interpolation. EEG data were then down-sampled from 2048 Hz to 1000 Hz. Electrodes and epochs with mechanical artefacts were identified by means of visual inspection and rejected.

After this step, each condition contained at least 54 artefact free trials. Specifically, TMS10 contained on average across participants 58 ± 4, TMS130 57 ± 4, TMS160 55 ± 4, TMS190 55 ± 4 and TM220 56 ± 4 trials in

the experimental group contralateral M1 stimulation and TMS10 contained 55 ± 7, TMS130 56 ± 4, TMS160 56 ± 4, TMS190 56 ± 4 and TMS220 56 ± 4 trials in the experimental group ipsilateral M1 stimulation group. In the experimental group contralateral M1 stimulation 3 ± 1 electrodes (i.e. 5 ± 0 % of total electrodes), and in experimental group ipsilateral M1 stimulation 3 ± 1 electrodes (i.e. 5 ± 2 % of total electrodes) were deleted on average across participants.

Data were then submitted to an ICA decomposition using the FASTICA algorithm (Korhonen et al., 2011) and components representing TMS evoked muscle artefacts were identified and rejected. In the experimental group contralateral M1 stimulation, 2 ± 1 components (i.e. 3 ± 1 % of total ICA components) and in the experimental group ipsilateral M1 stimulation, 3 ± 2 components (i.e. 6 ± 3 % of total ICA components) on average across participants were rejected.

Data between - 2 and +15 ms around the TMS pulse were removed and replaced with artefact free data using data from - 7 to - 2 and + 15 to + 20 ms using cubic interpolation. A bandpass filter (1-80 Hz, zero-phase Butterworth filter, order = 4) and bandstop filter (48-52 Hz, zero-phase Butterworth filter, order = 4) to remove line noise (50 Hz) were applied. Then, a second round of ICA decomposition was performed and all the remaining artefacts (eye-blinks, lateral eye movements, electrode movement and electrical artefacts) were identified and removed.

In the experimental group contralateral M1 stimulation, 34 ± 4 components (i.e., 57 ± 7 % of total ICA components) and in the experimental group ipsilateral M1 stimulation 27 ± 7 components (i.e., 46 ± 11 % of total ICA components) were rejected on average across participants. Deleted electrodes were interpolated using a spherical interpolation and the data were re-referenced to common average. A more detailed description of the pre-processing steps can be found in Chapter 3 (General Methods; section 3.6.3).

To examine TMS-evoked responses in the time domain, all clean trials were baseline corrected (- 800 to - 100 ms pre-TMS) and then averaged for each

electrode. The average of cleaned epochs for each electrode is referred to as TEP.

5.3.3.3. TEP – ERP subtraction

Since the TMS pulse in each condition is delivered during the visual and motor preparation potential and we wanted to limit the number of confounding factors, which could potentially contribute to differences of TEPs across conditions, we subtracted each average TMS-evoked response with the average evoked-response (locked to the visual cue) recorded in the no-TMS condition. After this subtraction, TEP peak components were evaluated and the peak amplitudes were extracted and analysed for each TMS condition.

5.3.3.4. Whole scalp

TEPs were calculated for each participant as a function of time. Using butterfly TEP plots of the cleaned data, commonly observed TMS–EEG deflections were identified. For the TEP peak amplitude extraction of each TEP component, the following time windows of interest: P30: 25-40 ms, N45: 35-60 ms, P60: 50-70 ms, N100: 75-150 ms, and P190: 160-220 ms were used, based on our data and in line with previous TMS-EEG literature (Farzan et al., 2013; Komssi et al., 2004; Mutanen et al., 2016; Paus et al., 2001; Premoli et al., 2014).

Specifically, TEP peak analysis was performed in every electrode using the tep_extract function of the TESA toolbox. Peaks were defined as a data point that is greater than (positive) or less than (negative) 5 data points on either side of the peak. If multiple peaks were detected within a time window, the largest peak was used.

5.3.3.5. Region of Interests (ROIs)

For local TEPs two ROIs covering the ipsilateral motor region of the stimulated hemisphere were selected. The ROI was composed of the two electrodes closest from the stimulated brain region, i.e. FC1 and C1 for the left M1 stimulation (experimental group contralateral M1 TMS stimulation) and FC2

and C2 for the right M1 stimulation (experimental group ipsilateral M1 stimulation).

5.4. Statistics

Unless stated otherwise, all data were assessed using parametric statistical tests following confirmation of normal distribution of data using the Shapiro-Wilk test. All statistical procedures were performed using SPSS (IBM SPSS Statistics for Windows, Version 24.0).

All data were assessed for normality using the Shapiro-Wilk test and sphericity using the Mauchly test. All data met the assumption for normality, however since kinematic data, MEPs (expressed as percentage change from TMS10) and TEP components violated the assumption of sphericity, a Greenhouse-Geisser correction was applied when running ANOVAs.

5.4.1. Kinematics

First, it was investigated if there were differences in TMS stimulation site and TMS delays on kinematic measures. A MANOVA was performed with TMS stimulation site (contralateral M1 stimulation versus ipsilateral M1 stimulation) as between-subject factor and TMS delays (6 levels: no-TMS, TMS10, TMS130, TMS160, TMS190 and TMS220) was performed. Dependent variables were movement onset, offset, movement time and summed errors. If a significant effect of TMS stimulation site, TMS delay or an interaction was detected, follow-up ANOVAs were performed on each of the dependent variables independently. Whenever a main effect of TMS delay was found, post-hoc paired t-tests with Bonferroni correction for multiple comparisons was applied to analyse the differences between no-TMS condition and TMS I, with i =10, 130, 160, 190, 220 (5 comparisons, p < 0.01).

5.4.2. MEPs

Since this study had an adequate baseline condition (TMS10, as opposed to study I), MEPs, expressed as percentage change from TM10 to reduce subject variability between subjects were taken for statistical analysis. The main effects of TMS stimulation site (between-subject factor) and TMS delay

(within-subjects factor), as well as their interaction, were examined. The mixed-model ANOVA had a between-subject factor of TMS stimulation site (contralateral M1 TMS stimulation versus ipsilateral M1 TMS stimulation) and a within-subject factor of TMS delay (5 levels: TMS10, TMS130, TMS160, TMS190 and TMS220). Whenever a main effect of TMS delay was found, post-hoc paired t-tests with Bonferroni correction for multiple comparisons was applied to analyse the differences between TMS10 condition and TMS I, with i = 130, 160, 190, 220 (4 comparisons, $p < 0.0125$).

Since MEP that results from a single-pulse of TMS is affected by the state of the activation of the target muscle. Therefore, we quantified the state of the muscles at 100 ms pre-TMS, calculated as the mean full-wave rectified EMG activity 100 ms pre-TMS pulse. Repeated-measure ANOVA (5 levels: TMS10, TMS130, TMS160, TMS190 and TMS220) were performed for the pre-TMS EMG activity in the contralateral M1 stimulation group.

5.4.3. TEPs

First, it was investigated if there were differences in TMS stimulation site and TMS delays on TEP peak amplitudes of the ipsilateral ROI (electrodes closest to the stimulation site). A MANOVA was performed with TMS stimulation site (contralateral M1 stimulation versus ipsilateral M1 stimulation) as between-subject factor and TMS delays (6 levels: no-TMS, TMS10, TMS130, TMS160, TMS190 and TMS220) was performed. The dependent variables were the five TEP components: P30, N45, P60, N100 and P190. If a significant effect of TMS stimulation site, TMS delay or an interaction was detected, follow-up ANOVAs were performed on each of the dependent variables separately. Whenever a main effect of TMS delay was found, post-hoc paired t-tests with Bonferroni correction for multiple comparisons was applied to analyse the differences between no-TMS condition and TMS I, with i =10, 130, 160, 190, 220 (5 comparisons, $p < 0.01$).

5.5. Results

Unless stated otherwise, all results presented in text, Figures and Tables are given in mean ± SD.

5.5.1. Kinematics

The MANOVA showed that there was a significant main effect on kinematic measures of TMS delay (Pillai's trace= 0.553, $F(15, 375)$= 5.648, $p < 0.0001$, $\eta2$ =0.184) and a significant interaction between TMS stimulations site and TMS delay (Pillai's trace = 0.263, $F(15, 375)$ = 2.402, $p = 0.002$, $\eta2 = 0.088$) with no main effect of TMS stimulation site (Pillai's trace = 0.221, $F(3,23)$ = 2.174, $p= 0.118$, $\eta2 = 0.221$).

Separate follow-up ANOVAs revealed a significant main effect of TMS delay for movement onset ($F (2.32, 55.57)$ = 10.75, $p < 0.0001$, $\eta2 = 0.31$) and offset ($F (1.88, 46.97)$ = 11.45, $p < 0.0001$, $\eta2 = 0.285$), but there was no main effect on overall movement time ($F (1.70, 42.59)$ = 3.02, $p < 0.0001$, $\eta2 = 0.108$) and on summed errors ($F(2.92, 73.06)$ = 2.40, $p=0.076$, $\eta2 = 0.098$).

No main effect of TMS stimulation site was found in any kinematic measure. A significant interaction between TMS delay and TMS stimulation site was only seen in summed errors ($F (2.92, 73.06)$ = 4.00, $p = 0.011$, $\eta2 = 0.155$). Post-hoc t-tests showed that TMS delay had no significant effect for contralateral M1 stimulation, but it significantly lowered summed errors with increasing TMS delay from visual cue for the ipsilateral M1 stimulation. For detailed statistical values (Mean ± SD and ANOVA results) refer to Table 5-1 and Table 5-2 and Figure 5-3.
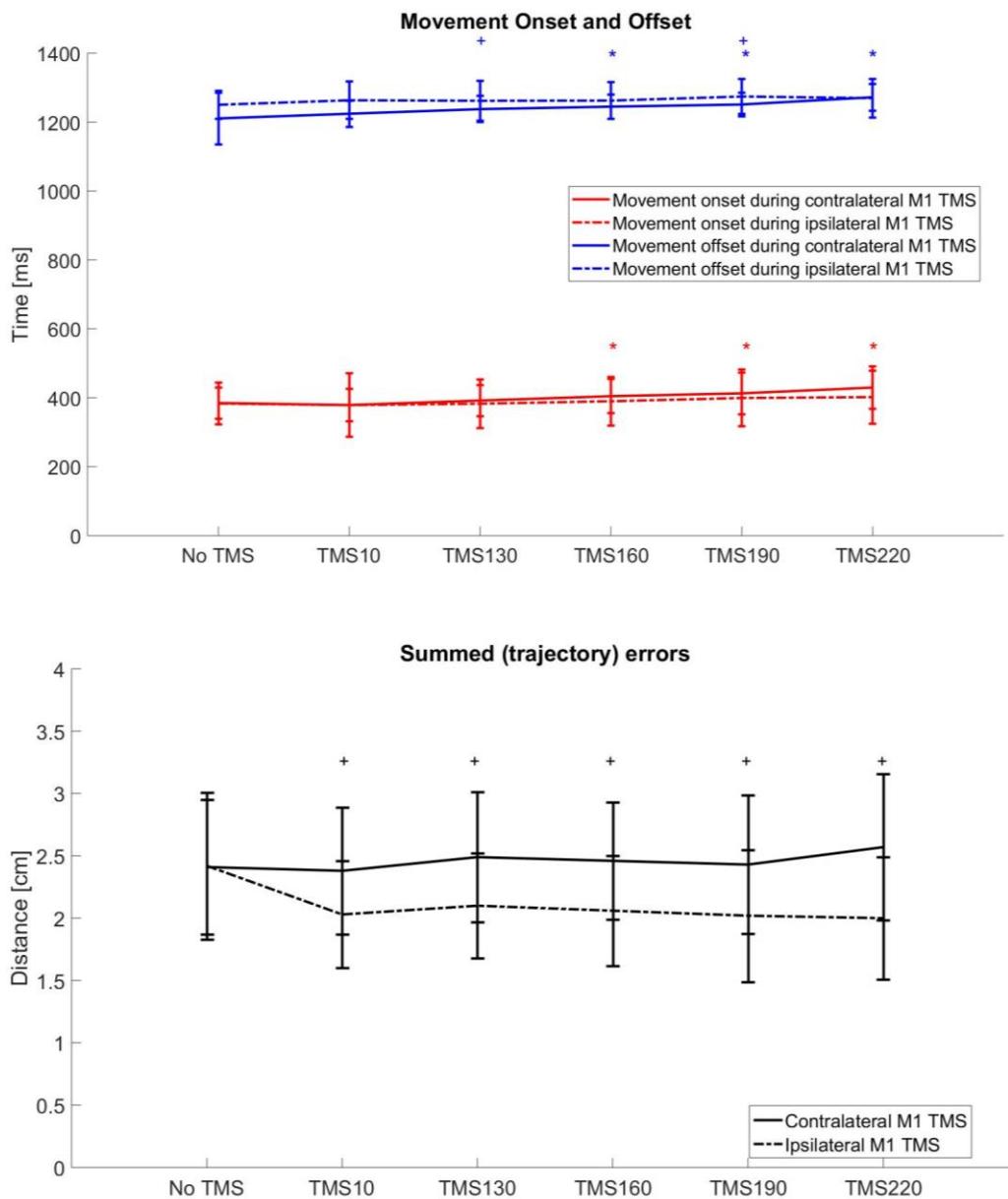
Figure 5-3: Kinematic results (Mean ± SD). The upper panel represents movement onset (in red) and movement offset (in blue) and the lower panel represents summed errors. Contralateral M1 stimulation are shown with solid lines and ipsilateral M1 TMS stimulation in dashed lines. *p < 0.001 post-hoc significant difference between TMS10 and all other TMS conditions for contralateral (left) M1 TMS and + p < 0.001 for ipsilateral (right) M1 TMS.

Table 5-1: ANOVA results for kinematic data. The mixed model ANOVA had a between -subject factor of TMS stimulation site (2 levels: contralateral (left) M1 versus ipsilateral (right) M1) and a within-subject factor of TMS delay (6 levels: no-TMS, TMS10, TMS130, TMS160, TMS190 and TMS220).

	Within-subject				Between-subject				Interaction			
Kinematics	TMS delay				TMS stimulation site				TMS delay*TMS stimulation site			
	F	df, Errors	p	η2	F	df, Errors	p	η2	F	df, Errors	p	η2
Movement Onset	10.75	2.32, 55.57	<0.0001	0.31	0.254	1, 25	0.618	0.01	2.18	2.32, 55.57	0.115	0.055
Movement Offset	11.45	1.88, 46.97	<0.0001	0.285	4.152	1, 25	0.53	0.142	1.23	1.88, 46.97	0.284	0.08
Movement Time	3.02	1.70, 42.59	0.067	0.108	4.142	1.25	0.053	0.142	0.299	1.703,42.587	0.708	0.012
Summed Errors	2.40	2.92, 73.06	0.076	0.098	4.933	1, 25	0.06	0.13	4.00	2.92, 73.06	0.011	0.155

Table 5-2: Post-hoc paired-t-tests for kinematic data (Mean ± SD). Bonferroni correction for multiple comparisons was applied to analyse the differences between no-TMS and TMS I, with i = 10, 130, 160, 190, 220 (5 comparisons, *p < 0.01) for the contralateral and ipsilateral M1 stimulation group.

Kinematics	no TMS	TMS10	TMS130	TMS160	TMS190	TMS220
Contralateral M1 TMS stimulation group						
Movement Onset [ms]	385 [46]	379[47]	392[46]	404[50]*	413[60]*	430[61]*
Movement Offset [ms]	1211[75]	1224[38]	1237[38]	1245[35]*	1251[34]*	1272[39]*
Movement Time [ms]	826[77]	845[58]	845[60]	840[55]	838[60]	842[61]
Summed Errors [cm]	2.41[0.54]	2.38[0.51]	2.49[0.52]	2.46[0.47]	2.43 [0.56]	2.57 [0.59]
Ipsilateral M1 TMS stimulation group						
Movement Onset [ms]	383[61]	379[91]	383[71]	390[71]	400[82]	402[77]
Movement Offset [ms]	1250[40]	1263[54]	1262[58]*	1263[54]	1274[50]*	1269[56]
Movement Time [ms]	860[68]	884[75]	880[75]	874[71]	876[73]	870[73]
Summed Errors [cm]	2.42[0.59]	2.03[0.43]*	2.1[0.42]*	2.06[0.44]*	2.02[0.53]*	2[0.49]*

5.5.2. MEPs

EMG traces are shown in one representative participants from the contralateral M1 TMS stimulation group in Figure 5-4 and for one in the ipsilateral M1 TMS stimulation group in Figure 5-5. When TMS was applied over the contralateral M1 during movement preparation it elicited an MEP in the task arm (right BB) and showed increased EMG activity around movement onset. When TMS was applied over the ipsilateral M1 during movement preparation it elicited an MEP in the non-task arm (left BB).

There was no significant main effect of TMS delay ($F_{(2.734, 71.095)} = 2.143$, $p = 0.108$, $\eta2 = 0.076$), no significant main effect of TMS stimulation site ($F_{(1, 26)} = 0.208$, $p = 0.652$, $\eta2 = 0.008$) and no significant interaction between TMS delay and TMS stimulation site ($F_{(2.734, 71.095)} = 0.145$, $p = 0.919$, $\eta2 = 0.006$) (Figure 5-6). When the two experimental condition groups were analysed independently, there was also no statistically significant difference in MEP amplitudes across TMS delay in the contralateral M1 TMS stimulation group ($F_{(3.528, 43.869)} = 1.573$, $p = 0.203$, $\eta2 = 0.108$) and in the ipsilateral M1 TMS stimulation group ($F_{(1.184, 15.389)} = 0.681$, $p = 0.452$, $\eta2 = 0.05$).

To ensure that MEP amplitudes were not influenced by pre-TMS voluntary EMG activity in the right BB associated with movement preparation and execution in the contralateral (left) M1 stimulation group, the average 100 ms pre-TMS EMG activity was evaluated. There was no significant difference in baseline rectified mean pre-TMS EMG activity: $F_{(1.45, 18.8)} = 1.07$, $p = 0.38$, $\eta2 = 0.076$) across conditions (TMS10 = 0.008 ± 0.026 mV, TMS130= 0.007 ± 0.026 mV, TMS160 = 0.006 ± 0.029 mV, TMS190 = 0.008 ± 0.0028 mV, TMS220 = 0.008 ± 0.029 mV.
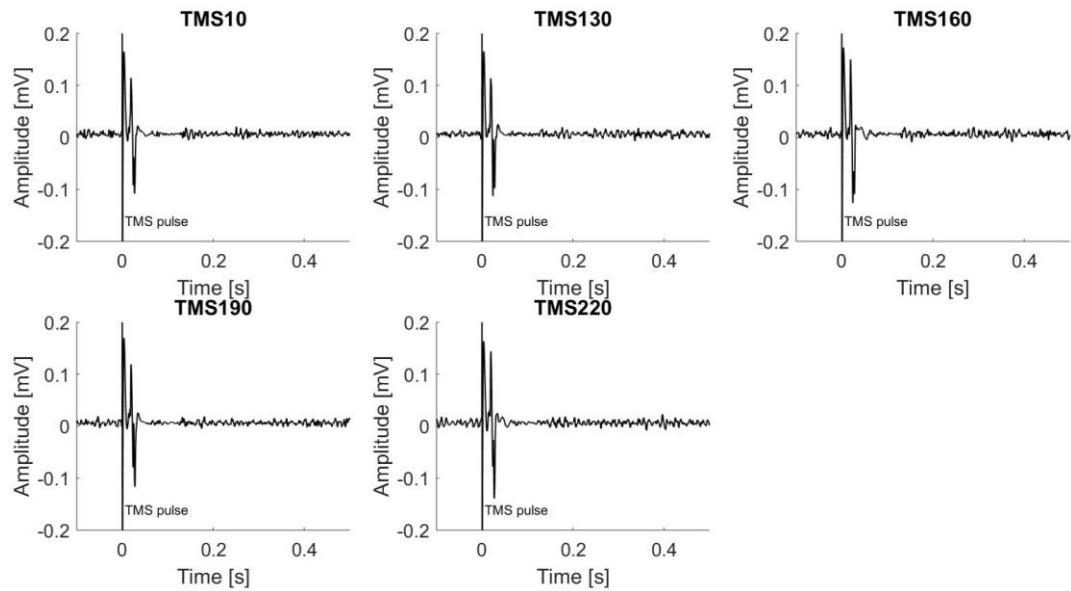
Figure 5-4: EMG traces for the five TMS conditions in one representative participant in the contralateral TMS stimulation condition. Each EMG trace shows the MEP response following contralateral (left) M1 stimulation recorded from the right BB EMG during right arm reaching preparation. MEP peak-to-peak amplitude was extracted between 10-40 ms post-TMS.
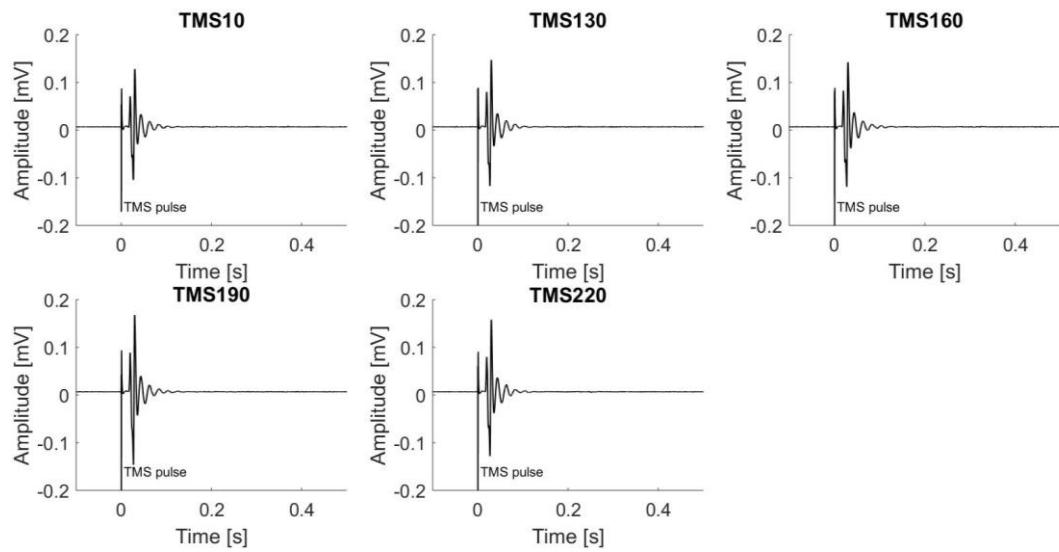
Figure 5-5: EMG traces for the five TMS conditions in one representative participant in the ipsilateral TMS stimulation condition. Each EMG trace shows the MEP response following ipsilateral (right) M1 stimulation recorded from the left BB EMG during right arm reaching preparation. MEP peak-to-peak amplitude was extracted in between 10-40 ms post-TMS.
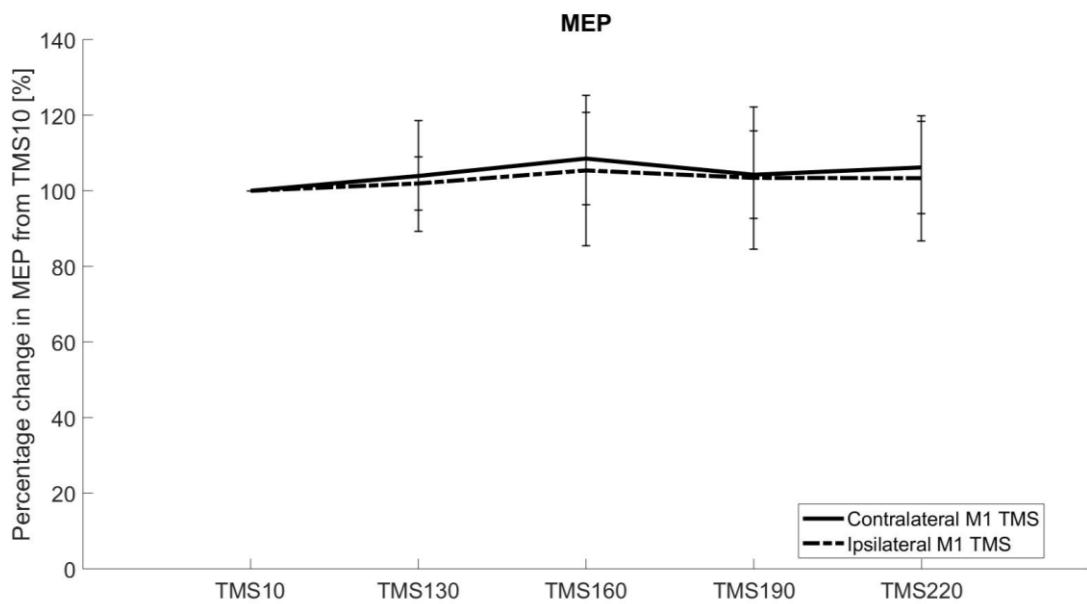
Figure 5-6: MEP modulation during movement preparation. Changes from TMS10 in group mean (± SD) MEP amplitudes for contralateral (solid black lines) and ipsilateral (dashed black lines) M1 TMS stimulation at different time delays from the visual cue during movement preparation. MEPs for contralateral M1 TMS stimulation were recorded from the task arm (right BB), and for ipsilateral M1 TMS stimulation from the non-task arm (left BB).

5.5.3. EEG Natural reaching

In line with the literature (Naranjo et al., 2007) and based on previous lab findings (Desowska and Turner, 2018; Pizzamiglio, 2017), a positive deflection around 140 ms post-visual cue and a negative deflection around 300 ms post-visual cue in the contralateral M1 (FC1, C1) and ipsilateral M1 (FC2, C2) to the reaching arm was detected. ERP activations during movement preparation are shown in all electrodes in butterfly plots and in the ROI ipsilateral to the targeted stimulation site in the subsequent TMS conditions in Figure 5-7.
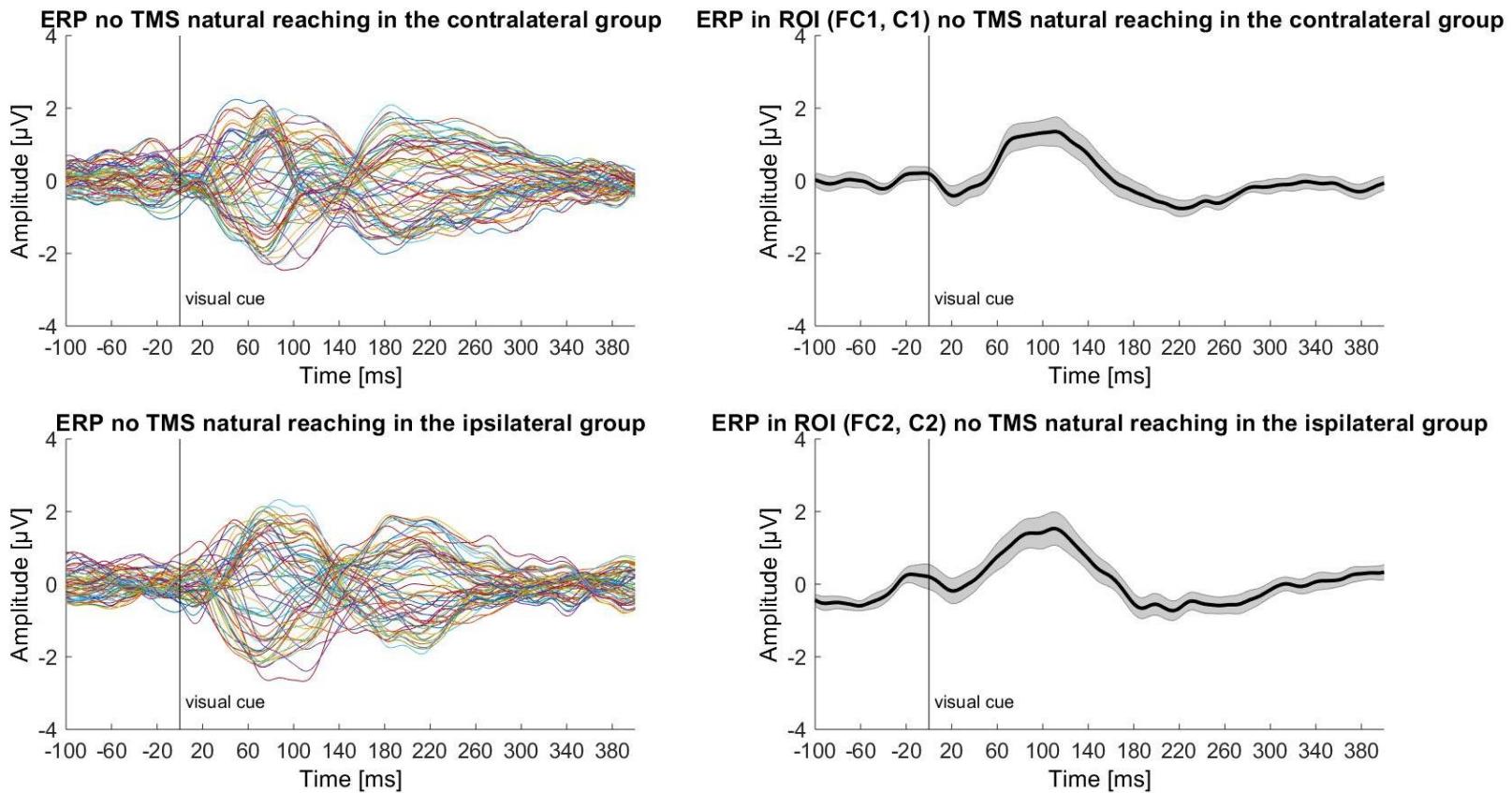
Figure 5-7: Grand-average ERP during natural reaching (no TMS condition). ERP activity is shown for the contralateral M1 TMS stimulation group (N = 14) in the upper panel and for the ipsilateral M1 TMS stimulation group (N = 14) in the lower panels. Grand-average ERPs in all electrodes are shown in the left upper and lower panel for both groups and grand-average (± SEM, shaded area) are shown in the right panels in the electrodes overlying the brain region targeted by TMS during the subsequent TMS conditions.

5.5.4. TMS-EEG: TEPs

Single-pulse TMS over the contralateral (Figure 5-8) and ipsilateral (Figure 5-9) M1 during movement preparation produced several positive and negative deflections as can be seen in the butterfly plots.

Raw TEPs from all TMS conditions in the ROI ipsilateral to the stimulation site are shown in Figure 5-10 in the left panels and TEPs from all TMS conditions subtracted with the ERP from the no-TMS condition are shown in the right panel for the ipsilateral and ipsilateral M1 stimulation group
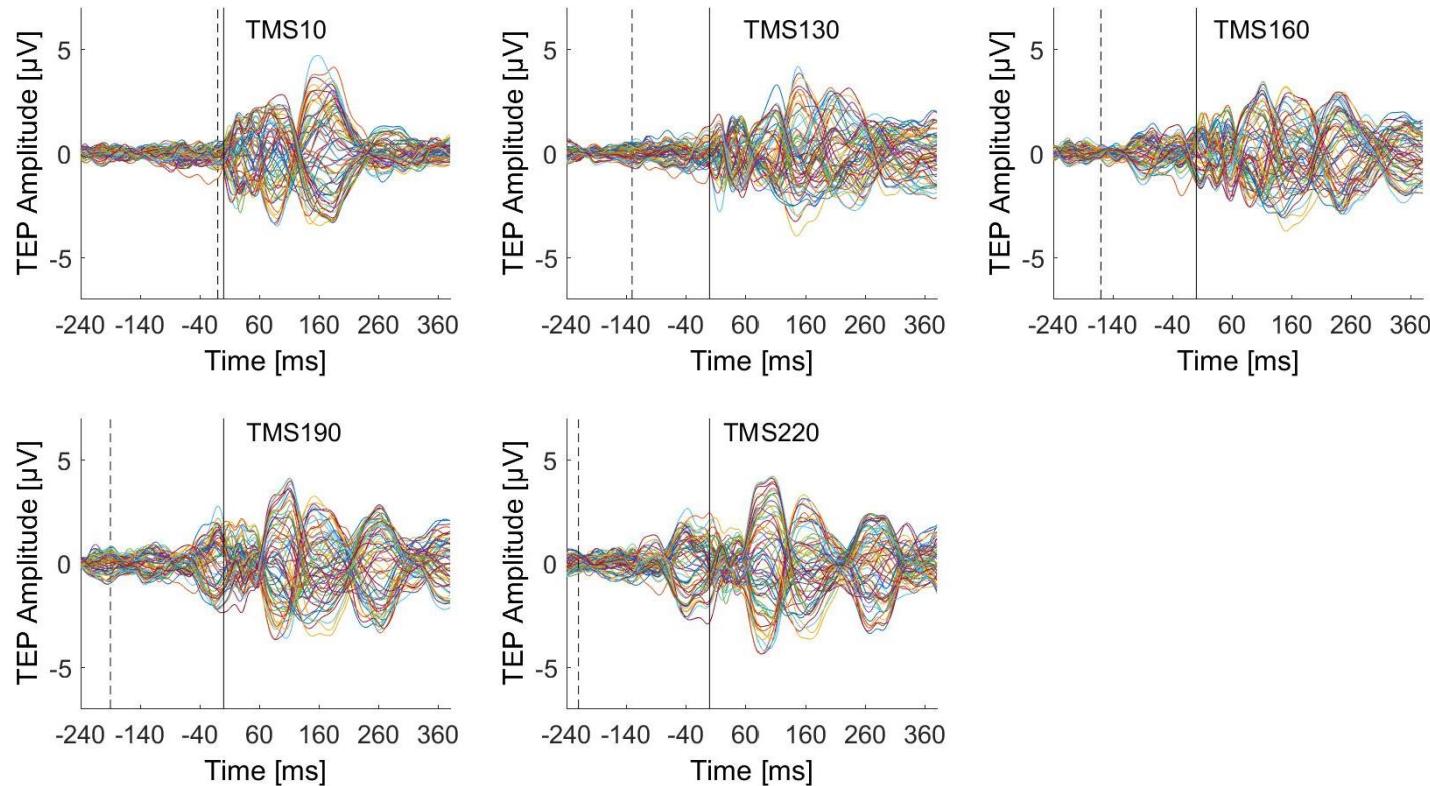
Figure 5-8: Raw TEP during movement preparation in the contralateral M1 stimulation group in the five TMS conditions: TMS10, TMS130, TMS160, TMS190 and TMS220. contralateral raw TEPs. Grand-average (N=14) TEPs in all electrodes are shown in subplots for each condition. The dashed vertical line represents the timing of visual cue and the solid black line the timing of the TMS pulse.
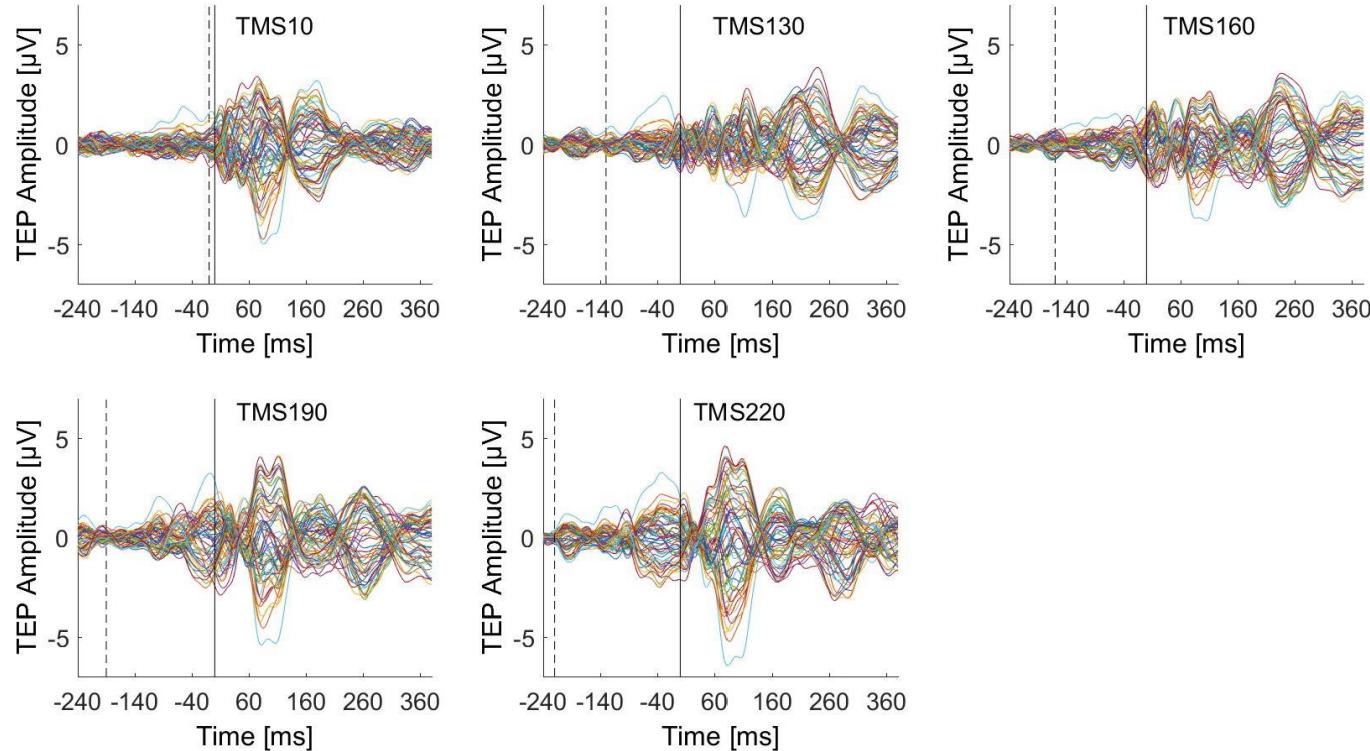
Figure 5-9: Raw TEP during movement preparation in the ipsilateral M1 stimulation group in the five TMS conditions: TMS10, TMS130, TMS160, TMS190 and TMS220. contralateral raw TEPs. Grand-average (N=14) TEPs in all electrodes are shown in subplots for each condition. The dashed vertical line represents the timing of visual cue and the solid black line the timing of the TMS pulse.
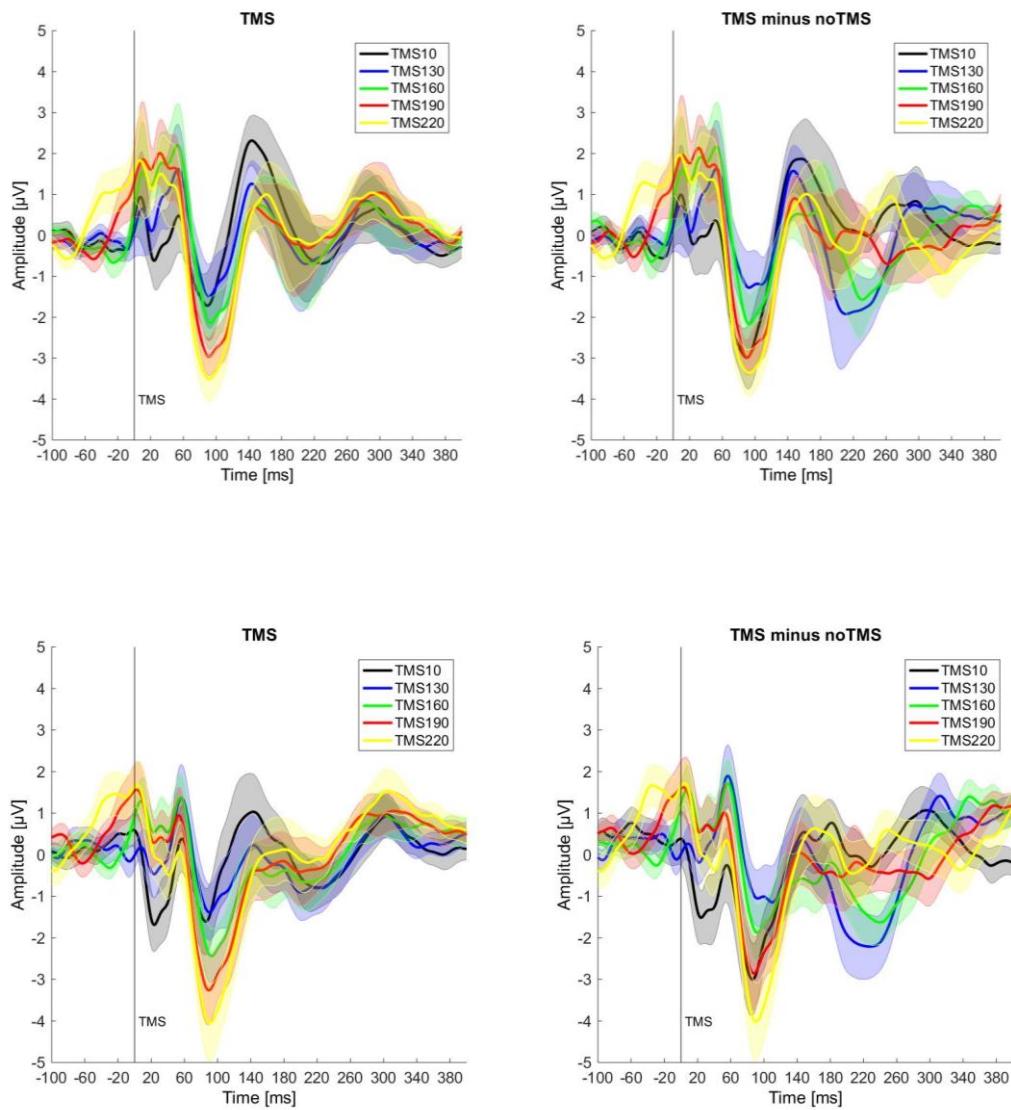
Figure 5-10: TEPs in the ipsilateral ROI in the five TMS delay conditions. TEP activity is shown for the contralateral M1 TMS stimulation group (N = 14) in the upper panels and for the ipsilateral M1 TMS stimulation group (N = 14) in the lower panels. Grand-average TEPs (± SEM, shaded area) are shown before subtraction in the left panels and after subtraction in the right panels in the ROI ipsilateral to the stimulation site (FC1, C1 for the contralateral M1 stimulation group and FC2, C2 for the ipsilateral M1 stimulation group).

The MANOVA showed that there was a significant main effect on TEP peak amplitudes of TMS delay (Pillai's trace= 0.680, $F_{(20,412)}$ = 4.219, $p < 0.0001$, $\eta2$ = 0.170), no significant effect of TMS stimulation site (Pillai's trace = 0.370, $F_{(5, 22)}$ = 2.579, p= 0.056, $\eta2$ = 0.370) and no significant interaction between TMS stimulation site and TMS delay (Pillai's trace = 0.112, $F_{(20, 412)}$ = 0.592, p = 0.919, $\eta2$ = 0.028).

Follow-up ANOVAs for the between-subject-factor TMS stimulation site revealed only a significant effect for the dependent variable P190 ($F_{(1, 26)}$ = 14.052, p= 0.001, $\eta2$ = 0.351). There was no effect of TMS stimulation site on any other TEP component: P30 ($F_{(1, 26)}$ = 1.289, p = 0.267, $\eta2$ = 0.047), N45 ($F_{(1, 26)}$ = 0.484, p = 0.493, $\eta2$ = 0.018), P60 ($F_{(1, 26)}$ = 2.473, p = 0.128, $\eta2$ = 0.087) and N100 ($F_{(1, 26)}$ = 0.068, p = 0.796, $\eta2$ = 0.03).

Follow-up univariate ANOVA results with factor TMS stimulation site and TMS delay are summarised in Table 5-2, and separate ANOVA results for each TMS stimulation site group with post-hoc paired t-tests results are reported in Table 5-3. All TEP component amplitudes (Mean ± SD) and statistical results are shown in Figure 5-11.

5.4.1.1.   Contralateral (left) M1 TMS stimulation

Repeated-measure ANOVA for the contralateral M1 TMS stimulation site group revealed a significant effect of TMS delay in the P30 component ($F_{(2.66, 1.8)}$ = 6.94, $p < 0.0001$, $\eta2$ = 0.346) , the N45 component ($F_{(2.8, 1.79)}$ = 5.87, $p < 0.0001$, $\eta2$ = 0.262), the P60 component ($F_{(2.28, 2.11)}$ = 5.38, p = 0.01, $\eta2$ = 0.249) and the N100 component ($F_{(2.19, 2.37)}$ = 3.7 ,p = 0.03, $\eta2$ = 0.265), and no significant effect on the P190 component ($F_{(2.64, 1.91)}$ = 1.27, p = 0.3, $\eta2$ = 0.045). Post-hoc paired t-tests between each between TMS10 condition and TMS I, with I = 130, 160, 190, 220 (4 comparisons, $p < 0.0125$) revealed a significant difference in the P30, N45 and P60 component. For individual statistics refer to Table 5-4.

5.4.1.2. Ipsilateral (left) M1 TMS stimulation

Repeated-measure ANOVA for the contralateral M1 TMS stimulations site group revealed a significant effect of TMS delay in the P30 component ($F_{(1.5, 10.84)} = 4.34$, $p = 0.04$, $\eta2 = 0.250$) , the N45 component ($F_{(2.66, 2.97)} = 6.00$, $p < 0.0001$, $\eta2 = 0.316$), the P60 component ($F_{(2.02, 4.16)} = 6.04$, $p = 0.01$, $\eta2 = 0.317$) and the N100 component ($F_{(1.84, 5.76)} = 3.68$ $p = 0.04$, $\eta2 = 0.221$), and no significant difference across condition for the P190 component ($F_{(2.68, 4.47)} = 1.46$, $p = 0.24$, $\eta2 = 0.101$). Post-hoc paired t-tests between each between TMS10 condition and TMS I, with i= 130, 160, 190, 220 (4 comparisons, $p < 0.0125$) revealed a significant difference in the P30, N45 and P60 component. For individual statistics refer to Table 5-4.
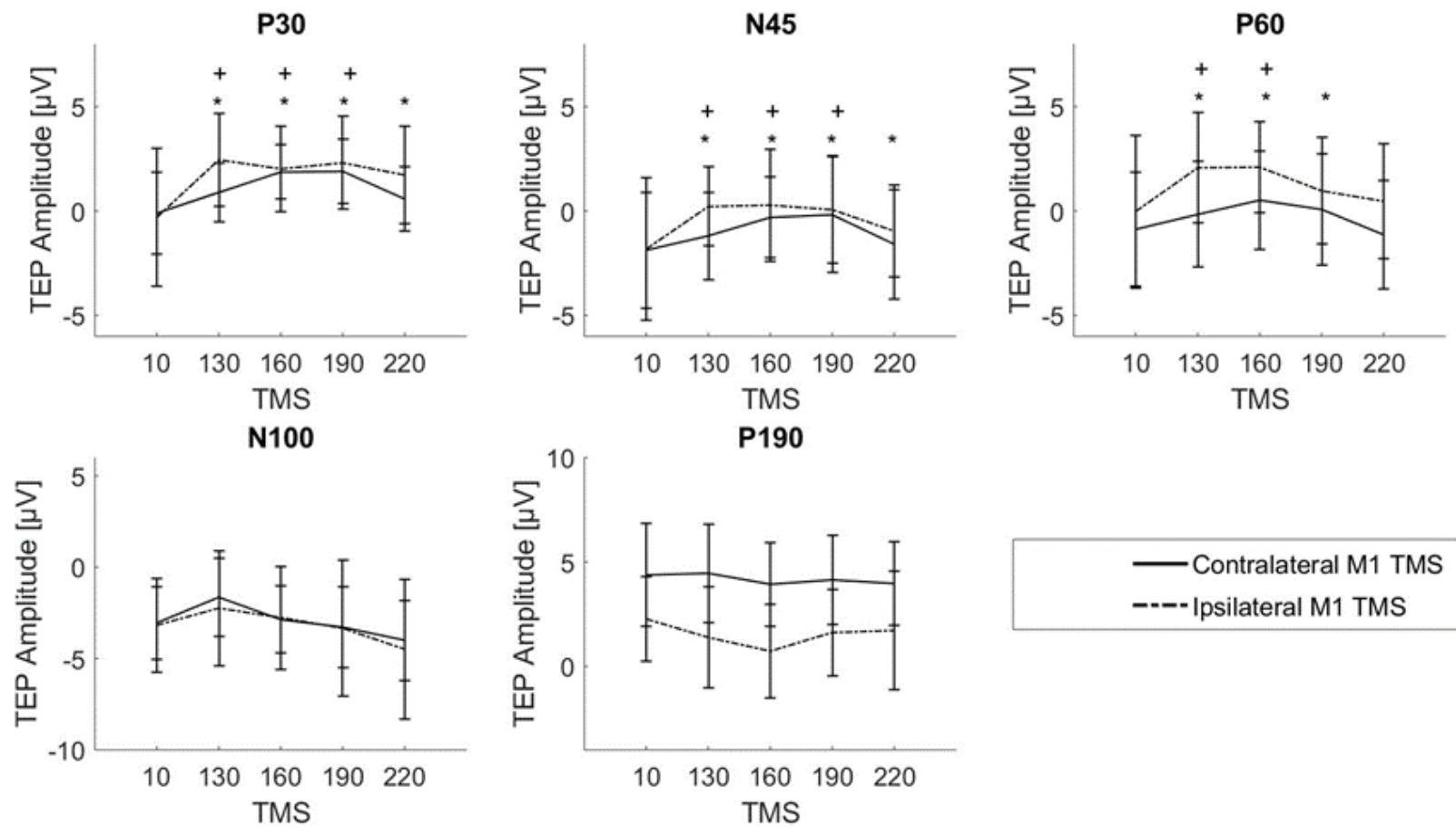
Figure 5-11: TEP components P30, N45, P60, N100 and P190. Line plots represent mean (± SD) of the TEP components averaged from the electrodes in the ipsilateral ROI (closest to the stimulation site; FC1, C1 for contralateral M1 TMS and FC2, C2 for ipsilateral M1 TMS stimulation). The experimental group contralateral M1 TMS are presented with solid lines and the experimental group ipsilateral M1 TMS stimulation in dashed lines. *p < 0.001 post-hoc significant difference between TMS10 and all other TMS conditions for contralateral (left) M1 TMS and + p < 0.01 for ipsilateral (right) M1 TMS.

Table 5-3: Mixed repeated-measure ANOVA results for TEP amplitudes. The within-subject factor was TMS delay (5 levels (TMS10, TMS130, TMS190, TMS220) and the between-subject factor TMS stimulation site (2 levels: contralateral M1 stimulation and ipsilateral M1 stimulation).

| Peak | Within-subject Factor | | | | Between-subject Factor | | | | Interaction | | | |
| | TMS delay | | | | Condition | | | | TMS delay * Condition | | | |
	F	df, Errors	p	η2	F	df, Errors	p	η2	F	df, Errors	p	η2
P30	8.73	1.97, 51.227	0.001	0.251	1.29	1, 26	0.267	0.047	1.32	1.97, 51.227	0.276	0.048
N45	9.7	2.86, 74.317	< 0.0001	0.272	0.48	1, 26	0.493	0.018	1.01	2.86, 74.317	0.39	0.037
P60	9.35	2.54, 65.917	< 0.0001	0.264	2.47	1, 26	0.128	0.087	1.29	2.54, 65.917	0.286	0.047
N100	8.02	2.31, 60.085	< 0.0001	0.236	0.07	1, 26	0.796	0.03	0.26	2.31, 60.085	0.805	0.01
P190	1.63	2.91, 75.66	0.191	0.059	14.05	1, 26	0.001	0.351	0.78	2.91, 75.66	0.504	0.029

Table 5-4: Repeated-measure ANOVA results for TEP amplitudes (Mean ± SD). Repeated-measure ANOVA are reported for each TMS stimulation site group separately with within factor TMS-delay (5 levels: TMS10, TMS130, TMS190, TMS220). Post-hoc paired t-tests were performed between TMS10 condition and TMS I, with i= 130, 160, 190, 220 (4 comparisons, * p < 0.0125).

Contralateral (left) M1 TMS stimulation

	TMS10	TMS130	TMS160	TMS190	TMS220	F	df,error	p	η2
P30	-0.1[1.96]	0.89[1.4]*	1.87[1.3]*	1.9[1.53]*	0.57[1.54]*	6.94	2.66,1.8	<0.0001	0.346
N45	-1.87[2.78]	-1.19[2.09]*	-0.31[1.93]*	-0.18[2.78]*	-1.59[2.62]*	5.87	2.8,1.79	<0.0001	0.262
P60	-0.88[2.72]	-0.16[2.53]*	0.52[2.53]*	0.08[2.68]*	-1.14[2.59]	5.38	2.28,2.11	0.01	0.249
N100	-3.04[1.99]	-1.65[2.14]	-2.87[1.84]	-3.28[2.21]	-4[2.2]	3.7	2.19,2.37	0.03	0.265
P190	4.38[2.47]	4.46[2.36]	3.94[2.01]	4.14[2.15]	3.97[1.99]	1.27	2.64,1.91	0.3	0.045

Ipsilateral (right) M1 TMS stimulation

	TMS10	TMS130	TMS160	TMS190	TMS220	F	df,error	p	η2
P30	-0.3[3.31]	2.45[2.24]*	2.02[2.04]*	2.3[2.22]*	1.72[2.32]	4.34	1.5,10.84	0,04	0.250
N45	-1.82[3.4]	0.21[1.9]*	0.28[2.68]*	0.06[2.57]*	-0.96[2.19]	6	2.66,2.97	<0.0001	0.316
P60	-0.02[3.65]	2.07[2.65]*	2.1[2.17]*	0.96[2.56]	0.47[2.76]	6.04	2.02,4.16	0,01	0.317
N100	-3.17[2.56]	-2.24[3.14]	-2.76[2.82]	-3.34[3.74]	-4.49[3.83]	3.68	1.84,5.76	0,04	0.221
P190	2.27[2.02]	1.39[2.42]	0.73[2.23]	1.62[2.08]	1.72[2.84]	1.46	2.68,4.47	0,24	0.101

5.6.   Discussion

The present study examined the time course of bilateral motor excitability during movement preparation of a robot-mediated unimanual reaching task.

While it was expected that cortical excitability will be significantly more modulated in the contralateral compared to the ipsilateral M1 during unimanual reaching preparation, the study reported no significant difference in TEPs or MEPs between the contralateral and ipsilateral M1. However, as hypothesised a temporal dynamic modulation of cortical excitability in both hemispheres was seen, as revealed by modulations in TEP amplitudes, suggesting increases and decreases of excitatory and inhibitory processes at different stages of movement preparation. Importantly, cortical components were significantly modulated at different times during movement preparation, reflected by phases of increased and decreased amplitudes of TEP components; no changes, however, were found in the amplitude of MEPs, suggesting that modified excitability did not affect the output of the corticospinal pyramidal cells. This could also suggest that EEG can detect the onset of excitability modulations earlier than MEPs. Thus, this study highlights the practical value of the combined TMS-EEG approach in using both cortical (TEPs) and corticospinal (MEPs) readouts to assess modulations in excitability. It demonstrates that co-registering TMS–EEG is a complementary method for the evaluation of cortical effects of TMS, enabling to measure TMS-induced neuronal activation in the millisecond time-scale.

However, since even TEPs can be influenced by corticospinal pathways due to somatosensory feedback resulting from MEPs when stimulating at supra-threshold intensities (Fecchio et al., 2017), it does not allow to explicitly delineate cortical from corticospinal excitability changes. One way to investigate whether differences in excitability have a cortical or subcortical origin is to stimulate at subthreshold intensities without evoking MEPs and by recording TEPs (for review see Farzan et al., 2016). Another method to differentiate between cortical and subcortical mechanisms, is to use TMS stimulation over the cervico-medullary junction or spinal cord level to elicit cervico-medullary or spinal MEPs and compare them to cortically evoked

MEPs to delineate cortical from spinal contributions (Nuzzo et al., 2016, Zewdie et al., 2014).

The study further showed that TMS applied to M1 during unimanual movement preparation interferes with subsequent movement by delaying movement onset and offset, without changing overall movement time for both ipsilateral and contralateral M1 stimulation. Interfering with the ipsilateral M1 during movement preparation seems to improve subsequent movement by decreasing trajectory errors (i.e. summed errors), whereas interfering with the contralateral M1 has no significant effect on subsequent trajectories.

5.6.1. Kinematics

5.6.1.1. Movement onset and offset

Applying single-pulse or repetitive TMS (rTMS) pulses to different cortical areas can disrupt or enhance cortical and cognitive processes (for review see Luber and Lisanby, 2014). This study found that applying single-pulse TMS to both the contralateral and ipsilateral M1 during movement preparation can interfere with movement execution, by prolonging movement onset and movement offset without affecting the overall reaching time. The finding supports previous TMS studies over the contralateral M1 applied during movement preparation in simple or choice-reaction time tasks delayed reaction times (Day et al., 1989; Hashimoto et al., 2004; Leocani et al., 2000; Ziemann et al., 1997). The results of ipsilateral M1 stimulation reported in this Chapter are in line with findings from Meyer and Voss (2000), who applied single-pulse TMS to the ipsilateral M1 during preparation to move and reported delayed executions of rapid finger movements. Taken together, it is plausible to assume that TMS inhibited neuronal populations within M1 involved in movement planning and thereby delayed their intervention in movement execution. Applying TMS over M1 might have inhibited neurons in the brain, making them unresponsive for a short period of time to command signals which initiate the motor program of the muscles needed for the movement. Importantly, Day et al. (1983), have shown that the delay cannot be explained by spinal motor neuron inaccessibility after TMS stimulus, but

must stem from a cortical mechanism, nor that it can be solely due to the participant's intention to respond.

5.6.1.2. Movement accuracy

Interestingly, TMS over the contralateral and ipsilateral M1 had different effects on movement accuracy, measured with summed errors (derivations from the ideal trajectory). Specifically, while TMS over the ipsilateral M1 improved movement accuracy (decreasing summed errors), TMS over the contralateral M1 had no significant effects on movement accuracy. This result suggests that interfering with the ipsilateral M1 during movement preparation might be beneficial for movement accuracy, bringing new insights into the functional role of the ipsilateral M1 during movement preparation. Similarly, it has been shown that disruption of cortical function can improve behaviour (for review: Luber and Lisanby, 2014). rTMS over M1 has been used to temporarily reduce the excitability of the ipsilateral M1 (Kobayashi et al., 2009, 2004). One study has found that rTMS applied to the ipsilateral M1 to the moving hand shortened reaction times (improved performance) while contralateral M1 rTMS did not make any changes (Kobayashi et al., 2004). Suppressing M1 activity with slow-frequency rTMS enhances ipsilateral learning of a simple motor task whereas it disrupts learning in the contralateral hand (Kobayashi et al., 2009), suggesting that reducing cortical excitability of M1 with rTMS may improve motor performance in the ipsilateral hand by releasing the contralateral M1 from transcallosal inhibition.

Taken together, the concept of interhemispheric "rivalry", namely, suppressing ipsilateral M1 activity seems to have a facilitatory effect on the unstimulated contralateral M1 presumably via suppression of activity in the ipsilateral M1 and transcallosal inhibition.

5.6.2. Corticospinal excitability

MEP amplitude is a measure of corticospinal excitability; increased MEP amplitudes reflect increased excitability and decreased amplitudes reflect increased inhibition. This Chapter failed to report any significant modulations in MEPs for both TMS applied to the contralateral and ipsilateral M1.

Specifically, the delay at which TMS was applied during movement preparation cue had no significant effect on MEP amplitudes. This result is in line with a previous study which used a similar TMS protocol during movement preparation of a reaching movement in an unperturbed (similar to the present study) and perturbed (velocity-dependent force-field) environment (Hunter et al., 2011). In particular, Hunter et al. (2011) reported no significant changes in corticospinal excitability during movement preparation in the unperturbed reaching condition (similar to the present study), and a significant increase in corticospinal activity in the perturbed reaching condition, during which participants had to adapt to a force-field. Their findings suggest that an increase in corticospinal activity in M1 is associated with an internal model formation linked to motor adaptation and does not reflect a mechanism of movement preparation (unperturbed reaching).

One reason for the negative findings reported in this study could be attributed to a too small sample size (N = 28). A post-hoc power analysis calculation using the G power software revealed that a sample size of 80 individuals was needed to detect a significant effect of TMS delay in MEP amplitudes with a power of 80%. This was based on an estimated effect size derived from the present data of f = 0.29, and α significance level of p = 0.05 in a mixed design with a between and within-subject factors with a total of 2 groups and 5 measures. To detect a significant effect of TMS stimulation site, the sample size needed derived from an f = 0.089 with the same parameters was estimated at 840 individuals. Since, significant modulations in TMS delay were detected with more cortical readouts (TEPs), it could be suggested that TEPs are a more sensitive measure of cortical excitability and can be used to detect effects with smaller sample sizes compared to MEPs.

5.6.2.1. Corticospinal excitability of the task arm

Increased corticospinal excitability preceding movement onset has been reported in reaction time task in which right thumb movements were required (Kičić et al., 2008, Leocani et al., 2000; Nikulin et al., 2003; Zaaroor et al., 2003). During unilateral movement preparation of right index fingers, using a simple reaction time task (Nikolova et al., 2006), MEPs amplitudes gradually

increased in the pre-movement period and were strongly amplified in a period of 90-100ms before the voluntary EMG onset.

In contrast to these findings, this Chapter failed to report significant modulations of corticospinal excitability preceding movement onset. This discrepancy can be explained in two ways: First, TMS was applied at different delays during movement preparation, with the ones reported in the literature being closer to the actual movement onset compared to the presented study (the closest TMS was applied to movement onset in this Chapter was 160 ms pre-movement). A future experiment should seek to apply TMS even closer to movement onset in order to investigate if this will have an impact on MEP amplitudes similar to the ones reported in the literature. Second, it is noteworthy that the motor task required in the previously cited studies required simple finger, thumb abductions which are different from reaching arm movements which are more complex and require the coordination of a large number of muscles (Pizzamiglio et al., 2017b). The difference in motor tasks required makes direct comparisons of results difficult.

5.6.2.2. Corticospinal excitability of the non-task arm

The present study showed no significant modulation in MEPs in the non-task (left BB) arm during right arm reaching preparation. This is in partial agreement with previous research using simple motor tasks. While it is in line with findings of Kičić et al. (2008) who reported no significant modulations in MEPs during movement preparation in a simple reaction time task requiring thumb abductions, others found significant increases in MEPs in the task-limb during wrist movement preparation. This discrepancy can again be related to the difference in the motor task and movement. In fact, it has been shown that even depending on the kind of movement: extension or flexion for instance, MEP amplitudes are differently modulated during movement preparation (McMillan et al., 2006) and execution (Howatson et al., 2011).

5.6.3. Cortical excitability

This Chapter reports that applying TMS at different times during the delay period in movement preparation significantly modulates the amplitude of

several TEP components which have been associated with cortical excitability. This suggests that cortical excitability goes through dynamic cortical excitability changes, namely transitioning from increased excitability to decreased excitability phases. This is in line with previous studies, which have established that motor preparation is involving the recruitment of both excitatory and inhibitory neural mechanisms (Greenhouse et al., 2015; Hannah et al., 2018). By applying TMS during the movement preparation phase and by measuring MEPs, it has been evidenced that task-relevant, as well as task-irrelevant muscles, were inhibited (Greenhouse et al., 2015). Hannah et al. (2018), showed that only a specific subset of cortical neurons are inhibited during movement preparation: namely they showed that only specific inputs to the corticospinal system are affected by inhibitory mechanisms and that this specific suppression of cortical neurons is correlated with reaction time and therefore crucial for a successful movement preparation.

5.6.3.1. P30 and P60

The generators of the P30 and P60 after stimulation of M1 remain unclear, but it has been shown that these components excitatory activity (Cash et al., 2017). Specifically, these components increase with higher TMS stimulation intensities (Komssi et al., 2004) and are generally inhibited in long-intracortical inhibition TMS paradigms (Rogasch et al., 2013) and cortical silent period TMS paradigms (Farzan et al., 2013). The P30 is mainly recorded in central regions (Paus et al., 2001) and the in regions over the stimulation site (Bonato et al., 2006). In good agreement with these studies, this Chapter reports that for both ipsilateral and contralateral M1 TMS during right arm reaching preparation elicited P30 and P60 components in the ipsilateral ROI of the stimulated site. Moreover, it was found that the delay from visual cue at which TMS was applied to M1 significantly affected the P30 and P60 amplitudes irrespective of stimulation site (contralateral and ipsilateral M1 TMS stimulation). Specifically, P30 and P60 amplitudes first increased with increasing delay from the visual cue and then decreased before movement onset in a bell-shaped manner. The significant modulation of both suggests

that during movement preparation, the excitability of the contralateral and ipsilateral motor cortex is dynamically modulated and goes through transitions of increased excitability followed by phases of decreased excitability. The present findings did not show any significant differences between the contralateral and ipsilateral M1 TMS condition.

5.6.3.2. N45

Previous TMS-EEG studies identified N45 as a marker of inhibitory processes, reflecting the N45 the activity of $GABA_A$ receptors (Premoli et al., 2014). It has further been suggested that the N45 is dependent on circuits within M1 (Van Der Werf et al., 2006). This Chapter reports that for both ipsilateral and contralateral M1 TMS during right arm reaching preparation elicited N45 components in the ipsilateral ROI of the stimulated site. Moreover, it was found that the delay from visual cue at which TMS was applied to M1 significantly affected the N45 amplitude irrespective of stimulation site (contralateral and ipsilateral M1 TMS stimulation). Specifically, N45 amplitudes first increased with increasing delay from the visual cue and then decreased before movement onset in a bell-shaped manner. The significant modulation of the N45 component which is associated with cortical excitability could suggest that during movement preparation, the excitability of the contralateral and ipsilateral motor cortex is dynamically modulated and goes through transitions of increased excitability followed by phases of decreased excitability. The present findings did not show any significant differences between the contralateral and ipsilateral M1 TMS condition.

5.6.3.3. N100

Several TMS-EEG studies applied to the motor cortex generate a well characterised EEG peak around 100 ms post-TMS reflecting inhibitory activity involving $GABA_B$ receptor-mediated neurotransmission (Bonnard et al., 2009; Farzan et al., 2013; Nikulin et al., 2003; Premoli et al., 2014). N100 reflects the balance between local GABA and glutamate receptors (Du et al., 2018). This Chapter reports that the delay from visual cue at which TMS was applied to M1 significantly affected the N100 amplitude irrespective of stimulation site

(contralateral and ipsilateral M1 TMS stimulation). Although post-hoc t-tests (comparing TMS10 to all other TMS conditions) were not significant, a trend of attenuated N100 amplitude followed by a phase of increase of the N100 amplitude was seen, suggesting that the M1 goes through transitions of decreased inhibition followed by increased inhibition. This is in slight discrepancy with Nikulin et al. (2003) – a TMS-EEG study, who showed that compared to a resting condition, the N100 was attenuated and the MEPs larger in the preparation period of a simple finger movement (abduction with the right thumb). The difference in both findings can be due to the fact that Nikulin et al. (2003) applied TMS at a later time point during movement preparation compared to the present study.

5.6.3.4.   P190

Very little is known about the P190 component; initially it was believed to be a response to the clicking noise of the TMS coil when discharging (Nikouline et al., 1999; Tiitinen et al., 1999), however, later studies have masked the coil sound without fully eliminating the P190 peak, concluding that the P190 does indeed reflect cortical contributions (Komssi et al., 2004; ter Braack et al., 2015). Applying TMS to either the contralateral or ipsilateral M1 at different time delays from visual cue during movement preparation of right arm movement did not affect P190 amplitudes. However, this Chapter reports a significant difference between stimulation sites; contralateral M1 TMS stimulation elicited higher P190 components compared to ipsilateral M1 TMS stimulation, suggesting that during later stages of movement preparation (captured with later TEP components such as the TEP 190) the contralateral M1 becomes more engaged and activated compared to the ipsilateral M1.

5.6.4. The functional role of the contralateral and ipsilateral M1

Stimulating the contralateral or ipsilateral M1 during movement preparation of right arm movements did not show any differences in early TEP components (P30, N45, P60 and N100), indicating that both M1s are equally modulated during movement preparation. Only the P190 TEP component was significantly different between both stimulation sites, applying TMS over the

contralateral M1 resulted in higher P190 amplitudes compared to ipsilateral M1 stimulation, which could reflect the higher engagement of the contralateral compared to the ipsilateral M1 during later stages of movement preparation.

This Chapter did not report major differences between the contralateral and ipsilateral M1 during right arm movement preparation. This result might seem unexpected, as it was hypothesised that due to its superior role the contralateral M1 would be more modulated than the ipsilateral M1. However, the difference in excitability between the motor cortices was close to significance as measured with TEPs (p= 0.056, observed power = 68 %) and the lack of significance could be related to a too small sample size (28 individuals). A post-hoc power analysis calculation using the G power software revealed that a sample size of 40 individuals was needed to detect a significant effect of TMS stimulation site in TEP amplitudes (5 components) with a power of 80%. This was based on an estimated effect size derived from the present data of f = 0.76, and α significance level of p = 0.05 in a mixed design with a between and within-subject factors with a total of 5 measures and 10 conditions.

The present findings show that cortical excitability is significantly modulated in the contralateral and ipsilateral M1 during unilateral arm reaching preparation, as reflected by changes in the P30, P60 and N45 TEP amplitudes. This is in good agreement with previous research which has shown that the excitability modulation of the ipsilateral M1 mirrors the modulation of the contralateral M1 during unilateral movement preparation in a reaction time task requiring left wrist movements (Chye et al., 2018). The amount of facilitation in the ipsilateral M1 during unilateral wrist contractions correlates with the number of callosal fibres measured with fractional anisotropy using fMRI (Chiou et al., 2014). Taken together, these results suggest that the ipsilateral M1 mirrors the activity of the contralateral M1 during unilateral hand movement preparation and execution via transcallosal fibres. Specifically, ipsilateral excitability changes mirroring contralateral excitability changes reported in the present study can be explained by transcallosal interactions between both M1. The contralateral M1 may send

efferent copies to the ipsilateral M1 and thus activity in both M1 can be coupled. An alternative hypothesis for the modulation of neural activity by ipsilateral movements is that the non-task arm and the axial musculature may be active (Cisek et al., 2003). However, this can be partly ruled out in the present study as the EMG of the BB of the ipsilateral non-task arm was continuously monitored and did not show any activity. Even though, the functional role of the ipsilateral M1 cannot be derived from the present study, its significant excitatory and inhibitory modulation point to a significant involvement in movement preparation.

5.6.5. The role of the ipsilateral M1 and its impact for neurorehabilitation

Interhemispheric imbalances are commonly observed following stroke affecting motor regions, showing an enhanced bilateral activation during unilateral movement of the affected limb (for review see Dodd et al., 2017). Commonly, an enhanced contralesional (analogous to the ipsilesional M1 in healthy individuals) compared to the ipsilesional hemisphere (contralateral M1 in healthy individuals) to the affected hand is seen. The role of the contralesional M1 (i.e. ipsilateral M1) during unilateral movement is still not completely understood. Specifically, it is unclear whether the increased contralesional M1 is beneficial or detrimental to unilateral limb recovery (Hummel et al., 2009). Mcdonnell and Stinear's meta-analysis (2017) suggests that facilitating the ipsilesional M1 excitability directly might be more beneficial than suppressing the contralesional M1 excitability to promote post-stroke recovery with NIBS. Moreover, it has been shown that inhibiting the ipsilesional M1 could have detrimental effects on recovery since it has an active role in unilateral movement. For instance, it has been demonstrated that the contralesional M1 could assist recovery through uncrossed ipsilateral CST fibres, accounting for approximately 10% of the CST fibres (Brus-Ramer et al., 2009). Enhanced activation of the contralesional hemisphere could also provide the recruitment of additional neural regions and thereby support recovery (Riecker et al., 2010).

The present study showed that activity in ipsilateral M1 is significantly modulated during movement preparation, suggesting its active involvement

during unilateral movement. This is supported by the fact that deriving ipsilateral M1 activity using BCI represents a therapeutic target in the context of neurorehabilitation. For instance, Bundy et al. (2017) demonstrated that using neural activity form the contralesional M1 to drive a BCI-controlled exoskeleton significantly improves motor recovery of the affected upper limb.

5.6.6. Limitations and future work

Although we have used white noise to mask the auditory artefact, we cannot rule out that our data were not contaminated with the artefact contaminating the N100 amplitude. We can also not rule out that the somatosensory evoked potential coming from the stimulated muscle might have affected the TEP peak amplitudes, but since the MEP amplitudes showed no statistically significant difference across conditions, and that the stimulation intensity was kept constant across conditions, we can assume that the auditory and somatosensory evoked potentials were similar for all conditions and did not influence our findings.

This study is the first one to use simultaneous TMS-EEG to investigate cortical excitability modulations during preparation of a robot-mediated unimanual reaching task. Although this study tried to address methodological issues related to confounding visuomotor cortical activations and TMS-induced activations. Specifically, visually triggered EEG responses and motor responses could influence TMS-evoked responses but by subtracting the ERPs from the no-TMS condition from the TEPs in TMS conditions, it was tried to reduce this confounding factor. A future study should aim to specifically disentangle visual and motor processing by adding an experimental condition in which TMS is applied in the time delays as in this study in two conditions: movement and no movement condition at different time delays from the visual cue. This would allow to compare modulatory effects of movement-related activity and visual processing alone. Chapters conclusions and novelty of findings

This study is novel in two ways: it is the first study to use TMS-EEG during movement preparation of a more complex task, namely a reaching arm

movement compared to simple finger or wrist movements. It is also the first to apply TMS-EEG to both the contralateral and ipsilateral M1 using such a complex task.

The findings of bi-hemispheric modulation during movement preparation might have implication for neurorehabilitation. Namely, when one hemisphere is damaged after brain injury, the contralesional (i.e. ipsilateral M1 to the affected limb) could become more important in controlling unilateral movement (for review see Dodd et al., 2017). This is in line with the fact that limb kinematics can reliably be decoded from ipsilateral M1 to control an external prosthesis in the context of neurorehabilitation (Ganguly et al., 2009).

Chapter 6 - Neural Correlates and Predictors of Motor Adaptation

6.1. Introduction

Goal-directed reaching relies on complex neural motor commands needed to achieve the desired goal and trajectory. The mechanism relies on inverse models making transformations from the desired movement trajectory in the visual space, to motor commands, the motor space (Wolpert et al., 1998). The visuomotor transformations are updated by integrating motor commands with sensory feedback mechanisms (for review see Scott et al., 2015; Shadmehr et al., 2010). Visually-guided movement relies on visuomotor transformations engaging fronto-parietal regions (Dipietro et al., 2014; Naranjo et al., 2007), as well as optimal feedback control involving cortical and subcortical regions such as the cerebellum and the basal ganglia (for review see Scott, 2012).

Human movement control is flexible by producing variable motor commands adapted to both internal (i.e. body) and external changes (i.e. environment). However, noise in motor production, movement execution errors and unexpected environmental perturbations are all factors that can hinder reaching behavioural goals. An adaptive internal model of the body and world enables flexible and accurate movements (for review see Scott, 2012, Shadmehr et al., 2010). Such internal models consist of a map of the dynamics of the motor task, which facilitates prediction and compensation in mechanical behaviour (Shadmehr and Mussa-Ivaldi, 1994). Predictions of these internal models transform motor commands into sensory consequences, termed feedforward mechanisms and improve the system's ability to estimate the state of the body and the world around it. Error signals play a key role in aiding the motor system to make smooth movement corrections (Desmurget and Grafton, 2000; Diedrichsen et al., 2005). Reaching errors can be divided into two types, target errors and execution errors. The former occurs due to unpredictable changes in the location of the target, while the latter arises due to a miscalibration of internal models. This miscalibration can be caused by dynamical changes, such as force-fields that alter limb dynamics or kinematic

changes or prisms which alter visual feedback (Diedrichsen et al., 2005). Such errors engage active corrections leading to trial-by-trial adaptation to the novel environment, which is referred to as error-based learning (Donchin et al., 2003; Thoroughman and Shadmehr, 2000). Motor adaptation is a form of motor learning during which sensory prediction errors are used to recalibrate internal models. Specifically, persistent mismatches between predictions and actual sensory outcomes are used as feedback error signals that update subsequent motor commands (for review see Scott et al., 2015). Corrective responses that are adapted to the new environments are made using these error signals to update internal models that predict sensory consequences of motor behaviour (for review see Haith and Krakauer, 2012).

Adaptation to an external force-filed usually causes an initial decrease in performance followed by close to exponential trial-by-trial return to natural reaching performance, a process referred to as motor adaptation. When the perturbation is removed, movements are typically overcompensated to the opposite direction (i.e. after-effects) of the previously applied perturbation and return to natural reaching performance trial-by-trial (i.e. washed-out), a process referred to as de-adaptation (Hunter et al., 2009). These short-lived after-effects are thought to reflect the formation of a predictive internal model to the new environment and demonstrate that the learner anticipates the expected dynamics of the new environment rather than simply reacting to environmental changes (Huberdeau et al., 2015).

Kinematic measures such as velocity, accuracy, consistency and forces are typically used to characterise movement performance. Motor learning and motor adaptation capacities are then derived from these kinematic measures. A common method to quantify the motor learning and adaptation capacity is derived from movement errors (deviations from an ideal straight trajectory). For example, an increasingly used index of learning (sometimes referred to as motor learning index; MLI), is calculated as the averaged errors during the first reaching trials over the last reaching trials during motor adaptation (Faiman et al., 2018; Ozdenizci et al., 2017; Patton et al., 2006; Vahdat et al., 2011).

Neuroimaging tools such as fMRI, PET and EEG have been used to identify the neural mechanisms in error-based learning. Error-based learning involves the medial frontal cortex (including the ACC and SMA), basal ganglia and cerebellum (for review see Scott, 2012; Seidler et al., 2013; Shadmehr et al., 2010).

Erroneous responses lead to increased negativity in medial-frontal regions peaking around the timing of error commission and is typically referred to as ERN (Anguera et al., 2009; Krigolson et al., 2015; MacLean et al., 2015). This activity has been linked to error processes, such as error monitoring, online error correction and response compensation, and is believed to originate in the ACC (for review see Gehring et al., 2018). In motor adaptation processes, the ERN is proposed to be involved in the modification of internal models of the task (Contreras-Vidal and Kerick, 2004; Desowska and Turner, 2019; Torrecillos et al., 2014).

Sensorimotor adaptation relies on perceptual learning as well as sensory plasticity (Ostry and Gribble, 2016; Vahdat et al., 2011). Motor adaptation drives cortical plasticity changes in both sensory and motor regions including M1, the primary sensory motor cortex (S1), SMA and ventral premotor cortex. Vahdat et al. (2011) demonstrated that motor adaptation leads to functionally specific changes in distinct resting-state networks, comprising M1, the dorsal premotor cortex and the cerebellar cortex that are all linked to motor learning. The behavioural relevance of plasticity modulations in motor adaptation is still debated. Diving motor cortical plasticity using non-invasive transcranial direct current stimulation (tDCS) during learning is associated with improved motor learning (Stagg et al., 2011) and during adaptation with greater retention of internal models without improving motor learning (Hunter et al., 2009).

Fore-field adaptation tasks have been applied to investigate the neural mechanisms underlying the updating or adaptation of such internal models. Robot-mediated force-fields during a reaching task can be applied to introduce of a physical perturbation which distorts both the visual and proprioceptive consequences of motor commands (Fine and Thoroughman, 2007; Hunter et al., 2009; Krebs et al., 1998; Shadmehr and Mussa-Ivaldi, 1994).

Adaptation is thought to support motor recovery by reinforcing neural plasticity (for review see Bastian, 2008, Basteris et al., 2014). Specifically, exposing subjects to novel force-fields during a robot-mediated task can lead to the formation of an internal model that is generalised to unconstrained movement (Patton et al., 2004, 2006). Adaptation is therefore important for rehabilitation and can make movement flexible and help to determine if patients can generate a more normal motor pattern (for review see Haith and Krakauer, 2013). Gaining more insights into the mechanisms underlying motor adaptation processes on a neuronal level might provide novel insights to design better neurorehabilitation therapies.

The response variability in motor adaptation capacities has included differences in resting-state functional connectivity and oscillatory power. Faiman et al. (2018) reported that resting-state functional connectivity between contralateral M1 and anterior prefrontal cortex in the beta band frequency band predicted the subsequent degree of motor adaptation. Ozdenizci et al. (2017) observed that resting-state and pre-trial beta power magnitude was associated with subsequent motor adaptation performance, showing that higher rates of adaptation were predicted by lower pre-trial beta oscillatory power (Ozdenizci et al., 2017). However, the neurophysiological and functional role of this mechanism remain to be clarified.

At a neurochemical level, motor learning has been linked to GABA (inhibitory activity) concentrations (Kolasinski et al., 2019; Nowak et al., 2017; Stagg et al., 2011). Higher GABA concentrations have been associated with poorer learning in a subsequent motor learning task (Kolasinski et al., 2019), suggesting that higher levels of cortical inhibition could be a barrier to motor learning. However, Nowak et al. (2017) reported that increasing GABA inhibition using transcranial alternating current stimulation over M1 was associated with beneficial effects on motor learning, suggesting that a higher inhibitory capacity improves motor performance, possibly due to increased precision of GABAergic transmission.

Cortical plasticity related to motor learning has been extensively studied using TMS over M1 as reviewed by Tyc and Boyadjian (2006) by measuring

topographical reorganisation quantified with shifts in cortical output maps or with increases in cortical excitability, indexed with increases in MEPs in the targeted muscle. These two methods both rely on an intact CST and provide an indirect measure of cortical excitability in neuronal activity in M1.

The added value of TMS-EEG co-registration as opposed to only measuring TMS-MEPs is highlighted by a recent study reporting that intermittent theta burst stimulation of the cerebellum showed only a significant effect on cortical reactivity as measured with significant modulation of TEPs captured with EEG without altering MEPs captured with EMG. This finding demonstrates that TMS-EEG enables to capture cortical effects, that would have remained undetected by solely measuring corticospinal activity, such as with MEPs (Harrington and Hammond-Tooke, 2015). Simultaneous recordings of TMS-EEG can also give a more complete picture of cortical excitability changes at the neuronal level in a wider range of brain regions (also outside the M1), by measuring TMS-evoked responses over the whole scalp (for review see Farzan et al., 2016). Specifically, single-pulse TMS applied over M1 produces a well characterised negative deflection, referred to as TEP N100, around 75-150 ms post-stimulation over the stimulated region (M1). The functional role and origin of the TEP N100 component has been extensively studied and has been established as a biomarker of inhibitory processes, representing the activity of $GABA_B$ receptors (Bonnard et al., 2009; Casula et al., 2014; Premoli et al., 2014; Spieser et al., 2010). The N100 amplitude has been linked to the duration of the CSP, an index of GABAergic inhibition after motor cortex stimulation (Farzan et al., 2013). Further support of the inhibitory role of the N100, has been revealed in a pharmacological TMS-EEG study (Premoli et al., 2014) who showed that M1 stimulation produced a larger N100 after intake of the $GABA_B$-agonist baclofen, suggesting that the activity of $GABA_B$-receptors contributes to the generation of this TEP component. The N100 component reflects the local GABA and glutamate balance (Du et al., 2018). To sum up, a larger N100 amplitude reflects increased inhibition, whereas a small amplitude reflects decreased inhibition. As such, the TEP N100 amplitude can measure cortical excitability and provide an indirect measure of plasticity, by quantifying changes in TEP amplitudes (for review see Farzan et

al., 2016). For instance, Casula et al. (2014) showed that the N100 amplitude increases following low-frequency rTMS, suggesting that this TEP component is a reliable marker of cortical inhibition and can quantify neuromodulatory effects. Given the functional role of the N100 as an inhibitory biomarker, the current study investigated how the initial cortical activity measured with the N100 amplitude before a robot-mediated adaptation task is related to the subsequent degree of motor learning.

This study used a robot-mediated reaching task in an unperturbed (non-adapting condition) and in a force-field perturbed (adapting condition) environment while EEG was recorded to identify the neural correlates and biomarkers of error-based learning. TMS over the contralateral (left) M1 was applied before and after the motor adaptation condition to measure cortical excitability with TMS-EEG and link it to motor performance. The first aim was to investigate neural correlates of motor adaptation by identifying neural activity related to error-processing using EEG and sensorimotor plasticity changes accompanying adaptation using TMS-EEG. The second aim was to identify the neurophysiological mechanism of inter-subject variability in motor learning by testing if a resting-state cortical biomarker can predict subsequent performance improvement.

It was hypothesised that:

i)   Participants will adapt to the applied force-field based on previous findings reported in the literature, showing temporary after-effects once the force-field is removed, and eventually returning to a baseline performance (Hunter et al., 2009; Krebs et al., 1998; Milner and Franklin, 2005; Pizzamiglio et al., 2017b).

ii)   Brain regions involved in the development of adaptive compensatory strategies optimising performance during motor adaptation will be actively engaged during perturbed reaching. This will be reflected in increases of an error-related ERP components (i.e. P/N300) during perturbed (i.e. adaptation) compared to unperturbed (i.e. non-adaptation condition) reaching (Pizzamiglio, 2017, Torrecillos et al., 2014).

iii)   The N300 ERP component (i.e. ERN-like activity) during motor adaptation will correlate with motor learning (Beaulieu et al., 2014).

iv)   Cortical excitability will be modulated (i.e. neuroplastic changes) after motor adaptation (for review see Tyc and Boyadjian, 2006), as reflected by decreases in TEP N100 amplitudes post- compared to pre-motor adaptation.

v)   Cortical excitability measured at rest prior to motor adaptation will be linked to the variability in motor learning capacities. Specifically, the TEP N100 amplitude, an inhibitory biomarker, will be predictive of subsequent motor learning. Since from the literature it not clear if enhanced or decreased inhibition is beneficial for motor learning (Kolasinski et al., 2019; Nowak et al., 2017; Stagg et al., 2011), no hypothesis on the direction of the correlation between the TEP N100 and motor learning was made.

6.2. Methods

6.2.1. Research design

This study employed a within-subject design to investigate behavioural and neural mechanisms related to motor adaptation (Figure 6-1). Before the start of the experiment TMS was applied over the left M1 and the hotspot as well as the RMT to elicit MEPs in the right BB muscle were determined.

The experimental protocol consisted of a reaching task with three conditions: familiarisation, motor adaptation and late wash-out. 50 TMS pulses were applied at rest just before and just after motor adaptation to assess cortical excitability. The whole experiment, including EEG cap preparation lasted around 4 hours.

The effect of motor adaptation was assessed on the following outcome measures: kinematic data (movement onset, offset, movement time, maximum velocity, summed errors and maximum force) and ERP components (main outcome measure: N/P300, control outcome measures: N/P100 and N/P170).

Changes in cortical excitability (i.e., neuroplastic changes) were assessed with TMS-EEG by comparing the amplitude of the TEP N100 pre- and post-motor adaptation.

Cortico-behavioural associations were assessed between performance improvement (MLI) and the N300 amplitude and the TEP N100 amplitude.

6.2.2. Participants

Fifteen right-handed healthy young participants (8 females, mean age ± SD = 23 ± 4 years, age range: 19 - 32 years) were recruited for the study. Prior to the study, participants were assessed for any contraindications to TMS (Rossi et al., 2009). The sample size used in this study was based on previous work from the lab (N = 14, 7 females (Hunter et al., 2009) and on previous reaching movement and motor adaptation studies (N = 15, 9 females (Frank et al., 2005), (N = 9, 3 females (Naranjo et al., 2007) , N = 7, gender not specified (Dipietro et al., 2012), N = 8, 5 females (Formaggio et al., 2015), N = 10, 3 females (Storti et al., 2016), N = 14, 7 females (De Marchis et al., 2018).. However, in case negative findings were reported, post-hoc power calculations were performed in order to determine if lack of significance could be due to an inadequate sample size.

6.2.3. EEG recording and TMS targeting

Prior to the experiment, participants were sat in a comfortable chair in the experiment room and the EEG cap was placed on their head to record cortical signals and EMG electrodes were placed on the right BB muscle to record EMG activity. For a detailed description of TMS hotspot definition and EMG recording refer to Chapter 3 (General Methods, Section 3.4.1).

The RMT of the left M1 targeting the right BB was determined after the positioning of the EEG cap on the head. The RMT intensity corresponded to an average of 47 ± 8 % of maximum stimulator output (MSO). 50 single-pulse TMS were applied pre-and post-MA to the left M1 at 100% RMT at rest (Figure 6-1). TMS was applied at a lower intensity compared to study I and II to limit the somatosensory feedback from the triggered muscle and because the

major goal in this study was to investigate cortical excitability directly by means of TEPs and not MEPs. The interstimulus interval between TMS pulses was, on average, 5 s (random intertrial interval variation of 20% to reduce anticipation of the next trial). To minimise the auditory evoked potentials resulting from the TMS discharge, participants listened to white noise played through earplugs (<70 dB in each ear) for a duration of the TMS session.

For a detailed description of the EMG and EEG recording and the set-up refer to **Chapter 3** (section 3.4.1.2 and 3.4.2 respectively). EEG was continuously recorded during the motor adaptation protocol and the TMS-EEG protocol.

6.2.4. Experimental task: Motor adaptation

Participants performed visually-triggered reaching movement with their dominant (right) hand rested in a robotic manipulandum (IMT2, Interactive Motion Technologies, Cambridge, MA, USA). The experiment was composed of 288 reaching trials. Each trial consisted in performing a voluntary movement with the right arm to a north-west target starting after the presentation of the visual cue from a central position, followed by a passive robot-assisted return to the starting position. Before each trial the participants were to hold the joystick within the starting central circle and wait for a visual cue; movement initiation was then indicated by the peripheral target turning from red to yellow (Figure 6-1A). The intertrial interval (interval between visual cues) was 6 s. For a detailed description of the reaching task and the kinematic recordings refer to the General Method section 3.6.1.

The experiment comprised three experimental conditions: A familiarisation (FAM), motor adaptation (MA) and wash-out (WO) condition, each composed of 96 trials (Figure 6-1B). During the familiarisation and wash-out conditions, the reaching movement was performed under a null-field, hence participants movements were unperturbed by the robot. In the motor adaptation condition, the robot applied a velocity-dependent force-field in the clockwise direction of + 25 Ns/ m absolute intensity, perpendicular to the trajectory of the joystick and as such perturbed participants movements in a consistent manner across trials. Each condition had four blocks of 24 trials. After each block of 24 trials,

a break of one minute was given. Each experiment started with four blocks of familiarisation, followed by four blocks of motor adaptation and ending with four blocks of wash-out. Before and after motor adaptation 50 single-pulse TMS were applied to the left M1 at rest.

A)

B)
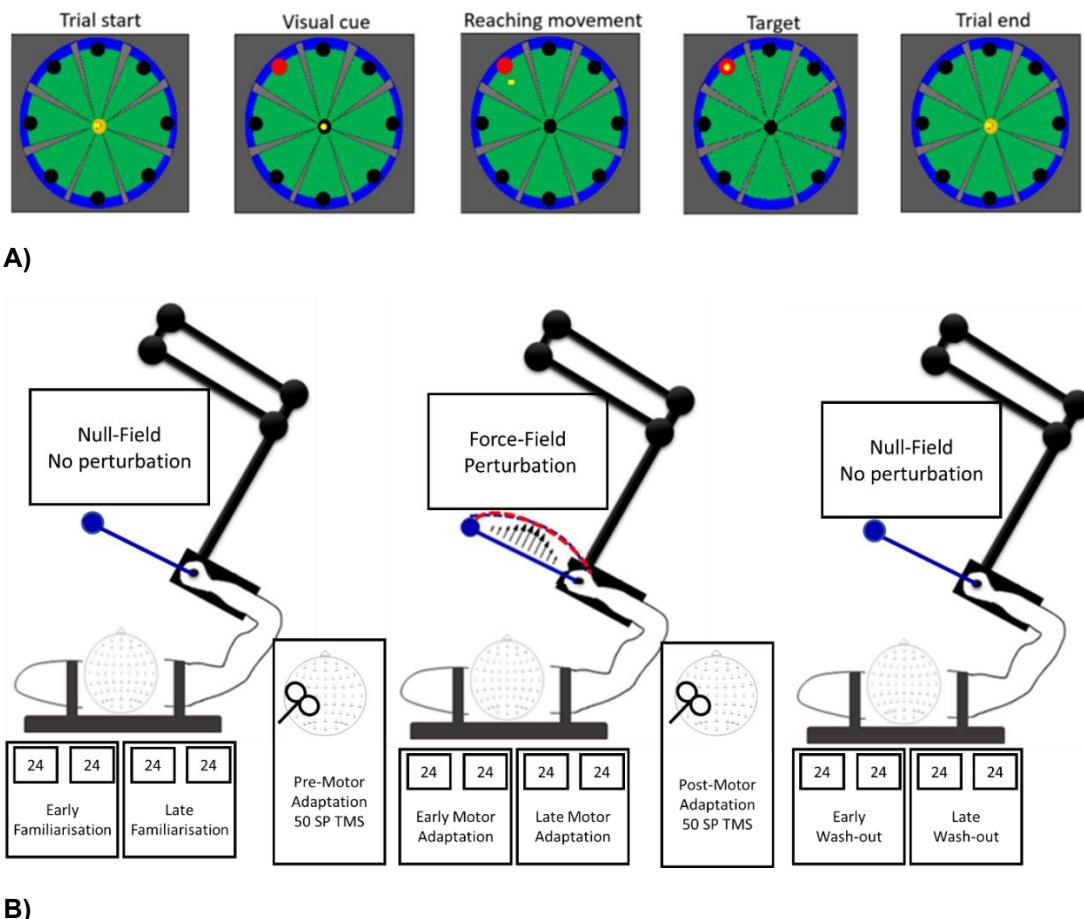
Figure 6-1. Experimental set-up and protocol. A) The visual display during the reaching task from a cathode-ray tube monitor. The screen displayed a dartboard including a central circle (diameter of 1 cm) and eight peripheral target circles (each of 1 cm in diameter) positioned at a constant radial distance of 14 cm and a 45 ° intervals relative to the central circle. A cursor (yellow dot) tracked the real-time hand position of participants and was projected on the screen. Each trial started with the yellow cursor at the central position (orange dot). After the appearance of the visual cue at the target circle (north-west direction), indicated by the target turning red, the participant was required to move the yellow cursor towards the target circle and hold this position until the cursor (i.e. the hand) is passively returned by the robot to the central start position. **B) Experimental task and timeline.** The experimental task consisted of three experimental conditions, namely familiarisation, motor adaptation and wash-out, each comprising four blocks of 24 reaching trials. Each block was separated by one-minute breaks to prevent muscle fatigue. During familiarisation and wash-out the robot-mediated reaching was performed in an unperturbed environment (null-field). During motor adaptation, a velocity-dependent force-field in the clockwise direction was applied by the robot during reaching movements. Before and after motor adaptation 50 single-pulse TMS was applied to the left M1 at rest. EEG was continuously recorded throughout the experimental task and during TMS stimulation.

6.2.5. Trajectory recording

During each condition, trial-by-trial kinematic measures were recorded with 16-bit position encoders embedded within the robot actuator system. Specifically, the angular position of was recorded and used to extract the position and velocity of the joystick in Cartesian coordinates. The position (m) and velocity (m/ s) of the end-effector in the horizontal plane (along the x and y axes), as well as the forces exerted by the participant in the 3D space (along the x, y and z axes; N) were recorded with a sampling rate of 200 Hz and stored for offline analyses on the computer.

6.2.6. Motor adaptation data analysis design

EEG and kinematic data acquired during the motor adaptation were analysed using data acquired during the three experimental conditions: familiarisation, motor adaptation and wash-out (Figure 6-2). The first two blocks (48 trials) and last two blocks (48 trials) of each condition were pooled together and referred to as early familiarisation, late familiarisation, early motor adaptation, late motor adaptation, early wash-out and late wash-out. Late familiarisation rather than early familiarisation was considered to be the baseline to prevent that task novelty effects are present. Early motor adaptation was considered to reflect the early stage adaptation as these blocks encompassed the initial exposure to the force-field, and late motor adaptation to more adapted stages. Late wash-out was included in the analysis, to test if de-adaptation to the removed force-field occurred and activity returned to baseline (Pizzamiglio, 2017; Pizzamiglio et al., 2017b). To obtain sufficient trial counts for the ERP, measures, the trials of each condition were pooled together and averaged in the following conditions, late familiarisation, early and late motor adaptation and late wash-out, similar to the literature (Anguera et al., 2009; Frank et al., 2005; Pizzamiglio, 2017).
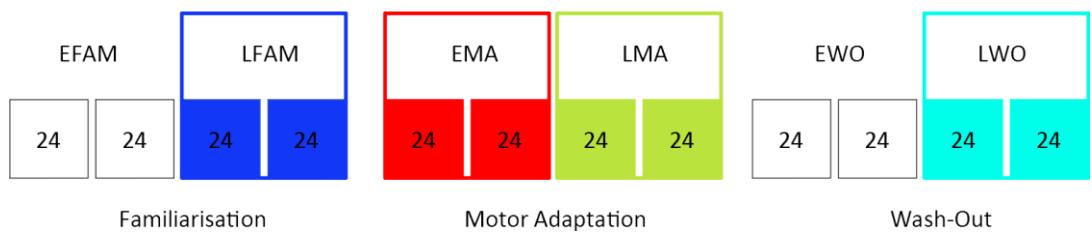
Figure 6-2: Conditions used for statistical analysis. Late familiarisation (LFAM), early motor adaptation (EMA), late motor adaptation (LMA) and late wash-out (LWO) were the conditions (each consisting of 48 trials) considered for statistical analysis.

6.2.7. Kinematic pre-processing

Reaching movements were described by a starting time point (movement onset, defined by a speed profile exceeding a threshold of 0.03 m/ s) and by an end time point (Movement offset, defined by a speed profile lower than the threshold of 0.03 m/ s after movement onset) (Figure 6-5). Modulations of movement onset and offset were monitored throughout the whole duration of the experiment to capture eventual changes in reaction times and movement durations. Reaching movements could ideally evolve following a straight trajectory connecting the start point and the end target but even practised movements show small deviations from this ideal straight path, which are likely to be enhanced when external force-fields are applied.

To quantify movement accuracy, summed errors (Hunter et al., 2009) were calculated as the sum of the perpendicular distance (path offset) between the actual and the ideal trajectory at each time point from movement onset to offset. Since changes in movement speed and exerted forces to counteract the applied perturbation and to support the adaptation process were expected (Hunter et al., 2009; Pizzamiglio et al., 2017b), maximum velocity (m/s) and maximum force (N) were also evaluated and monitored during movement execution.

To determine the degree of force-field learning the Motor Learning Index (MLI) (Faiman et al., 2018; Ozdenizci et al., 2017) was calculated for each participant. To this end the average summed errors were computed for the first five trials (T1) and for the last five trials (T2) (Figure 6-6 and 6-9) for each participant during the MA condition and the MLI calculated as the percentage change from T1 with the following equation:

$$\text{MLI} = \frac{\text{T1} - \text{T2}}{\text{T1}} * 100$$

Equation 6-1: Motor Learning Index (MLI).

The percentage change was chosen rather than using the difference between T1 and T2, in order to facilitate the comparability between this study and

previous studies using the same measure to identify neural correlates of motor performance improvements (Faiman et al. 2018, Ozdenizci et al., 2017).

6.2.8. EEG Pre-processing

6.2.8.1. Pre-processing

First, EEG data from each condition (familiarisation, motor adaptation and wash-out) were merged into one file and pre-processed together. Then, a bandpass filter (1-80 Hz, zero-phase Butterworth filter, order = 4) and bandstop filter (48-52 Hz, zero-phase Butterworth filter, order = 4) to remove line noise (50Hz) were applied. Data were epoched from -1 to 2 s around the visual cue. Electrodes and trials with mechanical artefacts were identified by means of visual inspection and rejected. On average across participants and conditions at least 44 artefact free trials remained (early Fam 46 ± 2, late FAM 44 ± 2, early MA 44 ± 3, late MA 46 ± 2, early WO 45 ± 2 and late WO 45 ± 3) and 5 ± 2 electrodes (i.e. 8 ± 3 % of total electrodes) were deleted. To remove artefacts such as eye-blinks, lateral eye movements and electrode movements, an ICA decomposition was performed using the FASTICA algorithm (Korhonen et al., 2011). Deleted electrodes were then interpolated using spherical interpolation and the data were re-referenced to common average. To examine evoked responses in the time domain, all clean trials were baseline corrected (-800 to 0 ms pre-visual cue) and then averaged for each electrode. The average of cleaned trials for each electrode is referred to as event-related potential (ERP).

ERPs were calculated for late, early motor adaptation, late motor adaptation, late wash-out in every participant and every electrode as simple mathematical averages across trials. This analysis aimed to investigate ERPs correlates of the natural reaching movement and demonstrate the presence/absence of significantly different neural responses to the reaching task between perturbed and unperturbed conditions.

6.2.8.2. ERP – component selection and analysis

After specific literature investigation (Naranjo et al., 2007) and based on previous lab findings (Desowska and Turner, 2019; Pizzamiglio, 2017), specific ERP components were selected in the following time windows: 90-110 ms for the N/P100, 140-240 ms for the N/P170; and 280-360 ms for the N/P300 ERP component. To check if these components were found in our data we visually inspected the ERPs in all electrodes (Figure 6-10) as well as the GMFA (a measure of global brain activation calculated as the root-mean-squared value of the EEG signal across all electrodes (Lehmann and Skrandies, 1980) (Figure 6-11).

The mean amplitude averaged in the specified time windows were then calculated in every electrode for each defined ERP component (N/P100, N/P170 and N/P300) and used for statistical analysis. Since late ERP components, such as the N/P300 have been associated with learning and error-processing (Krigolson et al., 2015), it was hypothesised that this component would be significantly different in motor adaptation conditions compared to non-adaptation conditions. Earlier components such as the N/P100 and N/P170 were not expected to be significantly modulated across conditions since they are mainly related to the visual cue processing which was kept constant in all conditions.

6.2.9. TMS-EEG Pre-processing

6.2.9.1. Pre-processing

EEG data from both TMS conditions (pre- and post-MA) were merged into one file and pre-processed together. Data were epoched (- 1 to +2 s) around the TMS pulse. Epochs were demeaned by subtracting the average between - 1 to + 2 s from each epoch to remove the DC offset. The TMS pulse artefact was removed from - 2 to + 10 ms around the TMS pulse and removed data was replaced with artefact free data using data from -7 to - 2 and + 10 to +15 ms using cubic interpolation. EEG data was then down-sampled from 2048 Hz to 1000 Hz. Electrodes and epochs with mechanical artefacts were identified by means of visual inspection and rejected. After this step, each

condition contained at least 45 artefact free trials. Specifically, the pre-MA condition contained 45 ± 6 and the post-MA condition contained 46 ± 2 on average across participants. On average across participants 4 ± 2 electrodes (i.e. 6 ± 3 % of total electrodes) were deleted. Data was then submitted to an ICA decomposition using the FASTICA algorithm (Korhonen et al., 2011) and components representing TMS evoked muscle artefacts were identified and rejected. On average across participants, 4 ± 2 components (i.e. 7 ± 3 % of total ICA components) were rejected. Data between - 2 and + 15 ms around the TMS pulse were removed and replaced with artefact free data using data from - 7 to - 2 and + 15 to + 20 ms using cubic interpolation. A bandpass filter (1-80 Hz, zero-phase Butterworth filter, order = 4) and bandstop filter (48-52 Hz, zero-phase Butterworth filter, order = 4) to remove line noise (50 Hz) were applied. Then, a second round of ICA decomposition was performed and all the remaining artefacts (eye-blinks, lateral eye movements, electrode movement and electrical artefacts) were identified and removed. On average across participants, 30 ± 5 components (i.e. 51 ± 9 % of total ICA components) were rejected. Deleted electrodes were interpolated using a spherical interpolation and the data were re-referenced to common average. A more detailed description of the pre-processing steps is described in **Chapter 3** (General Methods section 3.6.3).

To examine TMS-evoked responses in the time domain, all clean trials were baseline corrected (- 800 to - 100 ms pre-TMS). TEPs were then calculated for each participant, condition (pre-and post-MA) and electrode as simple mathematical averages across trials.

6.2.9.2. Peak extraction

To investigate how motor adaptation modulated cortical excitability (pre-versus post-motor adaptation) and to test whether pre-motor adaptation cortical excitability can predict motor learning, the peak amplitude of the N100 TEP component was extracted. This component was chosen as it was reliably observed as seen in the EEG butterfly plot (Figure 6-14A), and according to the literature this component is a biomarker of inhibitory mechanisms (Farzan et al., 2013), reflecting the balance of inhibitory (GABA$_B$-receptor-mediated

neurotransmission) (Premoli et al., 2014) and excitatory (Glutamate) processes (Du et al., 2018).

The peak amplitude of the N100 TEP component was extracted in the time window of 75-150 ms based on the TEP butterfly plot and in line with previous TMS-EEG literature (Farzan et al., 2013; Komssi et al., 2004; Paus et al., 2001). TEP peak analysis was performed in every electrode using the tep_extract function of the TESA toolbox. Peaks were defined as a data point that is greater than (positive) or less than (negative) 5 data points on either side of the peak. If multiple peaks were detected within a time window, the largest peak was used.

6.2.10. Statistics

6.2.10.1. Kinematics

All data were assessed for normality using the Shapiro-Wilk test and sphericity using the Mauchly test. All data met the assumption for normality, however since kinematic data violated the assumption of sphericity, a Greenhouse Geisser correction was applied when running ANOVAs.

It was investigated if there were differences between conditions (late familiarisation, early motor adaptation, late motor adaptation and late wash-out) on kinematic measures. A MANOVA was performed with a within-subject factor of Condition (late familiarisation, early motor adaptation, late motor adaptation and late wash-out) with the following dependent variables: movement onset, offset, time, maximum velocity, maximum force and summed errors. If a significant effect was detected, follow-up ANOVAs were performed on each of the dependent variables separately. Whenever a main effect of Condition was detected, post-hoc Bonferroni-adjusted paired t-tests were performed between late familiarisation and all other conditions (early motor adaptation, late motor adaptation and late wash-out).

6.2.10.2. ERP

To investigate the neural correlates of motor adaptation, differences across conditions on the N/P300 amplitude were assessed using a one-way repeated-measure ANOVAs with Condition (late familiarisation, early motor adaptation, late motor adaptation and late wash-out) as a within-subject factor. To see if significant effects were specific to the N/P300 component, repeated-measure ANOVAs were also performed on the N/P100 and N/P170 amplitude as a control analysis.

Since the ERP statistical analysis was performed on a whole scalp (63 electrodes) level, non-parametric permutation-based repeated-measure ANOVAs (2000 permutations) were used to assess differences across conditions in each electrode for each ERP component separately. If a significant main effect of Condition was found, non-parametric permutation-

based paired t-tests were used to compare each condition with the late familiarisation condition as well as between early and late motor adaptation. Significance level was set to 0.05 for the ANOVA and to 0.0125 for the post-hoc paired t-tests, and all p-values were FDR adjusted to control for multiple comparisons (i.e. 63 electrodes). Statistical results were plotted on scalp maps, and significant electrodes were highlighted in each plot.

Since the N300 component has been linked to error processing and motor learning (Anguera et al., 2009; Torrecillos et al., 2014) as well as to performance improvements (Beaulieu et al., 2014), a correlation between the N300 amplitude and the MLI was performed. Since the N300 amplitude and the MLI measures were normally distributed, a Pearson correlation was employed.

6.2.10.3. TEP N100

The N100 peak analysis was first performed on a whole scalp level and then the activity of significant electrodes was averaged and used for further analysis. Namely, to determine the global effect of motor adaptation the N100 amplitude at each electrode between pre- and post-motor adaptation using permutation-based t-tests (2000 permutations) were compared. TEPs from the significant electrodes were then averaged and the N100 amplitude was extracted pre-and post-motor adaptation. Statistical results were plotted on scalp maps (significant electrodes were highlighted in each plot) and in bar plots of the averaged N100 amplitude.

To test whether the N100 amplitude averaged from the significant electrodes can predict the MLI, a simple linear regression was performed.

Statistical significance was set to 0.05.

6.3. Results

Unless stated otherwise, all results presented in text, Figures and Tables are given in mean ± SD.

6.3.1. Kinematics

6.3.1.1. Trajectory results

As expected, at the beginning of motor adaptation, participants' trajectories considerably deviated from the ideal trajectory, resulting in curved trajectories compared to the familiarisation condition. With repetitive exposure to the force-field, participants were able to counteract the forces resulting in straight-lined trajectories and velocity profiles similar to those profiles in baseline movements. When the force-field was removed (wash-out condition), a first overcompensation towards the left (opposite) direction (after-effects of motor adaptation) was then followed by trajectories with very small deviations from the straight line. The motor adaptation process can be seen at a single-subject level and at a group-level (Figure 6-3 and 6-4 respectively).
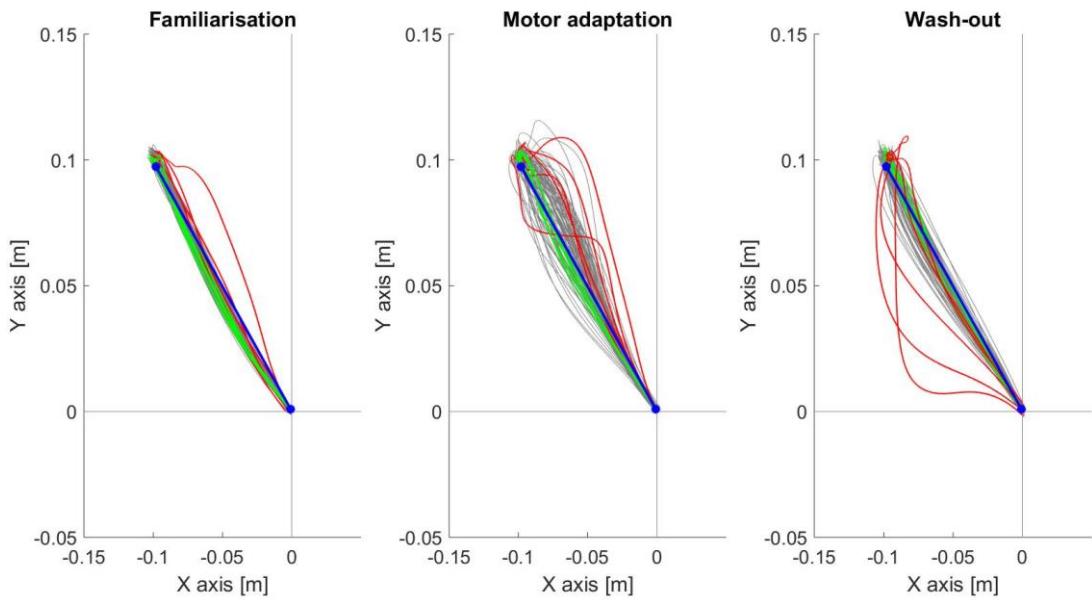
Figure 6-3: Trajectories during familiarisation, motor adaptation and wash-out in one representative participant. Trial-by-trial trajectories (i.e. thin grey lines) performed in the three experimental conditions of familiarisation (left panel), motor adaptation (middle panel) and wash-out (right panel). Thick blue lines illustrate the ideal straight line from the central starting point (x = 0; y = 0) to the peripheral target. During the familiarisation condition, actual trajectories are very close to the ideal trajectory as no perturbation (NF) is applied. Introduction of a clockwise force-field during the motor adaptation condition induce big deviations from the ideal trajectory towards the right-hand side at the beginning (red trajectories = first 5 trials), which are slowly reduced trial-by-trial (grey lines) until they get close to the ideal straight trajectory (green trajectories = last 5 trials). Removal of the perturbation (NF) during wash-out, induce a first overcompensation towards the left direction (red trajectories = first 5 trials), which are reduced trial-by-trial (grey lines) until they get very close to the ideal straight trajectory (green trajectories = last 5 trials).
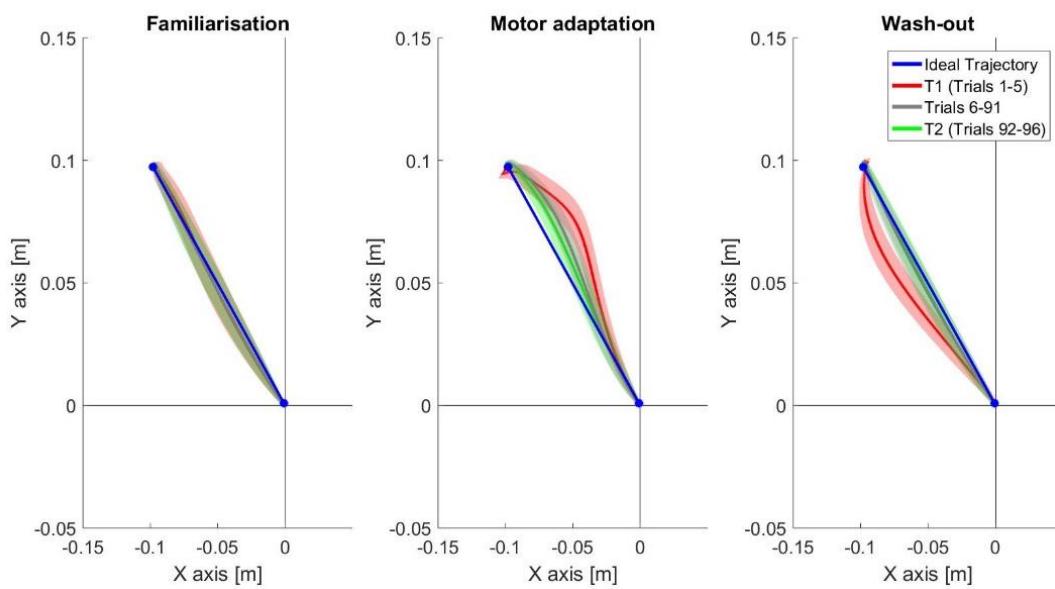
Figure 6-4: Group-level trajectories during familiarisation, motor adaptation and wash-out. Each panel represents group-level (N = 15) trajectories (shaded curve traces represent ±1 SEM) In each condition, the blue line illustrates the ideal trajectory from the central starting point (x = 0; y = 0) to the peripheral target, the red line the average of the first five trials, the green line the average of the last five trials and the grey line the average of the trials in between.

6.3.1.2. Behavioural motor adaptation process

Kinematic data were derived from trajectory profiles and velocity profile (Figure 6-5).

To get an overview of the details of behavioural changes during the motor adaptation, five kinematic measures are presented on a trial-by-trial basis (Figure 6-6).

The MANOVA showed that there was a significant main effect on kinematic measures of Condition (Pillai's trace= 1.273, $F_{(15, 120)}$ = 5.901, $p < 0.0001$, $\eta2 = 0.424$).

Follow-up repeated-measure ANOVA between conditions (LFAM, EMA, LMA and LWO) showed that movement onset ($F_{(2.33, 32.55)}$ = 0.35, $p = 0.741$, $\eta2 = 0.024$). movement offset $F_{(1.99, 27.985)}$ = 4.18, $p = 0.06$, $\eta2 = 0.23$) and movement time $F_{(1.89, 26.466)}$ = 3.431, $p = 0.05$, $\eta2 = 0.197$) were not significantly different across conditions, whereas averaged summed errors $F_{(1.45, 20.29)}$ = 47.87, $p < 0.0001$, $\eta2 = 0.774$), maximum velocity $F_{(1.936, 27.10)}$ = 15.41, $p < 0.0001$, $\eta2 = 0.524$) and maximum force $F_{(1.41, 19.76)}$ = 345, $p < 0.0001$, $\eta2 = 0.961$) were significantly different across conditions. Post-hoc t-tests showed that maximum force, summed errors and maximum velocities were significantly higher during motor adaptation compared to familiarisation (Figure 6-7). Exact statistical ANOVA and post-hoc paired t-test results are shown in Figure 6-7 and reported in Table 6-1.

To gain a deeper insight into the evolution of behaviour during different stages of motor adaptation as has been done in an earlier study (Pizzamiglio, 2017) kinematic data were also averaged into smaller blocks of trials, and statistical analysis is reported in **Appendix G.1**.
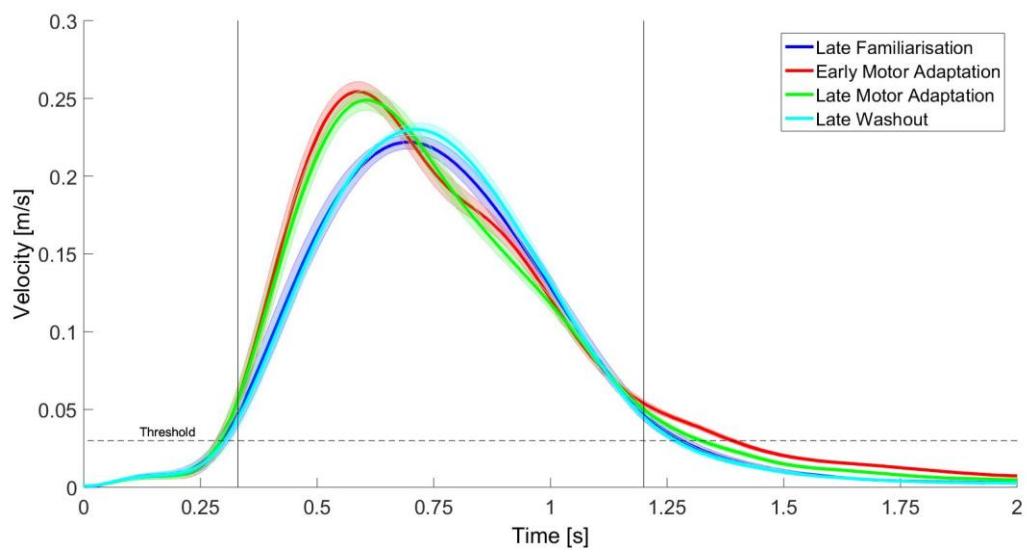
Figure 6-5: Velocity profile. Group-level (N = 15) velocity profile average (shaded curve traces represent ± 1 SEM) during familiarisation, motor adaptation and wash-out. Velocity profiles were used to derive and calculate movement onset, movement offset and maximum velocity for each participant. Specifically, movement onset (first dashed vertical line) was defined a speed profile exceeding a threshold of 0.03 m/s (dashed horizontal line), movement offset (second dashed horizontal line) by a speed profile lower than the threshold of 0.03 m/s after movement onset and maximum velocity as the peak velocity between movement onset and movement offset.
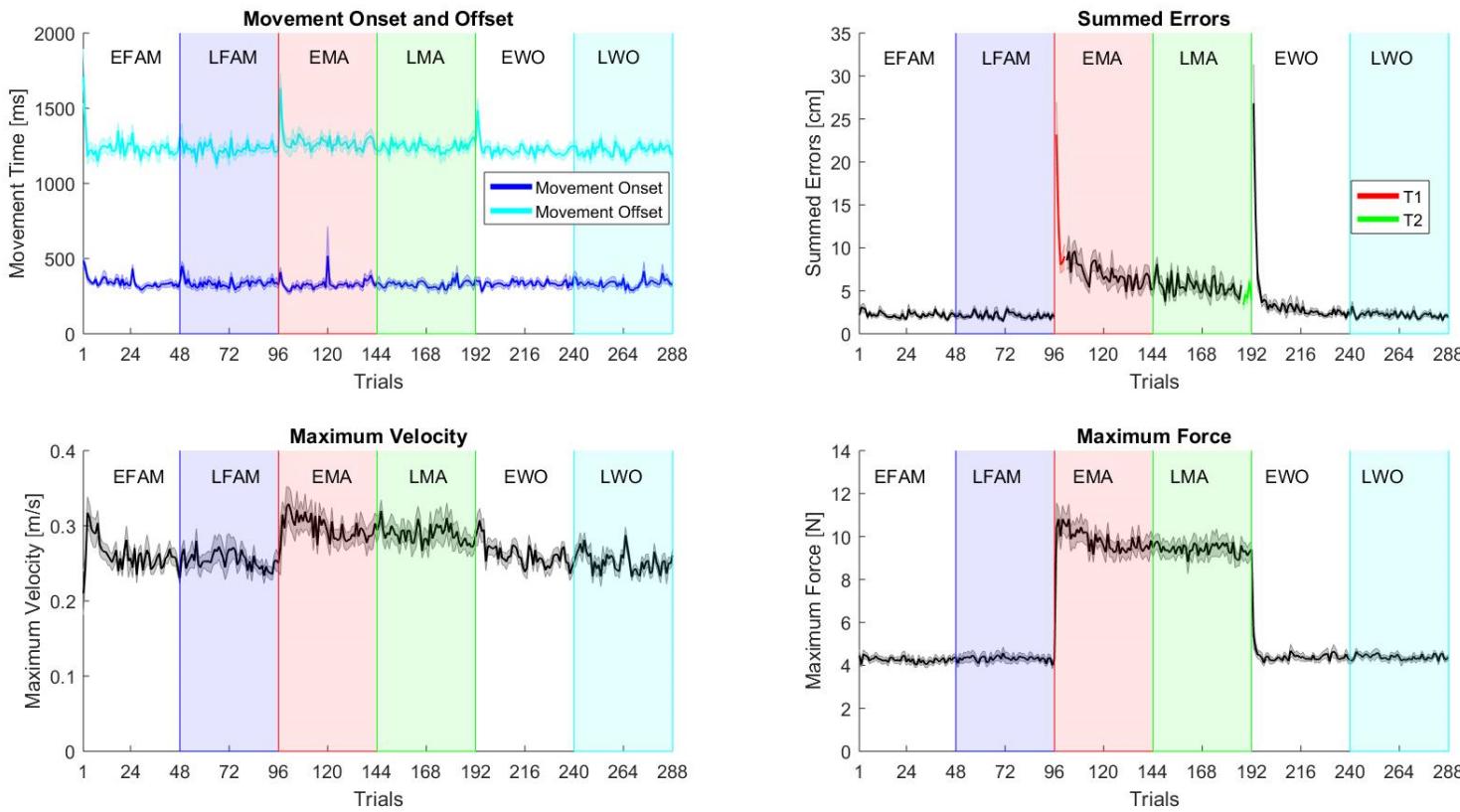
Figure 6-6: Trial-by-trial kinematic measures. A trial-by-trial population average (N = 15) profile with shaded standard error for each kinematic measure for all conditions. Trials taken for the averages considered for statistical analysis are highlighted in grey (LFAM, EMA, LMA and LWO). The upper left panel shows movement onset (blue line) and offset (turquoise line), lower left panel the maximum velocity and the lower right panel the maximum forces. The upper right panel shows the summed errors, here the trials were taken to calculate the MLI are shown in red (T1: first five trials of MA) and green (T2: last five trials of MA). EFAM: early familiarisation; LFAM: late familiarisation; EMA: early motor adaptation; LMA: late motor adaptation; LWO: late wash-out
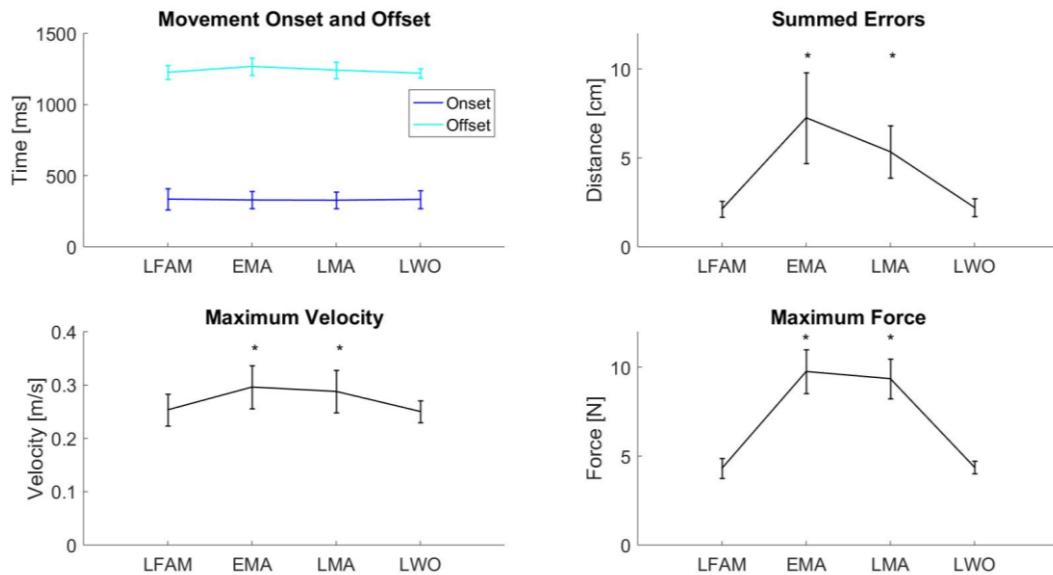
Figure 6-7: Kinematic measures in late familiarisation, early motor and late motor adaptation and late wash-out. Group averages (± SD) are shown for movement onset and offset (upper right panel), summed errors (upper right panel), maximum velocity (lower left panel) and maximum force (lower right panel). Repeated-Measure ANOVA with factor Condition (LFAM, EMA, LMA, LWO) showed a significant difference for summed errors, maximum velocity and maximum force. Significant post-hoc paired t-tests between LFAM and all other conditions are shown with * p < 0.0167.

Table 6-1: ANOVA results for kinematic data (Mean ± SD). Repeated Measure ANOVA with factor Condition (late familiarisation, early motor adaptation, late motor adaptation and late wash-out) was performed for all kinematic measures separately. Significant post-hoc t-tests between late familiarisation and all other conditions are highlighted with * p < 0.0167.

Kinematic Measure	LFAM	EMA	LMA	LWO	ANOVA			
					F	Df, Error	p	η2
Movement Onset [ms]	335[74]	329[60]	328[57]	333[62]	0.35	2.33, 32.55	0.741	.024
Movement Offset [ms]	1226[49]	1268[59]*	1242[57]	1220[33]	4.18	1.99, 27.985	0.06	.230
Movement Time [ms]	892[75]	938[53]	914[67]	887[56]	3.431	1.89, 26.466	0.05	0.197
Maximum Velocity [m/s]	0.25[0.03]	0.3[0.04]*	0.29[0.04]*	0.25[0.02]	15.41	1.936, 27.10	< 0.0001	.524
Maximum Force [N]	4.32[0.57]	9.76[1.24]*	9.36[1.13]*	4.38[0.36]	345	1.41, 19.76	< 0.0001	.961
Summed Errors [cm]	2.13[0.44]	7.26[2.55]*	5.34[1.48]*	2.21[0.5]	47.87	1.45, 20.29	< 0.0001	.774

217

6.3.1.3. The motor learning index (MLI)

Each participant made less errors (fewer deviations from the ideal straight line) in the final stages of motor adaptation (T1: 10.96 ± 4.70 cm > T2: 4.42 ± 1.28 cm) (Figure 6-8), reflected by positive MLI values (Figure 6-9). At a group level, paired t-tests revealed that in T2 summed errors were significantly lower compared to T1 ($t(14) = 5.6$ $p < 0.0001$, $\eta2 = 3.4$). Figure 6-9 shows that the MLI (53 ± 22 %) varied largely across participants ranging from 7.9 to 80.55 % reflecting a high variability in motor learning capacity.

The probability density graph displaying the frequency distribution of the MLI illustrates the variability of the MLI in Figure 6-9B and is similar to a previous lab finding (Faiman et al., 2018).
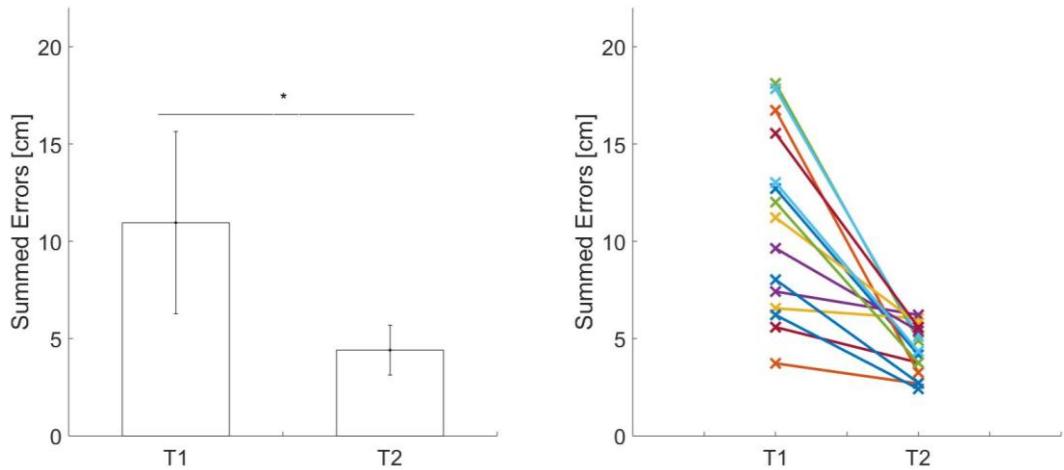
Figure 6-8: Trajectory errors during motor adaptation. Barplots (Mean ± SD) in the left panel represent group-level results. Significant differences between T1 and T2 are marked with asterisks. ∗p < 0.05. A paired t-test between pre-and post-motor adaptation resulted in a significant decrease in errors t (14) = - 5.6, p < 0.0001. Single-subject errors are shown in the right panel, where T1 and T2 errors are connected with lines.
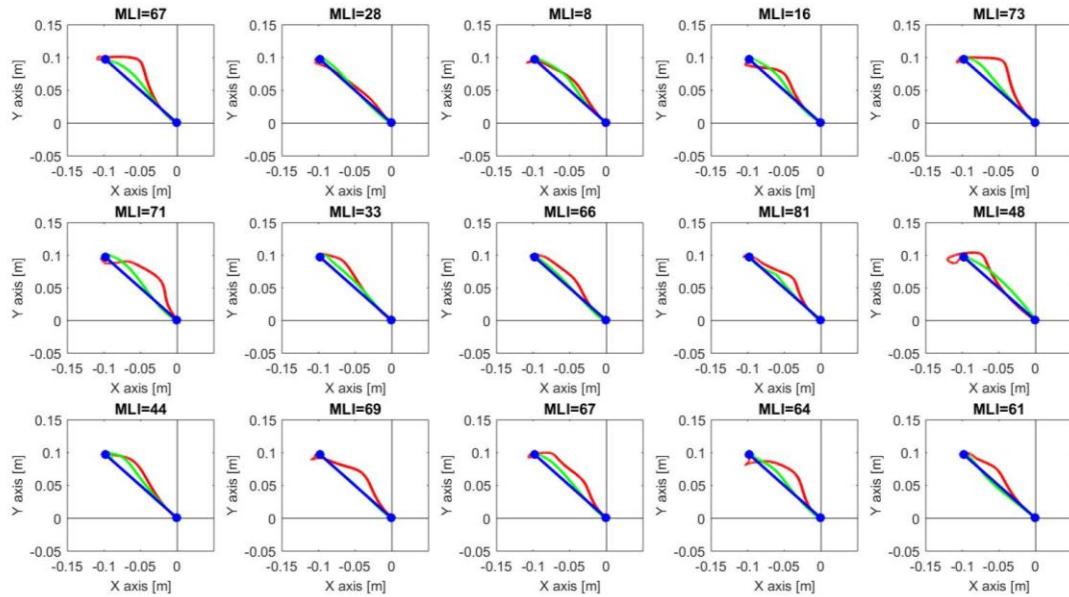
A)
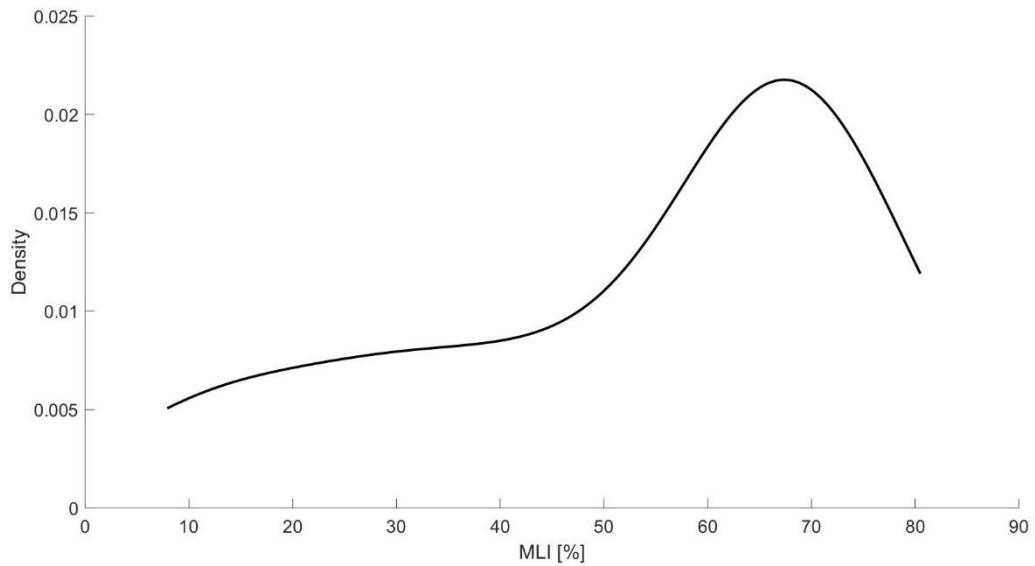
B)

Figure 6-9: The motor learning index (MLI in %) during motor adaptation. A) Each subplot (N = 15) represents the trajectories of a single-subject. Lines represent the averaged trajectories in the first five trials of motor adaptation (T1) in red, the last five trials of motor adaptation (T2) in green and the blue line represents the ideal trajectory. When a clockwise force-field (FF) is applied, deviations from the ideal trajectory are pronounced towards the right-hand side in the beginning (T1) and reduced at the end of motor adaptation (T2). The MLI (% improvement) of each participant is written above each subplot to show that motor adaptation (ability to adapt to the FF and make straight trajectories) is variable across participants. **B) Probability density graph.** The graph displays the sample probability density (y-axis) for the kinematic measure of Motor Learning Index (MLI; x-axis).

6.3.2. EEG

6.3.2.1. Error-related negativity

Three well characterised ERP components related to reaching movements were identified after visual inspection of ERPs in all electrodes (Figure 6-10) as well as in the GMFA (Figure 6-11). The specific ERP components were selected in the following time windows: 90-110 ms for the N/P100, 140-240 ms for the N/P170; and 280-360 ms for the N/P300 ERP component and used for statistical analysis.

However, it was ambiguous which time interval to take for the N/P170 component as it appeared as if there were two peaks between 140-240 ms. A control analysis, for the N/P170 component, was performed whereby the mean amplitude between 140-190ms and 190-240ms were calculated separately to see if it yielded a significant difference. (The results remained non-significant; results and Figures are reported in **Appendix G.2**).
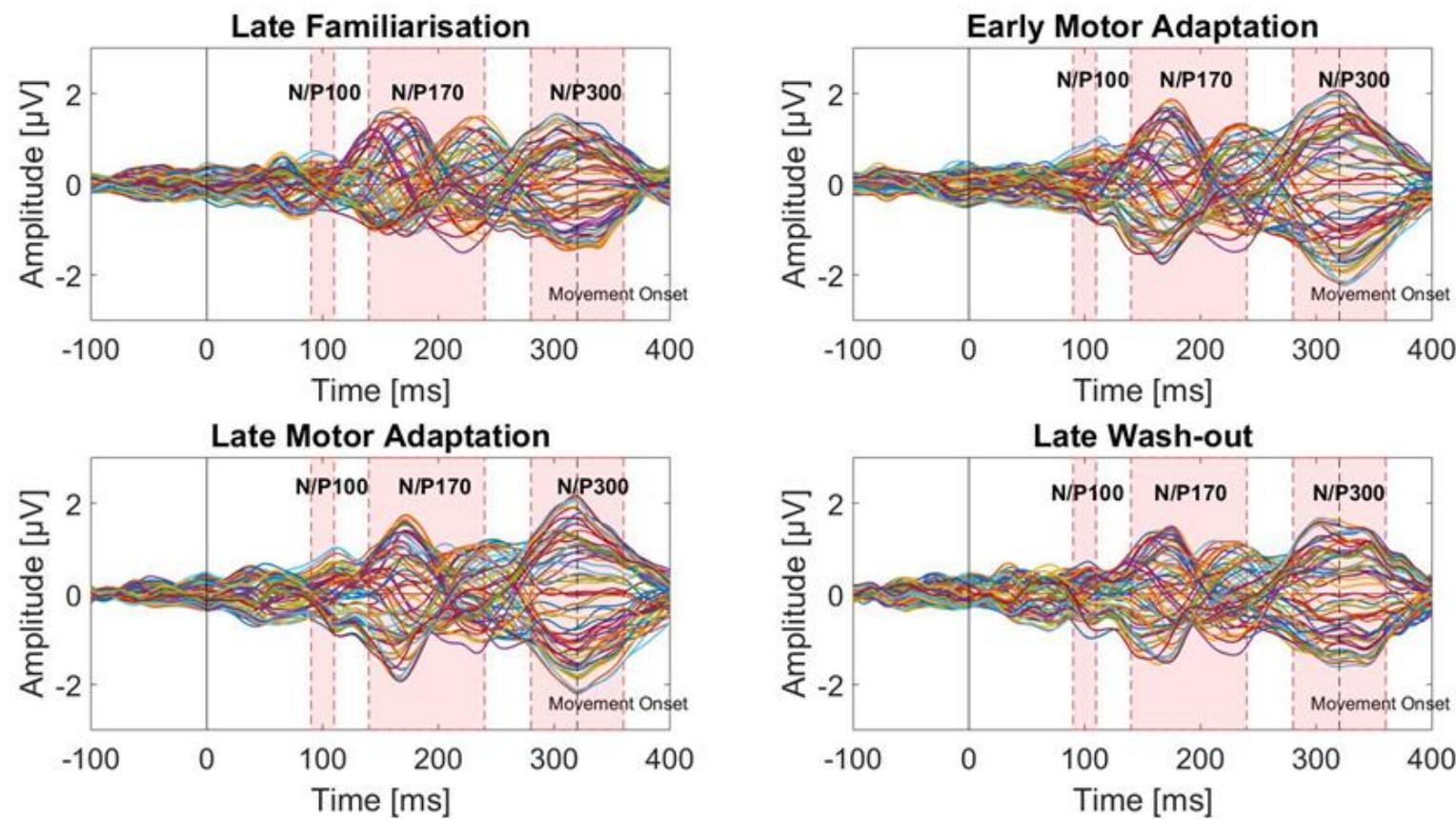
Figure 6-10: ERPs during the four blocks of interest: late familiarisation, early motor adaptation, late motor adaptation and late wash-out condition. Group-level (N = 15) grand-average of ERPs time evolution in each electrode (N = 63). Three time-windows of interest of the three ERP components have been identified for the N/P100, N/P170 and N/P300 and are highlighted with shaded red areas.
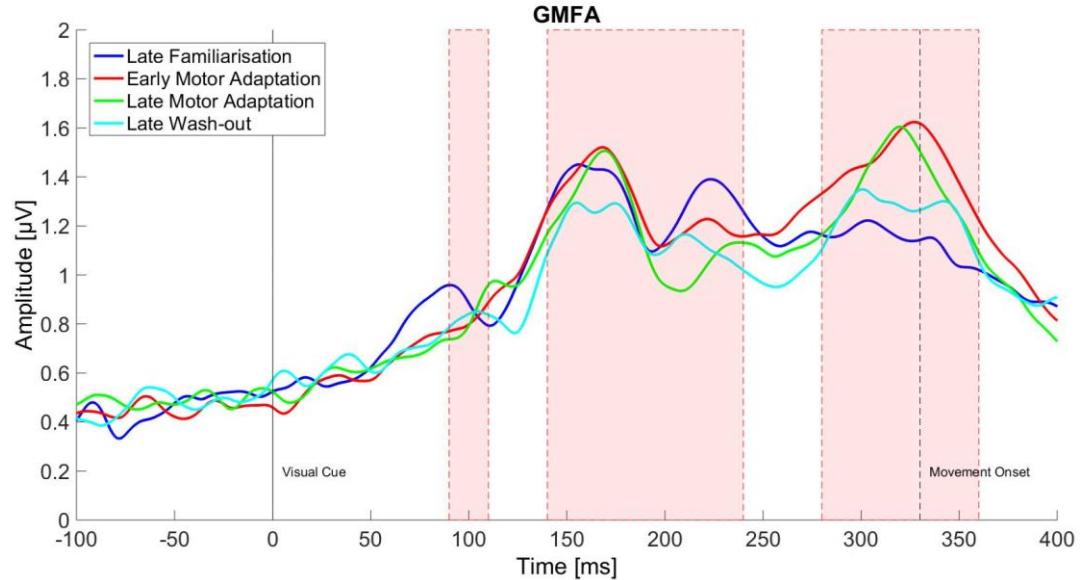
Figure 6-11: GMFA during late familiarisation, early motor adaptation, late motor adaptation and late wash-out condition. Group-level (N = 15) grand-average of GMFA time evolution is plotted and the three identified time-windows of interest of the three ERP components for the N/P100, N/P170 and N/P300 are highlighted with shaded red areas.

The repeated-measure ANOVA revealed no significant effect of Condition in the N/P100 and N/170 in any electrode (all $p > 0.05$) but a significant effect of Condition in the N/P300 in electrodes mainly overlying central brain regions and the exact F-values are represented on topographical maps in Figure 6-12. Post-hoc t-tests showed that N/P300 amplitudes were significantly larger during motor adaptation compared to familiarisation.

Specifically, the N/P300 was larger during early motor adaptation compared to late familiarisation in the following electrodes:

- **N300:** bilateral fronto-central regions (Fp1, F3, Fz, F4, FC5, FC1, FC2, C3, Cz, CP6, AF7, AF3, AF4, F5, F1, F2, FC3, FCz, FC4, C1, C2, C6)
- **P300:** bilateral posterior regions (P7, P4, P8, POz, O1, O2, P5, P2, P6, PO5, PO3, PO4, PO6, TP7, TP8, PO7, PO8, Oz, M1, M2)

N/P300 was larger during late motor adaptation compared to late familiarisation in the following electrodes:

- **N300:** contralateral sensorimotor regions to the reaching arm (Fz, FC1, C3, Cz, CP1, CP6, FC3, FCz, C1, C6)
- **P300:** ipsilateral posterior regions to the reaching arm (T8, M2, P6, TP8, P8)

The N300 (ERN) is seen over fronto-central regions during motor adaptation (Anguera et al., 2009; Krigolson and Holroyd, 2006) and is significantly different from familiarisation. No significant difference in the N/P300 between early and late motor adaptation was detected. Exact statistics are reported in topographical t-maps in Figure 6-12.
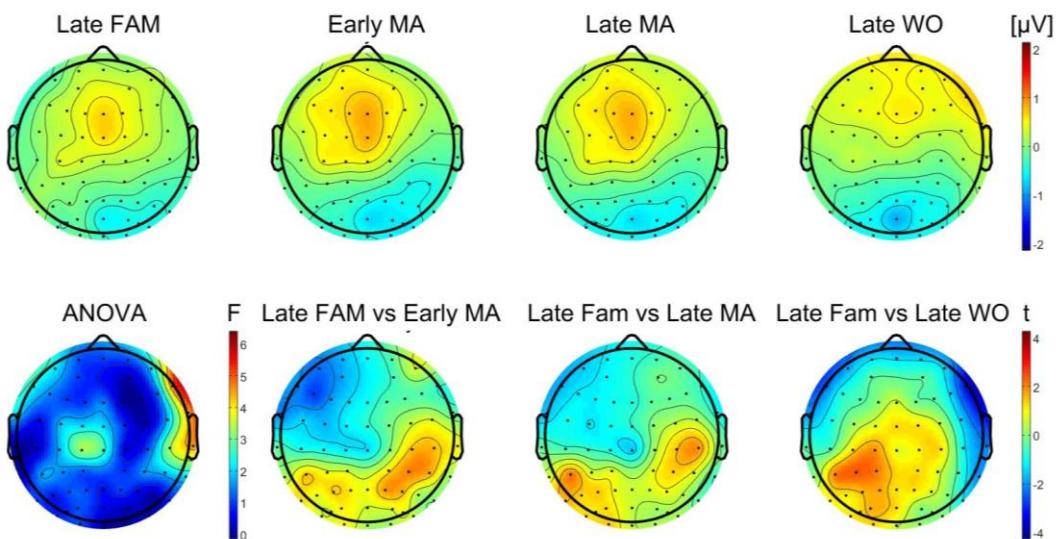
A)
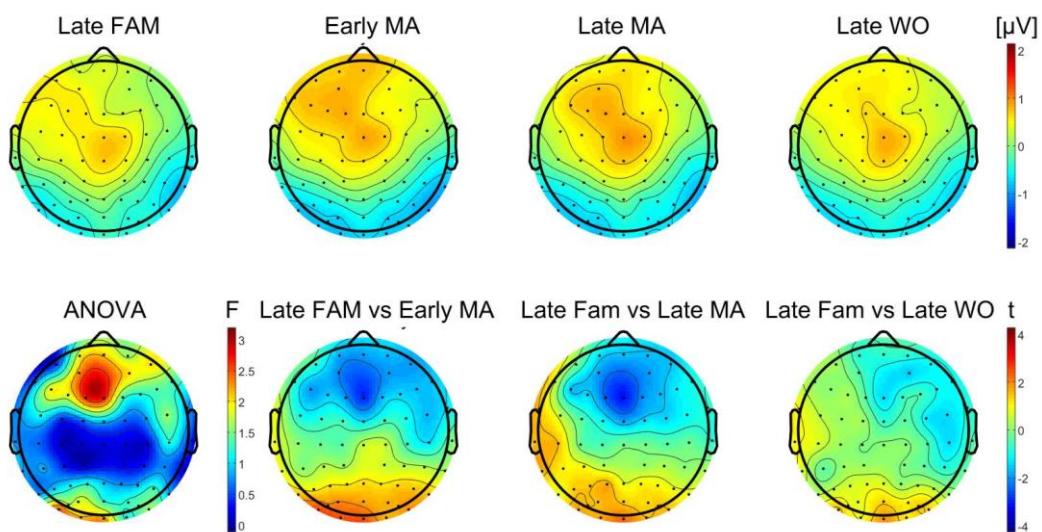
B)
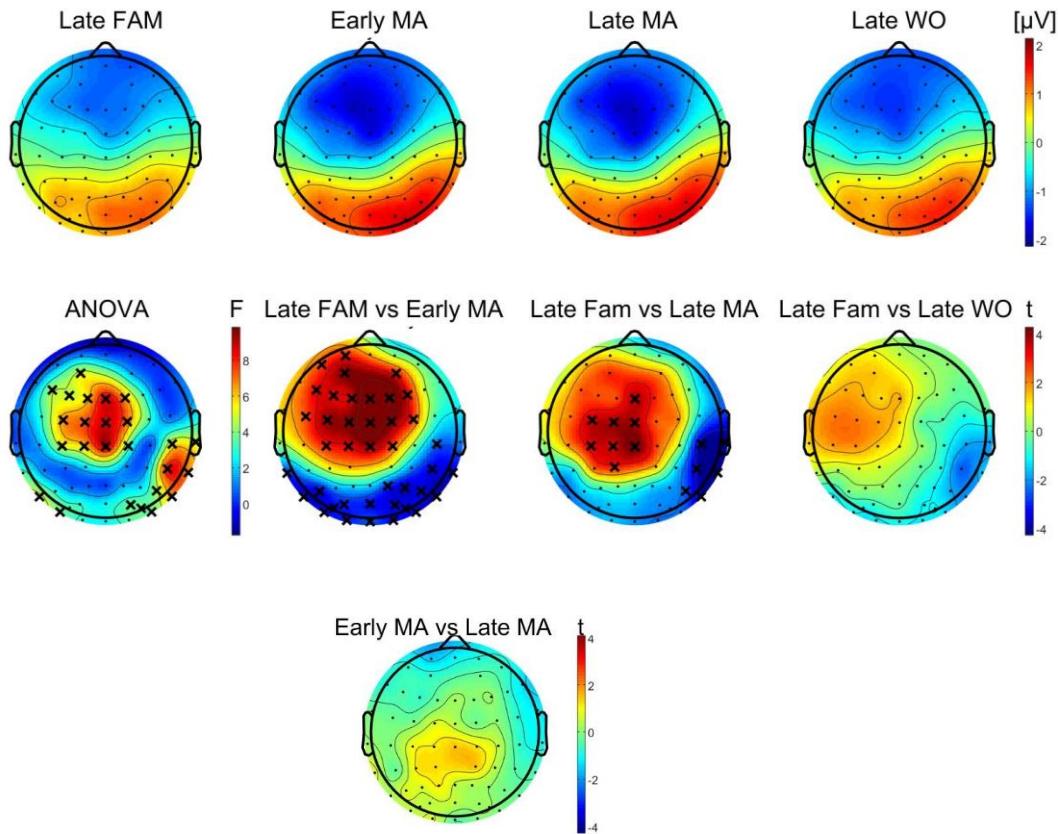
C)

Figure 6-12: ERPs activations and statistical comparisons for the P/N100 (A), P/N170 (B) and P/N300 (C) component. ERPs activations (µV) in the four conditions are shown in the first row. Statistical significance was obtained through non-parametric permutation-based permutation repeated measure ANOVA, followed by pairwise non-parametric permutation-based t-tests comparing late familiarisation with all other conditions as well as early and late motor adaptation. Significance level was set to 0.05 for the ANOVA and to 0.0125 for the post-hoc tests. All p-values were FDR adjusted to control for multiple comparisons (63 electrodes). Significant electrodes are highlighted with a cross in the second row for comparisons between late familiarisation with all other conditions. In the t-statistics maps, blue colours represent an increased N/P300 amplitude compared to late familiarisation, whereas red colours indicate decreased N/P300 amplitudes compared to baseline. Asterisk on the t-statistics maps represent the electrodes showing a significant difference (late familiarisation versus the other conditions as well as early versus late motor adaptation) (p < 0.0125). The paired t-test between early and late motor adaptation revealed no significant difference.

6.3.2.2. Cortico-behavioural correlation

To investigate the correlation between the N300 amplitude and motor performance during motor adaptation, the averaged N300 amplitude of the electrodes that were significantly different from late familiarisation in the early and late motor adaptation condition were calculated and used for the correlation. Since the data were normally distributed, Pearson correlations were used to test for significant correlations (3 correlations, Bonferroni adjusted significance with $p < 0.0167$).

There was a significant negative correlation between the MLI and the N300 in early motor adaptation (r= - 0.62, p = 0.014) and late motor adaptation (r= - 0.613, p = 0.015) (Figure 6-13). There was also a significant negative correlation between the MLI and the averaged N300 amplitude from early and late MA (in electrodes showing a significant modulation from late familiarisation) (r= - 0.671, p = 0.006), indicating that a larger N300 amplitude during motor adaptation is associated with higher MLI values.

As a control analysis, we tested whether the N300 amplitude was specifically correlated to motor performance improvement (MLI) or also to summed errors. The additional control correlation analysis revealed that the averaged errors during early and late motor adaptation did not significantly correlate with the N300 amplitude in early motor adaptation (r= - 0.049, p = 0.861) nor in late motor adaptation (r= - 0.188, p = 0.503).
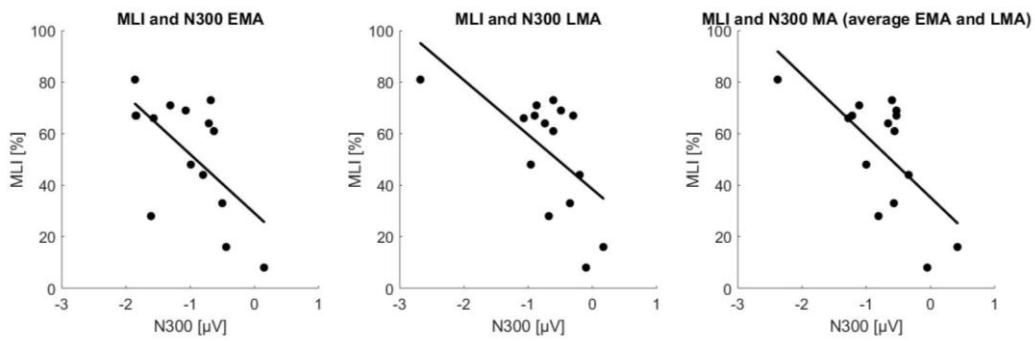
Figure 6-13: The association between the MLI and the N300 amplitude in early and late motor adaptation in the averaged electrodes showing a significant modulation from late familiarisation. The MLI was significantly negatively correlated with the N300 amplitude in early MA (average of significantly modulated electrodes compared to late familiarisation) ($r = -0.62$, $p = 0.014$) and the late MA N300 amplitude (average of significantly modulated electrodes compared to late familiarisation) ($r = -0.613$, $p = 0.015$). The MLI was also significantly correlated with the averaged N300 amplitude from early and late MA (in electrodes showing a significant modulation from late familiarisation) ($r = -0.671$, $p = 0.006$). (Bonferroni adjusted $p < 0.0167$, for three correlations).

6.3.3. TMS-EEG

6.3.3.1. Modulation of the N100 amplitude

Single-pulse TMS to left M1 reliably produced identifiable peaks in the EEG data as can be seen in the TEP butterfly plot in Figure 6-14A. The N100 peak amplitude occurred in a time window between 75 - 150 ms post-TMS in accordance with the literature (Farzan et al., 2013; Komssi et al., 2002; Paus et al., 2001). Group-level N100 peak amplitudes (N = 15) are plotted in topographical maps in Figure 6-14B. The N100 peak amplitude was significantly smaller post-MA compared to pre-MA. The exact distribution and t-test results for each electrode are plotted in topographical maps in Figure 6-14B. The electrodes showing a significant modulation are mainly overlying sensorimotor regions: FZ, FC1, FC2, CZ, CP1, CP2, F2, FC3, FCZ, F4, C1, C2, P1. The averaged N100 amplitude of these electrodes was then calculated and used for subsequent statistical analysis.
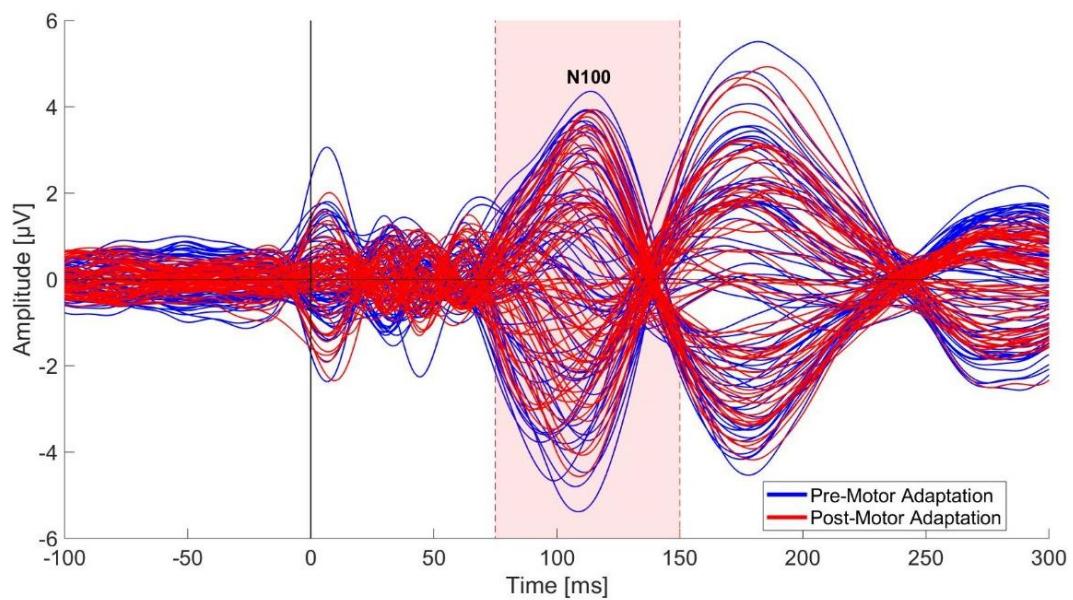
A)
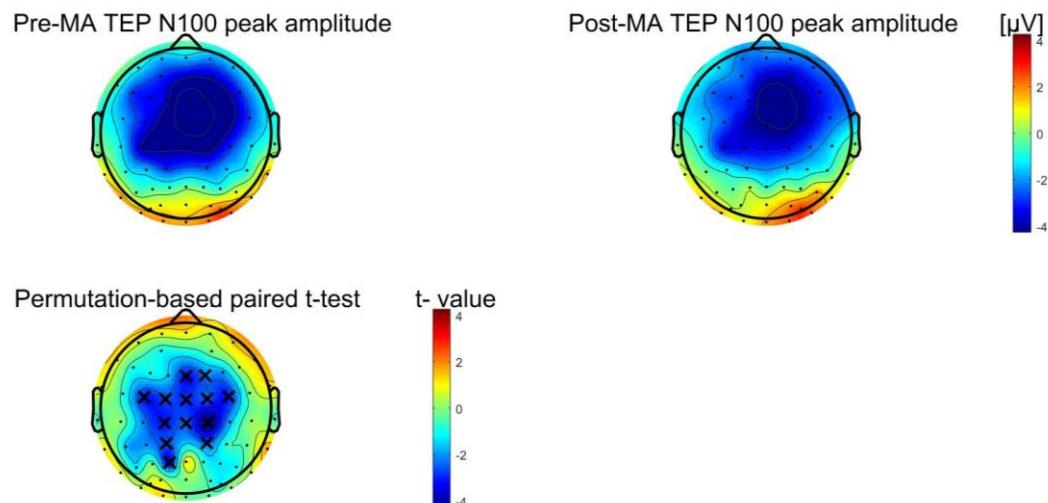
B)

Figure 6-14: TEPs pre- and post-motor adaptation. A) Group-level (N = 15) grand-average of TEPs time evolution in every electrode (N = 63). B) Topographical surface voltage plots of the N100 TEP component. Topoplots pre-MA (upper left column) and post-MA (upper right column) and topographic distribution of the t-values from a permutation-based paired t-test (p < 0.05) (lower left column) showing the difference between pre-and post-MA N100 TEP component. Blue represents decreases in negativity or increases in positivity. Crosses on the t-statistics maps represent the electrodes showing a significant difference (pre-MA versus post-MA) (p < 0.05).

TMS-evoked potentials are plotted for the averaged significant electrodes in Figure 6-14B. Single-pulse TMS to M1 reliably produced well-characterised positive and negative deflections in the EEG signal and the TEP N100 component, seen as a negative deflection around 100 ms post-TMS was reliably detected in all participants (Figure 6-15).

N100 amplitudes (from the averaged significant electrodes shown Figure 6-14B were significantly smaller N100 post- compared to pre-motor adaptation (t (14) = - 4.33, p = 0.001) (Figure 6-16). Single-subject and group-level (N = 15) N100 peak amplitudes are shown in Figure 6-16. The N100 amplitude decreased in 14 out of 15 participants.

The N100 modulation calculated as [(Post-Pre)/ Pre] *100 in the averaged electrodes (shown in Figure 6-14B) did not correlate with MLI (rho = - 0.021, p = 0.941).
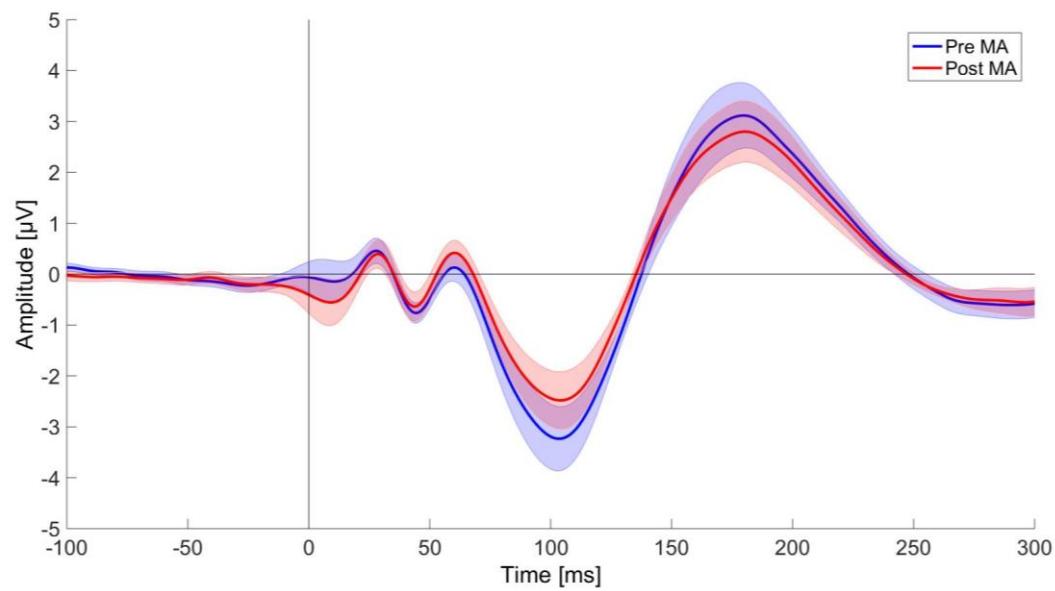
Figure 6-15: TEP modulation. Pre-motor adaptation (blue) and post-motor adaptation (red) grand-averages and SEM (shaded areas). Each line in the TEP plot represents the grand-average across electrodes that showed a significant difference in the N100 TEP between pre- and post-MA as indicated in Figure 6-14B.
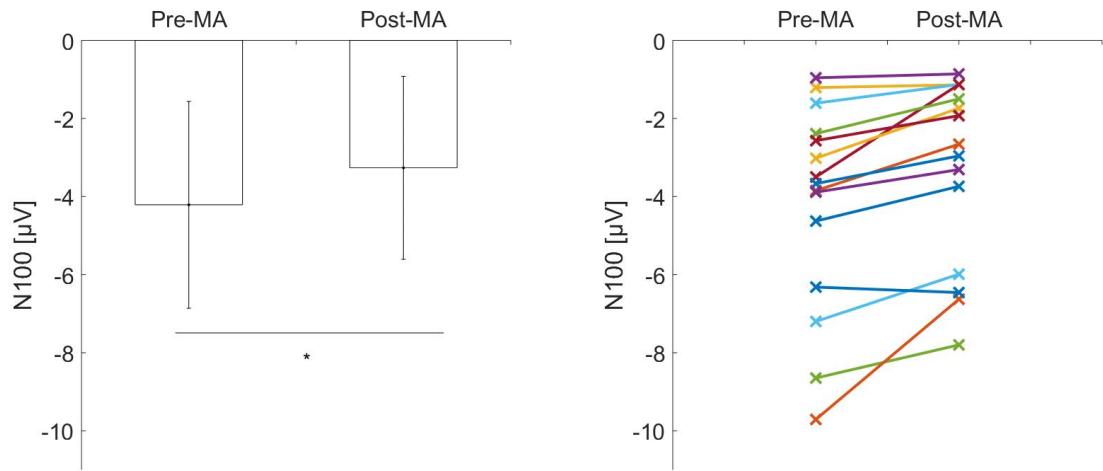
Figure 6-16: The N100 peak amplitude pre- and post-motor adaptation. Barplots (Mean ± SD) in the left panel represent group-level results of the N100 peak amplitude (in the averaged significant electrodes in Figure 6-14B). Significant differences between conditions are marked with asterisks. ∗p < 0.05. A paired t-test between pre-and post-motor adaptation showed that the N100 was significantly smaller post-compared to pre-motor adaptation (t (14) = - 4.33, p = 0.001). Single-subject N100 peak amplitudes are shown in the right panel, where pre- and post-MA N100 peak amplitudes are connected with lines. At a group-level, the N100 is attenuated post-MA compared to pre-MA.

6.3.3.2. The pre-motor adaptation N100 amplitude and MLI

The simple linear regression between the resting-state pre-motor adaptation N100 peak amplitude (average the electrodes shown in Figure 6-14B) and the MLI showed that the pre-MA N100 peak amplitude explained 35 % of the variance ($R^2 = 0.353$, $F(1, 14) = 7.09$, $p = 0.02$) and significantly predicted MLI of participants ($\beta = 32$, $p = 0.004$) and significantly predicted MLI of participants ($\beta = 33$, $p = 0.003$) (Figure 6-17). Residuals were normally distributed and plotted in Figure 6-18.
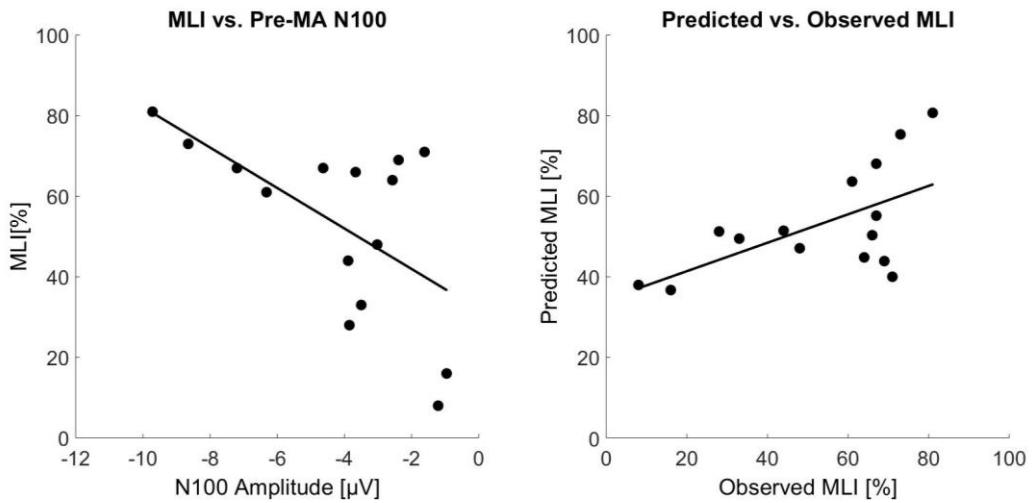
Figure 6-17. The association between the MLI and pre-motor adaptation N100 amplitude. The left scatterplot represents the MLI versus the N100 amplitude pre-motor adaptation (averaged N100 amplitude in the significant electrodes shown in Figure 6-14B) and the right scatterplot the predicted MLI versus the observed MLI. The simple linear regression revealed that the pre-MA N100 peak amplitude was a significant predictor and explained 35 % of the variance (R^2 = 0.353, F (1, 14) = 7.09, p = 0.02) and significantly predicted MLI of participants (β = 32, p = 0.004). The right panel shows the observed versus predicted MLI measures.
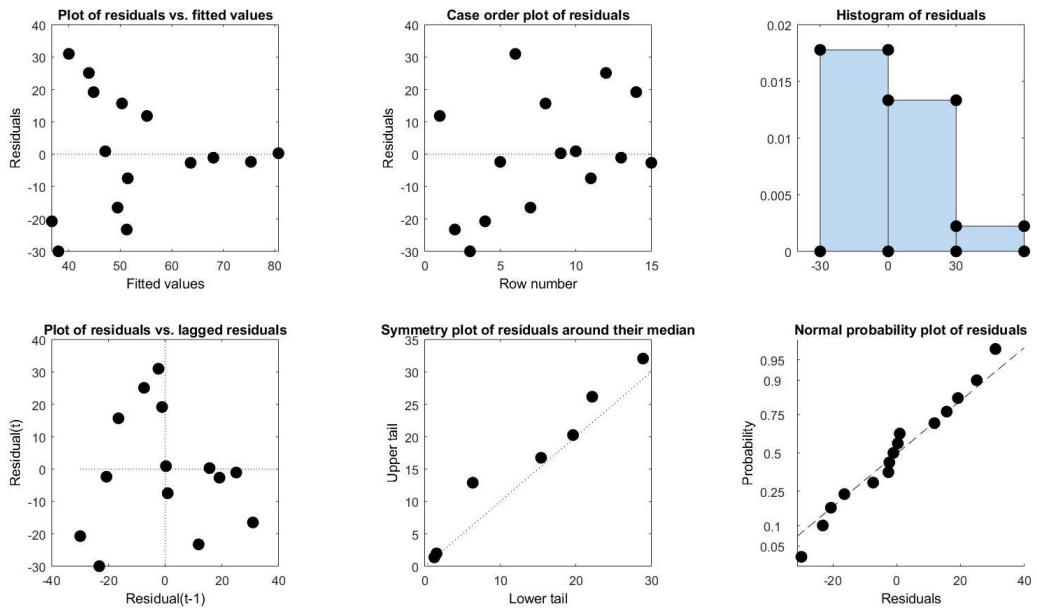
Figure 6-18: Plots of residuals of linear regression with MLI as the dependent variable and pre-motor adaptation N100 amplitude as the independent variable. The residuals versus fits plot were used to verify the assumption that the residuals have a constant variance. The residuals versus order plot were used to verify the assumption that the residuals are uncorrelated with each other. The histogram of residuals was used to determine whether the data are skewed or whether outliers exist in the data. The normal plot of residuals was used to verify the assumption that the residuals are normally distributed.

6.4. Discussion

The present study examined the electrophysiological correlates of error-based learning to assess sensorimotor excitability and plasticity related to motor adaptation. EEG and TMS-EEG were employed to investigate the neural mechanisms underlying inter-subject variability in motor performance in healthy individuals.

As expected, individuals successfully adapted to the force-field environment and showed strong-after effects once the force-field was removed.

During motor adaptation neural activity around movement onset (N300) was significantly enhanced compared to non-adaptation conditions and resembled the ERN activity, related to error processing (for review see Gehring et al., 2018). As expected, this activity was related to motor performance: The magnitude of the N300 (i.e. ERN) was associated with the degree of motor adaptation, calculated with the MLI. This finding corroborated previous studies showing that the ERN is involved in error-processing and motor learning (Anguera et al., 2009; Torrecillos et al., 2014) as well as to performance improvements (Beaulieu et al., 2014). Thus, the fronto-central ERN activity detected during motor adaptation in this study could reflect the formation of a predictive internal model adapted to the force-field environment.

As hypothesised, motor adaptation underlay neuroplastic changes within sensorimotor regions, as reflected by modulations in cortical excitation measured with decreases in the TEP N100 amplitude post- compared to pre-motor adaptation.

Finally, the study reported that a native resting-state inhibitory biomarker (i.e. TEP N100 amplitude pre-motor adaptation) predicted the degree of subsequent motor performance during motor adaptation.

6.4.1. Kinematic measures

The Chapter investigated how participants adapt to an external perturbation (force-field). Participants performed a visually-triggered reaching task in the

horizontal plane both in a null-field (i.e. unperturbed reaching) and force-field velocity-dependent environment (i.e. perturbed reaching). Participants completely familiarised with the experimental task when they performed unperturbed reaching movements (during familiarisation), demonstrated by a reduction in trajectory errors (smaller offsets from the ideal straight line (Figure 6-4). Subsequently, a clockwise velocity-dependent FF disrupted the movement causing big deviations from the ideal straight line. The initial big deviations from the straight line were slowly replaced by smaller deviations, i.e. smaller errors trial-by-trial, according to a nearly exponential trend (Figure 6-6), in line with previous reports (Huberdeau et al., 2015; Hunter et al., 2009; Pizzamiglio et al., 2017b). Strong after-effects were observed after the removal of the force-field, as participants over-compensated in the opposite direction of the previously applied force-field in the very first trials of wash-out. After the first few trials, participants performance improved again and returning almost to baseline levels with little errors at the end of the wash-out phase. The after-effects observed during wash-out demonstrate that individuals did not simply react to environmental changes but anticipated the expected the dynamic of the new environment most probably as a result of the formation of a predictive internal model to the new environment (Hunter et al., 2009).

The present results are consistent with the literature suggesting that motor adaptation is a reaction to specific changes in the environment with which the participant is interacting, consisting of a gradual reduction of performance error and a return to baseline performance (Donchin et al., 2003; Thoroughman and Shadmehr, 2000). During motor adaptation, each participant made fewer errors in the last five trials compared to the first five trials. However, the capacity to learn varied widely across participants, as indexed with the MLI ranging from 8 to 81 %. The underlying neural correlates yielding inter-subject variability in the capacity to learn were further explored using EEG and TMS-EEG.

6.4.2. Neural correlates of motor adaptation ERP N300 (i.e. ERN)

6.4.2.1. Neural correlates of motor adaptation

The ERP component differentiating perturbed (motor adaptation condition) and unperturbed reaching was the negative deflection around 280-360 ms (N300, ERN) post-visual cue (peaking around movement onset). This is of particular interest as this component has previously been linked with error-processing. Thus, it can be suggested that the neural correlates of motor adaptation are related to the ERN component which has been investigated and linked to error-related learning (Anguera et al., 2009; Holroyd and Coles, 2002; Krigolson and Holroyd, 2006; MacLean et al., 2015). Specifically, the N300 component was significantly larger during motor adaptation compared to unperturbed reaching (late familiarisation). The N300 were larger in electrodes overlying fronto-central, bilateral premotor and motor brain areas in early stages of motor adaptation and larger in electrodes located over fronto-central, contralateral premotor and motor brain regions in late stages of motor adaptation, which could be interpreted as a more focused activation pattern.

However, and even though errors during late motor adaptation were significantly higher compared to late motor adaptation (t (14) = 3.62, p = 0.003, this did not translate into cortical activation differences, as comparisons between early and late motor adaptations showed no significant difference in the N300 amplitude. Moreover, the N300 amplitude was not correlated with the averaged error magnitude during early and late motor adaptation. This finding contradicts Anguera et al. (2009) who reported that the ERN was larger when higher errors are made, smaller when smaller errors are made and that the ERN is larger in early compared to late adaptation. The discrepancy between the present findings and those of Anguera et al. (2009) can be explained through key methodological differences: First, Anguera et al. (2009) used a visuomotor adaptation task involving using a rotation of the visual feedback as opposed to a force-field mediated reaching task. Second, the ERN waveform occurred in time windows during movement as opposed to before movement onset as reported in the present study. As such the ERN

activity in Anguera et al.'s (2009) study is likely to be confounded with the magnitude of the movement and could not only reflect error-processing but also feedback-related activity. Third, Anguera et al. (2009) studied longer periods of motor adaptation by using a total of 364 trials for the motor adaptation condition and trials between early and late motor adaptation were separated by 308 adaptation trials. In the present study, however, the motor adaptation condition consisted of 96, with the first half of trials considered as early motor adaptation and the second half as late motor adaptation. The significantly higher cortical activity during late motor adaptation together with significantly higher averaged errors compared to late familiarisation suggest that the present motor adaptation task investigated short adaptation. This could also explain why cortical activation between early and late motor adaptation was not seen in the current study and did not show a significant shift of activity from cortico-striatal brain regions (early adaptation) to more posterior regions, including the posterior parietal cortex and cerebellum (late adaptation) reported by a previous motor adaptation study using more trials per motor adaptation condition (160 for early and 160 for late motor adaptation (Krebs et al., 1998). Moreover, Shadmehr and Holcomb (1997) demonstrated that the shift from prefrontal cortical regions to premotor, posterior parietal and cerebellar brain regions occurs 6 hours after motor adaptation practice and is attributable to motor consolidation.

6.4.2.2. ERN and motor learning

The larger N300 amplitude seen during motor adaptation compared to unperturbed reaching is likely to reflect motor adaptation processes underlying error-based learning. However, it could also be argued that the increased activity during motor adaptation reflects how the brain deals with a more complex motor task requiring higher muscle forces and cognitive engagement compared to unperturbed reaching (Hardwick et al., 2013; Lage et al., 2015), rather than reflecting error processing and motor learning. This hypothesis is unlikely to be the case in the present study, as the N300 amplitude is correlated with performance improvements, suggesting its active role in error-processing. This study reports a significant correlation between

the N300 amplitude during early and late motor adaptation with motor performance, calculated with the MLI. Specifically, larger N300 amplitudes were associated with better motor performance improvement, reflected by higher MLI scores. Interestingly, the N300 was only linked to performance improvement and not to the net error magnitude, demonstrated by a lack of significant correlation between the N300 and errors during motor adaptation. This finding is in agreement with a previous study reporting a significant correlation between the ERN and the performance improvement in a serial reaction time task (Beaulieu et al., 2014) and not raw errors, supporting the idea that the N300 is associated with the reduction in errors and not averaged error commission. The hypothesis that the ERN is related to error reduction rather than merely reflecting error commission and detection is further supported by Frank et al. (2005), in which larger ERNs were associated with better performance on a cognitive reinforcement task as well as being associated to learn to avoid negative events as opposed to seeking positive events.

The functional role of the ERN in motor performance improvement is further supported by studies involving clinical populations. Specifically, using the same motor adaptation task as discussed in this study, it has been shown that the ERN was smaller in stroke patients compared to healthy controls when adapting to an external force-field (Desowska and Turner, 2019). Similarly, disconnections between lateral and frontal cortices in stroke patients lead to smaller ERN amplitudes and are associated with poorer performance in a choice reaction time task (Hogan et al., 2006). In a patient with a lesion in the ACC, ERN amplitudes were attenuated and corresponded to lower error-correction rates (Swick and Turken, 2002), suggesting a dissociation between error monitoring and detection. Crucially, even in the absence of an ERN production due to lesions in the medial prefrontal cortex, patients can still be aware of (i.e. detect) errors (Stemmer et al., 2004). Together with the present study, showing a significant correlation between the N300 and performance improvement (higher MLI) and a lack of correlation between the N300 and net error magnitude, it can be argued that the ERN (N300) is linked to optimisation

strategies aiming to reduce errors rather than reflecting error detection and commission.

6.4.2.3. ERN and internal model formation

It is generally accepted that the CNS learns and holds internal models of sensorimotor transformations necessary for accurate movement control (Kawato and Wolpert, 1998). Specifically, an internal model is a neural system that mimics the behaviour of the sensorimotor system and objects in the outer world. The formation and modification of these internal models rely on the constant interaction of the body part being controlled and the controller and plays a key role for normal motor control and learning. Motor adaptation is commonly defined as error-driven learning relying on predictions from internal models formed by repetition to adapt to environmental perturbations (for review see Shadmehr et al., 2010). It is thought that the mechanism underlying the formation and modification of internal models rely on both feedback and feedforward signals.

The acquisition of an internal model during force-field mediated adaptation task is necessary to anticipate and counteract perturbing forces (Hunter et al., 2009; Kawato and Wolpert, 1998). The formation of this internal model to the external forces is generally manifested by after-effects errors in reaching trajectories in the first trials in which the force-field has been removed (Hunter et al., 2009). As the present study reports initial errors in the opposite direction of the previously applied force-field in the wash-out conditions, it can be assumed that participants acquired a predictive model to the previously applied force-field during motor adaptation. Since the overshooting errors vanished at the end of the wash-out condition and returned back to baseline, it can be assumed that the previously acquired internal model dissolved. In the present study, the formation of the internal model during motor adaptation seemed to coincide with increases in the ERN amplitude in fronto-central regions during motor adaptation compared to unperturbed reaching. During late wash-out when the after-effects of the previously applied force-field have vanished, the ERN also returns to baseline. These findings suggest that the

242

ERN is based on information stored in the internal model and might reflect the creation of an internal model specific to the perturbed environment.

ERN activity has been mainly localised in fronto-central regions (Anguera et al., 2009; Contreras-Vidal and Kerick, 2004) and associated with the formation and modulation of an internal model of the visuomotor representation to the perturbed environment. The exact function of the ERN activity in the modification of the internal model remains to be clarified. Some have argued that the ERN activity reflects the comparison of predicted and intended responses supporting its role in feedback mechanism (Anguera et al., 2009; Swick and Turken, 2002), whereas others have credited the ERN with the formation of predictive models (Desowska and Turner, 2019; Krigolson and Holroyd, 2006; Pizzamiglio, 2017). The second hypothesis seems more plausible in the current study, as the peak ERN activity was detected before movement onset, hence prior to error commission similar to Krigolson and Holroyd (2006). This study, therefore, suggests that the ERN is likely to reflect error processing rather than simple feedback mechanisms and might play a key role to build a representation of predicted error to account for environmental perturbations.

6.4.3. Cortical excitability and plasticity underlying motor adaptation

6.4.3.1. Cortical excitability modulation indicates neuroplastic changes

As hypothesised force-field adaptation was accompanied by changes in cortical excitability, as indexed with a significant modulation of the TEP N100 amplitude, a biomarker inhibitory processes (Du et al., 2018, Premoli et al., 2014). Specifically, the TEP N100 amplitude was significantly smaller post- compared to pre-motor adaptation over sensorimotor regions and was not restricted to M1. This finding corroborates previous TMS studies measuring corticomotor neuronal changes of excitability with MEPs (for review see Ljubisavljevic, 2006) and expanding them to regions outside M1 by measuring changes in excitability on a whole scalp level with TEPs. Specifically, the present study applied TMS over M1 pre- and post-motor adaptation at rest and recorded TMS-evoked cortical responses from the whole scalp. Permutation-based whole scalp paired

comparisons of the TEP N100 amplitude showed that significant modulations were seen over bilateral sensorimotor regions.

Since the N100 amplitude is thought to represent $GABA_B$-receptor activity (Premoli et al., 2014), the underlying neuronal mechanisms of sensorimotor excitability changes, as measured with the N100 amplitude are most likely reflecting modulations of $GABA_B$-mediated inhibitory pathways. The present Chapter suggests that decreases in the TEP N100 reflect GABA-related cortical inhibition decreases which could be related to motor adaptation. As shown by previous TMS studies investigating motor learning, these changes could be indicative of changes in membrane excitability and enhanced synaptic strength such as by LTP mechanism, as well as a concomitant modulation of cortical inhibition (for review see Ljubisavljevic, 2006).

However, the behavioural and functional relevance of the observed sensorimotor plasticity remains to be elucidated, since the present study did not find a significant correlation between the change in cortical plasticity as measured by the percentage decrease of the N100 amplitude from pre- to post-motor adaptation and performance improvement during motor adaptation. The lack of association between sensorimotor plasticity and behavioural performance improvement could imply that the observed neuroplastic changes in sensorimotor cortical regions only reflect an incomplete picture and that these changes could also at least in part be secondary to subcortical modulations. In fact, plasticity in the cerebellum appears to have a central role in motor adaptation (Krebs et al., 1998; Spampinato and Block, 2017). Moreover, it has been shown that driving neuroplasticity in the cerebellum by applying tDCS is associated with decreases in errors during adaptation, whereas tDCS over M1 has no behaviourally relevant effect (Galea et al., 2011). The idea that motor adaptation not only engaged distinct cortical regions but a whole network of brain regions was further demonstrated by functional specific changes in distinct resting-state networks following motor adaptation (for review see Ostry and Gribble, 2016). For instance, Vahdat et al. (2011) distinguished specific networks related to perceptual changes comprising the second somatosensory cortex, ventral premotor cortex, and supplementary motor

cortex from those relevant for motor aspects of learning including cerebellar cortex, the M1, and the dorsal premotor cortex. However, as EEG is unable to measure subcortical regions, such as the cerebellum, it might explain why the present study did not observe a direct relationship between plasticity changes and behavioural performance.

6.4.3.2. Native cortical excitability is linked to motor learning performance

Another explanation for the lack of cortical modulation in excitability and motor performance improvement during motor adaptation could be that differences in native (i.e. resting state pre-motor adaptation) excitability can influence subsequent brain activity and motor performance during the motor task (Lissek et al., 2013). Therefore, this study explored if resting state cortical excitability could serve as a better index for motor learning performance.

This Chapter examined how variations in intrinsic excitability measured with TMS-EEG at rest are related to behaviour, namely to performance improvement in the subsequent motor adaptation task. It was found that larger N100 amplitudes predicted better performance improvements (higher MLI), suggesting that inhibitory mechanisms play a central role in motor adaptation processes. It is noteworthy that the N100 amplitude was only correlated and predictive of subsequent motor adaptation measured with the MLI (R^2 = 0.353, F(1, 14) = 7.09, p = 0.02) and not with the magnitude of errors at the start of motor adaptation (T1 errors made in the first five trials of motor adaptation) (rho = - 0.264, p = 0.341). The level of inhibition at rest were related to motor learning and not to a baseline measurement of errors. The finding of an association of a larger N100 amplitude measured at rest with an improved degree of subsequent motor adaptation suggests that greater cortical inhibitory activity is related with better motor learning.

This might seem counter-intuitive, but it is partially consistent with previous motor learning studies: Some studies have shown that increased GABA levels at rest are linked with poorer motor learning (Kolasinski et al., 2019; Stagg et al., 2011). Conversely, it has also been reported that more inhibition at the start of the motor task is associated with better motor learning (Nowak

et al., 2017) and that higher GABA concentrations in M1 are related to better motor performance reflected by faster reaction times (Greenhouse et al., 2017). The association between higher inhibition before motor adaptation and better subsequent motor performance presented in this Chapter suggests that a higher inhibitory capacity could be beneficial for motor learning, possibly due to increased precision of GABAergic transmission. This hypothesis is supported in the literature reporting that a lack of inhibition can lead to poorer motor performance and to disorders such as dystonia (Beck et al., 2009; Stinear and Byblow, 2004).

6.4.4. Motor learning and metaplasticity

It has been shown that learning relies on the strengthening of horizontal connections within M1 (Rioult-Pedotti et al., 2000, 1998) and most likely depend on LTP-like mechanisms (Ziemann et al., 2004). In their review on motor learning and plasticity, Ziemann and Siebner (2008) proposed two strategies to boost motor learning underlying plasticity changes. The first strategy to improve motor learning, referred to as "gating", is to increase the excitability of M1 during motor practice by weakening intracortical inhibitory circuits. Another strategy to boost motor learning consists in lowering the threshold to induce synaptic plasticity by lowering neuronal activity (i.e. excitability) prior to learning. This mechanism is thought to be driven by homeostatic metaplasticity.

The present finding of higher resting-state inhibitory (i.e. lower excitatory activity) as a predictor of better motor learning is consistent with the mechanism of homeostatic metaplasticity: a decreased excitability (i.e. neuronal activity) prior to learning could promote LTP-like mechanisms to take place during motor adaptation and thus lead to better motor performance.

This study highlights that the individual differences in resting-state inhibitory capacity prior to motor adaptation explain the variability in motor performance improvement and the TEP N100 amplitude could serve as a biomarker to harness these differences to best utilise the brain's capacity to learn. Specifically, depending on the resting-state TEP N100 amplitude, an inhibitory

or excitatory NIBS could be applied prior to motor learning to promote LTP-like mechanisms during motor adaptation and thus boost motor performance.

For instance, Jung et al. (2009) demonstrated that paired associative brain stimulation of the M1 modulated subsequent motor learning. Specifically, motor learning was enhanced when an inhibitory paired associative brain stimulation (i.e. promoting LTD-like effects) was applied before motor practice. A future study could test whether an excitability-decreasing manipulation prior to the motor adaptation task used in the present study could have similar effects to the ones previously reported (Jung et al., 2009) and thereby boost motor learning. This could potentially be exploited in the clinical population to improve upper limb recovery.

Given the predictive value of the TEP N100 in motor learning capacity, this biomarker could potentially be used to understand the large inter-subject variability in motor learning and upper limb recovery in stroke patients. As shown by Davidson et al. (2016), finding a predictive readout, such as corticospinal excitability, would be helpful to determine who is likely to benefit from tDCS in the context of motor learning and exploited to further understand the inter-subject variability of tDCS during motor adaptation.

6.4.4. Limitations

6.4.4.1. No full motor adaptation

Although a typical adaptation profile in movement error was seen at a group-level, participants exponentially adapted to the applied external force-field; however, a complete adaptation did not occur as the group-level error in the last trials was still significantly higher compared to late familiarisation More trials would have been needed to reach full motor adaptation, but the choice of using 96 trials in total for each condition was a trade-off between full adaptation and avoiding fatigue and exhaustion. related to repetitive movements. Since the whole experiment with EEG preparation and TMS hotspot determination lasted up to 4 hours, giving longer breaks to the participant would have prolonged the experiment even more, it was not deemed reasonable to add additional trials to each condition. Moreover, it has

been reported that even after 336 trials during a visuomotor adaptation task, errors in the last block during motor adaptation were still significantly higher compared to baseline and even with this high amount of trials no full adaptation was obtained (Anguera et al., 2009). This group also reported significant differences in ERN amplitudes between early and late motor adaptation. The lack of significant difference between the ERN between early and late motor adaptation in the current study could, therefore, be attributed to the significantly lower amount of trials during motor adaptation. A future study ought to examine if by adding more adaptation trials between early and late motor adaptation, significant cortical activity differences would emerge.

6.4.4.2. No speed-accuracy trade-off

By design, the motor adaptation task used in the current study did not allow for speed-accuracy trade-offs as participants were instructed to move at a specific speed to the target and received feedback to ensure that they did so. This only allowed participants to optimise their reaching movement in one dimension: namely accuracy. However, it has been shown that motor adaptation relies on re-optimisation systems involving speed-accuracy trade-offs (Izawa et al., 2008; Peternel et al., 2017).

6.4.4.3. Specificity of neuromodulatory effect of motor adaptation

This present study used a motor adaptation protocol using 96 trials in which an external force-field was applied to reaching movements. Every participant adapted to the force-field resulting in positive motor learning indices. TMS-EEG applied to M1 revealed that the adaptation to the external perturbation modulated cortical excitability. However, it remains to be tested whether this neuromodulatory effect is specific to adaptation processes or if they are linked to repetitive movements. A future study could examine if repetitive reaching without an external perturbation (no-adaptation condition) has similar neuromodulatory effects. Based on the present study, it would be expected that perturbed reaching compared to unperturbed reaching has a stronger effect on cortical excitability changes since it is a more challenging task relying most probably on the formation of a new adaptive model.

In this study, TMS-EEG was applied over M1 and therefore tested local reactivity and plasticity within nearby neuronal populations. However, it is known that motor adaptation also involves other cortical and subcortical structures. A positron-electron tomography study to detect neural correlates of motor adaptation, reported that early learning activates striato-parietal and sensory cortical regions, whereas during late learning the pattern of activation shifted to a cortico-cerebellar feedback loops (Krebs et al., 1998). In light of this, some of the neuromodulatory effects caused by motor adaptation might have been missed and unmeasured with the current TMS-EEG protocol. Future studies should aim to target different cortical regions to establish the specificity of neuromodulation on different cortical structures. However, studying the effects on subcortical regions will not be feasible with currently available TMS-EEG equipment as it is not possible to measure EEG activity from these structures.

6.4.4.4. Limited value into clinical translation

Neurorehabilitation following stroke include robot-mediated therapy and different training modalities are used in clinical trials and practice, including assisted (Rodgers et al., 2019), passive and resistive (Patton et al., 2006) training. Despite of the increasing use of robots in the context of rehabilitation, there is still no consensus on what the best training modality and intensity is and how this kind of training can be translated into better recovery. In fact, a recent large multi-clinical trial with 770 stroke patients reported that robot assisted training (N = 257) was not better than more conventional treatments, namely enhanced upper limb therapy (N = 259), or usual care (N = 254) (Rodgers et al., 2019). Moreover, even if robot-assisted therapy resulted in improved upper limb impairment, as measured with the Fugl-Meyer assessment, it did not translate into better upper limb function. The present Chapter provides a predictive biomarker of motor performance during an adaptive training in healthy individuals and could help identify patients who would benefit the most from this kind of therapy, resulting in improved upper limb impairment. However, in light of Rodger et al.'s (2019) finding of the limited value of improved upper limb impairment on upper limb function, the

translation of these findings into clinical settings remains to be clarified in future studies.

6.4.4.5. Methodological consideration

Due to the length of the motor adaptation paradigm and the time required for the TMS-EEG set-up, the study was limited in the number of TMS pulses to use. The application of 50 single-pulse TMS pulses in each condition was chosen because previous studies have reported that this corresponds to the minimum number required to get reliable TEPs (Du et al., 2018; Farzan et al., 2013; Nikulin et al., 2003). This study elicited the N100 TEP component in all participants and confirmed that 50 TMS pulses are enough to reliably measure cortical excitability using the TEP N100 as a readout.

To limit the somatosensory feedback from the activated muscle by TMS, TMS was applied at an intensity of 100% RMT. Because of the limited amount of trials, this study did not seek to split the EEG data into trials where an MEP was present versus absent and did not store the EMG traces for offline analysis, as has been done in a previous study (100 trials per condition) (Petrichella et al., 2017) to investigate the effect of somatosensory feedback on the TEPs.

6.4.5. Conclusions

This Chapter demonstrated that individuals successfully formed an internal predictive model to the force-field environment, allowing them to make accurate movements in a perturbed environment. The formation of the internal model was reflected by the ERN-like activity in fronto-central regions.

Motor adaptation induced significant changes in cortical excitability over sensorimotor regions, suggesting that neuroplastic changes also outside the M1 are involved in motor adaptation mechanisms.

Finally, the finding of a predictive value of the inhibitory biomarker TEP N100 on motor learning provide a theoretical interpretation that resting state motor cortical excitability is a factor contributing to individual variations in motor learning.

Chapter 7 - Regional and Interregional Cortical Activity during Unperturbed and Perturbed reaching

This Chapter explores the neural correlates of reaching in an unperturbed and perturbed environment at a brain network level (i.e. regional and interregional cortical activity). It represents a secondary exploratory data analysis the EEG data recorded during the motor adaptation protocol of **Study III** (**Chapter 6**) and aims to expand the findings reported in the previous Chapter to the time-frequency domain to gain further insights into the dynamic fluctuations in brain network activity (i.e. functional connectivity between cortical regions) during robot-mediated reaching

7.1. Introduction

Regional and interregional cortical activity can be measured using functional neuroimaging techniques, such as EEG, MEG, fMRI and PET (for review see Bowyer, 2016) and can depict synchronous oscillations of neuronal populations. These neuroimaging techniques allow to quantify different brain network types depending on the mathematical processing technique used. Three main types exist, namely structural, functional and effective connectivity. This Chapter will focus on functional connectivity, which is defined as the temporal correlation between the time series of different brain regions sharing similar frequency, phase and/ or amplitude patterns. Functional connectivity measurements, as opposed to effective connectivity, provide only an information about the strength of connectivity without specifying the direction of information flow between regions.

Visually-triggered movements place high demands on the CNS, relying on visuomotor transformations engaging several brain regions including visual, motor and sensory areas (Classen et al., 1998; Naranjo et al., 2007). The preparation and execution of visually-triggered movements mobilise different brain regions which cooperate as a network to establish a stimulus-movement association (Classen et al., 1998; Formaggio et al., 2013; Naranjo et al., 2007). It has been shown that the strength of active involvement of specific

brain regions is modulated during different phases of visually-triggered reaching movements (Formaggio et al., 2013; Storti et al., 2016; Zaaroor et al., 2003), namely, early visual information processing (Thut et al., 2000), motor preparation (Simon et al., 2002), motor execution (Sainburg and Kalakanis, 2000) and movement termination (Andrew and Pfurtscheller, 1996). Movement preparation and execution during robot-mediated reaching have mainly been associated with decreased alpha and beta oscillatory power (Formaggio et al., 2013; Storti et al., 2016). Regional and interregional cortical activity is also modulated by task demand and is adaptively modified during different stages of sensorimotor learning (Andres and Gerloff, 1999; Gerloff and Andres, 2002; Perfetti et al., 2011). Furthermore, visuomotor adaptation studies have demonstrated that the formation of an internal model relies on the synchronised activity between segregated brain regions, specifically in the gamma frequency bands (Perfetti et al., 2011).

Studies employing robot-mediated arm reaching in unperturbed environments have reported movement-related desynchronisation in alpha and beta oscillatory power (Formaggio et al., 2015, 2013), as well as movement-related interregional coherence changes. Moreover, studies (Andres and Gerloff, 1999; Gerloff and Andres, 2002; Serrien and Brown, 2003) employing finger movement task to study motor learning have reported an increased interregional connectivity in early stages of and decreases in later stages of motor learning.

A better understanding of cortical modulations during robot-mediated reaching could be a useful tool to identify electrophysiological measures in healthy individuals and employed as baseline measurements to evaluate abnormal patterns in patients with upper limb impairments (Formaggio et al., 2015, 2013).

The present Chapter investigated cortical dynamical changes during visually-triggered reaching movements in an unperturbed (null-field, during familiarisation and wash-out) and perturbed environment (force-field applied during early and late motor adaptation). The signal recorded from the 64-electrode scalp EEG system from **Study III** (**Chapter 6**) was analysed in the

time-frequency domain to investigate the oscillatory power variation and connectivity between selected scalp (electrode) sites. The goal was to investigate the spatiotemporal patterns of task-related oscillatory brain activity during highly standardised motor performance using a robotic device. To this end this Chapter compared cortical activity during unperturbed (non-adaptation condition) and perturbed (adaptation condition) in terms of regional activity and functional connectivity.

The Chapter focussed on two main questions:

i) Are cortical regional changes and interregional cortical connectivity different between perturbed and unperturbed reaching?

ii) What is the temporal evolution of regional and interregional modulations during perturbed and unperturbed reaching?

It was hypothesised that:

i) Unperturbed and perturbed movement will engage similar cortical regions, but that regional and interregional cortical activity will be enhanced during perturbed (i.e. when adapting to an external force-field) compared to unperturbed reaching, due to the higher cognitive processing required during motor adaptation.

ii) Functional dynamics in regional activity and network configuration will be significantly modulated during different phases of robot-mediated reaching as revealed by changes in power and connectivity strength.

7.2. Methods

7.2.1. Research Design

This Chapter employed a within-subject design to investigate the patterns of task-related oscillatory regional and interregional cortical activity related to motor adaptation. EEG data from **Chapter 6** (**Study III**) during unperturbed (non-adaptation condition) and perturbed reaching (motor adaptation condition) were analysed in the time-frequency domain to identify the temporal

253

modulation of regional activity and interregional connectivity strength during different phases of reaching.

The effect of motor adaptation was assessed on regional oscillatory power modulations (i.e. event-related spectral perturbation (ERSP)) and interregional coherence modulations (i.e. task-related phase coherence (TR-ERPCOH)) in 6 different phases of reaching.

7.2.2. Data Analysis

The pre-processed EEG data were obtained from **Study III** (**Chapter 6**). For details on participant recruitment, experimental setup and protocol see **Chapter 6**.

7.2.2.1. Event-related spectral perturbation (ERSP)

Time frequency decomposition was obtained by using Wavelet transform (Morlet, 3.5 cycles) using newtimef function in EEGLAB from 6 to 80 Hz. Absolute spectra normalisation was first applied at the single-trial level performing full- epoch length single-trial correction and then by a pre-stimulus baseline correction (- 900 to – 100 ms pre-visual cue) on the resulting ERSP averaged across all artefact free trials (Grandchamp and Delorme, 2011). A sliding window size of 200 ms in width was applied to the single-trial clean data over a 3-second time interval (- 1000 ms to + 2000 ms post-visual cue) to optimally separate out both, the low and high-frequency components.

A two-tailed bootstrap significance probability was computed at each frequency by permutating baseline values across both time and trials and tested whether the original ERSP values lied in the 0.5 or 99.5 % tail of the surrogate distribution at any given frequency. If this criterion was met, the specific time-frequency point was considered significant at alpha < 0.01, number of permutations = 2000) with respect to baseline. Only significant values were considered for group analysis (Fecchio et al., 2017). Event-related power decreases are expressed as negative values and reflect event-related desynchronisation (ERD), whereas event-related power increases are expressed as positive values and reflect even-related synchronisation (ERS).

7.2.2.2. Task-related phase-coherence (TR-ERPCOH)

Event-related phase-coherence (ERPCOH) was introduced by Rappelsberger et al. (1994) and measures the coherence between EEG channels related to specific events across a temporal dimension. It provides information about the dynamic interaction of brain regions (Andrew and Pfurtscheller, 1996) and can be used as a measure of functional connectivity. In this thesis, only phase cross coherence (ERPCOH) (Delorme and Makeig, 2004), which estimates the complex linear relationship between two signals, was used. For a and b, two given time series (e.g. from two EEG channels), being F_k $(f,)$ the spectral estimate of trial k at frequency f and time t:

$$\text{ERPCOH}^{a,b}(f, t) = \frac{1}{n}\sum_{k=1}^{n} \frac{\sum_{k=1}^{n} F_k^a(f,t)\, F_k^b(f,t)^*}{|F_k^a(f,t)\, F_k^b(f,t)|} \quad,$$

Equation 7-1: ERPCOH.

N is the number of trials and $F_k^a(f, t)\, F_k^b(f, t)^*$ is the cross-spectrum between two given time series from *a* and *b*. ERPCOH values are real numbers between 0 and 1, where 1 symbolises perfect synchronisation and 0 an absence of synchronisation between two signals.

To reduce the effect of the averaged reference, volume conduction issues, inter-subject and inter-electrode variability, task-related coherence was employed. Specifically, ongoing coherence measurements were corrected for a baseline value. Task-related coherence was calculated by subtracting the baseline coherence (in a resting condition, e.g. before a visually cued movement) from an active condition (e.g. during visually guided movements) similar to previous studies (Formaggio et al., 2015; Fuggetta et al., 2005) according to following subtraction:

$$\text{TR} - \text{ERPCOH} = \text{ERPCOH(active)} - \text{ERPCOH(baseline)}$$

Equation 7-2: TR- ERPCOH.

Where positive values represent increases in coherence magnitude and negative values represent decreases in coherence.

To study the connections between scalp electrodes overlapping the fronto-parietal-occipital network, 21 electrodes of the 63 sites were selected. The electrode selection was based on previous studies on motor planning and reaching (Perfetti et al., 2011, Bernier et al., 2017). The electrode selection is in accordance with the extended 10/20 system covering medially and laterally the frontal, central and posterior regions of the left and right hemisphere. The selected electrodes were: FPZ, AF3, AF4, F3, F4, FC3, FC4, C3, C4, CP3, CP4, P3, P4, PO3, PO4, POZ, FZ, FCZ, CZ, PZ, OZ.

7.2.3. TOIs and FOIs

The averaged ERSP and TR-ERPCOH in six segments was calculated based on kinematic data derived from velocity profiles (Chapter 6, Figure 6-5). The window length for a segment was 300 ms without overlapping starting 0.3 s pre-visual cue and ending 1.5 s post-visual cue. Velocity profiles (Chapter 6, Figure 6-5) were used to define the time intervals to divide different movement stages and were in line with the literature (Formaggio et al., 2015; Perfetti et al., 2011), defined as the following:

- Pre- visual trigger: -0.3 to 0 s
- Movement preparation: 0 to 0.3 s
- Early Movement: 0.3 to 0.6 s
- Mid-Movement: 0.6 to 0.9 s
- Late Movement: 0.9 to 1.2 s
- Post Movement: 1.2 to 1.5 s

The following frequency ranges were selected: alpha (8 - 12 Hz), beta (13 - 30 Hz) (Formaggio et al., 2015), low gamma (30 - 45 Hz) and high gamma (45 - 80 Hz) (Ozdenizci et al., 2017).

7.3. Statistics

Since this was an exploratory analysis on a wide range of brain regions, the Benjamini and Hochberg (Benjamini and Hochberg, 1995) procedure for controlling for FDR was employed. This method was chosen because it is suggested to be the best suited for exploratory studies of focally (i.e. ROI) and broadly (i.e. whole brain) distributed effects (Groppe et al., 2011).

7.3.1. ERSP

Firstly, to investigate significant modulations in ERSPs in each condition (late familiarisation, early and late motor adaptation and late wash-out) compared to baseline (pre-visual cue), non-parametric permutation-based t-tests (2000 permutations) were used to evaluate whole scalp (63 electrodes).

Secondly, non-parametric permutation-based t-tests (2000 permutations, as previously used in **Chapter 6**) were used to evaluate whole scalp (63 electrodes) ERSPs differences between each condition (early and late motor adaptation and late wash-out) and late familiarisation and between early and late motor adaptation. Significance level was set to 0.0125, and all p-values were FDR adjusted to control for multiple comparisons (i.e. 63 electrodes).

7.3.2. TR-ERPCOH

Firstly, the aim was to study TR-ERPCOH changes among any pair of electrodes (210 combinations) during perturbed and unperturbed reaching. To identify significant TR-ERPCOH between electrodes, permutation-based (2000 permutations) one-sample t-tests (against 0) were performed using the statcond function in EEGLAB and p-values ($\alpha < 0.01$) were FDR corrected to adjust for multiple comparisons (210 electrode pairs). This was done for each of the four conditions (late familiarisation, early and late motor adaptation and late wash-out) separately.

Secondly, to investigate the difference between conditions, non-parametric permutation-based t-tests (2000 permutations) were used, comparing each condition (early and late motor adaptation and late wash-out) versus late

familiarisation and early versus late motor adaptation. Significance level was set to 0.0125, and all p-values were FDR adjusted to control for multiple comparisons (i.e. 210 electrode pairs).

7.3.3. Overall modulation across time and conditions

The overall oscillatory power modulation (ERSP) and the overall connectivity strength (TR-ERPCOH) was further assessed in the pre-selected ROI. Specifically, the net oscillatory power modulation was calculated by averaging the ERSP values in the electrodes of the pre-selected ROI (average of 21 electrodes). The net connectivity strength was computed by averaging the TR-ERPCOH values in the electrode pairs of the pre-selected ROI (average of 210 electrode pairs).

Effects of Condition and TIME on ERSP and TR-ERPCOH measures were assessed in the ROIs. Specifically, MANOVAs were performed with the factor of Condition (late familiarisation, early motor adaptation, late motor adaptation, late wash-out) and Time (-0.3-0, 0-0.3, 0.3-0.6, 0.6-0.9, 0.9-1.2 1.2-1.5) with the following FOIs as dependent variables: alpha, beta, low gamma and high gamma. If significant effects were found, follow-up two -way ANOVAs were then performed in each FOI separately.

7.4. ERSP results

Unless stated otherwise, all results presented in text, Figures and Tables are given in mean ± SD.

7.4.1. Results against baseline

Figure 7-1 illustrates significant modulations in oscillatory power during unperturbed reaching (late familiarisation and late wash-out) compared to baseline (0.9 - 0 s pre-visual cue) for every electrode. ERSP representations are colour coded showing significant decreases of power relative to baseline (Event-Related Desynchronisation, ERD, $p < 0.01$) in cold colours (i.e. light-blue/blue), and significant increases of power relative to the baseline (Event-Related Synchronization, ERS, $p < 0.01$) in warm colours (i.e. yellow/red). A

258

significant ERD relative to baseline is observed in alpha and beta band frequencies starting around movement onset (0.3 s post-visual cue) and sustained for the movement. During later movement (> 0.9 s post-visual cue), there is a significant ERS in high frequencies (low and high gamma) relative to baseline. Similar activation patterns are seen during perturbed reaching and are represented for early and late motor adaptation in Figure 7-2.

The spatiotemporal evolution of oscillatory power modulation is shown in Figures 7-3 and 7-4 in topographical maps for perturbed and unperturbed reaching respectively. Overall, there were no significant modulation in any frequency band before visual cue in unperturbed and perturbed reaching conditions at baseline (i.e. pre-visual cue). Alpha and Beta oscillatory power were the frequencies showing the most modulation, namely a strong ERD starting around movement onset which persisted until the end of the movement (0.3 -1.5 s post-visual cue). This modulation was mainly seen in bilateral sensorimotor regions
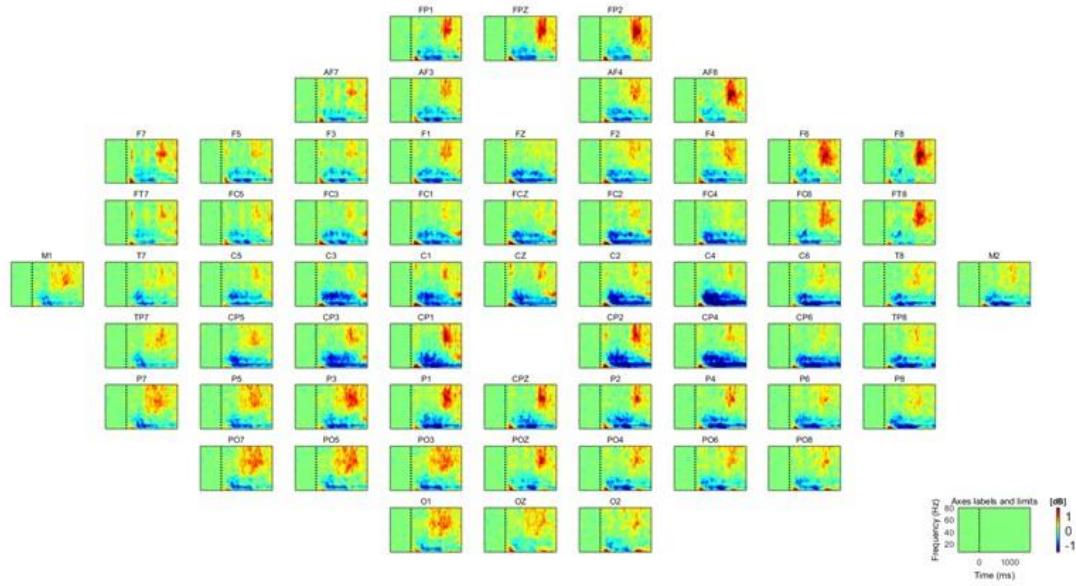
A)
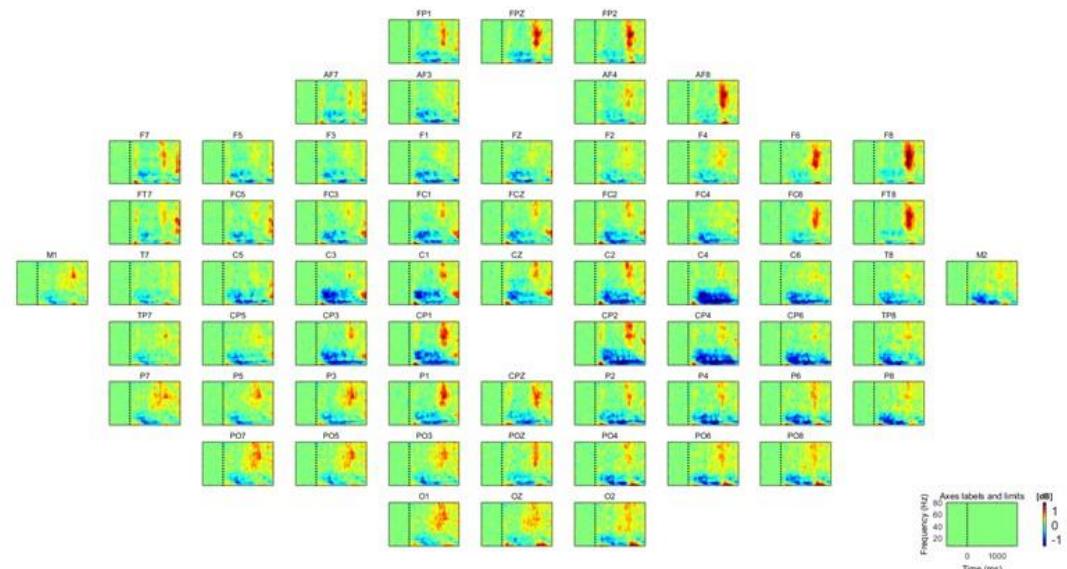
B)

Figure 7-1: ERSP during unperturbed reaching. 63 channel time-frequency spectral power during late familiarisation **(A)** and during late wash-out **(B)** are represented. X-axes represent time from 720 ms pre-visual cue to 1720 ms post-visual cue, Y axes represent frequencies from 6-80 Hz. Z-axes represent oscillatory power from -1.5 to 1.5 dB. The vertical dotted line represents the time of the visual cue. Modulations in the time-frequency domain were assessed using bootstrapping between baseline (from 0.9 s pre-visual cue) and task-related activation (period post-visual cue). Significant modulations of power with respect to baseline are colour-coded, with warmer colours (yellow/red) representing power increases (ERS) and colder colours (light-blue/ blue) representing power decreases (ERD) with respect to baseline. Green colours indicate non-significant modulations.

260
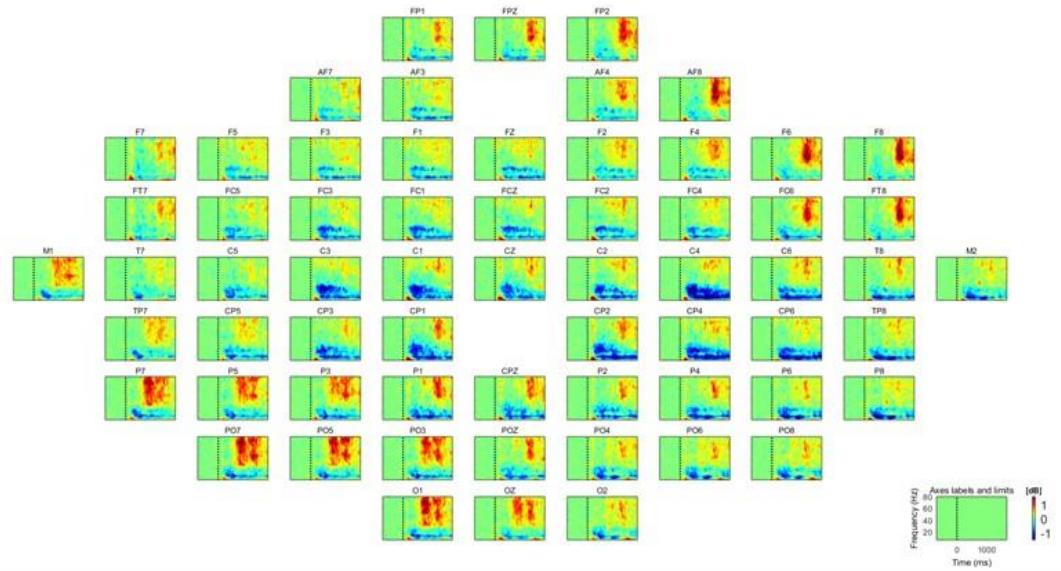
A)
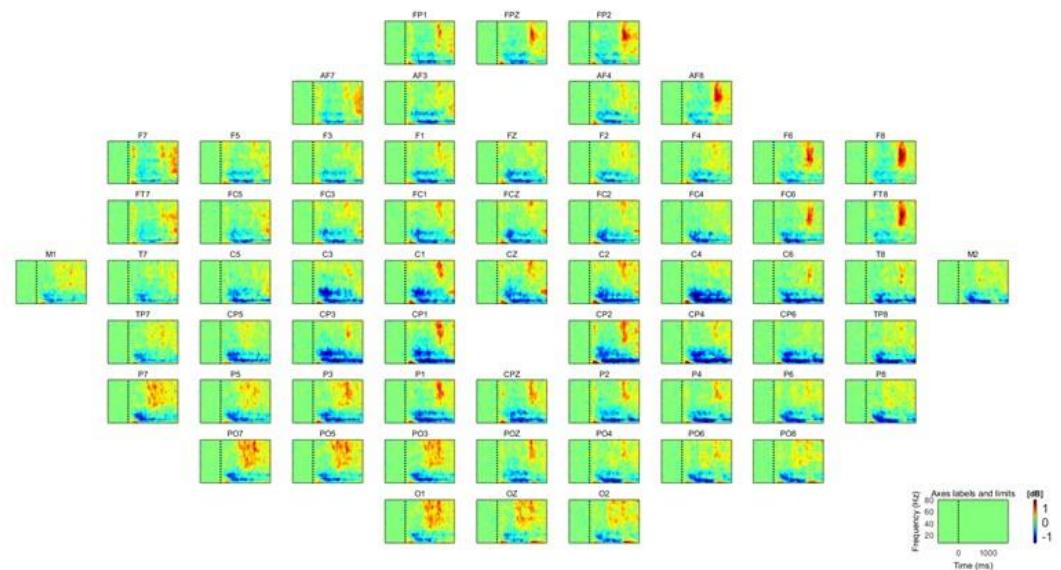
B)

Figure 7-2: ERSP during perturbed reaching. 63 channel time-frequency spectral power during early **(A)** and during late motor adaptation **(B)** are represented. X-axes represent time from 720 s pre-visual cue to 1720 ms post-visual cue, Y axes represent frequencies from 6-80 Hz. Z-axes represent oscillatory power from -1.5 to 1.5 dB. The vertical dotted line represents the time of the visual cue. Modulations in the time-frequency domain were assessed using bootstrapping between baseline (from 0.9 s pre-visual cue) and task-related activation (period post-visual cue). Significant modulations of power with respect to baseline are colour-coded, with warmer colours (yellow/red) representing power increases (ERS) and colder colours (light-blue/ blue) representing power decreases (ERD) with respect to baseline. Green colours indicate non-significant modulations.
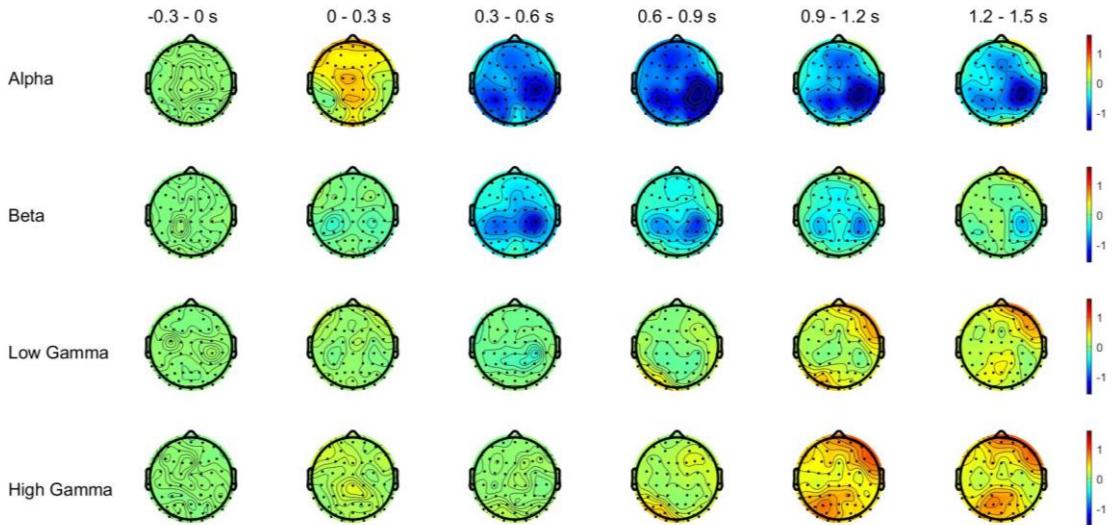
A)
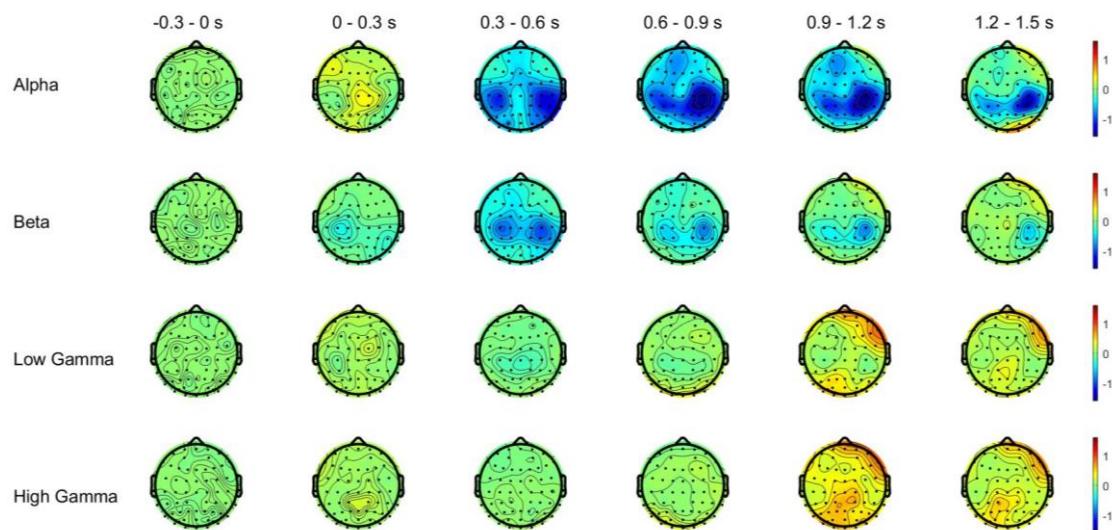
B)

Figure 7-3: ERSPs during unperturbed reaching in each FOI. ERSPs during late familiarisation **(A)** and late wash-out **(B)** condition divided into windows of 300 ms each starting from 0.3 s pre-visual to 1.5 s post-visual cue. Significant modulations of power with respect to baseline are colour-coded, with warmer colours (yellow/red) representing power increases (ERS) and colder colours (light-blue/ blue) representing power decreases (ERD) with respect to baseline in dB. Green colours indicate non-significant modulations. There were no significant modulations in any frequency band before visual cue. Alpha and Beta oscillatory power were the frequencies showing the most modulation, namely a strong ERD starting around movement onset and persisted until the end of the movement (0.3 - 1.5 s post-visual cue). This modulation was mainly seen in bilateral sensorimotor regions.

A)

B)

Figure 7-4: ERSPs during perturbed reaching in each FOI. ERSPs during early **(A)** and late **(B)** motor adaptation condition divided into windows of 300 ms each starting from 0.3 s pre-visual to 1.5s post-visual cue. Significant modulations of power with respect to baseline are colour-coded, with warmer colours (yellow/red) representing power increases (ERS) and colder colours (light-blue/ blue) representing power decreases (ERD) with respect to baseline in dB. Green colours indicate non-significant modulations. There were no significant modulations in any frequency band before visual cue. Alpha and Beta oscillatory power were the frequencies showing the most modulation, namely a strong ERD starting around movement onset and persisted until the end of the movement (0.3 - 1.5 s post-visual cue). This modulation was mainly seen in bilateral sensorimotor regions.

7.4.2. ERSP changes during motor adaptation compared to unperturbed reaching

Figure 7-5 to 7-7 show the statistical results in each FOI and TOI using permutation-based t-test comparisons between each condition (EMA, LMA and LWO) and LFAM and Figure 7-8 shows the comparison between LMA in and LFAM. Significant electrodes were highlighted with crosses (all p-values were FDR corrected). Exact statistics for each electrode (t-values) are represented in topographic plots.

7.4.2.1. Comparing each condition with late familiarisation

There was no significant difference in any TOI in any electrode in the alpha and gamma frequency band between late familiarisation and all other conditions. However, there was a significantly increased ERS in the gamma frequency band from late familiarisation to early motor adaptation (Figure 7-5):

- Increased low-gamma ERS during post-movement (1.2 - 1.5 s post-visual cue) in contralateral posterior brain regions (Oz, O1, PO7).
- Increased high-gamma ERS late movement (0.6 - 0.9 s) in bilateral motor regions (C4, C6, C3) and posterior contralateral brain regions (Oz, O1, PO7) and during post-movement (1.2 - 1.5 s) in ipsilateral motor regions (C4, FC4).

These significant effects were not seen in later stages of motor adaptation as shown in the t-statistic maps comparing late motor adaptation and late familiarisation (Figure 7-6). There were also no significant differences between late familiarisation and late wash-out (Figure 7-7).

7.4.2.2. Comparing late motor adaptation with early motor adaptation

To further investigate differences between early and late phases of motor adaptation the spectral power activation in both conditions was compared (Figure 7-8). Significant differences between late and early motor adaptation

in the gamma frequency band were found. Specifically, a decrease in ERS from late to early motor adaptation:

- In low-gamma during post-movement (1.2 - 1.5 s) in posterior brain regions (Oz, O1, PO7, P7)
- In high gamma during late movement (0.6 - 0.9 s) in widespread cortical regions including bilateral frontal, contralateral motor and ipsilateral posterior brain regions.
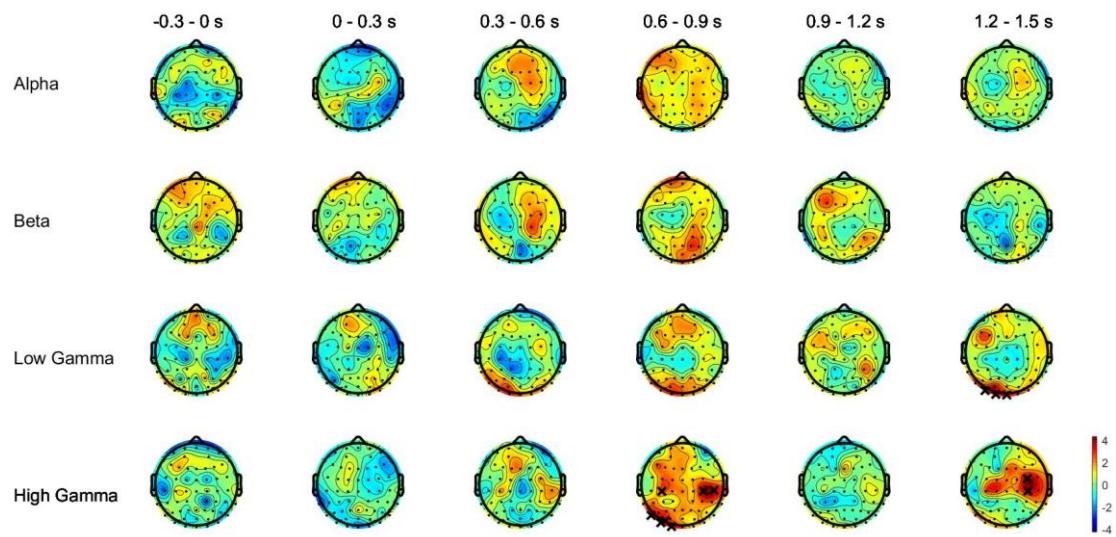
Figure 7-5: Topographical analysis (EMA vs LFAM). T-statistic maps of the ERSP of early motor adaptation versus late familiarisation differences divided into windows of 300 ms each starting from 0.3 s pre-visual cue to 1.5 s post-visual cue. Colour-codes are proportional to the t-values. Positive t-values (warmer colours) indicate an increase in ERS or a decrease in ERD from late familiarisation to early motor adaptation, whereas negative t-values (colder colours) represent an increase in ERD or a decrease in ERS from late familiarisation to early motor adaptation. Crosses indicate significant electrodes using non-parametric permutation statistics (all FDR corrected p-values < 0.01).
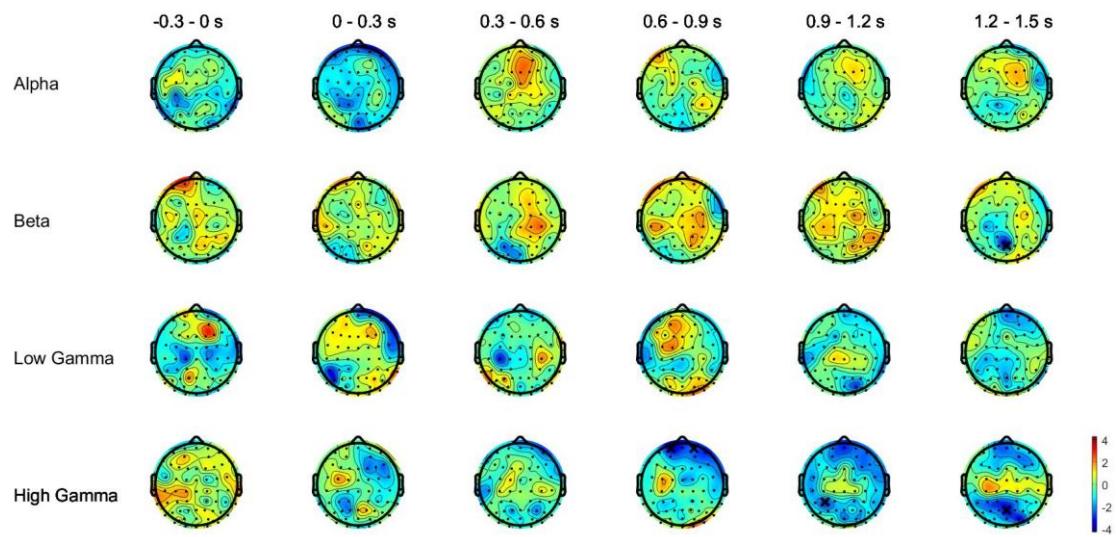
Figure 7-6: Topographical analysis (LMA vs LFAM). T-statistic maps of the ERSP of late motor adaptation versus late familiarisation differences divided into windows of 300 ms each starting from 0.3 s pre-visual cue to 1.5 s post-visual cue. Colour-codes are proportional to the t-values. Positive t-values (warmer colours) indicate an increase in ERS or a decrease in ERD from late familiarisation to late motor adaptation, whereas negative t-values (colder colours) represent an increase in ERD or a decrease in ERS from late familiarisation to late motor adaptation. Crosses indicate significant electrodes using non-parametric permutation statistics (all FDR corrected p-values <0.01).
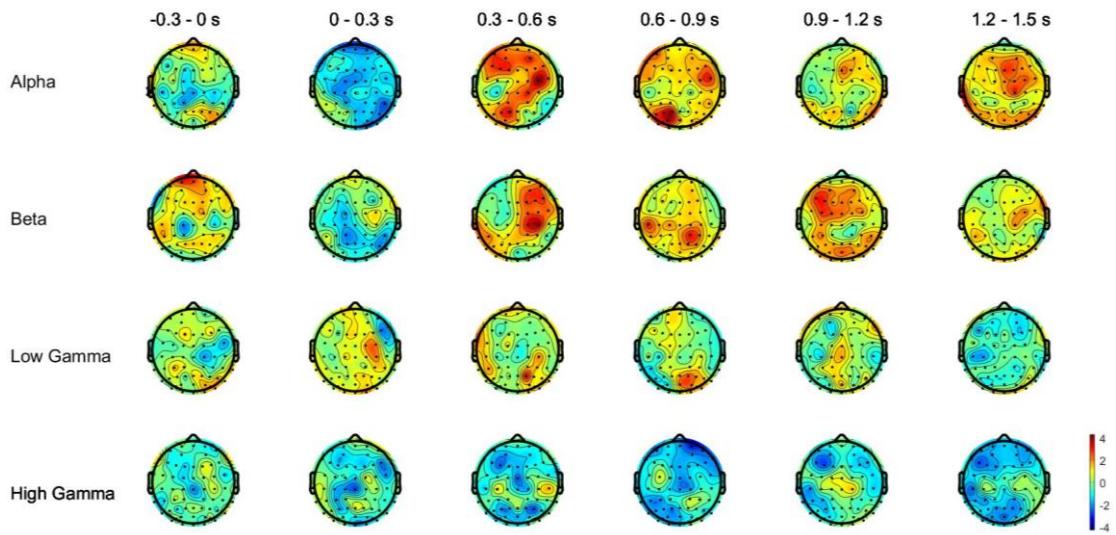
Figure 7-7: Topographical analysis (LWO vs LFAM). T-statistic maps of the ERSP of late wash-out versus late familiarisation differences divided into windows of 300 ms each starting from 0.3 s pre-visual cue to 1.5 s post-visual cue. Colour-codes are proportional to the t-values. Positive t-values (warmer colours) indicate an increase in ERS or a decrease in ERD from late familiarisation to late wash-out, whereas negative t-values (colder colours) represent an increase in ERD or a decrease in ERS from late familiarisation to late wash-out. Crosses indicate significant electrodes using non-parametric permutation statistics (all FDR corrected p-values < 0.01).
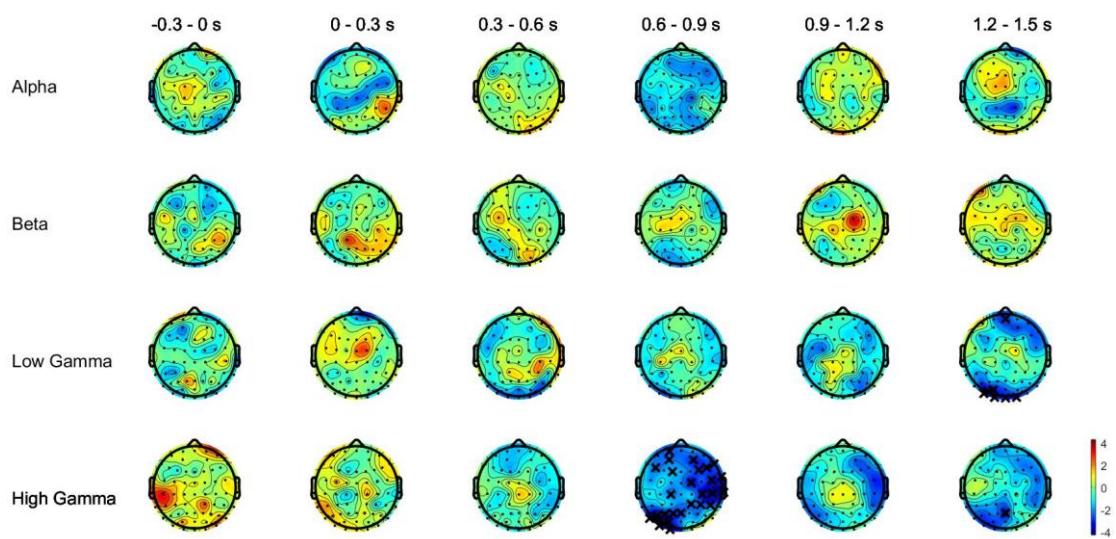
Figure 7-8: Topographical analysis (LMA vs EMA). T -statistic maps of the ERSP of late motor adaptation versus early motor adaptation differences divided into windows of 300 ms each starting from 0.3 s pre-visual cue to 1.5 s post-visual cue. Colour-codes are proportional to the t-values. Positive t-values (warmer colours) indicate an increase in ERS or a decrease in ERD from late to early motor adaptation, whereas negative t-values (colder colours) represent an increase in ERD or a decrease in ERS from late motor adaptation to early motor adaptation. Crosses indicate significant electrodes using non-parametric permutation statistics (all FDR corrected p-values < 0.01).

7.4.3. Overall ERSP modulation in ROI across time and conditions

The MANOVA revealed that there was no significant effect of Condition (Pillai's trace = 0.346, $F_{(12, 123)}$ = 1.337, p = 0.206, $\eta2$ = 0.115), but a significant effect of Time (Pillai's trace = 1.538, $F_{(20, 280)}$ = 8.741, p < 0.0001, $\eta2$ = 0.384) and a significant interaction between Condition and Time (Pillai's trace = 0.353, $F_{(60, 840)}$ = 1.354, p = 0.42, $\eta2$ = 0.088).

Post-hoc repeated-measure ANOVA showed a significant effect of Time in alpha ($F_{(1.527, 21.378)}$ = 25.262, p < 0.0001, $\eta2$ = 0.643), beta ($F_{(2.613, 36.585)}$ = 17.923, p < 0.0001, $\eta2$ =0.561) low gamma ($F_{(2.633, 36.868)}$ = 10.174, p < 0.0001, $\eta2$ =0.421) and high gamma ($F_{(2.063, 28.882)}$ = 11.413, p < 0.0001, $\eta2$ = 0.449). Post-hoc significant differences across time are shown in Figure 7-9. Detailed statistical results are reported in Table 7-1 and plotted in Figure 7-9.
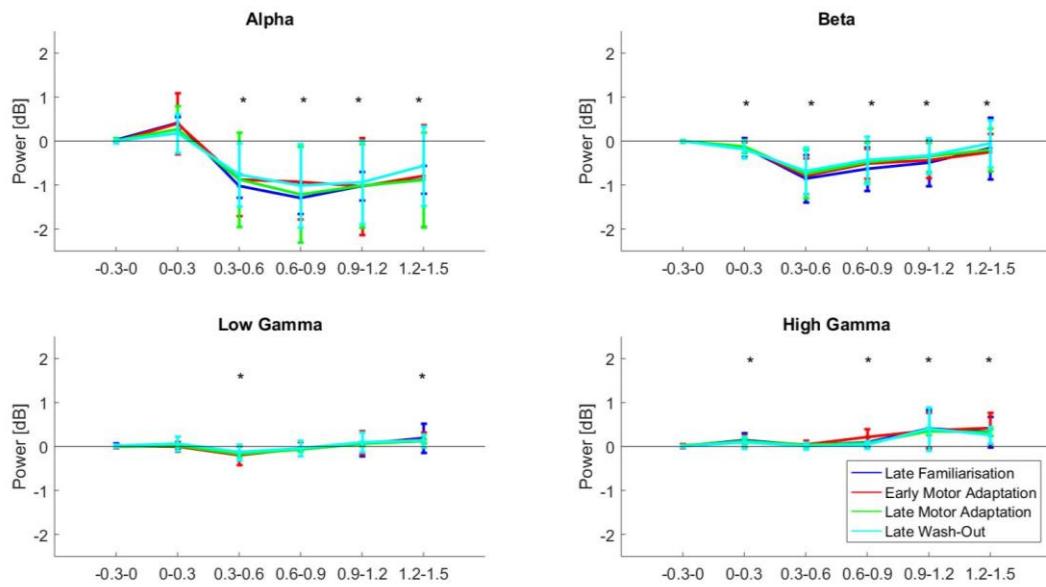
Figure 7-9: Overall oscillatory power modulation. Group-level averages (N = 15, bars represent ±1 SD) in the ROI during different phases of movement in late familiarisation, early, late motor adaptation and late wash-out. Repeated-Measure ANOVA showed a significant effect of Time in each FOI. *p < 0.05 (post-hoc contrasts comparing -0.3 - 0 versus all other time windows of interest). A significant effect of condition was only seen in the high Gamma, with post-hoc contrasts revealing a significant increase of ERS during movement (0.6 - 0.9 s post-visual cue) in early motor adaptation compared to late familiarisation and is highlighted with a red cross + p < 0.05.

Table 7-1: Post-hoc ANOVA results for ERSP modulations in the ROI in each frequency band. Repeated-Measure ANOVA with factor Condition (4 levels: late familiarisation, early motor adaptation, late motor adaptation and late wash-out) and factor Time (6 levels: -0-0.3, 0.3-0.6, 0.6-0.9, 0.9-1.2, 1.2-1.5) was performed.

	Condition				Time				Condition*Time			
FOI	F	df, Error	Sig.	η^2	F	df, Error	Sig.	η^2	F	df, Error	Sig.	η^2
Alpha	0.499	2.613, 36.581	0.66	0.034	25.262	1.527, 21.378	<0.0001	0.643	1.527	4.872, 68.206	0.194	0.098
Beta	1.354	2.628, 36.796	0.272	0.088	17.923	2.613, 36.585	<0.0001	0.561	1.36	4.92, 68.875	0.251	0.089
Low Gamma	0.573	2.764, 38.69	0.623	0.039	10.174	2.633, 36.868	<0.0001	0.421	0.777	6.054.59.658	0.591	0.053
High Gamma	2.243	2.398, 33.576	0.113	0.138	11.413	2.063, 28.882	<0.0001	0.449	1.92	4.261, 84.762	0.115	0.121

7.5. TR-ERPCOH results

7.5.1 Results against baseline

Figure 7-10 illustrates significant modulations in interregional connectivity during unperturbed reaching. Connectivity strength are colour coded so that statistically significant decreases of power relative to the 0 activity are coloured in red and increases in blue.

Interregional connectivity is mostly modulated during movement execution showing decreased connectivity in the alpha and beta band 0.6 - 0.9 s post-visual cue during late familiarisation. During late wash-out, however a widespread increase in connectivity between fronto-parieto-occipital regions is seen post-movement (1.2 – 1.5 s) in the alpha band and an increase in connectivity during movement (0.3 – 1.2 s) is seen in low gamma. For detailed significant connectivity modulations refer to Figure 7-10.

Figure 7-11 illustrates significant modulations in interregional connectivity during perturbed reaching. Interregional connectivity is mostly modulated during mid-movement execution (0.6 – 0.9 s post-visual cue) showing increased connectivity in the low gamma band during both early and late motor adaptation and during mid and late movement execution (0.6 – 1.2 s) in the high gamma band during early and late motor adaptation. In alpha and beta frequency-ranges, connectivity modulations were generally much less prominent during different reaching phases in motor adaptation. For detailed significant connectivity modulations refer to Figure 7-11.
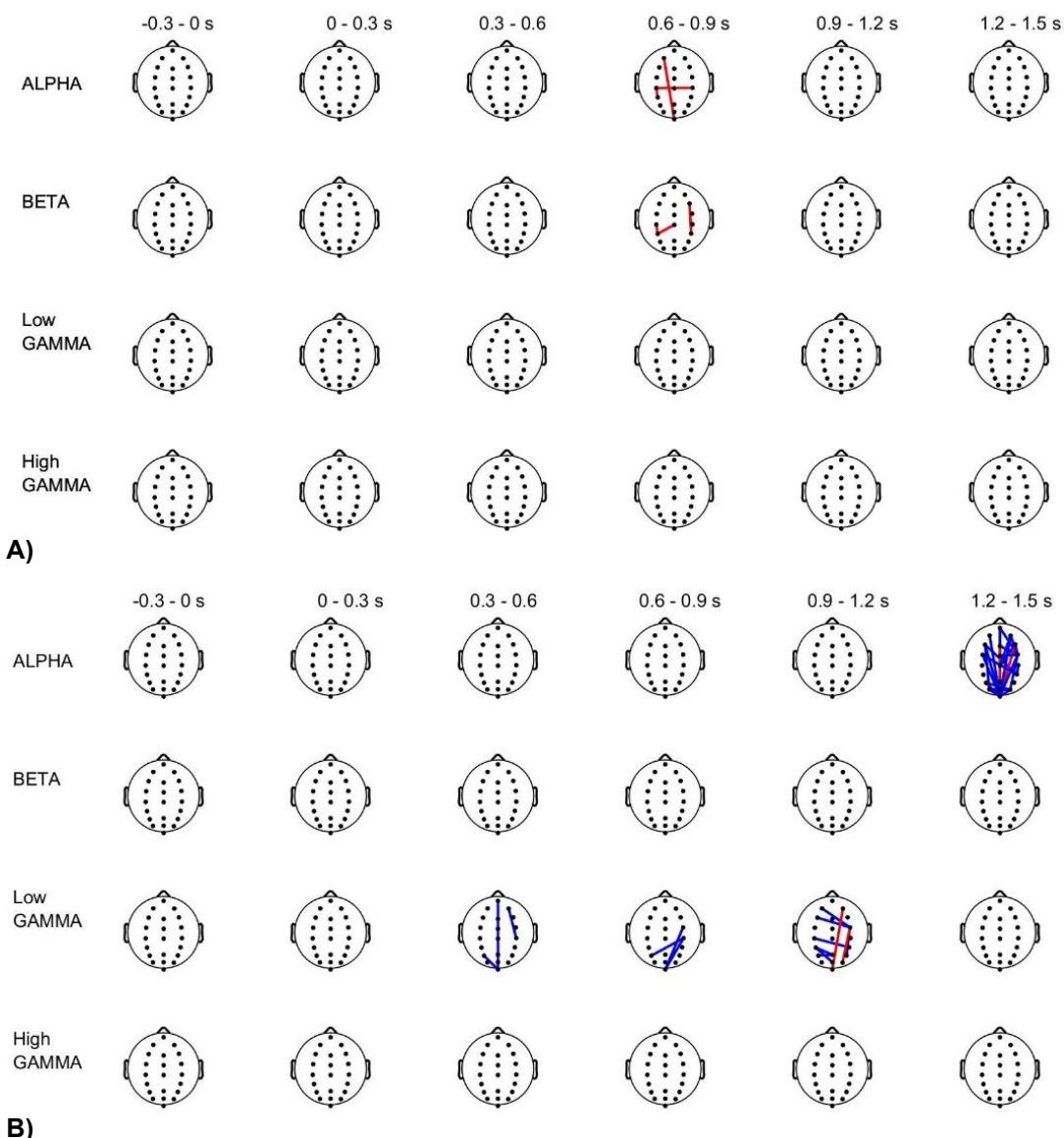
Figure 7-10: Connectivity maps during unperturbed reaching in the late familiarisation (A) and late wash-out (B) condition. TR-ERPCOH connectivity maps divided into windows of 300 ms each starting from 0.3 s pre-visual cue to 1.5 s post-visual cue. The blue lines represent TR-ERPCOH between electrodes that are significantly increased, while the red lines represent TR-ERPCOH between electrodes (all FDR corrected p-values <0.01).
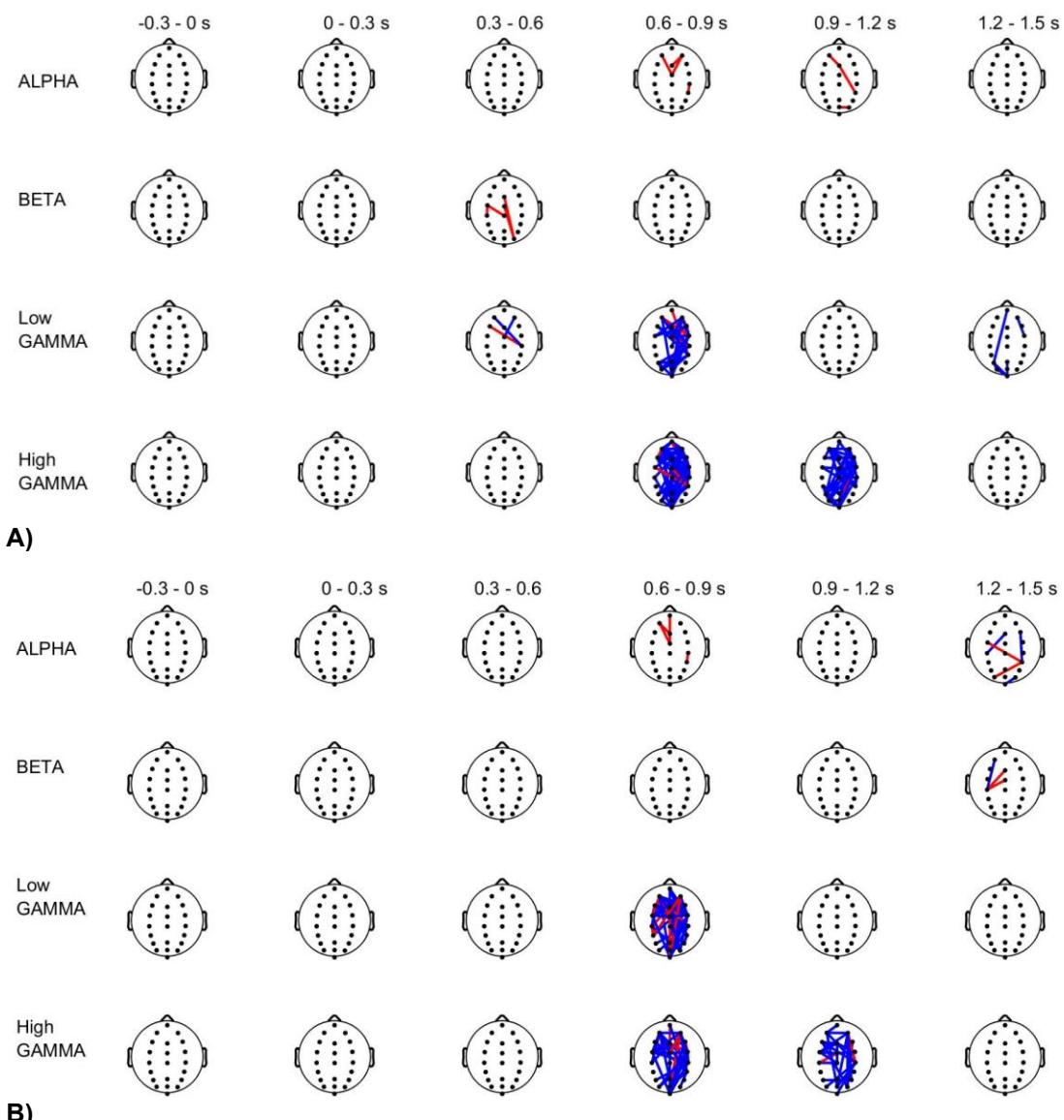
Figure 7-11: Connectivity maps during perturbed reaching in the early motor adaptation (A) and late motor adaptation (B) condition. TR-ERPCOH connectivity maps divided into windows of 300 ms each starting from 0.3 s pre-visual cue to 1.5 s post-visual cue. The blue lines represent TR-ERPCOH between electrodes that are significantly increased, while the red lines represent TR-ERPCOH between electrodes (all FDR corrected p-values <0.01).

7.5.2. TR-ERPCOH changes during motor adaptation compared to unperturbed reaching

No significant differences in interregional connectivity were detected between each condition (early, late motor adaptation, late wash-out) and late familiarisation in any TOI or FOI. However, during late reaching (0.9 - 1.2 s post-visual cue) connectivity was slightly higher in early compared late motor adaptation (Figure 7-12).
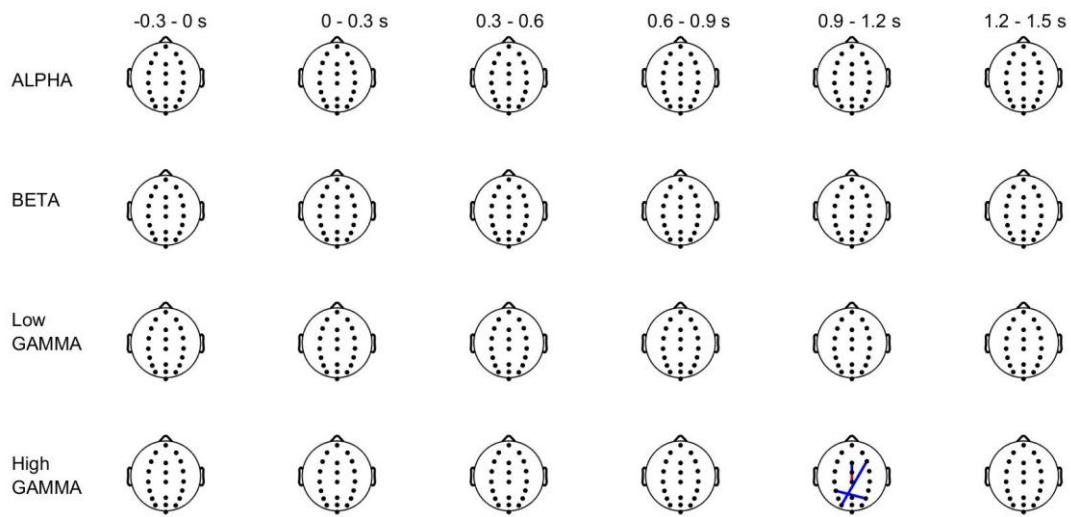
Figure 7-12: Connectivity analysis (LMA vs EMA). T -statistic maps of TR-ERPCOH of late motor adaptation versus early motor adaptation differences maps divided into windows of 300 ms each starting from 0.3 s pre-visual cue to 1.5 s post-visual cue. The blue lines represent higher coherence between electrodes in early motor adaptation compared to late motor adaptation and red colours a lower coherence between electrodes in early motor adaptation compared to late motor adaptation (all FDR corrected p-values < 0.01).

7.5.3 Overall TR-ERPCOH modulation in ROI across time and conditions

The MANOVA revealed no significant effect of Condition (Pillai's trace = 0.349, $F(12, 123) = 1.35$, p= 0.200, $\eta2$ =0.116) but a significant effect of Time (Pillai's trace = 0.798, $F(20, 280) = 3.486$, $p < 0.0001$, $\eta2 = 0.199$) and no significant interaction between Condition and Time (Pillai's trace = 0.252, $F(60, 840) = 0.942$, $p = 0.601$, $\eta2 = 0.063$).

Post-hoc repeated-measure ANOVA showed a significant effect of Time in alpha ($F(3.032, 42.45) = 3.782$, $p = 0.017$, $\eta2 = 0.231$) beta ($F(3.358, 47.01) = 4.572$, $p = 0.005$, $\eta2 = 0.246$), high gamma ($F(3.368, 47.15) = 7.767$, $p < 0.0001$, $\eta2 = 0.357$), but not in low gamma ($F(2.551, 35.72) = 1.729$, $p = 0.185$, $\eta2 = 0.11$). Post-hoc significant differences across time are shown in Figure 7-13. No significant effect of Condition was seen in any FOI. Detailed statistical results are reported in Table 7-2 and plotted in Figure 7-13.
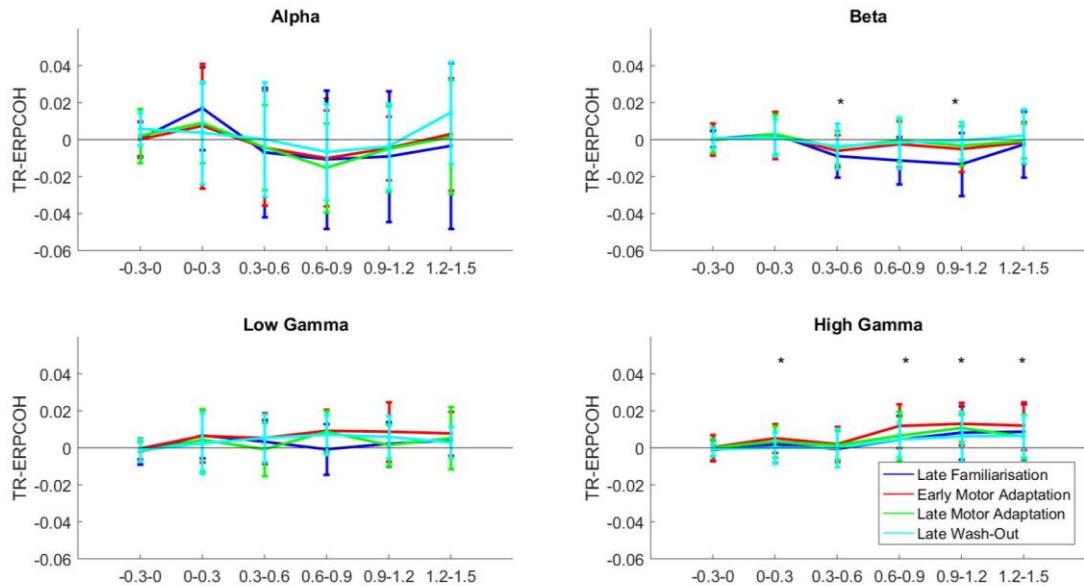
Figure 7-13: Overall connectivity strength. Group-level averages (N = 15, bars represent ±1 SD) in the ROI during different phases of movement in late familiarisation, early, late motor adaptation and late wash-out. Repeated-Measure ANOVA showed a significant effect of time in each FOI. *p < 0.05 (post-hoc contrasts comparing - 0.3 - 0 versus all other time windows of interest). No significant main effect of condition was reported in any FOI.

Table 7-2: Post-hoc ANOVA results for TR-ERPCOH in the ROI in each frequency band. Repeated-Measure ANOVA with factor Condition (4 levels: late familiarisation, early motor adaptation, late motor adaptation and late wash-out) and factor Time (6 levels: -0.3, 0.3-0.6, 0.6-0.9, 0.9-1.2 1.2-1.5) was performed.

	Condition				Time				Condition*Time			
	F	df, Error	p	η2	F	df, Error	p	η2	F	df, Error	p	η2
Alpha	0.359	2.57,35.95	0.752	0.025	3.782	3.032, 42,45	0.017	0.213	1.157	6.68, 93.54	0.335	0.076
Beta	1.848	2.56,35.88	0.163	0.117	4.572	3.358, 47.01	0.005	0.246	1.252	6.52, 91.24	0.285	0.082
Low Gamma	1.119	2.06, 28.83	0.342	0.074	1.729	2.551, 35.72	0.185	0.11	1.15	6.32, 88.53	0.34	0.076
High Gamma	2.006	2.37, 33.15	0.144	0.125	7.767	3.368, 47.15	<0.0001	0.357	0.541	7.26, 101,68	0.807	0.037

7.6. Discussion

This Chapter investigated the patterns of task-related oscillatory regional and interregional cortical activity during robot-mediated arm reaching using a standardised approach to study cortical aspects related to movement and motor adaptation. EEG data from **Chapter 6** (**Study III**) was analysed in the time-frequency domain to identify the temporal modulation of regional activity and interregional connectivity strength during different phases of reaching in an unperturbed and perturbed environment.

The Chapter found no significant difference between types of reaching (unperturbed and perturbed reaching) on how strongly they engaged regional and interregional brain regions as shown with shared net modulations in the time-frequency domain (i.e. ERSP and TR-ERPCOH pattern).

However as expected, the strength and connectivity between brain regions was significantly modulated during different stages of reaching, with the biggest changes observed during late movement.

Subtle differences between perturbed movement (motor adaptation condition) and unperturbed reaching were seen at the whole-scalp level in distinct regions (but not in overall activity) in the high-gamma frequency band and could suggest that increased gamma activity could play a role in motor adaptation processes.

7.6.1. ERSP: movement related ERD/ ERS modulations

The first EEG studies investigating brain modulations during movement preparations and execution mainly used ERP components (i.e. time-domain analysis) to examine cortical function (for review see Krigolson et al., 2015) Subsequent studies also focused on studying event-related power modulations related to movement preparation and execution (Formaggio et al., 2015; Storti et al., 2016; Waldert et al., 2008). These studies revealed that externally-cued voluntary reaching movements are characterized by an increase of oscillatory power in both low (< 8 Hz) and high (> 35 Hz) frequencies and by a decrease of oscillatory power at middle frequencies

(between 10 Hz and 30 Hz) with respect to a resting period (Storti et al., 2016; Waldert et al., 2008). It has further been shown that the increase and decrease of these oscillatory powers follow a particular time course during movement preparation and execution. Specifically, high-frequency oscillatory activity (gamma frequency band) increases, showing an ERS around movement onset and offset over the contralateral M1 (Ball et al., 2008) and frontal areas (Babiloni et al., 2016). These oscillations have been linked to fast information processing during movement execution. In contrast to this increased activity, oscillatory power of middle frequencies (alpha and beta frequency band) usually decreases, showing an ERD during voluntary movement and is thought to reflect ongoing sensorimotor integration processes (for review see Engel and Fries, 2010; Pfurtscheller and Andrew, 1999). After movement execution, beta-band oscillatory power usually increases and is commonly referred to as post-movement beta synchronisation or beta rebound. This phenomenon is thought to reflect neural processes related to movement accuracy such as trial-by-trial error detection and to update neural mechanisms of motor control (Tan et al., 2016; Torrecillos et al., 2014).

The present Chapter employed a laboratory-based robot-mediated arm reaching task to study related cortical changes in the time and frequency domain during unperturbed (non-adaptation condition) and perturbed reaching (motor adaptation condition). Overall, unperturbed and perturbed reaching seemed to have a similar topographical modulation of oscillatory power in low-frequency bands. Specifically, a strong increase of ERD was revealed in alpha and beta power starting around movement onset and lasting until post-movement in bilateral sensorimotor regions.

Two hypotheses for bilateral desynchronisation of ipsilateral and contralateral regions: have been proposed and could explain the reported bilateral involvement of sensorimotor regions: i) an inter-hemispheric cross-talk required to handle task of high difficulty (Derosiere et al., 2014; Formaggio et al., 2013), ii) an inhibitory mechanisms towards the opposite upper limb (van Wijk et al., 2012).

Higher frequency bands showed an opposite effect, namely a temporary increase in ERS around movement onset in sensorimotor regions. Cheyne et al. (2008) reported similar findings of increased gamma activity around movement onset in both upper and lower limb movements in the contralateral M1, and suggested that the modulation of oscillatory power is related to online feedback mechanisms. Overall the findings of this Chapter are in accordance with previous studies investigating movement-related oscillatory changes, thus confirming the validity of our experimental setup and of the analytical pipeline for the investigation of the spatiotemporal and spectral neural correlates of reaching movements.

The similar spatiotemporal activation during unperturbed and perturbed reaching could represent a shared cortical mechanism between unperturbed and perturbed reaching related to movement preparation and execution and not related to adaptation processes. This is not surprising, since it has been shown that even imaginary movements share the same functional networks activated during movement planning, preparation and execution of robot-assisted active and passive movement (Formaggio et al., 2013).

7.6.2. ERSP modulation related to motor adaptation

To identify cortical mechanisms related to motor adaptation, unperturbed (late familiarisation) and perturbed (early and late motor adaptation) reaching movements were compared. Modulations in beta power, reflective of GABA-ergic activity, have been linked to motor learning (Boonstra et al., 2007; Houweling et al., 2008; Pollok et al., 2014). This Chapter, however, failed to report significant alpha or beta ERD differences between late familiarisation and early, as well as late motor adaptation. The modulations in oscillatory power in sensorimotor regions were strikingly similar across different times of movement between perturbed and unperturbed conditions, suggesting that this modulation is reflective of a general mechanism involving visuomotor transformations necessary for movement and not specific to adaptation processes.

The Chapter reported significant differences in low and high gamma oscillatory power in early motor adaptation compared to late familiarisation during movement, indicating that gamma activity is related to neural mechanisms happening in early stages of motor adaptation during movement execution in distinct brain regions (but not in overall activity).

The Chapter shows subtle differences in ERS modulations during perturbed compared to unperturbed reaching revealing increased high gamma activity during late movement execution in bilateral motor and contralateral posterior regions during adaptation. This significant difference was only observed between early and not late motor adaptation compared to late familiarisation (unperturbed reaching), suggesting that increased gamma activity plays a role in early motor adaptation processes. Since the significant difference is only seen in early motor adaptation and not late motor adaptation, it rules out that the enhanced cortical activity is due to different motor demands during the motor adaptation (fore-field applied) and the unperturbed (no force-field applied) task. Moreover, this finding links gamma modulations to early adaptation processes and not to the physical training of repetitive arm reaching, as there are no significant differences between late familiarisation and late wash-out. This finding is in agreement with previous studies linking gamma activity with learning processes (Nowak et al., 2017; Rimsky-Robert et al., 2016; Stagg et al., 2011). A number of studies have shown that gamma activity is generated by GABA (for review see Nowak et al., 2018), glutamate and acetylcholine neurotransmitters and has been linked to different brain functions, including perception, attention, memory, consciousness, synaptic plasticity and motor control (Ahn et al., 2013; Amo et al., 2017; Corbetta and Shulman, 2002; Gonzalez Andino et al., 2005; Gruber et al., 1999; Tallon-Baudry et al., 1999). The present finding supports the idea that enhanced gamma is linked to visuospatial attention and reflective of the binding of sensory information and sensorimotor integration (Amo et al., 2017, 2016; Gruber et al., 1999).

7.6.3. TR-ERPCOH

TR-ERPCOH was employed to identify the possible cortico-cortical connectivity changes during different stages of arm reaching using a robot-mediated task. The net functional connectivity between fronto-parietal-occipital regions for each frequency band showed characteristic shared modulations across time during unperturbed and perturbed movement. Alpha and beta connectivity strength was reduced during movement, whereas high gamma connectivity strength was enhanced during movement and post-movement compared to baseline for both unperturbed and perturbed movement. The complex frequency- and time-specific changes in TR-ERPCOH suggest that modulated interregional connectivity might play an important role in different stages of arm reaching. No significant differences across conditions were found in overall connectivity strength in any frequency band, but increases in gamma connectivity strength in distinct electrode pairs in perturbed movement were observed. However, this increased gamma connectivity strength was not significantly different between perturbed and unperturbed movements. As such this study failed to find specific connectivity strength modulations associated with motor adaptation processes. This finding was unexpected since it has previously been shown that increased connectivity in the gamma band is specific to motor learning, reflecting a critical mechanism, integrating neural networks within and across brain structures during cognitive processes (Serrien and Brown, 2003). However, the present findings of increased interregional connectivity during both unperturbed and perturbed reaching seem to be related to a more general effect namely to movement and not to motor adaptation.

7.6.4. Limitations

7.6.4.1. Sample size

The failure to detect significant differences between perturbed and unperturbed reaching and thus to link specific neural mechanisms to motor adaptation processes in this Chapter could be attributed to the small sample size (N = 15). While this limited sample size is similar to previous studies who

reported no significant differences between active and passive robot-assisted reaching (Formaggio et al., 2013) or between active, passive and imagined reaching (Formaggio et al., 2015), collectively these negative findings reported cannot be taken as prove of no difference between these conditions. In fact, a post-hoc power analysis calculation using the G power software revealed that a sample size of 28 individuals was needed in the present study to detect a significant effect of Condition in cortical oscillations (ERSP or TR-ERPCOH measures) with a power of 80%. This was based on an estimated effect size derived from the present data of f = 0.36, and α significance level of p = 0.05 in a within-subjects design experiment with a total of 4 measures (4 frequency bands) and 4 conditions (late familiarisation, early motor adaptation, late motor adaptation and late wash-out).

7.6.4.2. Methodological consideration

The identified changes in spectral power and connectivity have been analysed in the sensor space corresponding to scalp locations that provide relatively low spatial resolution. Source space analysis (Muthuraman et al., 2014) could help to identify the corresponding brain regions giving rise to the reported findings and further our understanding of the underlying mechanism of motor adaptation in future studies.

It should be noted that although ICA decomposition was used to remove muscle activity from EEG data during pre-processing procedures, it cannot be ruled out that some cranial muscular artefacts are still present in the data. Since muscle activity and cortical activity are overlapping and share similar spectral properties in higher frequency bands (> 30 Hz), gamma oscillations might be contaminated with muscular artefacts (Muthukumaraswamy, 2013).

7.7. Conclusions

The goal of this Chapter was to investigate the spatiotemporal patterns of task-related oscillatory brain activity during highly standardised motor performance provided using a robotic device. It focused on the evaluation of the time course of spectral parameters during the preparation and execution of arm reaching in both an unperturbed and perturbed environment. This

Chapter reported distinct region and time-specific modulations occurring in the cortex during arm reaching. Since the results of this study are preliminary, no solid conclusions can be drawn from comparison of the two types of reaching (unperturbed and perturbed) and thus cannot be related to specific neural mechanisms of motor adaptation.

However, the modulations in cortical regional and interregional activity revealed at different phases of reaching (irrespective of the environment: perturbed or unperturbed) can provide important insights into the neural mechanisms underlying robot-mediated reaching. Since robot-mediated reaching is used in clinical research settings for stroke upper limb recovery (Turner et al., 2013), it is conceivable that extracting modulations in regional power and interregional connectivity could be used to detect abnormal neural activity patterns leading to impaired reaching in stroke patients. For instance, regional activation (measured with modulations in ERSP) and functional coupling (measured with modulations in TR-ERPCOH) features could be extracted in stroke patients to gain insights into the neural underpinnings of their reaching deficits. In the future, it is thinkable that these features could be targeted to establish a more normal pattern in stroke patients during reaching by enhancing or suppressing regional activity or functional coupling between regions.

The main finding of this study is the similar modulation of brain oscillations during highly standardised robotic perturbed and unperturbed reaching with significant increases and decreases of regional and interregional activity during different phases of reaching. The results of this study are preliminary and further investigations on larger populations are needed to establish the specific neural regional and interregional mechanism related to motor adaptation. Specifically, this study was most probably underpowered to detect significant differences between perturbed and unperturbed reaching.

Nonetheless, the time-resolved analyses of functional dynamics in regional activity and network configuration during robot-mediated reaching may represent an opportunity to examine normal patterns of activation related to unimanual reaching. In line with previous findings (Formaggio et al., 2015,

2013, Storti et al., 2016) this Chapter suggests that the neurophysiological analysis, performed using power spectra and functional connectivity during robot-mediated reaching, could be relevant for studying the mechanisms of brain plasticity and recovery following brain injury leading to upper limb (preparation and execution) impairments.

Chapter 8 – General Discussion

This thesis investigated unimanual upper limb movements focusing on three aspects that play a key role in motor control and can affect upper limb recovery, namely i) hemispheric asymmetries related to motor dominance, ii) bi-hemispheric motor cortical activity during movement preparation and iii) the ability to adapt movements to novel environments.

Specifically, this research employed two neuroimaging tools, namely EEG and TMS-EEG, in combination with a simple motor task (isometric contraction) as well as a highly standardised robot-mediated reaching task to gain further insights into the neural mechanisms underlying unimanual motor control. The three main aims of the thesis were to investigate hemispheric asymmetries related to motor dominance, to evaluate the relative contribution of the contralateral and ipsilateral M1 during unimanual reaching preparation and finally to identify the neural biomarkers underlying the formation of a predictive internal model enabling the adaptation of movements to new environments.

In sum, no motor cortical hemispheric asymmetries related to hand dominance at rest and during unimanual contraction and no motor cortical differences between the ipsilateral and contralateral M1 during unimanual reaching preparation were found. In fact, even unimanual motor control relied on bilateral hemispheric activations. As hypothesised a wide range of brain regions were engaged in unimanual movement control. The thesis reported significant bi-hemispheric modulations, showing complex interactions between excitatory and inhibitory processes during unimanual reaching preparation in both motor cortices. Finally, bilateral fronto-central activations during unimanual robot-mediated adaptation as well as plasticity changes in sensorimotor regions were identified.

The key findings will be reviewed and interpreted in the following section, before discussing their wider impact and contribution.

8.1. Key findings and hypothesis

The first aim of **Chapter 4** (**Study I**) was to replicate TMS-evoked cortical responses measured with EEG reported in the literature (for review see Farzan et al., 2016) to test whether TEPs and TMS-induced oscillations can reliably be used as readouts of cortical excitability. The study showed that applying TMS over the dominant and non-dominant M1 reliably produced well characterised patterns of activation in all individuals. The findings are consistent with previous studies in the time (TEP) (Paus et al., 2001; Petrichella et al., 2017; Premoli et al., 2014) and time-frequency (TRSP) (Fecchio et al., 2017) domain. Thus, these first results gave us confidence to use these TMS-evoked EEG responses to assess cortical excitability in the next studies.

The second aim of **Chapter 4** (**Study I**) was to identify cortical asymmetries related to motor dominance since it has been shown that motor (hand) dominance has an impact on upper limb recovery (Harris and Eng, 2006; Lüdemann-Podubecká et al. , 2015, Liew et al., 2018,). For instance, Lüdemann-Podubecká et al. (2015) demonstrated that patients with a lesion in the dominant as opposed to the non-dominant hemisphere present with poorer motor improvements of the affected upper limb. However so far, no clear neural mechanisms have been identified that can explain these differences in recovery. TMS has been used to assess differences in corticospinal excitability using MEPs as readouts but results on hemispheric asymmetries have been mixed: There are reports of no interhemispheric differences (Kazumoto et al., 2017; Saisanen et al., 2008) as well as higher levels of corticospinal excitability in the dominant (De Gennaro et al., 2004) or non-dominant hemisphere (Daligadu et al., 2013). Recent research suggests that hemispheric asymmetries are at a more cortical level and lies outside the CST (Howells et al, 2018, Westerhausen et al., 2006). Therefore, **Chapter 4 (Study I)** employed simultaneous TMS-EEG to identify possible neural correlates of motor dominance by using TMS-evoked EEG responses (TEPs and TRSPs) as well as EMG responses (MEPs and CSP durations) as readouts of cortical and corticospinal excitability respectively. Specifically, TMS-EEG was applied over the dominant and non-dominant M1 at rest and

during isometric contraction. The Chapter reported no significant difference in cortical and corticospinal excitability related to motor dominance. However, these negative results are not a prove of lack of hemispheric asymmetry and it is very likely that the sample size was too small to detect differences in excitability as measured with MEPs, CSPs and TEPs. A post-hoc power calculation revealed that a sample size of at least 34 individuals was needed to detect significant hemispheric differences. Since this study tested only 16 individuals, we strongly recommend that a future study uses a bigger sample size to expand these preliminary findings. Even though **Study I** was underpowered, it confirmed the reproducibility of TMS-evoked cortical EEG responses as a tool to assess cortical excitability in healthy individuals and thus suggested that future studies could use TEPs and TRSPs readouts to investigate cortical asymmetries related to motor dominance.

Chapter 5 (Study II) investigated the neurophysiological correlates of unimanual movement in the contralateral and ipsilateral M1 to the reaching arm. While the dominant role of the contralateral M1 in unimanual motor control is well established (for review see Lemon, 2008), the role of the ipsilateral M1 remains unclear. Studying the basic mechanisms of unimanual movement organisation can be valuable for understanding the critical role the ipsilateral M1 plays when the contralateral M1 is damaged (such as after stroke). While previous TMS studies have reported bilateral activation in motor cortices during preparation of simple unimanual tasks (Howatson et al., 2012, Kičić et al., 2008, McMillan et al., 2006), this **Chapter** explored excitability modulations in motor cortices during a more complex unimanual reaching task (Hunter et al., 2011), with an emphasis on the role of the ipsilateral M1. **Study II** used a between-subject design in which participants were divided into two groups, each receiving either stimulation to their ipsilateral or contralateral M1 during right-arm robot-mediated reaching preparation. TMS was applied at different time delays from visual cue to track excitability changes over time by measuring cortical EEG (i.e. TEPs) and

peripheral EMG (i.e. MEPs) responses. It was hypothesised that the contralateral M1 would be significantly more activated compared to the ipsilateral M1 but that both motor cortices would be engaged in the unimanual task as reflected by significant modulations in excitability during different times of movement preparation.

The **Chapter** reported no significant differences in corticospinal excitability between the task and non-task arm (i.e. indexed with MEPs) and no significant differences in cortical excitability between the ipsilateral and contralateral M1 (i.e. indexed with TEPs). However, the study found a significant bi-hemispheric modulation in cortical excitability (i.e. significant changes in TEP amplitudes over time) during different phases of reaching preparation. In line with previous findings reported in the contralateral M1 (Zaaroor et al., 2003), the time course of bi-hemispheric M1 excitability did not linearly increase closer to movement onset but reflected a complex interaction between inhibitory and excitatory mechanisms. The findings of **Study II** suggest that the ipsilateral M1 is also actively engaged during unimanual reaching and thus could represent an important substrate for unimanual reaching. For instance, the activity of the ipsilateral M1 could be exploited in the context of neurorehabilitation as has been shown by Ganguly et al. (2009) who used neural signals to control an external prosthesis.

This **Chapter** reported a bi-hemispheric modulation and engagement of motor cortices during unimanual reaching preparation but can only speculate on how the ipsilateral M1 contributes to unimanual movements. One hypothesis is that it could directly contribute to ipsilateral movements via the ipsilateral CST, the other that it facilitates ipsilateral movement at a higher-order processing level, such as movement selection and preparation (Gerloff et al., 2006). However, since we studied cortical excitability modulations prior to movement onset, our findings favour the latter theory.

In stroke, the imbalance of activity between the contralestional (i.e. ipsilateral) and ipsilesional (i.e. contralateral) M1 during unilateral movements can be detrimental and affect motor recovery (for review see Alawieh et al., 2017).

Specifically, it is unclear how imbalances between ipsi- and contralesional activity in M1 contribute to abnormal motor behaviour.

This imbalance of activity between hemispheres was investigated but this **Chapter** failed to report significant differences between the ipsilateral and contralateral M1 during unilateral movement preparation most probably due to an undersized sample (N = 28). Based on a power analysis derived from our results, we recommend that a future study ought to use a sample size of at least 40 participants to detect significant effects between hemispheres, using TEPs as readouts for cortical excitability. This would provide further insights into the role hemispheric imbalances between the motor cortices play in upper limb recovery such as after stroke (for review see Mcdonnell and Stinear, 2017)

Another important point to address is the impact motor dominance (studied in the previous **Chapter**) and how it could affect bi-hemispheric activity during unimanual movement preparation in M1. **Study II** recruited right-handed participants to perform a reaching task with their dominant (i.e. right hand). It could be possible that the observed bi-hemispheric activity would be different if participants performed the task with their non-dominant hand. In fact, Ziemann and Hallett (2001) demonstrated hemispheric asymmetries in the ipsilateral M1 activity during unilateral finger sequence movement tasks. Specifically, they found that there was a significant increase in corticospinal activity in the ipsilateral M1 when the non-dominant (left) hand was used and that it was less increased when the dominant (right) hand was used in the unimanual task. This asymmetry in activity of the ipsilateral M1 related to motor dominance could imply a stronger involvement of the dominant M1 in ipsilateral hand movements. This could be explained in several ways: a more prominent ipsilateral activation of the dominant M1, or a stronger interhemispheric inhibition of the non-dominant M1, or both. It could be argued that the asymmetry of ipsilateral motor cortex activation constitutes a property of motor dominance. In light of this finding, a future study should investigate whether similar hemispheric asymmetries in cortical excitability between the ipsilateral and contralateral M1 are observed using the reaching task used in

Study II, by comparing bi-hemispheric activations during unimanual movements performed with the dominant as well as the non-dominant hand. Since Ziemann and Hallett (2001) also demonstrated that hemispheric asymmetries depend on task complexity it could be possible that **Study I** (**Chapter 4**) failed to report significant differences between M1 excitability related to motor dominance due to the fact that a simple motor task (i.e. isometric contraction) rather than a more complex task such as robot-mediated reaching **(Study II)** was used.

Chapter 6 (Study III) investigated the neural correlates and predictors of motor adaptation (i.e. error-based learning) by employing a robot-mediated adaptation task. A large number of EEG studies have demonstrated that the brain's reactions to errors can be manifested in negative ERP deflections (referred to as ERN) (for review see Gehring et al., 2018). This negative deflection around movement onset (i.e. ERN) is also enhanced during motor adaptation compared to natural reaching (Pizzamiglio, 2017). **Study III** used EEG and TMS-EEG in combination with a robot-mediated adaptation task to further identify the neural correlates and neurophysiological mechanisms underlying motor adaptation. Participants were required to make right-arm reaching movements in an unperturbed (non-adaptation condition) and a perturbed (adaptation condition) while EEG was continuously recorded. TMS was applied to M1 pre- and post-motor adaptation to measure cortical excitability (i.e. indexed with the TEP N100 amplitude) and excitability changes (i.e. indexed with modulations in TEP N100 amplitude from pre- to post-motor adaptation).

It was expected that participants will adapt to the novel environment reflected in a reduction in trajectory errors during motor adaptation (Hunter et al., 2009) through the formation of an internal model of the perturbed environment. The hypothesis was that the formation of an internal model during motor adaptation would be reflected in enhanced neural activity in regions involved

with error processing (i.e. ERN) and that it will underly neuroplastic changes (modulations in excitability, reflected by modulations in the TEP N100 amplitude).

First, **Study III** confirmed and expanded Pizzamiglio's (2017) findings by linking the ERN activity to behavioural performance. As expected, all participants successfully adapted to the external perturbation (i.e. force-field) and produced over-shooting errors once the force-filed was removed, reflecting the formation of an internal model (Kawato and Wolpert, 1998). It was found that an increased ERN activity over fronto-central regions during motor adaptation correlated with better motor learning (i.e. motor performance improvement). This finding lends support to the notion that the ERN reflects the formation of a predictive internal model to the new environment enabling accurate movements. Given that the ERN activity started before movement onset, the data provides evidence that the ERN activity does not reflect feedback related processing since feedback is only available at later stages of movement, but rather that it is part of a prediction error system between the required and actually performed motor plan. Thus the generation of an ERN is likely to rely on an internal model that represents knowledge about mappings between actions and their consequences.

Since an increased amplitude of the ERN was associated with better motor learning during motor adaptation, it could represent an electrophysiological biomarker of efficient motor learning and thus be explored in clinical populations experiencing motor learning deficits. This theory is supported and appears to have validity in other motor learning tasks such as a finger sequence learning task. Specifically, Beaulieu et al. (2014) demonstrated that an increased ERN amplitude was significantly associated with sequence-specific reaction time improvements.

The **Chapter** proposes that the ERN amplitude could be collected in a test-retest manner to monitor changes in neural activity and link them to behavioural performance improvements over different sessions in order to assess its applicability in clinical settings. For instance, in stroke the ERN activity has been shown to be reduced during robot-mediated adaptation, thus

testing ERN changes over multiple sessions could help to gain deeper understandings into mechanisms involved in motor learning to regain normal motor behaviours.

Another important aspect of motor adaptation addressed in this **Chapter** is neuroplasticity (i.e. changes in cortical excitability). This was done in two ways: First, the **Chapter** investigated the underlying neuroplastic changes of motor adaptation measured in terms of cortical excitability changes and second to identify cortical resting state mechanisms that drive motor adaptation and can explain the variability of motor performance during motor learning across participants. The TEP N100, an inhibitory biomarker was taken as readout of cortical excitability and its change in amplitude from pre- to post-motor adaptation as marker of cortical excitability modulation (i.e. neuroplasticity).

Chapter 6 reported that the TEP N100 amplitude was significantly decreased in bilateral sensorimotor regions post- compared to pre-motor adaptation, suggesting that motor adaptation underlies neuroplastic changes, namely decreases in cortical inhibition (i.e. increases in cortical excitability). Since the N100 amplitude is thought to represent $GABA_B$-receptor activity (Premoli et al., 2014), the underlying neuronal mechanisms of sensorimotor excitability changes, as measured with the N100 amplitude are most likely reflecting modulations of $GABA_B$-mediated inhibitory pathways.

The identified neuroplastic changes in sensorimotor regions are in line with previous studies using neuroimaging tools other than EEG such as PET (Krebs et al., 1998), and fMRI (Vahdat et al., 2014, 2011). However, as highlighted by these studies, neuroplastic changes after motor learning are also observed in subcortical regions including the cerebellum. Since, EEG cannot capture subcortical activity, the observed neuroplastic changes over sensorimotor cortical regions in **Study III** might reflect an incomplete picture of neuroplasticity and these changes could also at least in part be secondary to subcortical modulations. In fact, no clear link between the neuroplastic changes over sensorimotor regions and performance improvements have

been established in this study, lending support to the idea that EEG only partly captured neuromodulations underlying motor learning.

A great amount of research has focussed on linking motor learning with changes in cortical excitability from pre- to post-training, however Lissek et al. (2003) suggested that initial native levels of cortical excitability should also be taken into account and could serve as a better index of motor learning. Therefore, **Chapter 6** did not only focus on changes in cortical excitability but also investigated whether intrinsic variability in cortical excitability measured at rest pre-motor adaptation is associated with motor performance improvements in the subsequent motor adaptation task. It was found that a larger TEP N100 amplitude measured at rest was correlated and predictive of subsequent motor learning improvements, suggesting that greater cortical inhibitory activity is related with better motor learning. This finding is consistent with the rule of homeostatic metaplasticity (for review see Ziemann and Siebner, 2008). According to this theory, a decreased excitability (i.e. neuronal activity) prior to learning could promote LTP-like mechanisms (driving neuroplasticity) to take place during motor adaptation and thus lead to better motor performance. **Chapter 6** proposes that the TEP N100 amplitude could serve as a biomarker to harness differences in native cortical excitability to best utilise the brain's capacity to learn. For instance, if healthy individuals or patients present with high levels of cortical excitability at rest, an excitability-decreasing manipulation prior to the motor adaptation task could be used to enhance motor learning (i.e. LTP-like mechanisms) and thereby be exploited to boost motor learning in healthy individuals and in the future maybe in the clinical population presenting with motor learning deficits. This has proven to be an effective strategy in healthy individuals: Jung et al. (2009) demonstrated that applying an inhibitory brain stimulation prior to a simple rapid thumb movement learning task facilitated motor learning. A future study could test this strategy using a more complex task such as the one used in **Study III**, since it is also used in clinical settings for upper limb recovery (for review see Bastian, 2008) and thus provide a strategy to boost motor learning in neurorehabilitation.

Chapter 7 represents a secondary exploratory approach using data acquired during robot-mediated reaching from **Study III** (**Chapter 6)** to investigate the spatiotemporal patterns of task-related oscillatory cortical activity focussing on the evaluation of the time course of spectral EEG features during unperturbed (non-adaptation condition) and perturbed reaching (adaptation condition). Previous studies investigating active, passive (Formaggio et al., 2013) as well as imaginary movements (Formaggio et al., 2015) during a highly standardised robot-assisted reaching task demonstrated that evaluating EEG data in the time-frequency domain represents a quantitative approach offering new opportunities for the neurological assessment of motor performance and are a powerful tool to understand the planning and execution of movement. This Chapter used a similar approach to extract spectral features from EEG data from **Study III** in a time-resolved manner to gain insights into modulations of regional strength (i.e. changes in ERSP) and interregional connectivity (i.e. changes in TR-ERPCOH) related to robot-mediated motor adaptation. Contrary to the hypothesis, no significant differences in overall strength in regional power or interregional connectivity were detected between perturbed and unperturbed reaching. As such, spectral power modulation reflected processes related to reaching and were not specific to adaptation processes. Only subtle differences in spectral power were detected during late phases of reaching between perturbed and unperturbed reaching, showing a significant increased gamma power (ERS) in bilateral motor regions and contralateral posterior regions during early motor adaptation. Similarly, interregional coherence in the gamma band was significantly increased during motor adaptation and not during unperturbed reaching in some electrode pairs in the fronto-parietal-occipital network. Together, these findings suggest that gamma-related activity could reflect mechanism involved in motor adaptation processes. However, the **Chapter** failed to establish a significant link between regional and interregional activity specific and motor adaptation, most probably due to an underpowered study (sample size N = 15). However, the preliminary results of this exploratory analysis could be exploited in future studies. Based on the present findings and post-hoc power calculations, we recommend that a future study should investigate differences in regional and interregional

activity between conditions using ERSPs and TR-ERPCOH as readouts including at least 28 individuals to detect specific effects related to motor adaptation.

As expected, the **Chapter** reported significant modulations in regional activity (ERSP) and interregional connectivity (TR-ERPCOH) during different phases of reaching (irrespective of the environment: unperturbed or perturbed). Specifically increases of ERD in alpha and beta oscillatory power were observed around movement onset and persisted throughout movement execution, suggesting that these activities reflect a common mechanism of reaching movement. Similarly, the net functional connectivity between fronto-parietal-occipital regions showed characteristic shared modulations across time and frequencies during unperturbed and perturbed reaching movements.

The **Chapter** proposes that EEG spectral features analysed in a time resolved manner during a highly standardised reaching task might provide a neurophysiological approach to index reaching-related regional activity as well as network reconfigurations that could serve as measures for efficient motor performance and in the future as baseline measures in upper-limb recovery. Specifically, since robot-mediated reaching is used in clinical research settings for stroke upper limb recovery (Turner et al., 2013), it is conceivable that extracting modulations in regional power and interregional connectivity could be used to detect the neurofunctional underpinnings leading to impaired reaching in stroke. For instance, regional activation, (measured with modulations in ERSP), and functional coupling (measured with modulation in TR-ERPCOH) features could be extracted in stroke patients to gain insights into the neural underpinnings of their upper limb impairments. These neurophysiological measures could further be relevant for studying the mechanisms of brain plasticity and recovery following brain injury leading to upper limb impairments. Together with previous research using robot-mediated reaching tasks in combination with EEG recordings (Formaggio et al., 2015, 2013), this **Chapter** suggests that spectral EEG regional and interregional features can offer new perspectives for the

evaluation of brain activity and the neurological assessment of motor performance to better understand the planning and execution of movement.

8.2. Impact of findings and wider contribution

In recent years, there has been much interest in extracting normal patterns of neural activity especially in the context of motor rehabilitation. These patterns of activity can be exploited in many ways and here are some selected examples addressed in this thesis: i) gaining a deeper understanding of the mechanisms necessary for accurate motor control ii) establishing a baseline of brain activity resulting in normal accurate motor behaviour that can be used as a guide for re-establishing normal patterns of activity following brain injury, iii) training patients to control these brain signals to improve their motor disabilities, iv) targeting brain regions with NIBS to regain a more normal activity pattern.

This thesis used EEG and TMS-EEG to extract normal patterns of activity related to unimanual motor control focussing on cortical excitability, plasticity and adaptation.

8.2.1. TMS-EEG

Collectively, the studies have shown that TMS-EEG is a useful tool to study cortical excitability providing reliable and reproducible readouts by measuring direct cortical responses to TMS with EEG (TEPs and TMS-induced oscillations) and corticospinal responses with EMG (MEP). **Study I** confirmed that TEP components commonly reported in the literature, namely the P30, N45, P60, N100, P190 and N280 (for review see Farzan et al., 2016) were reproducible across individuals when stimulating M1 in different motor states with the TMS-EEG set-up used in the lab. These results confirm previous findings (Lioumis et al., 2009) and further support the idea that TMS-EEG is a reliable tool to investigate cortical excitability as well as excitability changes (e.g. modulation from pre to post-intervention).

The thesis demonstrated that both readouts, MEPs and TEPs, provide complementary information about cortical function related to unimanual motor control. While MEP amplitudes were used as an index of corticospinal

excitability reflecting the excitation of pyramidal cells acting on motor output cells leading to a contraction in the targeted muscle, TEPs provided a more global and direct measure of cortical excitability on a whole scalp level by capturing the spreading of activity through cortico-cortical connections and was used to assess cortical excitability in a wider range of brain regions. Specifically, topographical representation on scalp maps of TEP activity were used (**Study I and III**) to assess local and distant effects of TMS by capturing excitability of the stimulated brain region (i.e. M1 in this thesis) and the spreading of TEPs in a broader cortical network. For instance, **Study III** applied TMS over M1 and recorded TEPs from the whole scalp. By comparing post- and pre-motor adaptation TEP N100 amplitudes, a significant modulation in cortical excitability was revealed not only in the stimulated area (i.e. M1) but also on a broader level, including bilateral sensorimotor regions.

Moreover, TEPs represent an additional readout of TMS that can help to identify changes in cortical excitability outside the CST and provide distinct information outside the corticospinal output. The value of TEP amplitudes as a readout in comparison to MEP amplitudes was highlighted in **Study II**. Namely, significant modulations of cortical excitability during unimanual reaching preparation were only seen in cortical activity measured with TEPs and not in the targeted muscle measured with MEPs, suggesting that the modulation of cortical activity was uncoupled from modulations in corticospinal activity. A similar dissociation was reported in a previous study (Kičić et al., 2008) who demonstrated that changes in the TMS-evoked inhibitory TEP N100 were dissociated from corticospinal modulations (MEPs). Together, these findings illustrate the crucial contribution brought by using both TEPs and MEPs as readouts to investigate functional cortical activity.

Finally, since TEPs can be elicited and measured without relying on the CST in contrast to MEPs, TEPs can be exploited to assess cortical excitability in populations with damages to the CST. This is especially relevant when studying clinical populations, such as stroke patients who commonly present with damages to the CST, limiting the use of MEPs as outcome measures (for review see Sato et al., 2015). In fact, TEPs have already been used to assess

cortical excitability and modulations in stroke patients as a measure of cortical plasticity used to track their motor recovery (for review see Tremblay et al., 2019). For instance, Manganotti et al. (2015) reported that the presence or absence of TEPs recorded from the ipsilesional M1 can be used as a prognostic factor of recovery in acute stroke. Another study in stroke patients demonstrated that TEPs and TMS-induced oscillations can be used to longitudinally to track the time-course of cortical plasticity in subcortical stroke patients (Pellicciari et al., 2018). In line with these studies, **Study III** supports the value of tracking cortical modulations with TEPs. In particular, we propose the TEP N100 as a reliable biomarker of inhibitory processes and the modulation of TEP N100 amplitudes as a biomarker of neuroplasticity related to motor adaptation and learning processes in healthy individuals. As such the TEP N100 could represent a valid biomarker to track plasticity changes related to learning. Since adaptation and learning are important aspects of rehabilitation in upper limb recovery driving neuroplastic changes, this thesis suggests that the TEP N100 can be exploited in stroke to track recovery in terms of plasticity changes. Since **Study III** also demonstrated the predictive value of the TEP N100 related to motor learning improvements, this component could be used in stroke patients to gain more insights into the inhibitory cortical mechanisms driving motor learning and thus recovery.

8.2.2. EEG and BCI

Upper limb impairments are often reported following stroke (Nichols-Larsen et al., 2005), and a major focus of rehabilitation is to recover normal brain function leading to recovery in motor function. In recent years, the use of BCI technologies have been increasingly explored to restore motor function for people with severe motor disabilities (for review see Grosse-Wentrup et al., 2011).

Two main approaches on how to use BCIs in the context of motor rehabilitation exist (for review see Daly and Wolpaw, 2008). The first strategy is to replace the loss of normal neuromuscular output by using brain signals to control a non-self-entity such as a neuroprosthetic limb (Ganguly and Carmena, 2009). The second consists in inducing activity-dependent brain

plasticity to restore normal brain function by requiring the activation or deactivation of specific brain signals (Linden et al., 2016). Here, the participant learns how to regulate his own brain signals by using real-time neurofeedback.

EEG has become an important tool in monitoring task-related activity in individuals and also to assess abnormal activity in neurological such as stroke. In the context of neurorehabilitation, it is important to target the impairment as directly as possible to restore normal motor function. As highlighted by Daly and Wolpaw (2008) one effective mechanism of motor learning and re-learning after brain injury is that of cortical plasticity. This thesis employed EEG to extract normal cortical activity patterns related to unimanual reaching and motor adaptation using a highly standardised robot-mediated task. Specifically, EEG recordings were employed to extract EEG features in a time-resolved manner to reflect dynamic fluctuations in cortical activity related to unimanual motor control. Using EEG signals, **Study III** identified two key features: An error-related negativity (ERN) linked to performance improvements (**Chapter 6**) as well as a dynamic fluctuation in network structure (i.e. modulation in regional activity and interregional connectivity) during unilateral reaching (**Chapter 7).** These features can be exploited for neurorehabilitation and are discussed below.

First, **Study III** identified ERN activity in fronto-central regions (including the SMA) reflecting the formation of a predictive internal model necessary to adapt movements to a novel environment and thus highlighting its role in motor learning. Since the ERN activity have been reported to be reduced in stroke patients (Desowska and Turner, 2019) and that a smaller ERN activity is linked to worse motor learning (Hogan et al., 2006), we propose the ERN in fronto-central areas (e.g. the SMA) as a target for BCI in the context of upper limb rehabilitation. Targeting the SMA seems appropriate and feasible, since it has been shown that upregulating activity in this brain region using real-time fMRI neurofeedback in stroke patients correlated with performance improvements during a motor imagery task (Yoo et al., 2008).

Second, the time-resolved analyses of cortical regional power and interregional connectivity strength observed during a highly standardised reaching task could be used in the clinical population: Namely, these features could serve as baseline measures for normal motor functioning. Since in stroke activity dependent cortical plasticity can have positive as well as negative effects on motor control, EEG data as extracted in **Study III** (**Chapter 7**) could be used to examine time-varying reconfigurations in global network structure during reaching and exploited for stroke rehabilitation. Specifically, since robot-mediated reaching tasks such as the one used in this thesis, provide a reliable tool to assess motor function in stroke patients (for review see Huang and Krakauer, 2009), deriving EEG features during movement preparation and execution during these highly standardised tasks can be used to evaluate abnormal brain activity in stroke leading to upper limb impairments. Moreover, these features could then be exploited in the context of upper limb rehabilitation. In agreement with previous studies (Formaggio et al., 2015, 2013) using robot-mediated reaching tasks, we propose that evaluating cortical oscillations at a regional and network level in a time-resolved manner can be useful to assess abnormal brain function in patients presenting with upper limb deficits due to brain injuries such as following stroke. In other words, this kind of neurophysiological evaluation could be used to study the mechanisms of brain plasticity and recovery or induced by rehabilitation treatments.

8.3. Methodological considerations

8.3.1. TMS-EEG

Although a growing number of research has provided strong evidence for the usefulness of simultaneous TMS-EEG to measure neural activity, the non-physiological effect of TMS in EEG recordings is an inherent source of ambiguity in which neural activity induced by transcranial neuronal excitation is confounded with neural activity due to somatosensory and auditory processing (Conde et al., 2019). Specifically, two main challenges remain to be solved to optimise experimental procedures: i) to disentangle the direct effects caused by TMS in the brain from non-cortical biological sources; and

ii) to automatise pre-processing algorithms for artefact rejections in order to make them less time consuming and less subjective.

TMS-evoked responses are contaminated by auditory evoked potentials (AEPs) produced by the loud clicking sound of the TMS pule and somatosensory evoked potentials (SEPs) produced by the activation of the peripheral muscle contraction (Conde et al., 2019). During experiments, auditory white noise can be used to reduce AEPs and TMS intensities can be lowered to subthreshold to reduce SEPs (for review see Farzan et al., 2016). However, even these measures do not fully remove their contribution to TMS-evoked potentials (Conde et al., 2019). Pre-processing pipelines have been developed to remove non-neural effects due to interactions from the EEG recording system with the large time-varying magnetic pulse from the TMS pulse. Specifically, ICA decomposition can be used to detect artefacts such as decay artefacts and electrode noise using semi-automated ICA component rejections. In this thesis, a semi-automated ICA detection algorithm for artefact rejection accustomed to our data was used (Atluri et al., 2016; Rogasch et al., 2014). Recently, laboratories have grouped together to design a fully-automated **art**efact rejection algorithm for **s**ingle-pulse **T**MS-EEG (ARTIST) (Wu et al., 2018). This newly developed pipeline provides a faster and more objective method to clean TMS-EEG data and thereby could make it easier to use in both basic research and clinical settings.

Another limitation of using TMS-EEG is the low spatial resolution, due to the fact that scalp EEG mainly captures neural activity from cortical neurons, thus recording of deeper subcortical structures from TMS-EEG recordings are not available (for review see Farzan et al., 2016). Combining TMS with fMRI overcomes this limitation and can provide local and more remote neural activations of TMS, but suffers from a poor temporal resolution (Bohning et al., 1999; Navarro de Lara et al., 2017; Ruff et al., 2009). Even though EEG suffers from a low spatial resolution, TMS has the potential to improve the spatial resolution by applying TMS over specific cortical regions, from which it can be inferred that the stimulated/targeted area is involved in generating the pattern of neural activity recorded with EEG. In other words, the source of

the earliest maximal EEG activity is likely to be located over the stimulated brain region with TMS (Conde et al., 2019; Petrichella et al., 2017). EEG source localisation algorithms can further help to localise the origins of the TMS-evoked responses (Petrichella et al., 2017).

Another important point to address when using TMS protocols, is the variability of TMS-evoked responses. In fact, it is known that TMS-evoked responses are highly variable within and across individuals at a single-trial level (Iscan et al., 2016). Importantly however, in contrast to the highly variable MEPs, averaged TMS-evoked EEG responses (e.g. TEPs) are highly reproducible within individuals as demonstrated by Lioumis et al. (2009), who reported that TEP components were highly reproducible up to 200 ms post-TMS with a correlation factor greater than 0.83. It is assumed that the variability of TMS-evoked responses within individuals are due to fact that TMS is applied during different brain states (i.e. higher or lower excitability) leading to higher or lower MEPs. For instance, it has been suggested that brain oscillations as measured with EEG can reflect spontaneous fluctuations of cortical excitability and be related to cortical excitability (for review see Berger et al., 2014). Specifically, in their review Berger et al. (2014) point out that instantaneous phase of oscillations at TMS stimulation site just before the TMS pulse is predictive of corticospinal excitability (i.e. the size of MEP amplitudes). For instance, Keil et al. (2014) demonstrated that oscillatory power and phase pre-TMS pulse correlated with the size of MEP amplitudes and Iscan et al. (2016) showed that pre-TMS alpha power variability was associated with MEP amplitude variability. Together, these findings provide evidence that ongoing brain oscillations directly influence neural excitability and suggest that EEG-extracted features can be used for closed-loop state-dependent brain stimulation (for review see Zrenner et al., 2016).

Traditionally, TMS-EEG has been used as input (TMS pulse) – output (e.g. EMG, EEG and behavioural output) measurement to study neurophysiological mechanisms. However, recently it has been shown that EEG parameters, revealing different brain states, can be extracted to guide TMS input parameters offline or even online through feedback mechanisms (closed-loop

systems) (Schaworonkow et al., 2019). In fact, EEG brain-state triggered TMS (EEG-TMS) can be used to interfere with ongoing brain activity with high temporal and spectral resolution and therefore be of potential use for neurorehabilitation and neurotherapeutics (for review see Zrenner et al., 2016).

In the context of motor control, EEG-extracted features such as ERD in alpha and beta band prior to movement onset (**Study III, Chapter 7**; Formaggio et al., 2015) could be valuable to detect the intention to move and trigger TMS administration to initiate the movement execution, by activating networks through the TMS pulse. This could, for example, be exploited to facilitate movement in stroke patients with upper limb dysfunctions by using brain-state dependent stimulation to detect the intention to move with EEG recordings and simultaneously applying brain stimulation to facilitate movement (Gharabaghi et al., 2014; Walter et al., 2012). A significant challenge that remains in closed-loop approaches using EEG-TMS is to decode the relevant EEG features, which can be confounded with TMS-artefacts. However, it has been shown that these stimulation after-effects can be removed using algorithms such as the Burg algorithm, linear interpolations or autoregressive models (Walter et al., 2012).

8.3.2. Robot-mediated reaching and neurorehabilitation

Study II and **III** employed a robot-mediated reaching task increasingly used in clinical settings (for review see Bastian, 2008) to investigate neurophysiological correlates of unimanual reaching with the hope to provide new perspectives for the assessment and recovery of motor function in neurorehabilitation settings. The experiments helped to gain insights into the mechanisms underlying unimanual motor control in terms of cortical excitability, modulation of excitability and activity. The findings can be exploited in neurorehabilitation settings, since robot-mediated reaching tasks are increasingly used in clinical settings and provide a robust method to assess motor function (for review see Huang and Krakauer, 2009). However, even if the findings from this thesis establish a theoretical mechanism in motor control and learning they cannot directly be translated into clinical settings.

This is highlighted by a recent multi-site clinical trial that compared robot-mediated upper limb therapy with conventional treatments in 770 stroke patients (Rodgers et al., 2019) and reported that improvements in upper limb impairment following robot-mediated therapy were not reflected in upper-limb functional improvements at a group-level. The authors suggested that this might in part be due to the fact that robot-mediated therapy might not work at a group-level but that rehabilitation protocols should be individualised and tailored to the characteristics of the patient. This thesis addressed this particular issue and identified neural correlates (i.e. ERN) and a predictor of motor learning (TEP N100 amplitude) during a robot-mediated reaching task (adaptation task). These two electrophysiological findings might represent a first step to gain a deeper understanding of the driving factors of motor learning and could be a way to delineate how intrinsic native cortical excitability (**Study III, Chapter 6**) can explain differences in motor learning across individuals. A future study could explore if these features can also explain the variability of motor learning and upper limb impairment recovery in stroke patients. These features could be one solution to stratify treatments in stroke patients using robot-mediated therapy targeting upper limb impairment recovery. However, the direct applicability of these findings into neurorehabilitation settings are still limited, since further research is needed to establish how upper limb impairment improvements translate into upper-limb function improvements and thus contribute to a better quality of life of stroke patients (Rodgers et al., 2019).

Another aspect to consider when employing robot-mediated therapy is the training modality. In stroke, robot-mediated therapy used in clinical trials and practice include assisted reaching (i.e. in an unperturbed environment) (Rodgers et al., 2019) and adaptive reaching (i.e. in a perturbed environment) (Patton et al., 2006) training. Both types of training consist of repetitive unilateral arm movements, but only in the adaptive reaching training movements are performed in the presence of perturbing forces (also called adaptive training and is similar to the task used in **Study III**). Patton et al. (2006) tested two types of adaptive trainings in stroke patients: one used forces that enhanced reaching errors and another that reduced reaching

errors. They demonstrated that improvements in upper limb impairments were only seen when the training forces enhanced errors, and not when they reduced errors or were near zero. These preliminary findings suggest that error-enhancing therapy (as opposed to guiding the arm closer to the correct trajectory) is more effective than therapy that reduces errors. Given that different training modalities are showing different clinical effects, establishing a relationship between behavioural outcome measures and brain activity patterns (as has been done in this thesis in healthy individuals) could shed light on the neural mechanisms driving different clinical effects in stroke patients.

8.4. Concluding remarks

Collectively, the series of experiments demonstrated that even unimanual motor control relies on complex interactions between excitatory and inhibitory mechanisms not only in the contralateral M1 but involves a wide range of brain regions, demonstrated by a bi-hemispheric activity during movement preparation, the formations of a predictive model in fronto-central regions and neuroplastic changes in sensorimotor regions underlying motor adaptation during unimanual reaching.

From a methodological point of view, the present thesis demonstrates that the complex relationship between the brain and behaviour, can be investigated with EEG-derived as well as TMS-EEG-derived cortical biomarkers for motor control in healthy individuals. Crucially, it has shown that TMS-EEG adds value to previously used TMS-EMG outcome measures by allowing to directly quantify cortical excitability and changes in cortical neurophysiological states on a whole-scalp level.

The use of a highly standardised robot task in this thesis allowing to accurately and reliably monitor motor performance enabled us to investigate motor control and adaptation in a highly standardised way and in combination with neuroimaging tools to derive neurophysiological underpinnings of unimanual reaching. Specifically, the identified neural mechanisms and substrates of unimanual motor control can be exploited for neurorehabilitation purposes

since EEG and TMS-EEG are cost-effective tools to assess neurophysiological functions and link them to behavioural outcome measures. The thesis proposes that recording cortical activity in stroke patients during robot-mediated training could provide insights into the dynamics of cortical reorganisation promoted by rehabilitation. Since the series of experiments in this thesis demonstrated that even unimanual movements depend on a widely distributed cortical network, we propose that it is not only important to focus on re-establishing a normal activity in distinct brain regions but also to monitor functional interactions between brain regions at a network level in the context of neurorehabilitation.

Apart from identifying neural correlates that constitute a functional brain system related to unimanual motor control, this thesis also focussed on establishing the role of motor dominance, bi-hemispheric activity and intrinsic native brain activity that can impact motor control and could represent key factors explaining the variability of upper limb recovery following brain injury. In fact, it has been shown that hemispheric asymmetries related to motor dominance, imbalances between contralateral and ipsilateral M1 excitability and the ability to adapt to novel environments can affect upper limb recovery (for review see Dodd et al, 2017). While the thesis failed to identify hemispheric asymmetries related to motor dominance, a significant ipsilateral as well as contralateral motor cortical activity was detected during unimanual reaching and a significant association between native levels of sensorimotor cortical excitability and unimanual motor learning was identified. These findings could represent a first step towards clarifying the contributions of these factors towards upper limb recovery. Specifically, neuronal reorganisation following stroke is often observed on both the ipsilesional and contralesional hemispheres during recovery to regain motor functionality but it remains unclear if a hyperactive contralesional M1 (i.e. ipsilateral M1) activity during unimanual movements of the paretic limb is detrimental or beneficial. Commonly, NIBS is used to either excite the ipsilesional M1 or inhibit the contralesional M1 to enhance stroke patient's recovery (for review see Mcdonnell and Stinear's meta-analysis, 2017). However, results have been mixed and inhibiting the contralesional hemisphere is not always the

best solution for all patients. In fact, **Chapter 5** (**Study II**) reports a significant bilateral M1 activation during unimanual reaching preparation which suggests an active role of the ipsilateral M1. This theory is supported by BCI paradigms who derive neural signals from the ipsilateral M1 to control unimanual movements of a prosthetic limb (Ganguly et al., 2009). In light of these findings, the thesis proposes that before applying an inhibitory NIBS protocol to the contralesional (i.e. ipsilateral) M1, the contribution of the ipsilateral M1 should first be established in each patient, for instance by assessing native cortical excitability of both hemispheres using TEPs as readouts. In fact, it has been shown that at least in a subset of stroke patients contralesional (i.e. ipsilateral) motor activity and the contralesional hemisphere appear to play a key role for upper limb recovery (for review see Dodd et al., 2017).

Similarly, robot-mediated learning is highly variable across healthy individuals (**Study III, Chapter 6**) as well as in stroke patients (Rodgers et al., 2019) and robot-mediated therapy does not lead to improved upper limb functional recovery at a group-level. The predictive value of native cortical excitability and motor learning improvements during a robot-mediated adaptation task reported in this thesis could serve as a biomarker to determine who is likely to benefit from robot-mediated therapy and thus to stratify treatments.

In this regard, this thesis aimed to assess key principles of upper limb motor control and motor learning that could pave the path to foster upper limb rehabilitation by providing deeper insights into the neurophysiological mechanisms underlying unimanual motor control in healthy individuals.

References

Ahn, M., Ahn, S., Hong, J.H., Cho, H., Kim, K., Kim, B.S., Chang, J.W., Jun, S.C., 2013. Gamma band activity associated with BCI performance: simultaneous MEG/EEG study. Front. Hum. Neurosci. 7, 848. https://doi.org/10.3389/fnhum.2013.00848

Airaksinen, K., Makela, J.P., Nurminen, J., Luoma, J., Taulu, S., Ahonen, A., Pekkonen, E., 2015. Cortico-muscular coherence in advanced Parkinson's disease with deep brain stimulation. Clin. Neurophysiol. Off. J. Int. Fed. Clin. Neurophysiol. 126, 748–755. https://doi.org/10.1016/j.clinph.2014.07.025

Akkal, D., Dum, R.P., Strick, P.L., 2007. Supplementary motor area and presupplementary motor area: targets of basal ganglia and cerebellar output. J. Neurosci. Off. J. Soc. Neurosci. 27, 10659–10673. https://doi.org/10.1523/JNEUROSCI.3134-07.2007

Alawieh, A., Tomlinson, S., Adkins, D., Kautz, S., Feng, W., 2017. Preclinical and Clinical Evidence on Ipsilateral Corticospinal Projections: Implication for Motor Recovery. Transl Stroke Res 8, 529–540. https://doi.org/10.1007/s12975-017-0551-5

Allen, J.J.B., Keune, P.M., Schönenberg, M., Nusslock, R., 2018. Frontal EEG alpha asymmetry and emotion: From neural underpinnings and methodological considerations to psychopathology and social cognition. Psychophysiology 55, e13028. https://doi.org/10.1111/psyp.13028

Alstermark, B., Ogawa, J., Isa, T., 2004. Lack of Monosynaptic Corticomotoneuronal EPSPs in Rats: Disynaptic EPSPs Mediated Via Reticulospinal Neurons and Polysynaptic EPSPs Via Segmental Interneurons. J. Neurophysiol. 91, 1832–1839.

Aman, J.E., Elangovan, N., Yeh, I.-L., Konczak, J., 2015. The effectiveness of proprioceptive training for improving motor function: a systematic review. Front. Hum. Neurosci. 8, 1075–1075. https://doi.org/10.3389/fnhum.2014.01075

Amo, C., de Santiago, L., Barea, R., López-Dorado, A., Boquete, L., 2017. Analysis of Gamma-Band Activity from Human EEG Using Empirical Mode Decomposition. Sensors 17, 989. https://doi.org/10.3390/s17050989

Amo, C., del Castillo, M.O., Barea, R., de Santiago, L., Martínez-Arribas, A., Amo-López, P., Boquete, L., 2016. Induced Gamma-Band Activity During Voluntary Movement: EEG Analysis for Clinical Purposes. Motor Control 20, 409–428.

Amunts, K., Schlaug, G., Schleicher, A., Steinmetz, H., Dabringhaus, A., Roland, P.E., Zilles, K., 1996. Asymmetry in the human motor cortex and handedness. Neuroimage 4, 216–222. https://doi.org/10.1006/nimg.1996.0073

Andres, F.G., Gerloff, C., 1999. Coherence of sequential movements and motor learning. J. Clin. Neurophysiol. Off. Publ. Am. Electroencephalogr. Soc. 16, 520–527.

Andrew, C., Pfurtscheller, G., 1996. Event-related coherence as a tool for studying dynamic interaction of brain regions. Electroencephalogr Clin Neurophysiol 98, 144–8.

Angstmann, S., Madsen, K.S., Skimminge, A., Jernigan, T.L., Baaré, W.F.C., Siebner, H.R., 2016. Microstructural asymmetry of the corticospinal tracts predicts right–left differences in circle drawing skill in right-handed adolescents. Brain Structure & Function 221, 4475–4489. https://doi.org/10.1007/s00429-015-1178-5

Anguera, J.A., Seidler, R.D., Gehring, W.J., 2009. Changes in Performance Monitoring During Sensorimotor Adaptation. J. Neurophysiol. 102, 1868–1879. https://doi.org/10.1152/jn.00063.2009

Annett, M., 2002. Handedness and brain asymmetry: The right shift theory. Psychology Press.

Armand, J., Olivier, E., Edgley, S.A., Lemon, R.N., 1997. Postnatal Development of Corticospinal Projections from Motor Cortex to the Cervical Enlargement in the Macaque Monkey. J. Neurosci. 17, 251. https://doi.org/10.1523/JNEUROSCI.17-01-00251.1997

Atluri, S., Frehlich, M., Mei, Y., Garcia Dominguez, L., Rogasch, N.C., Wong, W., Daskalakis, Z.J., Farzan, F., 2016. TMSEEG: A MATLAB-Based Graphical User Interface for Processing Electrophysiological Signals during Transcranial Magnetic Stimulation. Front. Neural Circuits 10. https://doi.org/10.3389/fncir.2016.00078

Aurlien, H., Gjerde, I.O., Aarseth, J.H., Eldøen, G., Karlsen, B., Skeidsvoll, H., Gilhus, N.E., 2004. EEG background activity described by a large computerized database. Clin. Neurophysiol. 115, 665–673. https://doi.org/10.1016/j.clinph.2003.10.019

Babiloni, C., Del Percio, C., Vecchio, F., Sebastiano, F., Di Gennaro, G., Quarato, P.P., Morace, R., Pavone, L., Soricelli, A., Noce, G., Esposito, V., Rossini, P.M., Gallese, V., Mirabella, G., 2016. Alpha, beta and gamma electrocorticographic rhythms in somatosensory, motor, premotor and prefrontal cortical areas differ in movement execution and observation in humans. Clin. Neurophysiol. Off. J. Int. Fed. Clin. Neurophysiol. 127, 641–654. https://doi.org/10.1016/j.clinph.2015.04.068

Baek, S.O., Jang, S.H., Lee, E., Kim, S., Hah, J.O., Park, Y.H., Lee, J.M., Son, S.M., 2013. CST recovery in pediatric hemiplegic patients: diffusion tensor tractography study. Neurosci. Lett. 557, 79–83.

Baker, M.R., Baker, S.N., 2003. The effect of diazepam on motor cortical oscillations and cortico-muscular coherence studied in man. J. Physiol. 546, 931–942. https://doi.org/10.1113/jphysiol.2002.029553

Baker, S.N., 2007. Oscillatory interactions between sensorimotor cortex and the periphery. Mot. Syst. Neurobiol. Behav. 17, 649–655. https://doi.org/10.1016/j.conb.2008.01.007

Baker, S.N., Pinches, E.M., Lemon, R.N., 2003. Synchronization in monkey motor cortex during a precision grip task. II. effect of oscillatory activity on corticospinal output. J. Neurophysiol. 89, 1941–1953. https://doi.org/10.1152/jn.00832.2002

Ball, T., Demandt, E., Mutschler, I., Neitzel, E., Mehring, C., Vogt, K., Aertsen, A., Schulze-Bonhage, A., 2008. Movement related activity in the high

gamma range of the human EEG. NeuroImage 41, 302–310. https://doi.org/10.1016/j.neuroimage.2008.02.032

Barker, A.T., Jalinous, R., Freeston, I.L., 1985. Non-invasive magnetic stimulation of human motor cortex. Lancet Lond. Engl. 1, 1106–1107.

Bashir, S., Perez, J., Horvath, J.C., Pascual-Leone, A., 2013. Differentiation of motor cortical representation of hand muscles by navigated mapping of optimal TMS current directions in healthy subjects. Journal of clinical neurophysiology: official publication of the American Electroencephalographic Society 30, 390–395.

Basmajian, J.V., Luca, C.J. de., 1985. Muscles Alive : their functions revealed by electromyography. Williams & Wilkins, Baltimore.

Basteris, A., Nijenhuis, S.M., Stienen, A.H.A., Buurke, J.H., Prange, G.B., Amirabdollahian, F., 2014. Training modalities in robot-mediated upper limb rehabilitation in stroke: a framework for classification based on a systematic review. J. Neuroengineering Rehabil. 11, 111–111. https://doi.org/10.1186/1743-0003-11-111

Bastian, A.J., 2008. Understanding sensorimotor adaptation and learning for rehabilitation. Curr. Opin. Neurol. 21, 628–633. https://doi.org/10.1097/WCO.0b013e328315a293

Bays, P.M., Flanagan, J.R., Wolpert, D.M., 2005. Interference between velocity-dependent and position-dependent force-fields indicates that tasks depending on different kinematic parameters compete for motor working memory. Exp. Brain Res. 163, 400–405. https://doi.org/10.1007/s00221-005-2299-5

Beaulieu, C., Bourassa, M.-È., Brisson, B., Jolicoeur, P., De Beaumont, L., 2014. Electrophysiological correlates of motor sequence learning. BMC Neurosci. 15, 102. https://doi.org/10.1186/1471-2202-15-102

Beck, S., Shamim, E.A., Pirio Richardson, S., Schubert, M., Hallett, M., 2009. Inter-hemispheric inhibition is impaired in mirror dystonia. Eur. J. Neurosci. 29, 1634–1640. https://doi.org/10.1111/j.1460-9568.2009.06710.x

Benjamini, Y., Hochberg, Y., 1995. Controlling the False Discovery Rate: A Practical and Powerful Approach to Multiple Testing. Journal of the Royal Statistical Society. Series B (Methodological) 57, 289–300.

Benjamini, Y., Yekutieli, D., 2001. The control of the false discovery rate in multiple testing under dependency. Ann Stat. 29, 1165–1188. https://doi.org/10.1214/aos/1013699998

Berger, H., 1929. On the electroencephalogram of man. Electroencephalogr. Clin. Neurophysiol. Suppl 28:37+.

Berger, B., Minarik, T., Liuzzi, G., Hummel, F.C., Sauseng, P., 2014. EEG oscillatory phase-dependent markers of corticospinal excitability in the resting brain. Biomed Res Int 2014, 936096–936096. https://doi.org/10.1155/2014/936096

Bernard, J.A., Taylor, S.F., Seidler, R.D., 2011. Handedness, Dexterity, and Motor Cortical Representations. Journal of Neurophysiology 105, 88–99.

Bernhard, C.G., Bohm, E., 1954. Cortical representation and functional significance of the corticomotoneuronal system. AMA Arch. Neurol. Psychiatry 72, 473–502.

Blakemore, S.J., Goodbody, S.J., Wolpert, D.M., 1998. Predicting the consequences of our own actions: the role of sensorimotor context estimation. The Journal of neuroscience: the official journal of the Society for Neuroscience 18, 7511–8.

Blank, A., Okamura, A.M., Kuchenbecker, K.J., 2008. Identifying the role of proprioception in upper limb prosthesis control: Studies on targeted motion. ACM Trans Appl Percept 7, 1–23.

Bohning, D., Shastri, A., McConnell, K., Nahas, Z., Lorberbaum, J., Roberts, D., Teneback, C., Vincent, D., George, M., 1999. A combined TMS/fMRI study of intensity-dependent TMS over motor cortex. Biol. Psychiatry 45, 385–394. https://doi.org/10.1016/S0006-3223(98)00368-0

Bonato, C., Miniussi, C., Rossini, P.M., 2006. Transcranial magnetic stimulation and cortical evoked potentials: a TMS/EEG co-registration study. Clin Neurophysiol 117, 1699–707. https://doi.org/10.1016/j.clinph.2006.05.006

Bonnard, M., Spieser, L., Meziane, H.B., de Graaf, J.B., Pailhous, J., 2009. Prior intention can locally tune inhibitory processes in the primary motor cortex: direct evidence from combined TMS-EEG. Eur J Neurosci 30, 913–23. https://doi.org/10.1111/j.1460-9568.2009.06864.x

Boonstra, T.W., Daffertshofer, A., Breakspear, M., Beek, P.J., 2007. Multivariate time-frequency analysis of electromagnetic brain activity during bimanual motor learning. NeuroImage 36, 370–7.

Bouton, C.E., Shaikhouni, A., Annetta, N.V., Bockbrader, M.A., Friedenberg, D.A., Nielson, D.M., Sharma, G., Sederberg, P.B., Glenn, B.C., Mysiw, W.J., 2016. Restoring cortical control of functional movement in a human with quadriplegia. Nature 533, 247.

Bowyer, S.M., 2016. Coherence a measure of the brain networks: past and present. Neuropsychiatr. Electrophysiol. 2, 1. https://doi.org/10.1186/s40810-015-0015-7

Brashers-Krug, T., Shadmehr, R., Bizzi, E., 1996. Consolidation in human motor memory. Nature 382, 252–255. https://doi.org/10.1038/382252a0

Brouwer, B., Sale, M.V., Nordstrom, M.A., 2001. Asymmetry of motor cortex excitability during a simple motor task: relationships with handedness and manual performance. Exp Brain Res 138, 467–76.

Brus-Ramer, M., Carmel, J.B., Martin, J.H., 2009. Motor cortex bilateral motor representation depends on subcortical and interhemispheric interactions. J Neurosci 29, 6196–6206. https://doi.org/10.1523/JNEUROSCI.5852-08.2009

Buetefisch, C.M., Revill, K.P., Shuster, L., Hines, B., Parsons, M., 2014. Motor demand-dependent activation of ipsilateral motor cortex. J. Neurophysiol. 112, 999–1009.

Bundy, D.T., Souders, L., Baranyai, K., Leonard, L., Schalk, G., Coker, R., Moran, D.W., Huskey, T., Leuthardt, E.C., 2017. Contralesional Brain-Computer Interface Control of a Powered Exoskeleton for Motor Recovery in Chronic Stroke Survivors. Stroke 48, 1908–1915. https://doi.org/10.1161/STROKEAHA.116.016304

Campfens, S.F., Schouten, A.C., van Putten, M.J.A.M., van der Kooij, H., 2013. Quantifying connectivity via efferent and afferent pathways in motor control using coherence measures and joint position perturbations. Exp. Brain Res. 228, 141–153. https://doi.org/10.1007/s00221-013-3545-x

Campfens, S.F., van der Kooij, H., Schouten, A.C., 2014. Face to phase: pitfalls in time delay estimation from coherency phase. J. Comput. Neurosci. 37, 1–8. https://doi.org/10.1007/s10827-013-0487-z

Cash, R.F.H., Noda, Y., Zomorrodi, R., Radhu, N., Farzan, F., Rajji, T.K., Fitzgerald, P.B., Chen, R., Daskalakis, Z.J., Blumberger, D.M., 2017. Characterization of Glutamatergic and GABAA-Mediated Neurotransmission in Motor and Dorsolateral Prefrontal Cortex Using Paired-Pulse TMS-EEG. Neuropsychopharmacol. Off. Publ. Am. Coll. Neuropsychopharmacol. 42, 502–511. https://doi.org/10.1038/npp.2016.133

Casula, E.P., Tarantino, V., Basso, D., Arcara, G., Marino, G., Toffolo, G.M., Rothwell, J.C., Bisiacchi, P.S., 2014. Low-frequency rTMS inhibitory effects in the primary motor cortex: Insights from TMS-evoked potentials. Neuroimage 98, 225–232. https://doi.org/10.1016/j.neuroimage.2014.04.065

Catani, M., 2017. A little man of some importance. Brain J. Neurol. 140, 3055–3061. https://doi.org/10.1093/brain/awx270

Chang, M.C., Jang, S.H., Seo, J.P., Lee, E., Kim, S., Won, Y.H., Son, S.M., 2015. Degenerative changes of the corticospinal tract in pediatric patients showing deteriorated motor function: A diffusion tensor tractography study. Dev. Neurorehabilitation 18, 290–295. https://doi.org/10.3109/17518423.2013.821538

Chen, R., 2004. Interactions between inhibitory and excitatory circuits in the human motor cortex. Exp. Brain Res. 154, 1–10. https://doi.org/10.1007/s00221-003-1684-1

Chen, R., Lozano, A.M., Ashby, P., 1999. Mechanism of the silent period following transcranial magnetic stimulation evidence from epidural recordings. Exp. Brain Res. 128, 539–542.

Cheyne, D., Bells, S., Ferrari, P., Gaetz, W., Bostan, A.C., 2008. Self-paced movements induce high-frequency gamma oscillations in primary motor cortex. NeuroImage 42, 332–42.

Chiou, S.-Y., Wang, R.-Y., Roberts, R.E., Wu, Y.-T., Lu, C.-F., Liao, K.-K., Yang, Y.-R., 2014. Fractional anisotropy in corpus callosum is associated with facilitation of motor representation during ipsilateral hand movements. PloS One 9, e104218.

Churchland, M.M., Abbott, L.F., 2012. Two layers of neural variability. Nat. Neurosci. 15, 1472–4.

Chye, L., Riek, S., de Rugy, A., Carson, R.G., Carroll, T.J., 2018. Unilateral movement preparation causes task-specific modulation of TMS responses in the passive, opposite limb. J. Physiol. 596, 3725–3738. https://doi.org/10.1113/JP275433

Cicinelli, P., Traversa, R., Bassi, A., Scivoletto, G., Rossini, P.M., 1997. Interhemispheric differences of hand muscle representation in human motor cortex. Muscle Nerve 20, 535–542.

https://doi.org/10.1002/(sici)1097-4598(199705)20:5<535::aid-mus1>3.0.co;2-a

Cisek, P., Crammond, D.J., Kalaska, J.F., 2003. Neural activity in primary motor and dorsal premotor cortex in reaching tasks with the contralateral versus ipsilateral arm. J. Neurophysiol. 89, 922–942. https://doi.org/10.1152/jn.00607.2002

Cisek, P., Kalaska, J.F., 2010. Neural mechanisms for interacting with a world full of action choices. Annu. Rev. Neurosci. 33, 269–298. https://doi.org/10.1146/annurev.neuro.051508.135409

Civardi, C., Cavalli, A., Naldi, P., Varrasi, C., Cantello, R., 2000. Hemispheric asymmetries of cortico-cortical connections in human hand motor areas. Clinical neurophysiology : official journal of the International Federation of Clinical Neurophysiology 111, 624–9.

Classen, J., Gerloff, C., Honda, M., Hallett, M., 1998. Integrative visuomotor behavior is associated with interregionally coherent oscillations in the human brain. J. Neurophysiol. 79, 1567–1573. https://doi.org/10.1152/jn.1998.79.3.1567

Cochet, H., Byrne, R.W., 2013. Evolutionary origins of human handedness: evaluating contrasting hypotheses. Anim. Cogn. 16, 531–542. https://doi.org/10.1007/s10071-013-0626-y

Conde, V., Tomasevic, L., Akopian, I., Stanek, K., Saturnino, G.B., Thielscher, A., Bergmann, T.O., Siebner, H.R., 2019. The non-transcranial TMS-evoked potential is an inherent source of ambiguity in TMS-EEG studies. NeuroImage 185, 300–312. https://doi.org/10.1016/j.neuroimage.2018.10.052

Contreras-Vidal, J.L., Kerick, S.E., 2004. Independent component analysis of dynamic brain responses during visuomotor adaptation. Neuroimage 21, 936–45. https://doi.org/10.1016/j.neuroimage.2003.10.037

Corballis, M.C., 2002. From hand to mouth: The origins of language., From hand to mouth: The origins of language. Princeton University Press, Princeton, NJ, US.

Corballis, M.C., 2017. The Evolution of Lateralized Brain Circuits. Front. Psychol. 8, 1021. https://doi.org/10.3389/fpsyg.2017.01021Cohen, J, 2013. Statistical power analysis for the behavioral sciences. Routledge.

Corbetta, M., Shulman, G.L., 2002. Control of goal-directed and stimulus-driven attention in the brain. Nat. Rev. Neurosci. 3, 201–15.

Coren, S., Halpern, D.F., 1991. Left-handedness: a marker for decreased survival fitness. Psychol. Bull. 109, 90–106.

Coren, S., Porac, C., 1977. Fifty centuries of right-handedness: the historical record. Science 198, 631–632.

Coryell, J.F., Michel, G.F., 1978. How supine postural preferences of infants can contribute toward the development of handedness. Infant Behav. Dev. 1, 245–257. https://doi.org/10.1016/S0163-6383(78)80036-8

Cragg, B.G., 1967. The density of synapses and neurones in the motor and visual areas of the cerebral cortex. J. Anat. 101, 639–654.

Cremoux, S., Tallet, J., Berton, E., Dal Maso, F., Amarantini, D., 2013. Does the force level modulate the cortical activity during isometric contractions after a cervical spinal cord injury? Clin. Neurophysiol. Off.

J. Int. Fed. Clin. Neurophysiol. 124, 1005–1012. https://doi.org/10.1016/j.clinph.2012.11.007

Dai, T.H., Liu, J.Z., Sahgal, V., Brown, R.W., Yue, G.H., 2001. Relationship between muscle output and functional MRI-measured brain activation. Exp. Brain Res. 140, 290–300.

Daligadu, J., Murphy, B., Brown, J., Rae, B., Yielder, P., 2013. TMS stimulus-response asymmetry in left- and right-handed individuals. Exp Brain Res 224, 411–6. https://doi.org/10.1007/s00221-012-3320-4

Daly, J.J., Wolpaw, J.R., 2008. Brain-computer interfaces in neurological rehabilitation. The Lancet. Neurology 7, 1032–43.

Davidson, T.W., Bolic, M., Tremblay, F., 2016. Predicting Modulation in Corticomotor Excitability and in Transcallosal Inhibition in Response to Anodal Transcranial Direct Current Stimulation. Frontiers in Human Neuroscience 10, 49. https://doi.org/10.3389/fnhum.2016.00049

Davidson, T., Tremblay, F., 2013. Hemispheric differences in corticospinal excitability and in transcallosal inhibition in relation to degree of handedness. PLoS One 8, e70286–e70286. https://doi.org/10.1371/journal.pone.0070286

Day, B.L., Brown, P., 2001. Evidence for subcortical involvement in the visual control of human reaching. Brain 124, 1832–1840. https://doi.org/10.1093/brain/124.9.1832

Day, B.L., Dressler, D., Maertens de Noordhout, A., Marsden, C.D., Nakashima, K., Rothwell, J.C., Thompson, P.D., 1989. Electric and magnetic stimulation of human motor cortex: surface EMG and single motor unit responses. J. Physiol. 412, 449–473. https://doi.org/10.1113/jphysiol.1989.sp017626

De Gennaro, L., Cristiani, R., Bertini, M., Curcio, G., Ferrara, M., Fratello, F., Romei, V., Rossini, P.M., 2004. Handedness is mainly associated with an asymmetry of corticospinal excitability and not of transcallosal inhibition. Clin. Neurophysiol. 115, 1305–1312.

De Marchis, C., Di Somma, J., Zych, M., Conforto, S., Severini, G., 2018. Consistent visuomotor adaptations and generalizations can be achieved through different rotations of robust motor modules. Sci. Rep. 8, 12657. https://doi.org/10.1038/s41598-018-31174-2

Della-Maggiore, V., Landi, S.M., Villalta, J.I., 2015. Sensorimotor adaptation: multiple forms of plasticity in motor circuits. Neurosci. Rev. J. Bringing Neurobiol. Neurol. Psychiatry 21, 109–125. https://doi.org/10.1177/1073858414545228

Delorme, A., Makeig, S., 2004. EEGLAB: an open source toolbox for analysis of single-trial EEG dynamics including independent component analysis. J Neurosci Methods 134, 9–21. https://doi.org/10.1016/j.jneumeth.2003.10.009

Delorme, A., Mullen, T., Kothe, C., Akalin Acar, Z., Bigdely-Shamlo, N., Vankov, A., Makeig, S., 2011. EEGLAB, SIFT, NFT, BCILAB, and ERICA: new tools for advanced EEG processing. Comput. Intell. Neurosci. 2011, 130714. https://doi.org/10.1155/2011/130714

Derosiere, G., Alexandre, F., Bourdillon, N., Mandrick, K., Ward, T.E., Perrey, S., 2014. Similar scaling of contralateral and ipsilateral cortical responses during graded unimanual force generation. NeuroImage 85 Pt 1, 471–477. https://doi.org/10.1016/j.neuroimage.2013.02.006

Desmurget, M., Epstein, C.M., Turner, R.S., Prablanc, C., Alexander, G.E., Grafton, S.T., 1999. Role of the posterior parietal cortex in updating reaching movements to a visual target. Nat. Neurosci. 2, 563–567. https://doi.org/10.1038/9219

Desowska, A., Turner, D.L., 2019. EEG correlates of motor adaptation in stroke. Presented at the OHBM.

Di Lazzaro, V., Oliviero, A., Profice, P., Saturno, E., Pilato, F., Insola, A., Mazzone, P., Tonali, P., Rothwell, J.C., 1998. Comparison of descending volleys evoked by transcranial magnetic and electric stimulation in conscious humans. Electroencephalogr. Clin. Neurophysiol. 109, 397–401.

Di Lazzaro, V., Ziemann, U., 2013. The contribution of transcranial magnetic stimulation in the functional evaluation of microcircuits in human motor cortex. Front. Neural Circuits 7, 18. https://doi.org/10.3389/fncir.2013.00018

Diedrichsen, J., White, O., Newman, D., Lally, N., 2010. Use-Dependent and Error-Based Learning of Motor Behaviors. J. Neurosci. 30, 5159–5166.

Dietz, V., 2002. Proprioception and locomotor disorders. Nat. Rev. Neurosci. 3, 781–790. https://doi.org/10.1038/nrn939

Dipietro, L., Krebs, H.I., Volpe, B.T., Stein, J., Bever, C., Mernoff, S.T., Fasoli, S.E., Hogan, N., 2012. Learning, not adaptation, characterizes stroke motor recovery: evidence from kinematic changes induced by robot-assisted therapy in trained and untrained task in the same workspace. IEEE Trans Neural Syst Rehabil Eng 20, 48–57. https://doi.org/10.1109/tnsre.2011.2175008

Dipietro, L., Poizner, H., Krebs, H.I., 2014. Spatiotemoral Dynamics of Online Motor Correction Processing Revealed by High-density Electroencephalography. J. Cogn. Neurosci. 26, 1966–1980. https://doi.org/10.1162/jocn_a_00593

Dodd, K.C., Nair, V.A., Prabhakaran, V., 2017. Role of the Contralesional vs. Ipsilesional Hemisphere in Stroke Recovery. Front Hum Neurosci 11, 469–469. https://doi.org/10.3389/fnhum.2017.00469

Donchin, O., Francis, J.T., Shadmehr, R., 2003. Quantifying generalization from trial-by-trial behavior of adaptive systems that learn with basis functions: theory and experiments in human motor control. J. Neurosci. Off. J. Soc. Neurosci. 23, 9032–9045.

Du, X., Rowland, L.M., Summerfelt, A., Wijtenburg, A., Chiappelli, J., Wisner, K., Kochunov, P., Choa, F.-S., Hong, L.E., 2018. TMS evoked N100 reflects local GABA and glutamate balance. Brain Stimulat. 11, 1071–1079. https://doi.org/10.1016/j.brs.2018.05.002

Duque, J., Lew, D., Mazzocchio, R., Olivier, E., Ivry, R.B., 2010. Evidence for two concurrent inhibitory mechanisms during response preparation. J. Neurosci. 30, 3793–3802.

Efron, B., Tibshirani, R., 1986. [Bootstrap Methods for Standard Errors, Confidence Intervals, and Other Measures of Statistical Accuracy]: Rejoinder. Stat. Sci 1. https://doi.org/10.1214/ss/1177013817

Engel, A.K., Fries, P., 2010. Beta-band oscillations--signalling the status quo? Curr Opin Neurobiol 20, 156–65. https://doi.org/10.1016/j.conb.2010.02.015

Escudero, J.V., Sancho, J., Bautista, D., Escudero, M., López-Trigo, J., 1998. Prognostic value of motor evoked potential obtained by transcranial magnetic brain stimulation in motor function recovery in patients with acute ischemic stroke. Stroke 29, 1854–1859.

Fagard, J., 1998. Changes in grasping skills and the emergence of bimanual coordination during the first year of life. Psychobiol. Hand, Clinics in developmental medicine No. 147. 123–143.

Fagard, J., Chapelain, A., Bonnet, P., 2015. How should "ambidexterity" be estimated? Laterality: Asymmetries of Body, Brain and Cognition 20, 543–570. https://doi.org/10.1080/1357650X.2015.1009089

Faiman, I., Pizzamiglio, S., Turner, D.L., 2018. Resting-state functional connectivity predicts the ability to adapt arm reaching in a robot-mediated force field. NeuroImage 174, 494–503. https://doi.org/10.1016/j.neuroimage.2018.03.054

Falkenstein, M., Hohnsbein, J., Hoormann, J., 1995. Event-related potential correlates of errors in reaction tasks. Electroencephalogr Clin Neurophysiol Suppl 44, 287–296.

Farzan, F., Barr, M.S., Hoppenbrouwers, S.S., Fitzgerald, P.B., Chen, R., Pascual-Leone, A., Daskalakis, Z.J., 2013. The EEG correlates of the TMS-induced EMG silent period in humans. NeuroImage 83, 120–134. https://doi.org/10.1016/j.neuroimage.2013.06.059

Farzan, F., Vernet, M., Shafi, M.M.D., Rotenberg, A., Daskalakis, Z.J., Pascual-Leone, A., 2016. Characterizing and Modulating Brain Circuitry through Transcranial Magnetic Stimulation Combined with Electroencephalography. Front. Neural Circuits 10, 73. https://doi.org/10.3389/fncir.2016.00073

Faul, F., Erdfelder, E., Lang, A.-G., Buchner, A., 2007. G*Power 3: A flexible statistical power analysis program for the social, behavioral, and biomedical sciences. Behavior Research Methods 39, 175–191. https://doi.org/10.3758/BF03193146

Fecchio, M., Pigorini, A., Comanducci, A., Sarasso, S., Casarotto, S., Premoli, I., Derchi, C.-C., Mazza, A., Russo, S., Resta, F., Ferrarelli, F., Mariotti, M., Ziemann, U., Massimini, M., Rosanova, M., 2017. The spectral features of EEG responses to transcranial magnetic stimulation of the primary motor cortex depend on the amplitude of the motor evoked potentials. PLOS ONE 12, e0184910. https://doi.org/10.1371/journal.pone.0184910

Feldman, A.G., 1986. Once more on the equilibrium-point hypothesis (λ model) for motor control. Journal of motor behavior 18, 17–54.

Ferreri, F., Pasqualetti, P., Maatta, S., Ponzo, D., Ferrarelli, F., Tononi, G., Mervaala, E., Miniussi, C., Rossini, P.M., 2011. Human brain connectivity during single and paired pulse transcranial magnetic stimulation. Neuroimage 54, 90–102. https://doi.org/10.1016/j.neuroimage.2010.07.056

Fields, E., Kuperberg, G.R., 2018. Having your cake and eating it too: Flexibility and power with mass univariate statistics for ERP data. https://doi.org/10.31234/osf.io/qfkgc

Finley, M.A., Dipietro, L., Ohlhoff, J., Whitall, J., Krebs, H.I., Bever, C.T., 2009. The effect of repeated measurements using an upper extremity robot on healthy adults. J. Appl. Biomech. 25, 103–110.

Formaggio, E., Storti, S.F., Boscolo Galazzo, I., Gandolfi, M., Geroin, C., Smania, N., Fiaschi, A., Manganotti, P., 2015. Time–Frequency Modulation of ERD and EEG Coherence in Robot-Assisted Hand Performance. Brain Topogr. 28, 352–363. https://doi.org/10.1007/s10548-014-0372-8

Formaggio, E., Storti, S.F., Boscolo Galazzo, I., Gandolfi, M., Geroin, C., Smania, N., Spezia, L., Waldner, A., Fiaschi, A., Manganotti, P., 2013. Modulation of event-related desynchronisation in robot-assisted hand performance: brain oscillatory changes in active, passive and imagined movements. J. Neuroengineering Rehabil. 10, 24.

Francis, J., 2005. Influence of the inter-reach-interval on motor learning. https://doi.org/10.1007/s00221-005-0062-6

Frank, M.J., Woroch, B.S., Curran, T., 2005. Error-Related Negativity Predicts Reinforcement Learning and Conflict Biases. Neuron 47, 495–501. https://doi.org/10.1016/j.neuron.2005.06.020

Fuggetta, G., Fiaschi, A., Manganotti, P., 2005. Modulation of cortical oscillatory activities induced by varying single-pulse transcranial magnetic stimulation intensity over the left primary motor area: A combined EEG and TMS study. NeuroImage 27, 896–908. https://doi.org/10.1016/j.neuroimage.2005.05.013

Fuhr, P., Agostino, R., Hallett, M., 1991. Spinal motor neuron excitability during the silent period after cortical stimulation. Electroencephalogr. Clin. Neurophysiol. Potentials Sect. 81, 257–262. https://doi.org/10.1016/0168-5597(91)90011-L

Gaetz, W., Cheyne, D., 2006. Localization of sensorimotor cortical rhythms induced by tactile stimulation using spatially filtered MEG. NeuroImage 30, 899–908. https://doi.org/10.1016/j.neuroimage.2005.10.009

Galea, J.M., Vazquez, A., Pasricha, N., de Xivry, J.-J.O., Celnik, P., 2011. Dissociating the roles of the cerebellum and motor cortex during adaptive learning: the motor cortex retains what the cerebellum learns. Cereb. Cortex N. Y. N 1991 21, 1761–70.

Ganguly, K., Carmena, J.M., 2009. Emergence of a stable cortical map for neuroprosthetic control. PLoS Biol. 7, e1000153.

Ganguly, K., Secundo, L., Ranade, G., Orsborn, A., Chang, E.F., Dimitrov, D.F., Wallis, J.D., Barbaro, N.M., Knight, R.T., Carmena, J.M., 2009. Cortical Representation of Ipsilateral Arm Movements in Monkey and Man. J. Neurosci. 29, 12948. https://doi.org/10.1523/JNEUROSCI.2471-09.2009

Gehring, W.J., Goss, B., Coles, M.G.H., Meyer, D.E., Donchin, E., 2018. The Error-Related Negativity. Perspect. Psychol. Sci. 13, 200–204. https://doi.org/10.1177/1745691617715310

Gehring, W.J., Goss, B., Coles, M.G.H., Meyer, D.E., Donchin, E., 1993. A Neural System for Error Detection and Compensation. Psychol. Sci. 4, 385–390. https://doi.org/10.1111/j.1467-9280.1993.tb00586.x

Georgopoulos, A.P., Carpenter, A.F., 2015. Coding of movements in the motor cortex. Curr. Opin. Neurobiol. 33, 34–39. https://doi.org/10.1016/j.conb.2015.01.012

Georgopoulos, A.P., Schwartz, A.B., Kettner, R.E., 1986. Neuronal population coding of movement direction. Science 233, 1416–1419.

Gerloff, C., Andres, F.G., 2002. Bimanual coordination and interhemispheric interaction. Acta Psychol. (Amst.) 110, 161–186.

Gerloff, C., Bushara, K., Sailer, A., Wassermann, E.M., Chen, R., Matsuoka, T., Waldvogel, D., Wittenberg, G.F., Ishii, K., Cohen, L.G., Hallett, M., 2006. Multimodal imaging of brain reorganization in motor areas of the contralesional hemisphere of well recovered patients after capsular stroke. Brain 129, 791–808. https://doi.org/10.1093/brain/awh713

Gesell, A., Ames, L.B., 1947. The development of handedness. J. Genet. Psychol. 70, 155–175.

Gharabaghi, A., Kraus, D., Leao, M.T., Spuler, M., Walter, A., Bogdan, M., Rosenstiel, W., Naros, G., Ziemann, U., 2014. Coupling brain-machine interfaces with cortical stimulation for brain-state dependent stimulation: enhancing motor cortex excitability for neurorehabilitation. Front. Hum. Neurosci. 8, 122. https://doi.org/10.3389/fnhum.2014.00122

Gonzalez Andino, S.L., Michel, C.M., Thut, G., Landis, T., Grave de Peralta, R., 2005. Prediction of response speed by anticipatory high-frequency (gamma band) oscillations in the human brain. Hum. Brain Mapp. 24, 50–58. https://doi.org/10.1002/hbm.20056

Grandchamp, R., Delorme, A., 2011. Single-trial normalization for event-related spectral decomposition reduces sensitivity to noisy trials. Front Psychol 2, 236. https://doi.org/10.3389/fpsyg.2011.00236

Grea, H., Pisella, L., Rossetti, Y., Desmurget, M., Tilikete, C., Grafton, S., Prablanc, C., Vighetto, A., 2002. A lesion of the posterior parietal cortex disrupts on-line adjustments during aiming movements. Neuropsychologia 40, 2471–2480.

Greenhouse, I., King, M., Noah, S., Maddock, R.J., Ivry, R.B., 2017. Individual Differences in Resting Corticospinal Excitability Are Correlated with Reaction Time and GABA Content in Motor Cortex. J. Neurosci. Off. J. Soc. Neurosci. 37, 2686–2696. https://doi.org/10.1523/JNEUROSCI.3129-16.2017

Greenhouse, I., Sias, A., Labruna, L., Ivry, R.B., 2015. Nonspecific Inhibition of the Motor System during Response Preparation. J. Neurosci. Off. J. Soc. Neurosci. 35, 10675–10684. https://doi.org/10.1523/JNEUROSCI.1436-15.2015

Groppe, D.M., Makeig, S., Kutas, M., 2009. Identifying reliable independent components via split-half comparisons. Neuroimage 45, 1199–1211. https://doi.org/10.1016/j.neuroimage.2008.12.038

Groppe, D.M., Urbach, T.P., Kutas, M., 2011. Mass univariate analysis of event-related brain potentials/fields I: a critical tutorial review. Psychophysiology 48, 1711–1725. https://doi.org/10.1111/j.1469-8986.2011.01273.x

Gruber, T., Muller, M.M., Keil, A., Elbert, T., 1999. Selective visual-spatial attention alters induced gamma band responses in the human EEG. Clin. Neurophysiol. Off. J. Int. Fed. Clin. Neurophysiol. 110, 2074–2085.

Gwin, J.T., Ferris, D.P., 2012. An EEG-based study of discrete isometric and isotonic human lower limb muscle contractions. J. NeuroEngineering Rehabil. 9, 35. https://doi.org/10.1186/1743-0003-9-35

Haith, A., Krakauer, J., 2013. Model-Based and Model-Free Mechanisms of Human Motor Learning. Advances in experimental medicine and biology 782, 1–21. https://doi.org/10.1007/978-1-4614-5465-6_1

Hallett, M., 2007. Transcranial magnetic stimulation: a primer. Neuron 55, 187–99. https://doi.org/10.1016/j.neuron.2007.06.026

Hammond, G., 2002. Correlates of human handedness in primary motor cortex: a review and hypothesis. Neurosci Biobehav Rev 26, 285–92.

Hannah, R., Cavanagh, S.E., Tremblay, S., Simeoni, S., Rothwell, J.C., 2018. Selective Suppression of Local Interneuron Circuits in Human Motor Cortex Contributes to Movement Preparation. J. Neurosci. Off. J. Soc. Neurosci. 38, 1264–1276. https://doi.org/10.1523/JNEUROSCI.2869-17.2017

Hardwick, R.M., Rottschy, C., Miall, R.C., Eickhoff, S.B., 2013. A quantitative meta-analysis and review of motor learning in the human brain. Neuroimage 67, 283–97. https://doi.org/10.1016/j.neuroimage.2012.11.020

Harrington, A., Hammond-Tooke, G.D., 2015. Theta Burst Stimulation of the Cerebellum Modifies the TMS-Evoked N100 Potential, a Marker of GABA Inhibition. PloS One 10, e0141284. https://doi.org/10.1371/journal.pone.0141284

Harris, J.E., Eng, J.J., 2006. Individuals with the dominant hand affected following stroke demonstrate less impairment than those with the nondominant hand affected. Neurorehabil Neural Repair 20, 380–389. https://doi.org/10.1177/1545968305284528

Hashimoto, T., Inaba, D., Matsumura, M., Naito, E., 2004. Two different effects of transcranial magnetic stimulation to the human motor cortex during the pre-movement period. Neurosci. Res. 50, 427–436. https://doi.org/10.1016/j.neures.2004.08.002

Heffner, R.S., Masterton, R.B., 1983. The Role of the Corticospinal Tract in the Evolution of Human Digital Dexterity. Brain. Behav. Evol. 23, 165–183. https://doi.org/10.1159/000121494

Heimer, L., 1995. The human brain and spinal cord: functional neuroanatomy and dissection guide. Springer-Verlag.

Herculano-Houzel, S., 2009. The human brain in numbers: a linearly scaled-up primate brain. Front. Hum. Neurosci. 3, 31–31. https://doi.org/10.3389/neuro.09.031.2009

Hermens, H.J., Freriks, B., Disselhorst-Klug, C., Rau, G., 2000. Development of recommendations for SEMG sensors and sensor placement procedures. J. Electromyogr. Kinesiol. Off. J. Int. Soc. Electrophysiol. Kinesiol. 10, 361–374.

Herrmann, C.S., Struber, D., Helfrich, R.F., Engel, A.K., 2016. EEG oscillations: From correlation to causality. Int. J. Psychophysiol. Off. J. Int. Organ. Psychophysiol. 103, 12–21. https://doi.org/10.1016/j.ijpsycho.2015.02.003

Hervé, P.-Y., Crivello, F., Perchey, G., Mazoyer, B., Tzourio-Mazoyer, N., 2006. Handedness and cerebral anatomical asymmetries in young adult males. Neuroimage 29, 1066–1079. https://doi.org/10.1016/j.neuroimage.2005.08.031

Hervé, P.-Y., Leonard, G., Perron, M., Pike, B., Pitiot, A., Richer, L., Veillette, S., Pausova, Z., Paus, T., 2009. Handedness, motor skills and

maturation of the corticospinal tract in the adolescent brain. Human brain mapping 30, 3151—3162. https://doi.org/10.1002/hbm.20734

Hervé, P.-Y., Mazoyer, B., Crivello, F., Perchey, G., Tzourio-Mazoyer, N., 2005. Finger tapping, handedness and grey matter amount in the Rolando's genu area. Neuroimage 25, 1133–1145. https://doi.org/10.1016/j.neuroimage.2004.12.062

Hess, C.W., Mills, K.R., Murray, N.M., 1987. Responses in small hand muscles from magnetic stimulation of the human brain. J. Physiol. 388, 397–419.

Hess, C.W., Mills, K.R., Murray, N.M.F., 1986. Magnetic stimulation of the human brain: facilitation of motor responses by voluntary contraction of ipsilateral and contralateral muscles with additional observations on an amputee. Neurosci. Lett. 71, 235–240.

Hochberg, L.R., Bacher, D., Jarosiewicz, B., Masse, N.Y., Simeral, J.D., Vogel, J., Haddadin, S., Liu, J., Cash, S.S., Van Der Smagt, P., 2012. Reach and grasp by people with tetraplegia using a neurally controlled robotic arm. Nature 485, 372.

Hogan, A.M., Vargha-Khadem, F., Saunders, D.E., Kirkham, F.J., Baldeweg, T., 2006. Impact of frontal white matter lesions on performance monitoring: ERP evidence for cortical disconnection. Brain 129, 2177–88. https://doi.org/10.1093/brain/awl160

Hollerbach, M.J., Flash, T., 1982. Dynamic interactions between limb segments during planar arm movement. Biol. Cybern. 44, 67–77.

Holroyd, C.B., Coles, M.G.H., 2002. The neural basis of human error processing: reinforcement learning, dopamine, and the error-related negativity. Psychol Rev 109, 679–709. https://doi.org/10.1037/0033-295x.109.4.679

Hortobágyi, T., Taylor, J.L., Petersen, N.T., Russell, G., Gandevia, S.C., 2003. Changes in segmental and motor cortical output with contralateral muscle contractions and altered sensory inputs in humans. J. Neurophysiol. 90, 2451–2459.

Hosp, J., Luft, A., 2011. Cortical Plasticity during Motor Learning and Recovery after Ischemic Stroke. Neural plasticity 2011, 871296. https://doi.org/10.1155/2011/871296

Houweling, S., Daffertshofer, A., van Dijk, B.W., Beek, P.J., 2008. Neural changes induced by learning a challenging perceptual-motor task. NeuroImage 41, 1395–1407. https://doi.org/10.1016/j.neuroimage.2008.03.023

Howatson, G., Taylor, M.B., Rider, P., Motawar, B.R., McNally, M.P., Solnik, S., DeVita, P., Hortobágyi, T., 2011. Ipsilateral motor cortical responses to TMS during lengthening and shortening of the contralateral wrist flexors. Eur. J. Neurosci. 33, 978–990.

Howells, H., Thiebaut de Schotten, M., Dell'Acqua, F., Beyh, A., Zappalà, G., Leslie, A., Simmons, A., Murphy, D.G., Catani, M., 2018. Frontoparietal Tracts Linked to Lateralized Hand Preference and Manual Specialization. Cereb. Cortex 28, 2482–2494. https://doi.org/10.1093/cercor/bhy040

Huang, V.S., Krakauer, J.W., 2009. Robotic neurorehabilitation: a computational motor learning perspective. J Neuroeng Rehabil 6, 5. https://doi.org/10.1186/1743-0003-6-5

Huberdeau, D.M., Krakauer, J.W., Haith, A.M., 2015. Dual-process decomposition in human sensorimotor adaptation. Mot. Circuits Action 33, 71–77. https://doi.org/10.1016/j.conb.2015.03.003

Hummel, F.C., Cohen, L.G., 2005. Drivers of brain plasticity. Curr. Opin. Neurol. 18, 667–674.

Hummel, F.C., Steven, B., Hoppe, J., Heise, K., Thomalla, G., Cohen, L.G., Gerloff, C., 2009. Deficient intracortical inhibition (SICI) during movement preparation after chronic stroke. Neurology 72, 1766–1772. https://doi.org/10.1212/WNL.0b013e3181a609c5

Hunter, T., Sacco, P., Nitsche, M.A., Turner, D.L., 2009. Modulation of internal model formation during force field-induced motor learning by anodal transcranial direct current stimulation of primary motor cortex. J Physiol 587, 2949–61. https://doi.org/10.1113/jphysiol.2009.169284

Hunter, T., Sacco, P., Turner, D.L., 2011. Changes in Excitability of the Motor Cortex Associated with Internal Model Formation during Intrinsic Visuomotor Learning in the Upper Arm. J. Behav. Brain Sci. Vol.01No.03, 13.

Hyvärinen, A., Oja, E., 1997. A Fast Fixed-Point Algorithm for Independent Component Analysis. Neural Comput. 9, 1483–1492. https://doi.org/10.1162/neco.1997.9.7.1483

Ingram, J.N., Kording, K.P., Howard, I.S., Wolpert, D.M., 2008. The statistics of natural hand movements. Exp Brain Res 188, 223–236. https://doi.org/10.1007/s00221-008-1355-3

Ilic, T.V., Ziemann, U., 2005. Exploring motor cortical plasticity using transcranial magnetic stimulation in humans. Ann. N. Y. Acad. Sci. 1048, 175–184. https://doi.org/10.1196/annals.1342.016

Illert, M., Tanaka, R., 1978. Integration in descending motor pathways controlling the forelimb in the cat. 4. Corticospinal inhibition of forelimb motoneurones mediated by short propriospinal neurones. Exp. Brain Res. 31, 131–141.

Ilmoniemi, R.J., Kičić, D., 2009. Methodology for Combined TMS and EEG. Brain Topogr. 22, 233. https://doi.org/10.1007/s10548-009-0123-4

Inghilleri, M., Berardelli, A., Cruccu, G., Manfredi, M., 1993. Silent period evoked by transcranial stimulation of the human cortex and cervicomedullary junction. J. Physiol. 466, 521–534.

Isa, T., 2017. The Brain Is Needed to Cure Spinal Cord Injury. Trends Neurosci. 40, 625–636. https://doi.org/10.1016/j.tins.2017.08.002

Iscan, Z., Nazarova, M., Fedele, T., Blagovechtchenski, E., Nikulin, V.V., 2016. Pre-stimulus Alpha Oscillations and Inter-subject Variability of Motor Evoked Potentials in Single- and Paired-Pulse TMS Paradigms. Front. Hum. Neurosci. 10. https://doi.org/10.3389/fnhum.2016.00504

Izawa, J., Rane, T., Donchin, O., Shadmehr, R., 2008. Motor adaptation as a process of reoptimization. J. Neurosci. Off. J. Soc. Neurosci. 28, 2883–2891. https://doi.org/10.1523/JNEUROSCI.5359-07.2008

Jasper, H., 1958. Progress and problems in brain research. J. Mt. Sinai Hosp. N. Y. 25, 244–253.

Jung, P., Ziemann, U., 2009. Homeostatic and non-homeostatic modulation of learning in human motor cortex. J Neurosci 29, 5597–5604. https://doi.org/10.1523/JNEUROSCI.0222-09.2009

Kalaska, J.F., Cohen, D.A., Hyde, M.L., Prud'homme, M., 1989. A comparison of movement direction-related versus load direction-related activity in primate motor cortex, using a two-dimensional reaching task. J. Neurosci. Off. J. Soc. Neurosci. 9, 2080–2102.

Kappenman, E., Luck, S., 2012. The Oxford Handbook of Event-Related Potential Components. https://doi.org/10.1093/oxfordhb/9780195374148.001.0001

Kasuga, S., Matsushika, Y., Kasashima-Shindo, Y., Kamatani, D., Fujiwara, T., Liu, M., Ushiba, J., 2015. Transcranial direct current stimulation enhances mu rhythm desynchronisation during motor imagery that depends on handedness. Laterality 20, 453–468. https://doi.org/10.1080/1357650X.2014.998679

Kawato, M., Wolpert, D., 1998. Internal models for motor control. Novartis Found. Symp. 218, 291–304; discussion 304-307.

Kazumoto, S., B., P.S., James, H., William, H., Yu-ichi, N., Nortina, S., M., M.J., Steve, V., C., K.M., 2017. Laterality of motor cortical function measured by transcranial magnetic stimulation threshold tracking. Muscle Nerve 55, 424–427. https://doi.org/10.1002/mus.25372

Keil, J., Timm, J., SanMiguel, I., Schulz, H., Obleser, J., Schönwiesner, M., 2014. Cortical brain states and corticospinal synchronization influence TMS-evoked motor potentials. Journal of neurophysiology 111, 513–519.

Kennefick, M., Maslovat, D., Carlsen, A.N., 2014. The Time Course of Corticospinal Excitability during a Simple Reaction Time Task. PLOS ONE 9, e113563. https://doi.org/10.1371/journal.pone.0113563

Kertesz, A., Geschwind, N., 1971. Patterns of pyramidal decussation and their relationship to handedness. Arch Neurol 24, 326–32.

Kičić, D., Lioumis, P., Ilmoniemi, R.J., Nikulin, V.V., 2008. Bilateral changes in excitability of sensorimotor cortices during unilateral movement: Combined electroencephalographic and transcranial magnetic stimulation study. Neuroscience 152, 1119–1129. https://doi.org/10.1016/j.neuroscience.2008.01.043

Kilavik, B.E., Confais, J., Riehle, A., 2014. Signs of timing in motor cortex during movement preparation and cue anticipation. Adv. Exp. Med. Biol. 829, 121–142. https://doi.org/10.1007/978-1-4939-1782-2_7

Kilner, J.M., Baker, S.N., Salenius, S., Hari, R., Lemon, R.N., 2000. Human cortical muscle coherence is directly related to specific motor parameters. J. Neurosci. Off. J. Soc. Neurosci. 20, 8838–45.

Kim, B.-R., Moon, W.-J., Kim, H., Jung, E., Lee, J., 2016. Transcranial Magnetic Stimulation and Diffusion Tensor Tractography for Evaluating Ambulation after Stroke. J. Stroke 18, 220–226. https://doi.org/10.5853/jos.2015.01767

Kleinjung, T., Steffens, T., Londero, A., Langguth, B., 2007. Transcranial magnetic stimulation (TMS) for treatment of chronic tinnitus: clinical effects. Prog. Brain Res. 166, 359–367. https://doi.org/10.1016/S0079-6123(07)66034-8

Klem, G.H., Luders, H.O., Jasper, H.H., Elger, C., 1999. The ten-twenty electrode system of the International Federation. The International Federation of Clinical Neurophysiology. Electroencephalogr. Clin. Neurophysiol. Suppl. 52, 3–6.

Kline, J.P., 2004. Frontal EEG asymmetry, emotion, and psychopathology: The first, and the next 25 years. Biological Psychology 67, 1–5. https://doi.org/10.1016/j.biopsycho.2004.03.001

Klove, H., 1963. Clinical Neuropsychology. Med. Clin. North Am. 47, 1647–1658.

Kluzik, J., Diedrichsen, J., Shadmehr, R., Bastian, A.J., 2008. Reach adaptation: what determines whether we learn an internal model of the tool or adapt the model of our arm? J. Neurophysiol. 100, 1455–1464. https://doi.org/10.1152/jn.90334.2008

Kobayashi, M., Hutchinson, S., Theoret, H., Schlaug, G., Pascual-Leone, A., 2004. Repetitive TMS of the motor cortex improves ipsilateral sequential simple finger movements. Neurology 62, 91–98. https://doi.org/10.1212/wnl.62.1.91

Kobayashi, M., Théoret, H., Pascual-Leone, A., 2009. Suppression of ipsilateral motor cortex facilitates motor skill learning. Eur. J. Neurosci. 29, 833–836. https://doi.org/10.1111/j.1460-9568.2009.06628.x

Koski, L., Schrader, L.M., Wu, A.D., Stern, J.M., 2005. Normative data on changes in transcranial magnetic stimulation measures over a ten hour period. Clinical Neurophysiology 116, 2099–2109. https://doi.org/10.1016/j.clinph.2005.06.006

Kolasinski, J., Hinson, E.L., Divanbeighi Zand, A.P., Rizov, A., Emir, U.E., Stagg, C.J., 2019. The dynamics of cortical GABA in human motor learning. J. Physiol. 597, 271–282. https://doi.org/10.1113/JP276626

Komssi, S., Aronen, H.J., Huttunen, J., Kesaniemi, M., Soinne, L., Nikouline, V.V., Ollikainen, M., Roine, R.O., Karhu, J., Savolainen, S., Ilmoniemi, R.J., 2002. Ipsi- and contralateral EEG reactions to transcranial magnetic stimulation. Clin. Neurophysiol. Off. J. Int. Fed. Clin. Neurophysiol. 113, 175–184.

Komssi, S., Kähkönen, S., Ilmoniemi, R.J., 2004. The effect of stimulus intensity on brain responses evoked by transcranial magnetic stimulation. Hum. Brain Mapp. 21, 154–164.

Kondo, T., Yoshihara, Y., Yoshino-Saito, K., Sekiguchi, T., Kosugi, A., Miyazaki, Y., Nishimura, Y., Okano, H.J., Nakamura, M., Okano, H., Isa, T., Ushiba, J., 2015. Histological and electrophysiological analysis of the corticospinal pathway to forelimb motoneurons in common marmosets. Neurosci. Res. 98, 35–44. https://doi.org/10.1016/j.neures.2015.05.001

Korhonen, R.J., Hernandez-Pavon, J.C., Metsomaa, J., Maki, H., Ilmoniemi, R.J., Sarvas, J., 2011. Removal of large muscle artifacts from transcranial magnetic stimulation-evoked EEG by independent component analysis. Med. Biol. Eng. Comput. 49, 397–407. https://doi.org/10.1007/s11517-011-0748-9

Krakauer, J.W., Pine, Z.M., Ghilardi, M.-F., Ghez, C., 2000. Learning of Visuomotor Transformations for Vectorial Planning of Reaching Trajectories. The Journal of Neuroscience 20, 8916–8924.

Krebs, H. I., Brashers-Krug, T., Rauch, S.L., Savage, C.R., Hogan, N., Rubin, R.H., Fischman, A.J., Alpert, N.M., 1998. Robot-aided functional imaging: application to a motor learning study. Hum Brain Mapp 6, 59–72.

Krebs, H.I., Hogan, N., Hening, W., Adamovich, S.V., Poizner, H., 2001. Procedural motor learning in Parkinson's disease. Exp. Brain Res. 141, 425–437. https://doi.org/10.1007/s002210100871

Krieg, S.M., Sollmann, N., Hauck, T., Ille, S., Foerschler, A., Meyer, B., Ringel, F., 2013. Functional Language Shift to the Right Hemisphere in Patients with Language-Eloquent Brain Tumors. PLOS ONE 8, e75403. https://doi.org/10.1371/journal.pone.0075403

Krigolson, O.E., Cheng, D., Binsted, G., 2015. The role of visual processing in motor learning and control: Insights from electroencephalography. -Line Vis. Control Action 110, 277–285. https://doi.org/10.1016/j.visres.2014.12.024

Krigolson, O.E., Holroyd, C.B., 2006. Evidence for hierarchical error processing in the human brain. Neuroscience 137, 13–7. https://doi.org/10.1016/j.neuroscience.2005.10.064

Kuchenbecker, K.J., Gurari, N., Okamura, A.M., 2007. Effects of visual and proprioceptive motion feedback on human control of targeted movement, in: 2007 IEEE 10th International Conference on Rehabilitation Robotics. IEEE, pp. 513–524.

Kuhlman, W.N., 1978. Functional topography of the human mu rhythm. Electroencephalogr. Clin. Neurophysiol. 44, 83–93.

Kuypers, H., 1981. Anatomy of the Descending Pathways. https://doi.org/10.1002/cphy.cp010213

Kwon, Y.M., Kwon, H.G., Rose, J., Son, S.M., 2016. The Change of Intra-cerebral CST Location during Childhood and Adolescence; Diffusion Tensor Tractography Study. Front. Hum. Neurosci. 10, 638–638. https://doi.org/10.3389/fnhum.2016.00638

Lage, G.M., Ugrinowitsch, H., Apolinario-Souza, T., Vieira, M.M., Albuquerque, M.R., Benda, R.N., 2015. Repetition and variation in motor practice: A review of neural correlates. Neurosci Biobehav Rev 57, 132–41. https://doi.org/10.1016/j.neubiorev.2015.08.012

Larsson, M., 2017. Did heart asymmetry play a role in the evolution of human handedness? J. Cult. Cogn. Sci. 1, 65–76. https://doi.org/10.1007/s41809-017-0009-z

Latash, M.L., Levin, M.F., Scholz, J.P., Schöner, G., 2010. Motor control theories and their applications. Medicina (Kaunas) 46, 382–392.

Lehmann, D., Skrandies, W., 1980. Reference-free identification of components of checkerboard-evoked multichannel potential fields. Electroencephalogr Clin Neurophysiol 48, 609–21.

Lemon, R.N., 2008. Descending pathways in motor control. Annu. Rev. Neurosci. 31, 195–218. https://doi.org/10.1146/annurev.neuro.31.060407.125547

Lemon, R.N., Griffiths, J., 2005. Comparing the function of the corticospinal system in different species: organizational differences for motor specialization? Muscle Nerve 32, 261–279. https://doi.org/10.1002/mus.20333

Leocani, L., Cohen, L.G., Wassermann, E.M., Ikoma, K., Hallett, M., 2000a. Human corticospinal excitability evaluated with transcranial magnetic stimulation during different reaction time paradigms. Brain 123 (Pt 6), 1161–73.

Leocani, L., Cohen, L.G., Wassermann, E.M., Ikoma, K., Hallett, M., 2000b. Human corticospinal excitability evaluated with transcranial magnetic stimulation during different reaction time paradigms. Brain J. Neurol. 123 (Pt 6), 1161–1173.

Li, X., Jahanmiri-Nezhad, F., Rymer, W.Z., Zhou, P., 2012. An Examination of the Motor Unit Number Index (MUNIX) in muscles paralyzed by spinal cord injury. IEEE Trans Inf Technol Biomed 16, 1143–1149. https://doi.org/10.1109/TITB.2012.2193410

Liew, S.-L., Garrison, K.A., Ito, K.L., Heydari, P., Sobhani, M., Werner, J., Damasio, H., Winstein, C.J., Aziz-Zadeh, L., 2018. Laterality of Poststroke Cortical Motor Activity during Action Observation Is Related to Hemispheric Dominance. Neural Plasticity 2018, 14

Linden, D.E.J., Turner, D.L., 2016. Real-time functional magnetic resonance imaging neurofeedback in motor neurorehabilitation. Curr. Opin. Neurol. 29, 412–8.

Lioumis, P., Kicic, D., Savolainen, P., Makela, J.P., Kahkonen, S., 2009. Reproducibility of TMS-Evoked EEG responses. Human brain mapping 30, 1387–96. https://doi.org/10.1002/hbm.20608

Lissek, S., Vallana, G.S., Gunturkun, O., Dinse, H., Tegenthoff, M., 2013. Brain activation in motor sequence learning is related to the level of native cortical excitability. PloS One 8, e61863. https://doi.org/10.1371/journal.pone.0061863

Liu, J., Sheng, Y., Liu, H., 2019. Cortico-muscular Coherence and Its Applications: A Review. Front. Hum. Neurosci. 13, 100. https://doi.org/10.3389/fnhum.2019.00100

Ljubisavljevic, M., 2006. Transcranial magnetic stimulation and the motor learning-associated cortical plasticity. Exp. Brain Res. 173, 215–222. https://doi.org/10.1007/s00221-006-0538-z

Luber, B., Lisanby, S.H., 2014. Enhancement of human cognitive performance using transcranial magnetic stimulation (TMS). NeuroImage 85 Pt 3, 961–970. https://doi.org/10.1016/j.neuroimage.2013.06.007

Lüdemann-Podubecká, J., Bösl, K., Theilig, S., Wiederer, R., Nowak, D.A., 2015. The Effectiveness of 1Hz rTMS Over the Primary Motor Area of the Unaffected Hemisphere to Improve Hand Function After Stroke Depends on Hemispheric Dominance. Brain Stimulation: Basic, Translational, and Clinical Research in Neuromodulation 8, 823–830. https://doi.org/10.1016/j.brs.2015.02.004

Lynch, A., Lee, H.M., Bhat, A., Galloway, J.C., 2008. No stable arm preference during the pre-reaching period: a comparison of right and left hand kinematics with and without a toy present. Dev. Psychobiol. 50, 390–398. https://doi.org/10.1002/dev.20297

Macdonell, R.A.L., Shapiro, B.E., Chiappa, K.H., Helmers, S.L., Cros, D., Day, B.J., Shahani, B.T., 1991. Hemispheric threshold differences for motor evoked potentials produced by magnetic coil stimulation. Neurology 41, 1441–1441.

MacLean, S.J., Hassall, C.D., Ishigami, Y., Krigolson, O.E., Eskes, G.A., 2015. Using brain potentials to understand prism adaptation: the error-related negativity and the P300. Front Hum Neurosci 9, 335. https://doi.org/10.3389/fnhum.2015.00335

MacNeilage, P.F., Rogers, L.J., Vallortigara, G., 2009. Origins of the left & right brain. Sci. Am. 301, 60–67.

Manganotti, P., Acler, M., Masiero, S., Del Felice, A., 2015. TMS-evoked N100 responses as a prognostic factor in acute stroke. Funct. Neurol. 30, 125–130.

Martin, J.H., 2005. The corticospinal system: from development to motor control. The Neuroscientist 11, 161–173.

Martini, F., Timmons, M.J., Tallitsch, R.B., 2012. Human Anatomy. Pearson Benjamin Cummings.

Matsumoto, J., Fujiwara, T., Takahashi, O., Liu, M., Kimura, A., Ushiba, J., 2010. Modulation of mu rhythm desynchronisation during motor imagery by transcranial direct current stimulation. J. Neuroengineering Rehabil. 7, 27. https://doi.org/10.1186/1743-0003-7-27

Maynard, E.M., Hatsopoulos, N.G., Ojakangas, C.L., Acuna, B.D., Sanes, J.N., Normann, R.A., Donoghue, J.P., 1999. Neuronal interactions improve cortical population coding of movement direction. J. Neurosci. Off. J. Soc. Neurosci. 19, 8083–8093.

McDonnell, M.N., Orekhov, Y., Ziemann, U., 2006. The role of GABA(B) receptors in intracortical inhibition in the human motor cortex. Exp Brain Res 173, 86–93. https://doi.org/10.1007/s00221-006-0365-2

McDonnell, M.N., Stinear, C.M., 2017. TMS measures of motor cortex function after stroke: A meta-analysis. Brain Stimul 10, 721–734. https://doi.org/10.1016/j.brs.2017.03.008

McGregor, H.R., Vesia, M., Rinchon, C., Chen, R., Gribble, P., 2017. Changes in corticospinal excitability associated with motor learning by observing. bioRxiv. https://doi.org/10.1101/205385

McManus, C., 2002. Right hand, left hand: The origins of asymmetry in brains, bodies, atoms and cultures., Right hand, left hand: The origins of asymmetry in brains, bodies, atoms and cultures. Harvard University Press, Cambridge, MA, US.

McMillan, S., Ivry, R.B., Byblow, W.D., 2006. Corticomotor excitability during a choice-hand reaction time task. Exp. Brain Res. 172, 230–245.

Meyer, B.U., Voss, M., 2000. Delay of the execution of rapid finger movement by magnetic stimulation of the ipsilateral hand-associated motor cortex. Exp. Brain Res. 134, 477–482.

Miall, R.C., Weir, D.J., Stein, J.F., 1986. Manual tracking of visual targets by trained monkeys. Behav. Brain Res. 20, 185–201.

Miall, R.C., Weir, D.J., Stein, J.F., 1985. Visuomotor tracking with delayed visual feedback. Neuroscience 16, 511–520.

Michel, G.F., 2018. How Might the Relation of the Development of Hand Preferences to the Development of Cognitive Functions be Examined During Infancy: A Sketch? Front. Neurosci. 11, 739. https://doi.org/10.3389/fnins.2017.00739

Michel, G.F., Ovrut, M.R., Harkins, D.A., 1985. Hand-use preference for reaching and object manipulation in 6- through 13-month-old infants. Genet. Soc. Gen. Psychol. Monogr. 111, 407–427.

Milner, T.E., Franklin, D.W., 2005. Impedance control and internal model use during the initial stage of adaptation to novel dynamics in humans. J. Physiol. 567, 651–664. https://doi.org/10.1113/jphysiol.2005.090449

Minsky, M., 1988. Society of mind. Simon and Schuster.

Morange, F., Bloch, H., 1996. Lateralization of the Approach Movement and the Prehension Movement in Infants from 4 to 7 Months. Early Dev. Parent. 5, 81–92. https://doi.org/10.1002/(SICI)1099-0917(199606)5:2<81::AID-EDP119>3.0.CO;2-M

Mountcastle, V.B., 1997. The columnar organization of the neocortex. Brain J. Neurol. 120, 701–722.

Muellbacher, W., Facchini, S., Boroojerdi, B., Hallett, M., 2000. Changes in motor cortex excitability during ipsilateral hand muscle activation in humans. https://doi.org/10.1016/S1388-2457(99)00243-6

Muller, K., Kass-Iliyya, F., Reitz, M., 1997. Ontogeny of ipsilateral corticospinal projections: a developmental study with transcranial magnetic stimulation. Ann Neurol 42, 705–711. https://doi.org/10.1002/ana.410420506

Muller, G.R., Neuper, C., Rupp, R., Keinrath, C., Gerner, H.J., Pfurtscheller, G., 2003. Event-related beta EEG changes during wrist movements induced by functional electrical stimulation of forearm muscles in man. Neurosci. Lett. 340, 143–147.

Murphy, J., C Wong, Y., C Kwan, H., 1985. Sequential activation of neurons in primate motor cortex during unrestrained forelimb movement. https://doi.org/10.1152/jn.1985.53.2.435

Mutanen, T.P., Kukkonen, M., Nieminen, J.O., Stenroos, M., Sarvas, J., Ilmoniemi, R.J., 2016. Recovering TMS-evoked EEG responses masked by muscle artifacts. NeuroImage 139, 157–166. https://doi.org/10.1016/j.neuroimage.2016.05.028

Muthukumaraswamy, S.D., 2013. High-frequency brain activity and muscle artifacts in MEG/EEG: a review and recommendations. Front. Hum. Neurosci. 7, 138–138. https://doi.org/10.3389/fnhum.2013.00138

Muthuraman, M., Hellriegel, H., Hoogenboom, N., Anwar, A.R., Mideksa, K.G., Krause, H., Schnitzler, A., Deuschl, G., Raethjen, J., 2014. Beamformer Source Analysis and Connectivity on Concurrent EEG and MEG Data during Voluntary Movements. PLOS ONE 9, e91441. https://doi.org/10.1371/journal.pone.0091441

Naranjo, J.R., Brovelli, A., Longo, R., Budai, R., Kristeva, R., Battaglini, P.P., 2007. EEG dynamics of the frontoparietal network during reaching preparation in humans. NeuroImage 34, 1673–1682. https://doi.org/10.1016/j.neuroimage.2006.07.049

Nathan, P.W., Smith, M.C., Deacon, P., 1990. The corticospinal tracts in man. Course and location of fibres at different segmental levels. Brain J. Neurol. 113 (Pt 2), 303–324.

Navarro de Lara, L.I., Tik, M., Woletz, M., Frass-Kriegl, R., Moser, E., Laistler, E., Windischberger, C., 2017. High-sensitivity TMS/fMRI of the Human Motor Cortex Using a Dedicated Multichannel MR Coil. NeuroImage 150, 262–269. https://doi.org/10.1016/j.neuroimage.2017.02.062

Netz, J., Lammers, T., Homberg, V., 1997. Reorganization of motor output in the non-affected hemisphere after stroke. Brain 120 (Pt 9), 1579–1586. https://doi.org/10.1093/brain/120.9.1579

Nichols-Larsen, D.S., Clark, P.C., Zeringue, A., Greenspan, A., Blanton, S., 2005. Factors influencing stroke survivors' quality of life during subacute recovery. Stroke 36, 1480–4.

Nikolova, M., Pondev, N., Christova, L., Wolf, W., Kossev, A.R., 2006. Motor cortex excitability changes preceding voluntary muscle activity in simple reaction time task. Eur. J. Appl. Physiol. 98, 212–219. https://doi.org/10.1007/s00421-006-0265-y

Nikouline, V., Ruohonen, J., Ilmoniemi, R.J., 1999. The role of the coil click in TMS assessed with simultaneous EEG. Clin. Neurophysiol. Off. J. Int. Fed. Clin. Neurophysiol. 110, 1325–1328.

Nikulin, V.V., Kicic, D., Kahkonen, S., Ilmoniemi, R.J., 2003. Modulation of electroencephalographic responses to transcranial magnetic stimulation: evidence for changes in cortical excitability related to movement. Eur. J. Neurosci. 18, 1206–1212.

Noskin, O., Krakauer, J.W., Lazar, R.M., Festa, J.R., Handy, C., O'Brien, K.A., Marshall, R.S., 2008. Ipsilateral motor dysfunction from unilateral stroke: implications for the functional neuroanatomy of hemiparesis. J Neurol Neurosurg Psychiatry 79, 401–406. https://doi.org/10.1136/jnnp.2007.118463

Nowak, D.A., Topka, H., Timmann, D., Boecker, H., Hermsdorfer, J., 2007. The role of the cerebellum for predictive control of grasping. Cerebellum Lond. Engl. 6, 7–17. https://doi.org/10.1080/14734220600776379

Nowak, M., Hinson, E., van Ede, F., Pogosyan, A., Guerra, A., Quinn, A., Brown, P., Stagg, C.J., 2017. Driving Human Motor Cortical Oscillations Leads to Behaviorally Relevant Changes in Local GABAA Inhibition: A tACS-TMS Study. J. Neurosci. Off. J. Soc. Neurosci. 37, 4481–4492. https://doi.org/10.1523/JNEUROSCI.0098-17.2017

Nowak, M., Zich, C., Stagg, C.J., 2018. Motor Cortical Gamma Oscillations: What Have We Learnt and Where Are We Headed? Curr. Behav. Neurosci. Rep. 5, 136–142. https://doi.org/10.1007/s40473-018-0151-z

Nuzzo, J.L., Trajano, G.S., Barry, B.K., Gandevia, S.C., Taylor, J.L., 2016. Arm posture-dependent changes in corticospinal excitability are largely spinal in origin. J Neurophysiol 115, 2076–2082. https://doi.org/10.1152/jn.00885.2015

Ocklenburg, S., Friedrich, P., Schmitz, J., Schlüter, C., Genç, E., Güntürkün, O., Peterburs, J., Grimshaw, G., 2018. Beyond frontal alpha: investigating hemispheric asymmetries over the EEG frequency spectrum as a function of sex and handedness. Laterality: Asymmetries of Body, Brain and Cognition 24, 1–20. https://doi.org/10.1080/1357650X.2018.1543314

Oldfield, R.C., 1971. The assessment and analysis of handedness: the Edinburgh inventory. Neuropsychologia 9, 97–113.

Olivier, E., Edgley, S.A., Armand, J., Lemon, R.N., 1997. An Electrophysiological Study of the Postnatal Development of the Corticospinal System in the Macaque Monkey. J. Neurosci. 17, 267. https://doi.org/10.1523/JNEUROSCI.17-01-00267.1997

Onton, J., Westerfield, M., Townsend, J., Makeig, S., 2006. Imaging human EEG dynamics using independent component analysis. Neurosci. Biobehav. Rev. 30, 808–822. https://doi.org/10.1016/j.neubiorev.2006.06.007

Orth, M., Rothwell, J.C., 2004. The cortical silent period: intrinsic variability and relation to the waveform of the transcranial magnetic stimulation pulse. Clin Neurophysiol 115, 1076–82. https://doi.org/10.1016/j.clinph.2003.12.025

Ostry, D.J., Gribble, P.L., 2016. Sensory Plasticity in Human Motor Learning. Trends Neurosci. 39, 114–123. https://doi.org/10.1016/j.tins.2015.12.006

Ozdenizci, O., Yalcin, M., Erdogan, A., Patoglu, V., Grosse-Wentrup, M., Cetin, M., 2017. Electroencephalographic identifiers of motor adaptation learning. J Neural Eng 14, 046027. https://doi.org/10.1088/1741-2552/aa6abd

Papousek, I., Schulter, G., 1999. EEG correlates of behavioural laterality: Right handedness. Perceptual and Motor Skills 89, 403–411. https://doi.org/10.2466/PMS.89.6.403-411

Park, D.-H., Shin, C.-J., 2017. Asymmetrical Electroencephalographic Change of Human Brain During Sleep Onset Period. Psychiatry Investig 14, 839–843. https://doi.org/10.4306/pi.2017.14.6.839

Park, H., Kim, J.S., Paek, S.H., Jeon, B.S., Lee, J.Y., Chung, C.K., 2009. Cortico-muscular coherence increases with tremor improvement after deep brain stimulation in Parkinson's disease. Neuroreport 20, 1444–1449. https://doi.org/10.1097/WNR.0b013e328331a51a

Parma, V., Brasselet, R., Zoia, S., Bulgheroni, M., Castiello, U., 2017. The origin of human handedness and its role in pre-birth motor control. Sci. Rep. 7, 16804. https://doi.org/10.1038/s41598-017-16827-y

Patton, J.L., Mussa-Ivaldi, F.A., 2004. Robot-assisted adaptive training: custom force fields for teaching movement patterns. IEEE transactions on bio-medical engineering 51, 636–46.

Patton, J.L., Stoykov, M.E., Kovic, M., Mussa-Ivaldi, F.A., 2006. Evaluation of robotic training forces that either enhance or reduce error in chronic hemiparetic stroke survivors. Exp. Brain Res. 168, 368–83.

Paus, T., Sipila, P.K., Strafella, A.P., 2001. Synchronization of Neuronal Activity in the Human Primary Motor Cortex by Transcranial Magnetic Stimulation: An EEG Study. J. Neurophysiol. 86, 1983–1990. https://doi.org/10.1152/jn.2001.86.4.1983

Pellicciari, M.C., Bonni, S., Ponzo, V., Cinnera, A.M., Mancini, M., Casula, E.P., Sallustio, F., Paolucci, S., Caltagirone, C., Koch, G., 2018. Dynamic reorganization of TMS-evoked activity in subcortical stroke patients. NeuroImage 175, 365–378. https://doi.org/10.1016/j.neuroimage.2018.04.011

Pellicciari, M.C., Veniero, D., Miniussi, C., 2017. Characterizing the Cortical Oscillatory Response to TMS Pulse. Front. Cell. Neurosci. 11, 38. https://doi.org/10.3389/fncel.2017.00038

Pelvig, D.P., Pakkenberg, H., Stark, A.K., Pakkenberg, B., 2008. Neocortical glial cell numbers in human brains. Neurobiol. Aging 29, 1754–1762. https://doi.org/10.1016/j.neurobiolaging.2007.04.013

Penfield, W., Boldrey, E., 1937. Somatic motor and sensory representation in the cerebral cortex of man as studied by electrical stimulation. Brain J. Neurol. 60, 389–443.

Perelle, I.B., Ehrman, L., 2005. On the Other Hand. Behav. Genet. 35, 343–350. https://doi.org/10.1007/s10519-005-3226-z

Perez, M.A., Butler, J.E., Taylor, J.L., 2013. Modulation of transcallosal inhibition by bilateral activation of agonist and antagonist proximal arm muscles. J. Neurophysiol. 111, 405–414.

Perez, M.A., Cohen, L.G., 2008. Mechanisms underlying functional changes in the primary motor cortex ipsilateral to an active hand. J. Neurosci. Off. J. Soc. Neurosci. 28, 5631–5640. https://doi.org/10.1523/JNEUROSCI.0093-08.2008

Perfetti, B., Moisello, C., Landsness, E.C., Kvint, S., Pruski, A., Onofrj, M., Tononi, G., Ghilardi, M.F., 2011. Temporal evolution of oscillatory activity predicts performance in a choice-reaction time reaching task. J. Neurophysiol. 105, 18–27. https://doi.org/10.1152/jn.00778.2010

Peternel, L., Sigaud, O., Babič, J., 2017. Unifying Speed-Accuracy Trade-Off and Cost-Benefit Trade-Off in Human Reaching Movements. Front. Hum. Neurosci. 11, 615. https://doi.org/10.3389/fnhum.2017.00615

Petrichella, S., Johnson, N., He, B., 2017. The influence of corticospinal activity on TMS-evoked activity and connectivity in healthy subjects: A TMS-EEG study. PloS One 12, e0174879. https://doi.org/10.1371/journal.pone.0174879

Pfurtscheller, G., Andrew, C., 1999. Event-Related changes of band power and coherence: methodology and interpretation. J Clin Neurophysiol 16, 512–9.

Pfurtscheller, G., Aranibar, A., 1979. Evaluation of event-related desynchronisation (ERD) preceding and following voluntary self-paced movement. Electroencephalogr. Clin. Neurophysiol. 46, 138–146.

Pfurtscheller, G., Neuper, C., Ramoser, H., Muller-Gerking, J., 1999. Visually guided motor imagery activates sensorimotor areas in humans. Neurosci. Lett. 269, 153–156.

Pistohl, T., Jackson, A., Gowrishankar, G., Joshi, D., Nazarpour, K., 2013. Artificial proprioception for myoelectric control. Conf. Proc. Annu. Int. Conf. IEEE Eng. Med. Biol. Soc. IEEE Eng. Med. Biol. Soc. Annu. Conf. 2013, 1595–1598. https://doi.org/10.1109/EMBC.2013.6609820

Pizzamiglio, S., 2017. Neuroimaging of human motor control in real world scenarios: from lab to urban environment. University of East London.

Pizzamiglio, S., De Lillo, M., Naeem, U., Abdalla, H., Turner, D.L., 2017a. High-Frequency Intermuscular Coherence between Arm Muscles during Robot-Mediated Motor Adaptation. Frontiers in Physiology 7, 668. https://doi.org/10.3389/fphys.2016.00668

Pizzamiglio, S., Desowska, A., Shojaii, P., Taga, M., Turner, D.L., 2017b. Muscle co-contraction patterns in robot-mediated force field learning to guide specific muscle group training. NeuroRehabilitation 41, 17–29. https://doi.org/10.3233/nre-171453

Pollok, B., Latz, D., Krause, V., Butz, M., Schnitzler, A., 2014. Changes of motor-cortical oscillations associated with motor learning. Neuroscience 275, 47–53.

Porter, R., Lemon, R., 1993. Corticospinal function and voluntary movement. Oxford University Press, USA.

Poston, B., Kukke, S.N., Paine, R.W., Francis, S., Hallett, M., 2012. Cortical silent period duration and its implications for surround inhibition of a hand muscle. Eur. J. Neurosci. 36, 2964–2971. https://doi.org/10.1111/j.1460-9568.2012.08212.x

Premoli, I., Castellanos, N., Rivolta, D., Belardinelli, P., Bajo, R., Zipser, C., Espenhahn, S., Heidegger, T., Muller-Dahlhaus, F., Ziemann, U., 2014. TMS-EEG signatures of GABAergic neurotransmission in the human cortex. J Neurosci 34, 5603–12. https://doi.org/10.1523/jneurosci.5089-13.2014

Propper, R., Pierce, J., Geisler, M., Christman, S., Bellorado, N., 2012. Asymmetry in Resting Alpha Activity: Effects of Handedness. Open Journal of Medical Psychology 01, 86–90. https://doi.org/10.4236/ojmp.2012.14014

Provins, K.A., 1992. Early infant motor asymmetries and handedness: A critical evaluation of the evidence. Dev. Neuropsychol. 8, 325–365. https://doi.org/10.1080/87565649209540531

Quoilin, C., Lambert, J., Jacob, B., Klein, P.-A., Duque, J., 2016. Comparison of Motor Inhibition in Variants of the Instructed-Delay Choice Reaction Time Task. PLOS ONE 11, e0161964. https://doi.org/10.1371/journal.pone.0161964

Rademacher, J., Bürgel, U., Geyer, S., Schormann, T., Schleicher, A., Freund, H.J., Zilles, K., 2001. Variability and asymmetry in the human precentral motor systemA cytoarchitectonic and myeloarchitectonic brain mapping study. Brain 124, 2232–2258. https://doi.org/10.1093/brain/124.11.2232

Ramsay, D.S., 1985. Fluctuations in unimanual hand preference in infants following the onset of duplicated syllable babbling. Dev. Psychol. 21, 318–324. https://doi.org/10.1037/0012-1649.21.2.318

Rappelsberger, P., Pfurtscheller, G., Filz, O., 1994. Calculation of event-related coherence--a new method to study short-lasting coupling between brain areas. Brain Topogr 7, 121–7.

Reichenbach, A., Thielscher, A., Peer, A., Bülthoff, H.H., Bresciani, J.-P., 2009. Seeing the hand while reaching speeds up on-line responses to a sudden change in target position. J. Physiol. 587, 4605–4616. https://doi.org/10.1113/jphysiol.2009.176362

Reynolds, C., Ashby, P., 1999. Inhibition in the human motor cortex is reduced just before a voluntary contraction. Neurology 53, 730–735.

Ridding, M.C., Rothwell, J.C., 2007. Is there a future for therapeutic use of transcranial magnetic stimulation? Nat Rev Neurosci 8, 559–567. https://doi.org/10.1038/nrn2169

Riddle, C.N., Baker, S.N., 2005. Manipulation of peripheral neural feedback loops alters human cortico-muscular coherence. J. Physiol. 566, 625–39.

Rimsky-Robert, D., Charpier, S., Corlier, J., Le Van Quyen, M., Lehongre, K., Adam, C., Navarro, V., Clémenceau, S., Lachaux, J.-P., Valderrama, M., Bastin, J., Kahane, P., 2016. Self-induced intracerebral gamma oscillations in the human cortex. Brain 139, 3084–3091. https://doi.org/10.1093/brain/aww246

Rioult-Pedotti, M.S., Friedman, D., Donoghue, J.P., 2000. Learning-induced LTP in neocortex. Science 290, 533–536. https://doi.org/10.1126/science.290.5491.533

Rioult-Pedotti, M.S., Friedman, D., Hess, G., Donoghue, J.P., 1998. Strengthening of horizontal cortical connections following skill learning. Nat Neurosci 1, 230–234. https://doi.org/10.1038/678

Rizzolatti, G., Arbib, M.A., 1998. Language within our grasp. Trends Neurosci. 21, 188–194.

Rodgers, H., Bosomworth, H., Krebs, H.I., van Wijck, F., Howel, D., Wilson, N., Aird, L., Alvarado, N., Andole, S., Cohen, D.L., Dawson, J., Fernandez-Garcia, C., Finch, T., Ford, G.A., Francis, R., Hogg, S., Hughes, N., Price, C.I., Ternent, L., Turner, D.L., Vale, L., Wilkes, S., Shaw, L., 2019. Robot assisted training for the upper limb after stroke (RATULS): a multicentre randomised controlled trial. The Lancet. https://doi.org/10.1016/S0140-6736(19)31055-4

Rogasch, N.C., Daskalakis, Z.J., Fitzgerald, P.B., 2013. Mechanisms underlying long-interval cortical inhibition in the human motor cortex: a TMS-EEG study. J. Neurophysiol. 109, 89–98.

Rogasch, N.C., Sullivan, C., Thomson, R.H., Rose, N.S., Bailey, N.W., Fitzgerald, P.B., Farzan, F., Hernandez-Pavon, J.C., 2017. Analysing concurrent transcranial magnetic stimulation and electroencephalographic data: A review and introduction to the open-source TESA software. NeuroImage 147, 934–951. https://doi.org/10.1016/j.neuroimage.2016.10.031

Rogasch, N.C., Thomson, R.H., Farzan, F., Fitzgibbon, B.M., Bailey, N.W., Hernandez-Pavon, J.C., Daskalakis, Z.J., Fitzgerald, P.B., 2014. Removing artefacts from TMS-EEG recordings using independent component analysis: importance for assessing prefrontal and motor cortex network properties. NeuroImage 101, 425–439. https://doi.org/10.1016/j.neuroimage.2014.07.037

Rogers, L.J., Zucca, P., Vallortigara, G., 2004. Advantages of having a lateralized brain. Proc. Biol. Sci. 271 Suppl 6, S420–S422. https://doi.org/10.1098/rsbl.2004.0200

Rosanova, M., Casali, A., Bellina, V., Resta, F., Mariotti, M., Massimini, M., 2009. Natural frequencies of human corticothalamic circuits. J Neurosci 29, 7679–85. https://doi.org/10.1523/jneurosci.0445-09.2009

Rossi, S., Hallett, M., Rossini, P.M., Pascual-Leone, A., 2009. Safety, ethical considerations, and application guidelines for the use of transcranial magnetic stimulation in clinical practice and research. Clin. Neurophysiol. Off. J. Int. Fed. Clin. Neurophysiol. 120, 2008–2039. https://doi.org/10.1016/j.clinph.2009.08.016

Rossini, P.M., Burke, D., Chen, R., Cohen, L.G., Daskalakis, Z., Di Iorio, R., Di Lazzaro, V., Ferreri, F., Fitzgerald, P.B., George, M.S., Hallett, M., Lefaucheur, J.P., Langguth, B., Matsumoto, H., Miniussi, C., Nitsche, M.A., Pascual-Leone, A., Paulus, W., Rossi, S., Rothwell, J.C., Siebner, H.R., Ugawa, Y., Walsh, V., Ziemann, U., 2015. Non-invasive electrical and magnetic stimulation of the brain, spinal cord, roots and peripheral nerves: Basic principles and procedures for routine clinical and research application. An updated report from an I.F.C.N. Committee. Clin Neurophysiol 126, 1071–107. https://doi.org/10.1016/j.clinph.2015.02.001

Rossini, P.M., Rossi, S., 1998. Clinical applications of motor evoked potentials. Electroencephalography Clin Neurophysiology 106, 180–194. https://doi.org/10.1016/s0013-4694(97)00097-7

Rothwell, J., Thompson, P., Day, B., Boyd, S., Marsden, C., 1991. Stimulation of the human motor cortex through the scalp. Exp. Physiol. 76, 159–200. https://doi.org/10.1113/expphysiol.1991.sp003485

Ruff, C.C., Driver, J., Bestmann, S., 2009. Combining TMS and fMRI: from "virtual lesions" to functional-network accounts of cognition. Cortex J. Devoted Study Nerv. Syst. Behav. 45, 1043–1049. https://doi.org/10.1016/j.cortex.2008.10.012

Rumelhart, D.E., Hinton, G.E., Williams, R.J., 1986. Learning representations by back-propagating errors. Nature 323, 533–536. https://doi.org/10.1038/323533a0

Sainburg, R.L., 2014. Convergent models of handedness and brain lateralization. Front. Psychol. 5, 1092. https://doi.org/10.3389/fpsyg.2014.01092

Sainburg, R.L., Duff, S.V., 2006. Does motor lateralization have implications for stroke rehabilitation? J Rehabil Res Dev 43, 311–322.

Sainburg, R.L., Kalakanis, D., 2000. Differences in control of limb dynamics during dominant and nondominant arm reaching. J. Neurophysiol. 83, 2661–75.

Saisanen, L., Pirinen, E., Teitti, S., Kononen, M., Julkunen, P., Maatta, S., Karhu, J., 2008. Factors influencing cortical silent period: optimized stimulus location, intensity and muscle contraction. J. Neurosci. Methods 169, 231–238. https://doi.org/10.1016/j.jneumeth.2007.12.005

Sato, S., Bergmann, T.O., Borich, M.R., 2015. Opportunities for concurrent transcranial magnetic stimulation and electroencephalography to characterize cortical activity in stroke. Front. Hum. Neurosci. 9.

Scharoun, S.M., Bryden, P.J., 2014. Hand preference, performance abilities, and hand selection in children. Front. Psychol. 5, 82–82. https://doi.org/10.3389/fpsyg.2014.00082

Schaworonkow, N., Triesch, J., Ziemann, U., Zrenner, C., 2019. EEG-triggered TMS reveals stronger brain state-dependent modulation of motor evoked potentials at weaker stimulation intensities. Brain Stimul. Basic Transl. Clin. Res. Neuromodulation 12, 110–118. https://doi.org/10.1016/j.brs.2018.09.009

Scheidt, R.A., Stoeckmann, T., 2007. Reach adaptation and final position control amid environmental uncertainty after stroke. J Neurophysiol 97, 2824–2836. https://doi.org/10.1152/jn.00870.2006

Schintu, S., Martin-Arevalo, E., Vesia, M., 2016. Paired-Pulse Parietal-Motor Stimulation Differentially Modulates Corticospinal Excitability across Hemispheres When Combined with Prism Adaptation 2016, 5716179. https://doi.org/10.1155/2016/5716179

Schomer, D.L., Silva, F.H.L. da, Wadman, W.J., Silva, F.H.L. da, 2017. Biophysical Aspects of EEG and MEG Generation, in: Niedermeyer's ElectroencephalographyBasic Principles, Clinical Applications, and Related Fields. Oxford University Press, Oxford, UK.

Schwartz, A.B., 2016. Movement: How the Brain Communicates with the World. Cell 164, 1122–1135. https://doi.org/10.1016/j.cell.2016.02.038

Schwartz, A.B., 2007. Useful signals from motor cortex. J. Physiol. 579, 581–601. https://doi.org/10.1113/jphysiol.2006.126698

Schwartz, A.B., Moran, D.W., 1999. Motor cortical activity during drawing movements: population representation during lemniscate tracing. J. Neurophysiol. 82, 2705–18.

Schwerin, S., Dewald, J.P., Haztl, M., Jovanovich, S., Nickeas, M., MacKinnon, C., 2008. Ipsilateral versus contralateral cortical motor projections to a shoulder adductor in chronic hemiparetic stroke: implications for the expression of arm synergies. Exp. Brain Res. 185, 509–519.

Schwerin, S.C., Yao, J., Dewald, J.P., 2011. Using paired pulse TMS to facilitate contralateral and ipsilateral MEPs in upper extremity muscles of chronic hemiparetic stroke patients. J. Neurosci. Methods 195, 151–160.

Scott, S.H., 2012. The computational and neural basis of voluntary motor control and planning. Trends Cogn. Sci. 16, 541–549. https://doi.org/10.1016/j.tics.2012.09.008

Scott, S.H., 2004. Optimal feedback control and the neural basis of volitional motor control. Nat. Rev. Neurosci. 5, 532.

Scott, S.H., 2000. Role of motor cortex in coordinating multi-joint movements: is it time for a new paradigm? Can. J. Physiol. Pharmacol. 78, 923–933.

Scott, S.H., Cluff, T., Lowrey, C.R., Takei, T., 2015. Feedback control during voluntary motor actions. Curr Opin Neurobiol 33, 85–94. https://doi.org/10.1016/j.conb.2015.03.006

Seidler, R.D., Kwak, Y., Fling, B.W., Bernard, J.A., 2013. Neurocognitive Mechanisms of Error-Based Motor Learning. Adv. Exp. Med. Biol. 782, 10.1007/978-1-4614-5465–6_3. https://doi.org/10.1007/978-1-4614-5465-6_3

Serrien, D.J., Brown, P., 2003. The integration of cortical and behavioural dynamics during initial learning of a motor task. Eur. J. Neurosci. 17, 1098–1104.

Shadmehr, R., 2010. From Equilibrium Point to Optimal Control. Motor Control 14, e25–e30. https://doi.org/10.1123/mcj.14.3.e25

Shadmehr, R., Holcomb, H.H., 1997. Neural correlates of motor memory consolidation. Science 277, 821–5.

Shadmehr, R., Krakauer, J.W., 2008. A computational neuroanatomy for motor control. Exp. Brain Res. 185, 359–381. https://doi.org/10.1007/s00221-008-1280-5

Shadmehr, R., Mussa-Ivaldi, F.A., 1994. Adaptive representation of dynamics during learning of a motor task. The Journal of neuroscience: the official journal of the Society for Neuroscience 14, 3208–24.

Shadmehr, R., Smith, M.A., Krakauer, J.W., 2010. Error correction, sensory prediction, and adaptation in motor control. Annu Rev Neurosci 33, 89–108. https://doi.org/10.1146/annurev-neuro-060909-153135

Shadmehr, R., Wise, S.P., 2005. The computational neurobiology of reaching and pointing: A foundation for motor learning., The computational neurobiology of reaching and pointing: A foundation for motor learning. MIT Press, Cambridge, MA, US.

Shishov, N., Melzer, I., Bar-Haim, S., 2017. Parameters and Measures in Assessment of Motor Learning in Neurorehabilitation; A Systematic

Review of the Literature. Front. Hum. Neurosci. 11, 82–82. https://doi.org/10.3389/fnhum.2017.00082

Shitara, H., Shinozaki, T., Takagishi, K., Honda, M., Hanakawa, T., 2013. Movement and afferent representations in human motor areas: a simultaneous neuroimaging and transcranial magnetic/peripheral nerve-stimulation study. Front. Hum. Neurosci. 7, 554. https://doi.org/10.3389/fnhum.2013.00554

Shojaii, P., Turner, D., 2019. The posterior parietal cortex has a greater role than the supplementary motor area in novel motor behaviour: A TMS-based virtual disruption study. Brain Stimul. Basic Transl. Clin. Res. Neuromodulation 12, 432–433. https://doi.org/10.1016/j.brs.2018.12.402

Siebner, H.R., Dressnandt, J., Auer, C., Conrad, B., 1998. Continuous intrathecal baclofen infusions induced a marked increase of the transcranially evoked silent period in a patient with generalized dystonia. Muscle Nerve 21, 1209–1212. https://doi.org/10.1002/(sici)1097-4598(199809)21:9<1209::aid-mus15>3.0.co;2-m

Simon, S.R., Meunier, M., Piettre, L., Berardi, A.M., Segebarth, C.M., Boussaoud, D., 2002. Spatial attention and memory versus motor preparation: premotor cortex involvement as revealed by fMRI. J. Neurophysiol. 88, 2047–2057. https://doi.org/10.1152/jn.2002.88.4.2047

Smith, M.A., Shadmehr, R., 2005. Intact ability to learn internal models of arm dynamics in Huntington's disease but not cerebellar degeneration. J. Neurophysiol. 93, 2809–2821. https://doi.org/10.1152/jn.00943.2004

Spampinato, D.A., Block, H.J., 2017. Cerebellar-M1 Connectivity Changes Associated with Motor Learning Are Somatotopic Specific 37, 2377–2386. https://doi.org/10.1523/jneurosci.2511-16.2017

Stagg, C.J., Bachtiar, V., Johansen-Berg, H., 2011. The role of GABA in human motor learning. Curr. Biol. CB 21, 480–484. https://doi.org/10.1016/j.cub.2011.01.069

Stancák, A., 2006. Cortical oscillatory changes occurring during somatosensory and thermal stimulation. Prog. Brain Res. 159, 237–252. https://doi.org/10.1016/s0079-6123(06)59016-8

Stefan, K., Wycislo, M., Gentner, R., Schramm, A., Naumann, M., Reiners, K., Classen, J., 2006. Temporary occlusion of associative motor cortical plasticity by prior dynamic motor training. Cereb. Cortex N. Y. N 1991 16, 376–385. https://doi.org/10.1093/cercor/bhi116

Stemmer, B., Segalowitz, S.J., Witzke, W., Schonle, P.W., 2004. Error detection in patients with lesions to the medial prefrontal cortex: an ERP study. Neuropsychologia 42, 118–30.

Stinear, C.M., Byblow, W.D., 2004. Impaired modulation of intracortical inhibition in focal hand dystonia. Cereb. Cortex N. Y. N 1991 14, 555–561. https://doi.org/10.1093/cercor/bhh017

Storti, S.F., Formaggio, E., Manganotti, P., Menegaz, G., 2016. Brain Network Connectivity and Topological Analysis During Voluntary Arm Movements. Clin EEG Neurosci 47, 276–290. https://doi.org/10.1177/1550059415598905

Strobbe, G., 2015. Advanced forward models for EEG source imaging.

Swick, D., Turken, A.U., 2002. Dissociation between conflict detection and error monitoring in the human anterior cingulate cortex. Proc Natl Acad Sci U A 99, 16354–9. https://doi.org/10.1073/pnas.252521499

Takiyama, K., Sakai, Y., 2016. Balanced motor primitive can explain generalization of motor learning effects between unimanual and bimanual movements. Sci. Rep. 6, 23331.

Tallon-Baudry, C., Kreiter, A., Bertrand, O., 1999. Sustained and transient oscillatory responses in the gamma and beta bands in a visual short-term memory task in humans. Vis Neurosci 16, 449–59.

Tan, H., Wade, C., Brown, P., 2016. Post-Movement Beta Activity in Sensorimotor Cortex Indexes Confidence in the Estimations from Internal Models. J. Neurosci. 36, 1516–1528. https://doi.org/10.1523/jneurosci.3204-15.2016

Tanji, J., Okano, K., Sato, K.C., 1988. Neuronal activity in cortical motor areas related to ipsilateral, contralateral, and bilateral digit movements of the monkey. J. Neurophysiol. 60, 325–343. https://doi.org/10.1152/jn.1988.60.1.325

Tarkka, I.M., Hallett, M., 1991. The cortical potential related to sensory feedback from voluntary movements shows somatotopic organization of the supplementary motor area. Brain Topogr 3, 359–63.

ter Braack, E.M., de Vos, C.C., van Putten, M.J., 2015. Masking the Auditory Evoked Potential in TMS-EEG: A Comparison of Various Methods. Brain Topogr 28, 520–8. https://doi.org/10.1007/s10548-013-0312-z

Thiebaut de Schotten, M., Ffytche, D.H., Bizzi, A., Dell'Acqua, F., Allin, M., Walshe, M., Murray, R., Williams, S.C., Murphy, D.G., Catani, M., 2011. Atlasing location, asymmetry and inter-subject variability of white matter tracts in the human brain with MR diffusion tractography. Neuroimage 54, 49–59. https://doi.org/10.1016/j.neuroimage.2010.07.055

Thoroughman, K.A., Shadmehr, R., 1999. Electromyographic correlates of learning an internal model of reaching movements. J Neurosci 19, 8573–88.

Thoroughman, K.A., Shadmehr, R., 2000. Learning of action through adaptive combination of motor primitives. Nature 407, 742–7.

Thut, G., Hauert, C., Viviani, P., Morand, S., Spinelli, L., Blanke, O., Landis, T., Michel, C., 2000. Internally driven vs. externally cued movement selection: a study on the timing of brain activity. Brain Res. Cogn. Brain Res. 9, 261–269.

Thut, G., Veniero, D., Romei, V., Miniussi, C., Schyns, P., Gross, J., 2011. Rhythmic TMS causes local entrainment of natural oscillatory signatures. Curr. Biol. CB 21, 1176–1185. https://doi.org/10.1016/j.cub.2011.05.049

Tiitinen, H., Virtanen, J., Ilmoniemi, R.J., Kamppuri, J., Ollikainen, M., Ruohonen, J., Naatanen, R., 1999. Separation of contamination caused by coil clicks from responses elicited by transcranial magnetic stimulation. Clin. Neurophysiol. Off. J. Int. Fed. Clin. Neurophysiol. 110, 982–985.

Tinazzi, M., Zanette, G., 1998. Modulation of ipsilateral motor cortex in man during unimanual finger movements of different complexities. Neurosci. Lett. 244, 121–124.

Todorov, E., Jordan, M.I., 2002. Optimal feedback control as a theory of motor coordination. Nature neuroscience 5, 1226–35.

Tofts, 1990. The distribution of induced currents in magnetic stimulation of the nervous system. Phys. Med. Biol. 35, 1119.

Torrecillos, F., Albouy, P., Brochier, T., Malfait, N., 2014. Does the processing of sensory and reward-prediction errors involve common neural resources? Evidence from a frontocentral negative potential modulated by movement execution errors. J Neurosci 34, 4845–56. https://doi.org/10.1523/jneurosci.4390-13.2014

Touzalin-Chretien, P., Ehrler, S., Dufour, A., 2009. Dominance of Vision over Proprioception on Motor Programming: Evidence from ERP. Cereb. Cortex 20, 2007–2016. https://doi.org/10.1093/cercor/bhp271

Tremblay, S., Rogasch, N.C., Premoli, I., Blumberger, D.M., Casarotto, S., Chen, R., Di Lazzaro, V., Farzan, F., Ferrarelli, F., Fitzgerald, P.B., Hui, J., Ilmoniemi, R.J., Kimiskidis, V.K., Kugiumtzis, D., Lioumis, P., Pascual-Leone, A., Pellicciari, M.C., Rajji, T., Thut, G., Zomorrodi, R., Ziemann, U., Daskalakis, Z.J., 2019. Clinical utility and prospective of TMS-EEG. Clin. Neurophysiol. Off. J. Int. Fed. Clin. Neurophysiol. 130, 802–844. https://doi.org/10.1016/j.clinph.2019.01.001

Triggs, W.J., Subramanium, B., Rossi, F., 1999. Hand preference and transcranial magnetic stimulation asymmetry of cortical motor representation. Brain Res 835, 324–329. https://doi.org/10.1016/s0006-8993(99)01629-7

Truccolo, W., Friehs, G.M., Donoghue, J.P., Hochberg, L.R., 2008. Primary motor cortex tuning to intended movement kinematics in humans with tetraplegia. J. Neurosci. Off. J. Soc. Neurosci. 28, 1163–78.

Turner, D.L., Ramos-Murguialday, A., Birbaumer, N., Hoffmann, U., Luft, A., 2013. Neurophysiology of robot-mediated training and therapy: a perspective for future use in clinical populations. Front. Neurol. 4, 184–184. https://doi.org/10.3389/fneur.2013.00184

Tyc, F., Boyadjian, A., 2006. Cortical plasticity and motor activity studied with transcranial magnetic stimulation. Rev Neurosci 17, 469–95.

Vahdat, S., Darainy, M., Milner, T.E., Ostry, D.J., 2011. Functionally specific changes in resting-state sensorimotor networks after motor learning. J. Neurosci. Off. J. Soc. Neurosci. 31, 16907–15.

Vahdat, S., Darainy, M., Ostry, D.J., 2014. Structure of plasticity in human sensory and motor networks due to perceptual learning. J. Neurosci. Off. J. Soc. Neurosci. 34, 2451–63.

van Beers, R.J., Sittig, A.C., Gon, J.J., 1999. Integration of proprioceptive and visual position-information: An experimentally supported model. J. Neurophysiol. 81, 1355–1364. https://doi.org/10.1152/jn.1999.81.3.1355

Van Der Werf, Y.D., Sadikot, A.F., Strafella, A.P., Paus, T., 2006. The neural response to transcranial magnetic stimulation of the human motor cortex. II. Thalamocortical contributions. Exp. Brain Res. 175, 246–255. https://doi.org/10.1007/s00221-006-0548-x

van Duinen, H., Renken, R., Maurits, N.M., Zijdewind, I., 2008. Relation between muscle and brain activity during isometric contractions of the first dorsal interosseus muscle. Hum. Brain Mapp. 29, 281–299. https://doi.org/10.1002/hbm.20388

van Wijk, B., Beek, P., Daffertshofer, A., 2012. Neural synchrony within the motor system: what have we learned so far? Front. Hum. Neurosci. 6, 252. https://doi.org/10.3389/fnhum.2012.00252

Velliste, M., Perel, S., Spalding, M.C., Whitford, A.S., Schwartz, A.B., 2008. Cortical control of a prosthetic arm for self-feeding. Nature 453, 1098.

Vernet, M., Bashir, S., Yoo, W.K., Perez, J.M., Najib, U., Pascual-Leone, A., 2013. Insights on the neural basis of motor plasticity induced by theta burst stimulation from TMS-EEG. Eur J Neurosci 37, 598–606. https://doi.org/10.1111/ejn.12069

Villringer, A., Long, X., Kuehn, E., Bazin, P.-L., Sereno, M.I., Schäfer, A., Dinse, J., Margulies, D.S., Jakobsen, E., 2017. Body Topography Parcellates Human Sensory and Motor Cortex. Cereb. Cortex 27, 3790–3805. https://doi.org/10.1093/cercor/bhx026

Volkmann, J., Schnitzler, A., Witte, O.W., Freund, H., 1998. Handedness and asymmetry of hand representation in human motor cortex. J Neurophysiol 79, 2149–2154. https://doi.org/10.1152/jn.1998.79.4.2149

Voss, P., Thomas, M.E., Cisneros-Franco, J.M., de Villers-Sidani, É., 2017. Dynamic Brains and the Changing Rules of Neuroplasticity: Implications for Learning and Recovery. Front. Psychol. 8, 1657–1657. https://doi.org/10.3389/fpsyg.2017.01657

Waldert, S., Preissl, H., Demandt, E., Braun, C., Birbaumer, N., Aertsen, A., Mehring, C., 2008. Hand Movement Direction Decoded from MEG and EEG. J. Neurosci. 28, 1000. https://doi.org/10.1523/JNEUROSCI.5171-07.2008

Walter, A., Ramos-Murguialday, A., Spüler, M., Rosenstiel, W., Birbaumer, N., Bogdan, M., 2012. Coupling BCI and cortical stimulation for brain-state-dependent stimulation: Methods for spectral estimation in the presence of stimulation after-effects. https://doi.org/10.3389/fncir.2012.00087

Wassermann, E.M., Fuhr, P., Cohen, L.G., Hallett, M., 1991. Effects of transcranial magnetic stimulation on ipsilateral muscles. Neurology 41, 1795–1799. https://doi.org/10.1212/wnl.41.11.1795

Werhahn, K.J., Kunesch, E., Noachtar, S., Benecke, R., Classen, J., 1999. Differential effects on motorcortical inhibition induced by blockade of GABA uptake in humans. J. Physiol. 517 (Pt 2), 591–597. https://doi.org/10.1111/j.1469-7793.1999.0591t.x

Westerhausen, R., Huster, R.J., Kreuder, F., Wittling, W., Schweiger, E., 2007. Corticospinal tract asymmetries at the level of the internal capsule: Is there an association with handedness? NeuroImage 37, 379–386. https://doi.org/10.1016/j.neuroimage.2007.05.047

Wiese, H., Stude, P., Sarge, R., Nebel, K., Diener, H.C., Keidel, M., 2005. Reorganization of motor execution rather than preparation in poststroke hemiparesis. Stroke 36, 1474–9. https://doi.org/10.1161/01.str.0000170639.26891.30

Wiesel, T.N., Hubel, D.H., 1965. Extent of recovery from the effects of visual deprivation in kittens. J. Neurophysiol. 28, 1060–1072. https://doi.org/10.1152/jn.1965.28.6.1060

Wilhelm, E., Quoilin, C., Petitjean, C., Duque, J., 2016. A Double-Coil TMS Method to Assess Corticospinal Excitability Changes at a Near-

Simultaneous Time in the Two Hands during Movement Preparation. Front. Hum. Neurosci. 10, 88–88. https://doi.org/10.3389/fnhum.2016.00088

Wise, S. & Shadmehr, R. ., 2002. Motor control. Elsevier Sci.

Witham, C.L., Wang, M., Baker, S.N., 2010. Cortico-muscular coherence between motor cortex, somatosensory areas and forearm muscles in the monkey. Front. Syst. Neurosci. 4, 38. https://doi.org/10.3389/fnsys.2010.00038

Wolpert, D., 2011. Transcript of "The real reason for brains" [WWW Document]. URL https://www.ted.com/talks/daniel_wolpert_the_real_reason_for_brains /transcript (accessed 6.22.19).

Wolpert, D.M., Miall, R.C., 1996. Forward Models for Physiological Motor Control. Neural Netw 9, 1265–1279.

Wolpert, D.M., Miall, R.C., Kawato, M., 1998. Internal models in the cerebellum. Trends Cogn. Sci. 2, 338–347.

Wong, A.L., Haith, A.M., Krakauer, J.W., 2014. Motor Planning. The Neuroscientist 21, 385–398. https://doi.org/10.1177/1073858414541484

Wu, J., Quinlan, E.B., Dodakian, L., McKenzie, A., Kathuria, N., Zhou, R.J., Augsburger, R., See, J., Le, V.H., Srinivasan, R., Cramer, S.C., 2015. Connectivity measures are robust biomarkers of cortical function and plasticity after stroke. Brain 138, 2359–69. https://doi.org/10.1093/brain/awv156

Wu, W., Keller, C.J., Rogasch, N.C., Longwell, P., Shpigel, E., Rolle, C.E., Etkin, A., 2018. ARTIST: A fully automated artifact rejection algorithm for single-pulse TMS-EEG data. Hum. Brain Mapp. 39, 1607–1625. https://doi.org/10.1002/hbm.23938

Yang, Y., Dewald, J.P.A., van der Helm, F., Schouten, A., 2017. Unveiling neural coupling within the sensorimotor system: directionality and nonlinearity. https://doi.org/10.1111/ejn.13692

Yoo, S.-S., Lee, J.-H., O'Leary, H., Panych, L.P., Jolesz, F.A., 2008. Neurofeedback fMRI-mediated learning and consolidation of regional brain activation during motor imagery. Int J Imaging Syst Technol 18, 69–78. https://doi.org/10.1002/ima.20139

Zaaroor, M., Pratt, H., Starr, A., 2003. Time course of motor excitability before and after a task-related movement. Neurophysiol. Clin. Clin. Neurophysiol. 33, 130–137.

Zewdie, E.T., Roy, F.D., Okuma, Y., Yang, J.F., Gorassini, M.A., 2014. Long-latency, inhibitory spinal pathway to ankle flexors activated by homonymous group 1 afferents. Journal of Neurophysiology 111, 2544–2553.

Zhou, W., Gotman, J., 2009. Automatic removal of eye movement artifacts from the EEG using ICA and the dipole model. Prog. Nat. Sci. 19, 1165–1170. https://doi.org/10.1016/j.pnsc.2008.11.013

Ziemann, U., 2017. Thirty years of transcranial magnetic stimulation: where do we stand? Exp. Brain Res. 1–12. https://doi.org/10.1007/s00221-016-4865-4

Ziemann, U., Hallett, M., 2001. Hemispheric asymmetry of ipsilateral motor cortex activation during unimanual motor tasks: further evidence for

motor dominance. Clinical neurophysiology: official journal of the International Federation of Clinical Neurophysiology 112, 107–13.

Ziemann, U., Ilic, T.V., Pauli, C., Meintzschel, F., Ruge, D., 2004. Learning modifies subsequent induction of long-term potentiation-like and long-term depression-like plasticity in human motor cortex. J. Neurosci. Off. J. Soc. Neurosci. 24, 1666–1672. https://doi.org/10.1523/JNEUROSCI.5016-03.2004

Ziemann, U., Ishii, K., Borgheresi, A., Yaseen, Z., Battaglia, F., Hallett, M., Cincotta, M., Wassermann, E.M., 1999. Dissociation of the pathways mediating ipsilateral and contralateral motor-evoked potentials in human hand and arm muscles. J Physiol 518 (Pt 3), 895–906. https://doi.org/10.1111/j.1469-7793.1999.0895p.x

Ziemann, U., Tergau, F., Netz, J., Homberg, V., 1997. Delay in simple reaction time after focal transcranial magnetic stimulation of the human brain occurs at the final motor output stage. Brain Res. 744, 32–40.

Zilles, K., Palomero-Gallagher, N., Schleicher, A., 2004. Transmitter receptors and functional anatomy of the cerebral cortex. J. Anat. 205, 417–432. https://doi.org/10.1111/j.0021-8782.2004.00357.x

Zrenner, C., Belardinelli, P., Müller-Dahlhaus, F., Ziemann, U., 2016. Closed-Loop Neuroscience and Non-Invasive Brain Stimulation: A Tale of Two Loops. Front. Cell. Neurosci. 10, 92–92. https://doi.org/10.3389/fncel.2016.00092

Appendix

A. Ethical Approval

A.1. Study I

8th February 2017

Dear Myriam,

Project Title:	**Understanding human cortical connectivity and excitability in healthy people and stroke patients using simultaneous Transcranial Magnetic Stimulation and Electro-Encephalography (TMS-EEG)**
Principal Investigator:	**Professor Duncan Turner**
Researcher:	**Myriam Taga**
Reference Number:	**UREC 1617 23**

I am writing to confirm the outcome of your application to the University Research Ethics Committee (UREC), which was considered by UREC on **Wednesday 18 January 2017.**

The decision made by members of the Committee is **Approved**. The Committee's response is based on the protocol described in the application form and supporting documentation. Your study has received ethical approval from the date of this letter.

Should you wish to make any changes in connection with your research project, this must be reported immediately to UREC. A Notification of Amendment form should be submitted for approval, accompanied by any additional or amended documents:
http://www.uel.ac.uk/wwwmedia/schools/graduate/documents/Notification-of-Amendment-to-Approved-Ethics-App-150115.doc

Any adverse events that occur in connection with this research project must be reported immediately to UREC.

Approved Research Site

I am pleased to confirm that the approval of the proposed research applies to the following research site.

Research Site	Principal Investigator / Local Collaborator
Neurorehabilitation Unit lab at the UEL Stratford campus	Professor Duncan Turner

The final list of documents reviewed and approved by the Committee is as follows:

Document	Version	Date
UREC application form	2.0	2 February 2017
Annexe 1. Medical questionnaire	1.0	8 December 2016
Annexe 2: Edinburgh Handedness Inventory	1.0	8 December 2016
Annexe 3: Advertising flyer/Email	1.0	8 December 2016
Annexe 4: Participant Information sheet	1.0	8 December 2016
Annexe 5: Consent form	1.0	8 December 2016

Approval is given on the understanding that the UEL Code of Practice in Research is adhered to.

The University will periodically audit a random sample of applications for ethical approval, to ensure that the research study is conducted in compliance with the consent given by the ethics Committee and to the highest standards of rigour and integrity.

Please note, it is your responsibility to retain this letter for your records.

With the Committee's wish best for the success of this project.

Yours sincerely,

Fernanda Silva

Administrative Officer for Research Governance

University Research Ethics Committee (UREC)

344

A.2. Study II-III

1st November 2017

Dear Myriam,

Project Title:	**Understanding human cortical connectivity and excitability** **using simultaneous Transcranial Magnetic Stimulation and** **Electro-Encephalography (TMS-EEG)**
Principal Investigator:	**Professor Duncan Turner**
Researcher:	**Myriam Taga**
Reference Number:	**EXP 1718 03**

I am writing to confirm the outcome of your application to the University Research Ethics Committee (UREC), which was considered by UREC on **Wednesday 1st November 2017.**

The decision made by members of the Committee is **Approved**. The Committee's response is based on the protocol described in the application form and supporting documentation. Your study has received ethical approval from the date of this letter.

Should you wish to make any changes in connection with your research project, this must be reported immediately to UREC. A Notification of Amendment form should be submitted for approval, accompanied by any additional or amended documents: http://www.uel.ac.uk/wwwmedia/schools/graduate/documents/Notification-of-Amendment-to-Approved-Ethics-App-150115.doc

Any adverse events that occur in connection with this research project must be reported immediately to UREC.

Approved Research Site

I am pleased to confirm that the approval of the proposed research applies to the following research site.

Approved Research Site

I am pleased to confirm that the approval of the proposed research applies to the following research site.

Research Site	Principal Investigator / Local Collaborator
Neurorehabilitation Unit lab at the UEL Stratford campus	Professor Duncan Turner

The final list of documents reviewed and approved by the Committee is as follows:

Document	Version	Date
UREC application form	3.0	19 October 2017
Annexe 1: Medical Questionnaire	2.0	18 October 2017
Annexe 2: Participant Information sheet	3.0	19 October 2017
Annexe 3: Edinburgh Handedness Inventory	2.0	18 October 2017
Annexe 4: Consent form	2.0	18 October 2017
Annexe 5: Advertisement/ Recruitment material	1.0	19 October 2017

Approval is given on the understanding that the UEL Code of Practice in Research is adhered to.

The University will periodically audit a random sample of applications for ethical approval, to ensure that the research study is conducted in compliance with the consent given by the ethics Committee and to the highest standards of rigour and integrity.

Please note, it is your responsibility to retain this letter for your records.

With the Committee's wish b**est** for the success of this project.

Yours sincerely,

Fernanda Silva

Administrative Officer for Research Governance

University Research Ethics Committee (UREC)

Email: **researchethics@uel.ac.uk**

B. Advertising Email/ Flyer

B.1. Study I

We are recruiting participants to take part in a study on hemispheric asymmetry related to handedness. This exciting project involves:

- Recording your brain activity
- Recording your muscle activity
- Handedness and hand skill assessment

If you are a right- or left-handed adult with no neurological history, you are eligible to take part in the study! So make sure to book your spot today, there are only 20 places available in each study group.

All the procedures are safe.

Your participation will lead to better understanding of hemispheric asymmetries which may reflect your handedness. In the future this study may help us to gain better insights in hemispheric imbalance between excitation and inhibition in stroke patients and could potentially lead to a better understanding of the pathology in order to design better neurorehabilitation therapies.
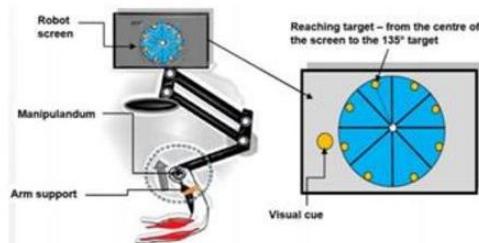
Please contact Myriam Taga u1621899@uel.ac.uk to record your interest and ask for the details.

Thank you!

Do you want to help us understand **how the brain controls arm movements?** Then come and participate in my study at UEL! You will not only help research but also get a **20 POUND AMAZON** voucher for participating!

Brain motor learning paradigm/ plasticity training.

Human brain after motor plasticity training.

Experiment Description:

We want to analyse the relationship between arm movements with brain activity. You will **play an interactive robot game** while we stimulate your brain with non-invasive brain stimulation and record your brain activity with electroencephalography (EEG).

Investigator/PhD student:

Myriam Taga

If you want to take part in the study, please email me: **m.taga@uel.ac.uk**

The Principal Investigator(s)

Professor Duncan Turner

School of Health, Sport and Bioscience,

University of East London, Stratford Campus,

London E15 4LZ +44 208 223 4514 [office] or 4065 [research lab] d.l.turner@uel.ac.uk

Duration of the study: The whole study with the preparation phase will take less than 3 hours.

Benefits of the study: There are no benefits of the study Risks involved Research Ethics Application Form February 2016 25. There are no medical risks to the participants of our study. Since we are collecting data only form 20 participants in each group of the study, the risk of identifying the data is a little increased, but we will use anonymizing procedures no make sure you will not be identified. Confidentiality of the Data You will be given a participant number and the data recorded will be stored under that number. The only time we ask your identifying data is the consent form that will be stored separately. The data will be kept at the research lab for 10 years for future analysis.

Location: The study will take place in the UEL Stratford campus Neurorehabilitation Unit research lab: room **UH 2.0.7**

Remuneration: After completing the experiment participants will receive a 20 pound amazon voucher. If the participant withdraws from the study half way through the experiment (without completing the experiment), the participant will get a 10 pound amazon voucher.

Disclaimer: You are not obliged to take part in this study, and are free to withdraw at any time during tests. Should you choose to withdraw from the programme you may do so without disadvantage to yourself and without any obligation to give a reason. If you decide to withdraw from the study, all the data gathered up to this point will be destroyed.

C. Medical Questionnaire

This questionnaire is designed for the purpose of understanding if you have any conditions that may result in excluding you from the research being conducted. All the data supplied in this questionnaire will remain private and confidential.

Date:
Participant Number:
Date of birth:
Gender: M / F
Handedness: Right / Left
Do you take any medication or recreational drugs?
Y / N
If Yes, state below:

_____

_____

How many units of alcohol do you consume per week on average:

_____

_____

Have you had any surgeries in the past?

_____

_____

Do you have any chronic illness?
Y / N
If Yes, state below:

_____

_____

Do you have any neurological disorders (e.g. stroke, spinal cord injury, colour blindness, dyslexia, Parkinson's or Alzheimer's disease, epilepsy/seizures, family history of these)?
Y / N
If Yes, state below:

_____

_____

Do you have a psychiatric history (e.g. schizophrenia, bipolar disorder, depression, obsessive-compulsive disorders, panic disorder, family history of these)? Y / N
If Yes, state below

_____

Do you have a cardio-respiratory Disease (asthma, angina, high blood pressure, respiratory distress)?
Y / N
If Yes, state below:

_____

_____

Do you have a musculoskeletal condition: (bone fracture, muscle or ligament tear)? Y / N
If Yes, state below:

_____

_____

Do you have any metal or electrical implants (e.g. pacemakers, intracranial plates, skeletal pins, vascular clips)?
Y / N
If Yes, state below:

_____

_____

If you are a woman are you pregnant or experiencing altered menstrual cycles?
Y / N
If Yes, state below:

_____

_____

D. Edinburgh Handedness Inventory

Please indicate with a one (1) your preference in using your left or right hand in the following tasks.

Where the preference is so strong you would never use the other hand, unless absolutely forced to, put a two (2).

If you are indifferent, put a one in each column (1 | 1).

Some of the activities require both hands. In these cases, the part of the task or object for which hand preference is wanted is indicated in parentheses.

Task / Object	Left Hand	Right Hand
1. Writing		
2. Drawing		
3. Throwing		
4. Scissors		
5. Toothbrush		
6. Knife (without fork)		
7. Spoon		
8. Broom (upper hand)		
9. Striking a Match (match)		
10. Opening a Box (lid)		
Total checks:	LH =	RH =
Cumulative Total	CT = LH + RH =	
Difference	D = RH − LH =	
Result	R = (D / CT) × 100 =	
Interpretation: (Left Handed: R < -40) (Ambidextrous: -40 ≤ R ≤ +40) (Right Handed: R > +40)		

E. Written Informed Consent

E.1. Study I

Consent to Participate in a Research Study

The purpose of this letter is to provide you with the information that you need to consider in deciding whether to participate in this study.

Project Title

Understanding the human cortical connectivity and excitability in healthy people and stroke patients using simultaneous Transcranial Magnetic Stimulation and Electro-Encephalography (TMS-EEG)

Project Description

Aim of the study

The purpose of the project is to use state of the art simultaneous transcranial magnetic stimulation (TMS) and electroencephalography (EEG) to investigate brain connectivity and excitability. We want to investigate how hemispheric asymmetries in the motor hand areas are correlated with handedness.

While you will be seated comfortably in a reclining chair, we will apply single and paired pulses of TMS over your motor cortex and record your brain activity and muscle hand activity.

Before that we will assess your handedness with a 10-item questionnaire and you will perform a small playful task in order to see which hand is your dominant.

Duration of the study

The whole study with the preparation phase will take about 3 hours.

Benefits of the study

There are no benefits of the study

Risks involved

There are no medical risks to the participants of our study. Since we are collecting data only form 20 participants in each group of the study, the risk of identifying the data is a little increased, but we will use anonymizing procedures no make sure you will not be identified.

Confidentiality of the Data

You will be given a participant number and the data recorded will be stored under that number. The only time we ask your identifying data is the consent form that will be stored separately. The data will be kept at the research lab for 10 years for future analysis.

Location

The study will take place in the UEL Stratford campus Neurorehabilitation Unit research lab.

Remuneration

There is no renumeration for the participation in the study.

Disclaimer

You are not obliged to take part in this study, and are free to withdraw at any time during tests. Should you choose to withdraw from the programme you may do so without disadvantage to yourself and without any obligation to give a reason. If you decide to withdraw from the study, all the data gathered up to this point will be destroyed.

Consent to Participate in a Programme Involving the Use of Human Participants.

Title:

Understanding the human cortical connectivity and excitability in healthy people and stroke patients using simultaneous Transcranial Magnetic Stimulation and Electro-Encephalography (TMS-EEG)

Researchers: The principle investigator: Professor Duncan Turner (BSc, PhD) Investigator/PhD student: Myriam Taga (BSc, MSc)

Please tick as appropriate:

	Yes	No
I have the read the information leaflet relating to the above programme of research in which I have been asked to participate and have been given a copy to keep. The nature and purposes of the research have been explained to me, and I have had the opportunity to discuss the details and ask questions about this information. I understand what is being proposed and the procedures in which I will be involved have been explained to me.		
I understand that my involvement in this study, and particular data from this research, will remain strictly confidential as far as possible. Only the researchers involved in the study will have access to the data. (Please see below)		
I understand that maintaining strict confidentiality is subject to the following limitations:		
If the sample size is small, or focus this may have implications for confidentiality / anonymity.		
My confidentiality will be maintained unless a disclosure is made that indicates that I or someone else is at serious risk of harm. Such disclosures may be reported to the relevant authority.		
I will be pseudo-anonymised in publications that will arise from the research.		
I am aware that the proposed methods of publication dissemination of research findings, includes: - Peer reviewed journals - Non-peer reviewed journals - Peer reviewed books - Publication in media or website - Conference presentation - Internal report - Promotional report and materials - Dissertation/Thesis - Presentation to participants or relevant community group		

I give permission for your team to use the data in future research.		
I give permission to be to be contacted for future research studies by your team. It has been explained to me what will happen once the programme has been completed.		
I understand that my participation in this study is entirely voluntary, and I am free to withdraw at any time during the research without disadvantage to myself and without being obliged to give any reason. I understand that my data can be withdrawn up to the point of data analysis and that after this point it may not be possible.		
I hereby freely and fully consent to participate in the study which has been fully explained to me and for the information obtained to be used in relevant research publications.		

Participant's Name (BLOCK CAPITALS)
………………………………………………………………………

Participant's Signature
……………………………………………………………………………………….

Investigator's Name (BLOCK CAPITALS)
……………………………………………………………………….

Investigator's Signature
………………………………………………………………………………………

Date: …………………………

END OF FORM.

E.2. Study II-III

University of East London Stratford Campus

London E15 4LZ England

University Research Ethics Committee

If you have any queries regarding the conduct of the programme in which you are being asked to participate, please contact:

Catherine Fieulleteau,

Research Integrity and Ethics Manager,

Graduate School, EB 1.43 University of East London,

Docklands Campus,

London E16 2RD

(Telephone: 020 8223 6683, Email: researchethics@uel.ac.uk).

The Principal Investigator(s)

Professor Duncan Turner

School of Health, Sport and Bioscience,

University of East London, Stratford Campus,

London E15 4LZ +44 208 223 4514 [office] or 4065 [research lab] d.l.turner@uel.ac.uk

Investigator/PhD student:

Myriam Taga m.taga@uel.ac.uk

Consent to Participate in a Research Study

The purpose of this letter is to provide you with the information that you need to consider in deciding whether to participate in this study.

Project Title

Understanding human cortical connectivity and excitability using simultaneous Transcranial Magnetic Stimulation and Electro-Encephalography (TMS-EEG)

Project Description

The purpose of the project is to use state of the art simultaneous transcranial magnetic stimulation (TMS) and electroencephalography (EEG) to investigate brain connectivity and excitability.

We want to analyse the relationship between arm movements with brain activity. You will play an interactive robot game while we stimulate your brain with non-invasive brain stimulation and record your brain activity with electroencephalography (EEG).

Duration of the study: The whole study with the preparation phase will take less than 3 hours.

Benefits of the study: There are no benefits of the study Risks involved Research Ethics Application Form February 2016 25. There are no medical risks to the participants of our study. Since we are collecting data only form 20 participants in each group of the study, the risk of identifying the data is a little increased, but we will use anonymizing procedures no make sure you will not be identified. Confidentiality of the Data You will be given a participant number and the data recorded will be stored under that number. The only time we ask your identifying data is the consent form that will be stored separately. The data will be kept at the research lab for 10 years for future analysis.

Location: The study will take place in the UEL Stratford campus Neurorehabilitation Unit research lab.

Remuneration: After completing the experiment participants will receive a 20 pound amazon voucher. If the participant withdraws from the study half way through the experiment, the participant will get a 10 pound amazon voucher.

Disclaimer: You are not obliged to take part in this study, and are free to withdraw at any time during tests. Should you choose to withdraw from the programme you may do so without disadvantage to yourself and without any obligation to give a reason. If you decide to withdraw from the study, all the data gathered up to this point will be destroyed.

Consent to Participate in a Programme Involving the Use of Human Participants.

Title:

Understanding the human cortical connectivity and excitability in healthy people and stroke patients using simultaneous Transcranial Magnetic Stimulation and Electro-Encephalography (TMS-EEG)

Researchers: The principle investigator: Professor Duncan Turner (BSc, PhD) Investigator/PhD student: Myriam Taga (BSc, MSc)

Please tick as appropriate:

	Yes	No
I have the read the information leaflet relating to the above programme of research in which I have been asked to participate and have been given a copy to keep. The nature and purposes of the research have been explained to me, and I have had the opportunity to discuss the details and ask questions about this information. I understand what is being proposed and the procedures in which I will be involved have been explained to me.		
I understand that my involvement in this study, and particular data from this research, will remain strictly confidential as far as possible. Only the researchers involved in the study will have access to the data. (Please see below)		
I understand that maintaining strict confidentiality is subject to the following limitations:		
If the sample size is small, or focus this may have implications for confidentiality / anonymity.		
My confidentiality will be maintained unless a disclosure is made that indicates that I or someone else is at serious risk of harm. Such disclosures may be reported to the relevant authority.		
I will be pseudo-anonymised in publications that will arise from the research.		
I am aware that the proposed methods of publication dissemination of research findings, includes: - Peer reviewed journals - Non-peer reviewed journals - Peer reviewed books - Publication in media or website - Conference presentation - Internal report - Promotional report and materials - Dissertation/Thesis - Presentation to participants or relevant community group		

I give permission for your team to use the data in future research.		
I give permission to be to be contacted for future research studies by your team. It has been explained to me what will happen once the programme has been completed.		
I understand that my participation in this study is entirely voluntary, and I am free to withdraw at any time during the research without disadvantage to myself and without being obliged to give any reason. I understand that my data can be withdrawn up to the point of data analysis and that after this point it may not be possible.		
I hereby freely and fully consent to participate in the study which has been fully explained to me and for the information obtained to be used in relevant research publications.		

Participant's Name (BLOCK CAPITALS)
………………………………………………………………………

Participant's Signature
………………………………………………………………………………..

Investigator's Name (BLOCK CAPITALS)
………………………………………………………………….

Investigator's Signature
………………………………………………………………………………….

Date: …………………………

END OF FORM.

F. Publications/ Abstracts/ Poster Presentations

Published Paper:

- PIZZAMIGLIO, S., DESOWSKA, A., SHOJAII, P., **TAGA, M.** & TURNER, D. L. 2017. Muscle co-contraction patterns in robot-mediated force-field learning to guide specific muscle group training. NeuroRehabilitation, 1-13.

Published Abstract:

- **TAGA, M.,** CURCI, A., LACAL, I., & TURNER, D. (2019). The N100 TEP as a neural predictor of motor learning: A TMS-EEG study. Brain Stimulation: Basic, Translational, and Clinical Research in Neuromodulation, 12(2), 445-446.

Poster Presentations at Conferences:

- **MYRIAM TAGA** and Professor DUNCAN TURNER (2017, Helsinki, Finland, TMS-EEG Conference). Frequency specific correlations between oscillatory power and the cortical silent period: Is it restricted to the dominant hemisphere?
- **MYRIAM TAGA** and Professor DUNCAN TURNER (2018, Helsinki, Finland, TMS-EEG Conference). Neural correlates of motor adaptation and motor performance measured with TMS-EEG

G. Additional Analysis – Chapter 6

G.1. Kinematic Block-by-block analysis

G.1.1. Statistics

The 288 trials were then divided into 18 blocks each containing 16 trials. Each condition (familiarisation, motor adaptation and wash-out) had six blocks. All trials in each block were then averaged and eight blocks of interest were then chosen for statistical analysis. Specifically, block 6 (average of trials 81-96 in the familiarisation condition), block 7 to 12 (average of trials 97-112, 113-128, 129-144, 145-160, 161-175, 176-191, respectively in the motor adaptation condition) and block 18 (average of trials 273-288 in the wash-out condition). For each measure, a one-way repeated-measure ANOVA with factor "block" (8 levels: Block 6-12, 18) was performed to highlight the presence of any variance across blocks. A Greenhouse-Geiger correction was applied whenever Mauchly's test indicated a lack of sphericity. Whenever a main effect of block was detected, post-hoc paired t-tests with Bonferroni correction for multiple comparisons was applied to analyse the differences between block 6 and block I, with i=7-12,18 (7 comparisons, $p < 0.007$). Unless otherwise stated, all data presented in text, Tables and Figures are represented as mean ± SD.

G.1.2. Results

Movement onset and offset were similar across conditions, whereas averaged summed errors, maximum velocity and maximum force were increased during motor adaptation compared to familiarisation and wash-out. Statistical block-by-block results of the selected kinematic measures are shown in the Figure below and reported in the table. The results are very similar to previously reported lab results (Pizzamiglio et al., 2017) confirming the robustness of the findings across experiments.
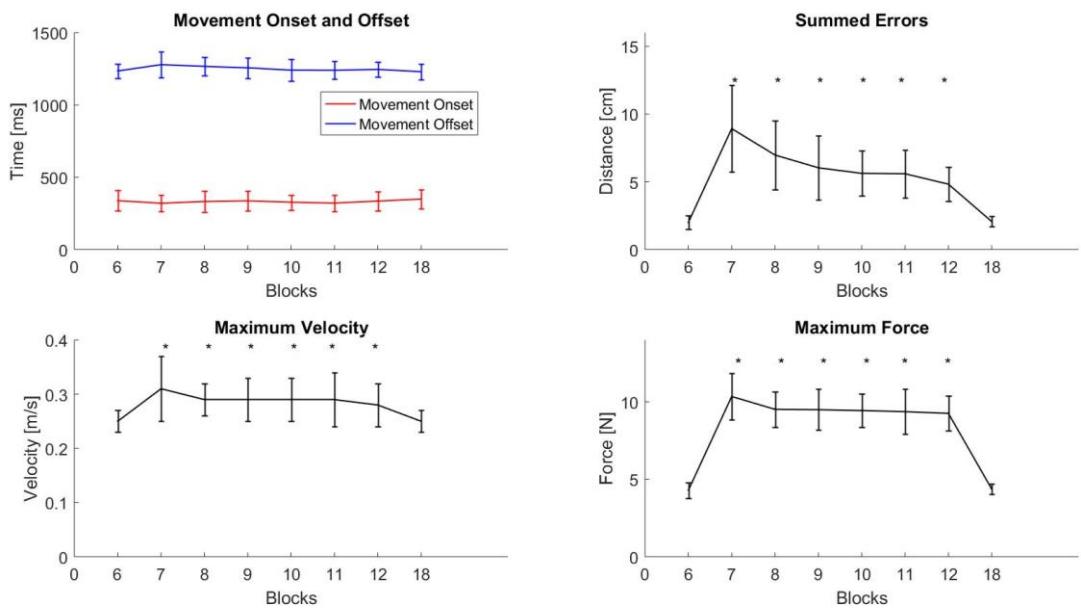
Figure G-1: Block-by-block kinematic measures. Block-by-block grand-average (N = 15 and bars represent ± 1 SD) are shown for every kinematic measure. Repeated-measures ANOVA revealed a significant effect of condition on summed errors, maximum velocity and maximum force. Significant post-hoc paired t-tests are highlighted with * (Block 6 versus Block$_i$ with I = 7, ...12, 18; 7 comparisons and Bonferroni corrected $p < 0.0071$).

Table G: Kinematics results (Mean [SD])
Block-by-block kinematic measures. Descriptives and repeated-measures ANOVA are reported for every kinematic measure. Significant post-hoc paired t-tests between Block 6 versus Block$_i$ with i = 7, ...12, 18; 7 are highlighted with * p < 0.0071 (Bonferroni corrected).

	Null-Field	Force-Field	Force-Field	Force-Field	Force-Field	Force-Field	Force-Field	Null-Field	ANOVA		
Kinematic Measure	**Block 6**	**Block 7**	**Block 8**	**Block 9**	**Block 10**	**Block 11**	**Block 12**	**Block 18**	**F**	**Df, Error**	**p**
Movement Onset [ms]	338[71]	320[58]	332[73]	337[68]	327[52]	321[57]	335[66]	349[66]	1.73	3.9, 55.03	0.16
Movement Offset [ms]	1235[48]	1279[88]	1267[62]	1257[71]	1241[77]	1240[61]	1246[53]	1230[56]	1.61	3.9, 54.36	0.19
Max Velocity [m/s]	0.25[0.02]	0.31[0.06]*	0.29[0.03]*	0.29[0.04]*	0.29[0.04]*	0.29[0.05]*	0.28[0.04]*	0.25 [0.01]	10.63	3.28, 45.88	< 0.0001
Max Force [N]	4.29[0.51]	10.35[1.52]*	9.52[1.16]*	9.5[1.32]*	9.44[1.07]*	9.37[1.45]*	9.26[1.13]*	4.37 [0.09]	177.57	3.13, 43.74	< 0.0001
Summed Errors [cm]	1.99[0.51]	8.92[3.21]*	6.97[2.56]*	6.03[2.35]*	5.62[1.65]*	5.59[1.77]*	4.82[1.27]*	2.06 [0.1]	36.04	2.4, 32.7	< 0.0001

G.2. ERP Component control analysis

Control P/N170: 140-190 ms
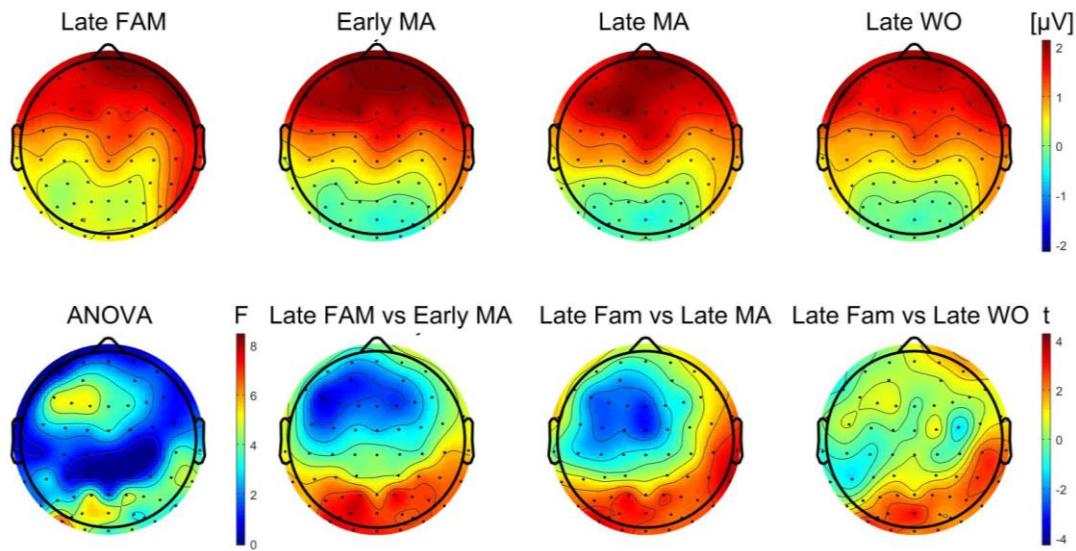
Control P/N170: 190-240 ms
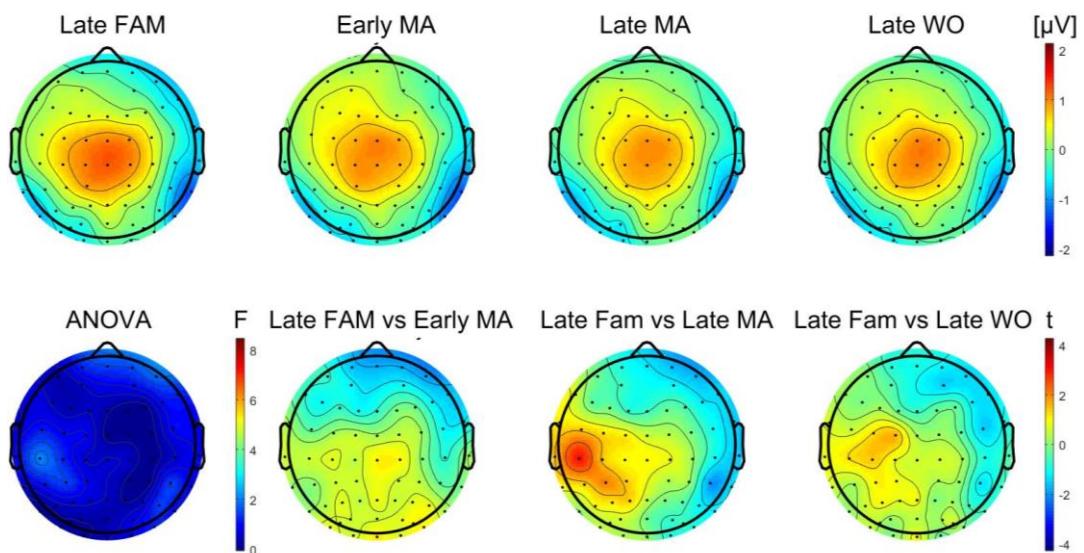
Figure G-2: ERPs activations and statistical comparisons for the P/N170 component in two control time windows (140-190 ms and 190-240 ms). ERP activations (µV) in the four conditions of interest are represented in the first row. Statistical significance was obtained through non-parametric permutation-based permutation repeated measure ANOVA, followed by pairwise non-parametric permutation-based t-tests comparing late familiarisation with all other conditions. Significance level was set to 0.05, and all p-values were FDR adjusted to control for multiple comparisons (63 electrodes). Significant electrodes are highlighted with a cross in the second row.